ISSN 0013-4686

THE JOURNAL OF THE INTERNATIONAL SOCIETY OF ELECTROCHEMISTRY

ELECTROCHIMICA Acta

Editor-in-Chief: R. D. ARMSTRONG, University of Newcastle upon Tyne, England
North American Editor: E. J. CAIRNS, University of California, Berkeley, CA

FOUR-YEAR SUBJECT INDEX

1990–1993

VOLUMES 35–38

PERGAMON

ELECTROCHIMICA ACTA

Published by Elsevier Science Ltd for the International Society of Electrochemistry (ISE)

Editor-in-Chief

R. D. ARMSTRONG

CHEMISTRY DEPARTMENT, THE UNIVERSITY,
NEWCASTLE UPON TYNE NE1 7RU, ENGLAND
(Tel: +44 91 2227858. Fax: +44 91 2226929)

Assistant Editor: **O. R. BROWN**, University of Newcastle upon Tyne
Editorial Assistant: **Mrs M. DODDS**, University of Newcastle upon Tyne

North American Editor

E. J. CAIRNS

ENERGY & ENVIRONMENT DIVISION, BUILDING 90,
LAWRENCE BERKELEY LABORATORY, UNIVERSITY OF CALIFORNIA,
BERKELEY, CA 94720, U.S.A.
(Tel: +1 510 4865028. Fax: +1 510 4865172)

Associate Editors

R. ALKIRE
Urbana, IL, U.S.A.

E. BUDEVSKI
Sofia, Bulgaria

M. FROMENT
Paris, France

H. GERISCHER
Berlin, Germany

R. HAASE
Aachen, Germany

D. J. HENDERSON
Sandy, UT, U.S.A.

Y. ITO
Kyoto, Japan

K. V. KORDESCH
Graz, Austria

J. KORYTA
Prague, Czech Republic

L. I. KRISHTALIK
Moscow, Russia

D. LANDOLT
Lausanne, Switzerland

J. OSTERYOUNG
Raleigh, NC, U.S.A.

S. K. RANGARAJAN
Bangalore, India

D. W. SHOESMITH
Pinawa, Manitoba, Canada

Z. W. TIAN
Xiamen, China

S. TRASATTI
Milan, Italy

W. VIELSTICH
Bonn, Germany

C. A. VINCENT
St Andrews, Scotland

Production Editor: S. TAYLOR, Elsevier Science Ltd, Oxford *(Tel: +44 865 743690)*

Please direct all queries in relation to accepted articles to the Production Editor at Elsevier Science Ltd.

Publishing, Subscription and Advertising Offices: Elsevier Science Ltd, The Boulevard, Langford Lane, Kidlington, Oxford OX5 1GB, U.K. (*Tel:* +44 865 794141; *Fax:* +44 865 60285), and Elsevier Science Inc., 660 White Plains Road, Tarrytown, NY 10591-5153, U.S.A. Annual Institutional Subscription Rates 1994: North, Central and South America, U.S.$1650.00, Rest of World, £1072.00. Associated Personal Subscription Rates are available on request for those whose institutions are library subscribers. Sterling prices exclude VAT. Non-VAT registered customers in the European Community will be charged the appropriate VAT in addition to the price listed. Prices include postage and insurance and are subject to change without notice. Issued free to paid-up members of the International Society of Electrochemistry (ISE). Subscription enquiries from customers in North America should be sent to: *Elsevier Science Inc., 660 White Plains Road, Tarrytown, NY 10591-5153, U.S.A.*, and for the remainder of the world to: *Elsevier Science Ltd, The Boulevard, Langford Lane, Kidlington, Oxford OX5 1GB, U.K.*

Copyright © 1994 Elsevier Science Ltd

Second class postage paid at Rahway, NJ and additional mailing offices. Postmaster send address corrections to Electrochimica Acta, c/o Elsevier Science Inc., 660 White Plains Road, Tarrytown, NY 10591-5153, U.S.A.

Whilst every effort is made by the publishers and editorial board to see that no inaccurate or misleading data, opinion or statement appear in this journal, they wish to make it clear that the data and opinions appearing in the articles and advertisements herein are the sole responsibility of the contributor or advertiser concerned. Accordingly, the publishers, the editorial board and editors and their respective employees, officers and agents accept no responsibility or liability whatsoever for the consequences of any such inaccurate or misleading data, opinion or statement.

ELECTROCHIMICA *Acta*

THE JOURNAL OF THE INTERNATIONAL SOCIETY OF ELECTROCHEMISTRY

Editor-in-Chief: R. D. ARMSTRONG
North American Editor: E. J. CAIRNS

SUBJECT INDEX 1990–1993

PERGAMON

AIMS AND SCOPE

This international journal is intended for the rapid publication of both original work and reviews in the field of electrochemistry. Electrochemistry should be interpreted to mean any of the Divisions of the International Society of Electrochemistry, *ie*

(1) Fundamental Interfacial Electrochemistry
(2) Electrode and Electrolyte Materials
(3) Analytical Electrochemistry
(4) Molecular Electrochemistry
(5) Electrochemical Energy Conversion
(6) Corrosion, Electrodeposition and Surface Treatment
(7) Industrial Electrochemistry and Electrochemical Engineering
(8) Bioelectrochemistry.

Publishing, Subscription and Advertising Offices: Elsevier Science Ltd, The Boulevard, Langford Lane, Kidlington, Oxford OX5 1GB, U.K. (*Tel:* +44 865 794141; *Fax:* +44 865 60285).

Back Issues: Back issues of all previously published volumes in both hard copy and microform are available direct from Elsevier Science offices.

Copyright © 1994 Elsevier Science Ltd

It is a condition of publication that manuscripts submitted to this journal have not been published and will not be simultaneously submitted or published elsewhere. By submitting a manuscript, the authors agree that the copyright for their article is transferred to the Publisher if and when the article is accepted for publication. However, assignment of copyright is not required from authors who work for organizations which do not permit such assignment. The copyright covers the exclusive rights to reproduce and distribute the article, including reprints, photographic reproductions, microform or any other reproductions of similar nature and translations. No part of this publication may be reproduced, stored in a retrieval system or transmitted in any form or by any means, electronic, electrostatic, magnetic tape, mechanical, photocopying, recording or otherwise, without permission in writing from the copyright holder.

Whilst every effort is made by the publishers and editorial board to see that no inaccurate or misleading data, opinion or statement appear in this journal, they wish to make it clear that the data and opinions appearing in the articles and advertisements herein are the sole responsibility of the contributor or advertiser concerned. Accordingly, the publishers, the editorial board and editors and their respective employees, officers and agents accept no responsibility or liability whatsoever for the consequences of any such inaccurate or misleading data, opinion or statement.

®™The paper used in this publication meets the minimum requirements of American National Standard for Information Sciences—Permanence of Paper for Printed Library Materials, ANSI Z39.48-1984.

Photocopying information for users in the U.S.A.

The Item-Fee Code for this publication indicates that authorization to photocopy items for internal or personal use is granted by the copyright holder for libraries and other users registered with the Copyright Clearance Center (CCC) Transactional Reporting Service provided the stated fee for copying beyond that permitted by Section 107 and 108 of the United States Copyright Law is paid. The appropriate remittance of $6.00 per copy per article is paid directly to the Copyright Clearance Center Inc., 222 Rosewood Drive, Danvers, MA 01923, U.S.A.

Permission for other use

The copyright owner's consent does not extend to copying for general distribution, for promotion, for creating new works, or for resale. Specific written permission must be obtained from the Publisher for such copying.

The Item-Fee Code for this publication is: 0013-4686/94 $6.00 + 0.00

A

abrading electrode method: effect of Cl^- on repassivation kinetics of Ni in 0.75M Na_2SO_4 aq, **37,** 2437
absolute electrode potentials, **36,** 1659
  a unifying approach, **35,** 269
absorption
  of hydrogen in metal membrane electrodes: theory of faradaic admittance, **38,** 2645
absorption spectra
  of complexes of lanthanides with acetylacetonate and tetraphenylporphyrin anions during oxidation and reduction, **38,** 689
acetate ions
  adsorption at Pt: effect on zinc acetate coatings, **36,** 2109
  effect on anodic dissolution and passivation of Fe in acetate buffers, **37,** 477
1-acetate-2-methylnaphthalene
  synthesis and oxidation at Pt anodes in HOAc-LiOAc, **35,** 1739
acetonaphthone
  electrochemical behaviour and effect on electrodeposition of Zn from acid sulphate, **38,** 1351
acetonitrile
  Ag(I) solvation and cryptate stability in mixtures with DMSO, **36,** 1427
  effect on anodic behaviour of Fe microelectrodes in acidic aqueous perchlorate, **35,** 501
acetonitrile-water mixtures
  precipitation of metal fluorides, pF^- scale, buffers and *E vs* pF^- diagrams, **35,** 1885
acetophenone
  asymmetric induction by cyclodextrins for dimerization in DMF-$TBABF_4$, **36,** 1911
  reduction at Pd or Pt supported on carbon felt cathodes in 0.1M KOH or 0.1M H_2SO_4 in EtOH aq, **38,** 199
acetophenones
  asymmetric induction by β-cyclodextrin during reductions at Hg in alkaline media, **35,** 1149
acetoxylation
  of ketones by electrogenerated $Pb(OAc)_4$, **36,** 1165
acetylacetonato complexes of lanthanides(III)
  polarography in DMSO, **35,** 1713
acetylacetonatolanthanide(III) phthalocyaninates
  synthesis and electrochemistry at Pt electrodes in DMSO-TEAP, **35,** 1707
acetylene see ethyne
acoustic calorimetry
  study of Peltier effect at the electrochemical interface, **35,** 25
acoustic microscopy
  of polyimide coatings on Al metallizations of Si substrates, **38,** 1877
acrylamide
  electrochemical polymerization in DMF solutions: effect of pH, **37,** 2083
activation energies and frequency factors
  apparent variations with potential during reductions of Zn(II) paludrine complexes at Hg cathodes, **38,** 735
activation energy
  for oxygen reduction at Pt in aqueous acids: relation to the Pt-O vibrational quantum, **37,** 1
activity coefficients
  of $AgNO_3$ in $AgNO_3$-KNO_3 melts in the range 513-583K, **37,** 91, 1155
  of $AgNO_3$ from EMF studies of the cells Ag / $AgNO_3$-KNO_3-$NaNO_3$ / NO_2, O_2, Pt, **38,** 1139
  of Cd^{2+} in LiCl-KCl eutectic, **35,** 1201
adatoms see also adsorption and underpotential deposits and underpotential deposition
  of Au: effect of adsorbed Cl^- or pyridine on surface diffusion on Au electrodes in 0.5M H_2SO_4 aq, **35,** 1331
additives see also surfactants
  N,N-bis(decaoxyethene)octadecylamine, cinnamaldehyde, benzalacetone and acetonaphthone: effects on electrodeposition of Zn, **38,** 1351
  effect of benzene, 2-methylfuran and 2-methylthiophene on behaviour of Li electrodes in propene carbonate, **37,** 119
  effect of TiO_2 and B_2O_3 on Al electrodeposition from cryolite baths, **37,** 1787
  to electroplating baths to control properties of the deposit, **37,** 2115
  inhibition of electrodeposition of Pb dendrites: effects of potential and RDE speed, **37,** 2249
adenosine
  two ranges of electrode potential for adsorption at Hg electrodes, **35,** 1291

admittance see impedance
admittance spectroscopy
interpretations of low-frequency dispersion, **35,** 1595
adsorption at electrodes
analytical model of differential capacitance based on the isotherm of quasi-chemical approximation, **37,** 1273
discussion of the "size ratio parameter" (number of solvent molecules displaced by each adsorbate molecule), **38,** 2663
of intermediates in electrodeposition reactions: impedance studies, **38,** 2043
of intermediates in electrode processes: inductive behaviour, **38,** 1803
of ions at the metal/electrolyte interface: effect on second harmonic generation, **36,** 1835
of non-symmetrical electrolytes at the metal interface, **35,** 545
of organic compounds, effects of nature and crystal face of the metal and of substituents in aromatics, **37,** 2137
of organic layers: electron tunnelling through, **36,** 421
and reorientation at electrified interphases: a statistical mechanical treatment, **38,** 1441
of several components: effects of lateral interactions, **36,** 1689
of strongly adsorbed substances from dilute solutions: phase transitions, **36,** 447
adsorption studies see also chemisorption
of acetate ions at Pt electrodes: effect on coatings of zinc acetate, **36,** 2109
of acetylenic alcohols on Fe in H_2SO_4 aq, **37,** 317
of adensosine at Hg electrodes: two ranges of electrode potential for adsorption, **35,** 1291
of albumin at vitreous carbon electrodes: effect of ionic strength on rate, **36,** 1811
of allyl alcohol and propargyl alcohol: interactions with reduced CO_2 at Pt electrodes in 0.5M H_2SO_4, **37,** 1083
of 3-amino-5-heptyl-1,2,4-triazole, inhibition of corrosion of Cu in 0.5M H_2SO_4, **37,** 2299
of anions at single crystal Au anodes: inhibition of oxidation of D-glucose in aqueous acids, **37,** 357
of 4,4'-bipyridyl at Au electrodes in acidic and neutral media, **35,** 591
of Br^- at Hg electrodes from propene carbonate solutions, **36,** 1971
of butanediols at Au electrodes from 0.02M $NaClO_4$ aq, **35,** 1345
of $C_{10}H_{21}(OC_2H_4)_{11}OH$ and $C_6F_{13}(C_2H_4O)_nH$ on Au in sodium sulphate aq, **37,** 2377
of Ca^{2+} at Pt electrodes, induced by adsorbed anions and molecules, **36,** 1453
of Cl^- on Ni electrodes in 0.75M Na_2SO_4 aq, **37,** 2437
of ClO_4^- at the Hg/$HClO_4$ aq and Hg/$HClO_4$-TEAP aq interfaces, **37,** 1753
of CN^- and CNS^- at Pt, Pd, Au and Ag electrodes: *in situ* IR spectroscopy, **36,** 1863
of CN^- and SCN^- at Pt electrodes from 0.1M $NaClO_4$ aq, **36,** 1849
of CO at Ni electrodes: inhibition of HER and anodic dissolution of Ni, **35,** 1777
of CO on noble metals: theory and experiment [R], **35,** 691
competitive and co-operative, involving organic residues and CO, **36,** 2183
competitive, of species on electrodeposited metals discussed in terms of hard and soft acids and bases, **37,** 2115
on constructional materials used in nuclear power stations: radiotracer studies, **35,** 817
of corrosion inhibitors at carbon steel from neutral solutions, **36,** 981
of cytochrome *c* at Hg electrodes, **35,** 473
of cytochrome *c* on Au electrodes from phosphate buffer solution: effect of 4,4'-bipyridyl disulphide, **37,** 403
of 1,2-diaminoethane at platinized Pt electrodes from 1M H_2SO_4 aq and from 0.1M NaOH aq, **35,** 111
of DMSO at the Hg/H_3PO_4 aq interface, **35,** 1901
of ethanal at Pt in 0.1M $HClO_4$ aq, **35,** 989
of Fe(III) hydroxo complexes on $Ni(OH)_2$ and NiOOH powders from aqueous alkali, **37,** 469
of Forafac ionic perfluorinated surfactants at Au electrodes, **38,** 2203
of D-glucose at platinized Pt in 1M H_2SO_4 aq, **37,** 2443
of $H_2PO_4^-$ and H_3PO_4 on Pt from acidic aqueous fluorides, **37,** 385
of hemic proteins at pyrolytic graphite electrodes, **35,** 177
of hydrogen, oxygen, metals or simple organics at treated Ir electrodes, **35,** 191
of L-hydroxyproline and D-allohydroxyproline at Hg electrodes in aqueous buffers, **36,** 109
of imidazole at Au electrodes from aqueous media, **38,** 947
of iron(II) tris(2,2'-bipyridyl) complex at Ag electrodes, **37,** 2347
of methylpyridines at Hg electrodes: capacitance studies, **38,** 1585
of methylpyridines at Hg electrodes: thermodynamic interpretation of electrocapillary data, **38,** 1573
of nitrobenzene and benzonitrile at Ag electrodes from 0.1M KCl aq, **36,** 1523
of *p*-nitrosodimethylaniline at flat single-crystal Ag electrodes, **36,** 1879

adsorption studies continued
1-octyn-3-ol at Fe electrodes in HCl aq: kinetic aspects, **36,** 1333
of *p*-toluene sulphonate anions at the polycrystalline Au/aqueous solution interface, **37,** 75
of *p*-nitroaniline at Ag and Au electrodes from aqueous perchlorates, **35,** 1037
of Pb^{2+} at Hg electrodes induced by Br^-, **35,** 1701
of phosphonium cations from Ph_4PCl and cetylBu_3PBr in 0.1M NaF at a stationary Hg electrode, **37,** 2447
of polyacrylamide at Au and steel electrodes from aqueous acids, **36,** 1315
of poly(styrene sulphonate) at polyaniline film electrodes in $HClO_4$ aq, **36,** 799
of primary amino compounds at Pt electrodes [R], **35,** 919
of propargyl, allyl, methyl and propyl alcohols at Pt electrodes from 0.5M H_2SO_4 aq, **36,** 2003
of pyridine or Cl^- at Au electrodes: effect on surface diffusivity of Au, **35,** 1331
of quinine and flumazenil at Hg electrodes, **35,** 1311
of reaction products at the Hg cathode during reduction of camphorquinone, **38,** 2209, 2217
and redox behaviour of cytochrome c_3 at basal plane pyrolytic graphite electrodes, **36,** 1423
and redox behaviour of mitoxantrone at Hg electrodes in 0.5M Na_2SO_4-McIlvaine buffers, **37,** 2059
of a redox surfactant at Pt and at ITO electrodes, **35,** 885
and reduction of N,N-bis(decaoxyethene)octadecylamine, cinnamaldehyde, benzalacetone and acetonaphthone at Hg cathodes, **38,** 1351
of SO_4^{2-} at Pt: bond restrictions caused by the applied electric field (second-order Stark effect), **37,** 2179
of SO_4^{2-} at smooth Cu electrodes in acidic and neutral media, **36,** 753
of sulphide, thiosulphate, sulphite and dithionite at Pt electrodes: inhibition of hydrogen oxidation, **37,** 2785
of surfactants: effect on polarographic discharge of Cd^{2+}, **35,** 1805
of terminal and vicinal aliphatic diols at Au electrodes from 0.02M $NaClO_4$ aq, **38,** 717
of the tetrasulphonated phthalocyanines of iron and cobalt at pyrolytic graphite, **36,** 2165, **37,** 769
of thiourea at polycrystalline Ag electrodes in methanolic KF, **36,** 965
of thymine at the (0001) basal face of Cd single-crystal electrodes: condensed 2-dimensional film behaviour, **37,** 2369
of thymine at the (111) face of Ag single-crystal electrodes, **37,** 2373
of trioctylphosphine oxide at Hg from methanolic electrolytes, **35,** 379
of ubiquinone-10 and 1-hexanol at Hg electrodes: θ inferred from *cv* ΔE for Cd^{2+}/Cd(Hg), **37,** 2395
of uracil at Hg electrodes from aqueous phosphate buffer pH8, **37,** 2663
of xylenes and their oxidation products at Pt and Au, **35,** 273
adsorption from gas phase
distinguishing hydration from reaction between co-adsorbed water and H or Cs, **36,** 1883
of oxygen and SO_2 at Li and Na, **37,** 731
adsorption, specific
of HSO_4^- ions on Au(100) in H_2SO_4 aq, **37,** 615
of hydrogen on polycrystalline Pt electrodes from 0.5M H_2SO_4 aq, **37,** 2629
of polar solvents at solid electrodes (Cu, Cd, Ag), **36,** 859
air electrode
based on carbon paper treated with H_2PtCl_6 aq: thermal preparation, **37,** 1327
albumin
effect of ionic strength on rate of adsorption on vitreous carbon electrodes, **36,** 1811
alcohols, lower aliphatic
chaotic and periodic switching in cyclic voltammetric responses in alkaline solutions at Pt anodes, **38,** 519
aldehydes
oxidations at anodes of Cu, Ag and Au: concomitant hydrogen evolution, **38,** 1067
algae
bound to vitreous carbon electrodes: uptake of redox couples, **35,** 1377
alizarin complexone
complex with La(III): effect of F^- on reduction mechanism at Hg cathodes, **35,** 1861
alkali-metal cations
electrochemical exchange intercalation in thin sputtered NiO films, **38,** 2765
alkenes
indirect cathodic reduction using Cr(II) complexes with polyaminocarboxylate ligands, **37,** 575
alkylation
using cathodically generated triphenylmethyl anions in DMF, **35,** 239
alkynes
indirect cathodic reduction using Cr(II) complexes with polyaminocarboxylate ligands, **37,** 575

D-allohydroxyproline
complexes with Cu^{2+}: kinetics of dissociation, **36,** 109
alloy see also alloys and aluminium alloys
Ag-Hg: growth kinetics of clusters at Pt cathodes, **38,** 535
Al-0.4%Mn: impedance of thin oxide films formed on anodes in borate buffer pH7.4, **37,** 1389
Al-5.03%Zn-1.67%Mg-0.23%Cu, pitting and repassivation processes in chloride solutions containing sulphate, **38,** 2741
AlMn05Mg05, characterization of chromate-phosphate conversion coatings by impedance spectroscopy and optical measurements, **38,** 2577
$CoGe_2$-Ge eutectic: electrochemical behaviour and structural changes in 0.5M H_2SO_4 aq, **36,** 1247
Cu_3Ge-Ge eutectic: electrochemical behaviour and structural changes in 0.5M H_2SO_4 aq, **36,** 1247
90%Cu-10%Ni: anodic dissolution of RDE in HCl aq, **36,** 2135
Fe25Cr: atmospheric oxidation of abraded and electrochemically polarized surfaces, **36,** 1623
$Fe_{80}B_{20}$: anodic films in borate buffer and acidic sulphate solutions, **38,** 205
$FeGe_2$-Ge eutectic: electrochemical behaviour and structural changes in 0.5M H_2SO_4 aq, **36,** 1247
$FeSn_2$ on tinplate: anodic stripping voltammetry in 1M HCl aq, **36,** 1501
misch metal-$Ni_{3.6}Mn_{0.4}Al_{0.3}Co_{0.7}$ in porous Ni substrate: modification for H_2 storage by KBH_4 treatment, **38,** 659
40%Ni-60%Co: thick oxide layers formed by fast square-wave potential pulses, **36,** 1963
NiGe-Ge eutectic: electrochemical behaviour and structural changes in 0.5M H_2SO_4, **36,** 1247
Pb-Sb: anodic behaviour in H_2SO_4 aq, **35,** 229
Pd-Ni: electrocatalytic hydrogenation of nitrobenzenes to anilines in methanol, **38,** 2683
Pt-Fe supported on carbon: preparations and characterizations, **38,** 2715
Ru-Ti: electrochemical behaviour in acidic solutions, **36,** 19
alloy electrocatalysts for direct oxidation of methanol: characterization [R], **36,** 2053
alloys see also alloy and aluminium alloys
Al-In: anodic behaviour in 4M KOH aq from -20 to 60°C, **36,** 79
Al-Mn: photoelectrochemical behaviour of oxide layers, **36,** 1179
Al-Zr: sputter-deposited and arc-melted: anodic polarization behaviours of both, **36,** 1227
amorphous Ni-Co-Si-B electrocatalysts and crystalline Ni-Co: voltammetric and XPS studies in 1M KOH aq, **37,** 2029
Au-Ag: surface reorganization after anodic dissolution of Ag, **36,** 905
Bi-Pb cathodes: effects of grain macrostructure and surface morphology on hydrogen evolution in H_2SO_4 aq:, **37,** 269
Co-Cr: potentiodynamic behaviours of Stellite and Ceramometallique in artificial saliva (AFNOR standard S90-701), **38,** 1769
co-deposited Pt-Pd: electrocatalysis of oxidation of ethane-1,2-diol in 0.1M NaOH, **36,** 353
Cu-Al-Ag: anodic oxidation in 0.5M NaOH aq, **36,** 1409
Cu-Au and Ag-Pd single phases: anodic dissolution in 12M LiCl aq and in acid, **36,** 49
Cu-Ni: impedance studies of electrodeposition, **35,** 1587
$Fe_{40}Ni_{40}P_{14}B_6$: electrocatalytic activity in 1M KOH aq, **38,** 821
$Fe_{60}Co_{20}Si_{10}B_{10}$: electrocatalytic activity in 1M KOH aq, **38,** 821
$Fe_{70}Cr_{10}X_{13}C_7$ where X = P or B: XPS study of anodic passivation in 0.5M H_2SO_4, **37,** 2269
Fe-Co: mechanism of deposition on vitreous carbon cathodes, **38,** 671
Fe-Cr: anodic behaviour in 0.5M H_2SO_4, **38,** 763
Fe-Cr: impedance studies of passive layers formed in neutral aqueous media, **38,** 1567
Fe-Cr(-Mo): role of Mo in passivation in 0.5M H_2SO_4, **36,** 1465
Fe-Ni: effects of Cl^- and alloy composition on passivation in H_2SO_4 aq, **35,** 69
Fe-Ni-Cr-Zr-B: electrocatalytic activity in 1M KOH aq, **38,** 821
α-Li-Al, β-Li-Al and $Li_5Al_5Fe_2$ as negatives in high temperature secondary lithium cells, **38,** 1269
misch metal-$Ni_{3.6}Mn_{0.4}Al_{0.3}Co_{0.7}$: modification for H_2 storage by deposition of Pd, Fe, Co or Ni, **38,** 787
$MmNi_{3.6}Mn_{0.5}Al_{0.4}M_{0.1}$ (Mm = Misch metal, M = Cr, Fe, Co or Cu) for hydrogen storage in Ni-H batteries, **38,** 1087
$Mm_xNi_{3.7}Mn_{0.5}Al_{0.4}$ (Mm = Misch metal, $0.885<x<1$) for hydrogen storage in Ni-H batteries, **38,** 1087
Ni-Co, amorphous and crystalline: electrocatalysts for anodic oxygen evolution, **37,** 169, 769
Ni-Co(-Si-B-P): catalysis of hydrogen evolution in 1M KOH aq, **36,** 537
Ni-P: anodic behaviour in 0.1M NaCl and in 0.05M Na_2SO_4 aq, **38,** 1979
Ni-P: electrodeposition on glassy carbon cathodes and anodic dissolution, **38,** 261
Ni-Sn electrodeposits on Cu: studies by Mossbauer and X-ray fluorescence spectra, **35,** 55
NiSn and porous NiZn electrodeposited coatings as anodes for water electrolysis in KOH aq, **37,** 29

alloys continued
Pd-Ni: cathodic hydrogen uptake, **36,** 1203
Pt-Ru bifunctional electrocatalysts for direct oxidation of methanol, **37,** 2361
reorganization of surfaces after selective anodic dissolution, **36,** 905
Sb-Pb: kinetics of reduction of the PbO film on Pb-Sb electrodes in H_2SO_4, **38,** 1131
Ti with implanted Ir and Rh near the surface: catalysis of chlorine evolution and XPS characterization of anodic layers, **38,** 1313
transition-metal: relation between hydrogen overpotential and electronic structure, **38,** 557
Zn-Ni: mechanism of electro-codeposition from aqueous chlorides, **37,** 545
Zr-Sn-Fe-Cr-Ni: anodic behaviour of Zircaloy-2 and Zircaloy-4 in aqueous media, **37,** 281
allyl alcohol
anodic stripping of adsorbed residues from Pt in 0.5M H_2SO_4, **36,** 2003
interaction with a Pt electrode, modified by reduced CO_2 in 0.5M H_2SO_4, **37,** 1083
on-line MS analysis of products of oxidation at Au anodes in 0.5M H_2SO_4 aq, **38,** 1337
alternating current
superimposed, effect of frequency on current yield of ferrate (VI) at Fe anodes in 14M NaOH aq, **38,** 1717
alumina see also aluminium and aluminium oxide
galvanoluminescence from porous anodic films, **35,** 825
growth and structure of anodic oxides in CrO_3-xH_2SO_4 aq, **35,** 955, 961
kinetics of galvanostatic growth of porous films on Al in H_2SO_4 aq, **36,** 709
structure of anodic films formed in H_2SO_4 aq and the mechanism of their hydration and pore closure at 100°C, **38,** 1413
β"-alumina
with Ca^{2+} as the divalent cation: preparation, properties and application as a solid electrolyte, **38,** 365
containing Ba^{2+} through ion exchange: production and characterization, **36,** 563
β- and β"-alumina
potentiometric study of activities in Na_2O-α-Al_2O_3 between 825K and 1400K, **36,** 791
aluminium
anodic dissolution in 0.33M $AlCl_3$-MeCN: inductive loops indicating adsorbed intermediates, **38,** 1803
anodization in CrO_3-xH_2SO_4 aq, **35,** 955, 961
barrier and porous anodic oxide films studied by spectroscopic ellipsometry and impedance spectra, **38,** 2103
containing Mn: photoelectrochemical behaviour of oxide layers, **36,** 1179
corrosion and anodic dissolution in alkali: impedance analysis, **35,** 1509
corrosion in deaerated HCl aq, **36,** 179
corrosion in Li_2CO_3-Na_2CO_3 aq: effects of Li^+, CO_3^{2-} and Cl^-, **37,** 2659
dissolution in aqueous media under cathodic conditions, **38,** 2541
dissolution during cathodic hydrogen evolution in neutral media, **35,** 1743
effect of added In on anodic behaviour in 4M KOH aq, **36,** 79
effect of BPh_4^- on surface modification during cycling in 0.1M $NaClO_4$ aq, **38,** 1073
effect of organic co-solvents on electrodeposition from $[Me_3PhN][Al_2Cl_7]$ melts, **38,** 245
effects of temperature and concentrations of OH^- and AlO_2^- on dissolution in KOH aq, **36,** 1631
electrodeposition and chemical dissolution at graphite electrodes in cryolite, **36,** 811
electroplating of Ag and Cu at anodized surfaces: effects of anions and alloy composition, **35,** 1019
electropolishing using alternating current, **36,** 93
growth kinetics for porous anodic oxide films in H_2SO_4 aq, **38,** 2351
impedance of passive films in aggressive (0.5M NaCl) and non-aggressive (0.5M Na_2SO_4-0.1M ammonium tartrate) media, **37,** 2283
impedance studies of thin oxide layers and their water content, **38,** 1957
impedance study of anodization in 0.5M NaCl aq, **35,** 1501
impedance study of corrosion in neutral and acidic media, **38,** 1989
impedance of thin oxide films formed on anodes in neutral borate buffer, **37,** 1389
kinetics of galvanostatic growth of porous oxide films in H_2SO_4 aq, **36,** 709
mechanism of hydration and pore closure during hydrothermal treatment of porous anodic films, **37,** 125
oxidation of soluble species in NaF-AlF_3-Al_2O_3 melts at carbon and W anodes, **36,** 31
aluminium alloys
characterization of chromate-phosphate conversion coatings by impedance spectroscopy and optical measurements, **38,** 2577
corrosion resistance of Al 6061-T6 bestowed by successively boiling in Ce^{3+} aq and anodizing in 0.1M Na_2MoO_4, **37,** 2277
impedance determinations of rates of pitting corrosion of coated metals, **38,** 1891

aluminium alloys continued
impedance studies in 1M KOH aq, **35,** 1559
aluminium chloride
effect of organic co-solvents on electrodeposition of Al from $[Me_3PhN][Al_2Cl_7]$ melts, **38,** 245
mixtures with 1-methyl-3-ethylimidazolium chloride: dissolution of Zn, **35,** 89
with Ph_3MeNCl or 1-methyl-3-ethylimidazolium chloride and ArCl or ArF co-solvents: reversible Al electrode, **37,** 1061
aluminium electrode see also aluminium
in chloroaluminates with aryl chloride and aryl fluoride co-solvents at room temperature, **37,** 1061
oxidizable substances formed during cathodic hydrogen evolution in NaCl aq, **35,** 1747
photocurrents at thin oxide films: photoemission at the Al/Al_2O_3 interface, **38,** 15
aluminium electrodeposition
calculations of local heat changes, **36,** 661
conductivities of Na_3AlF_6-Al_2O_3-(CaF_2)-(MgF_2) ternary and quaternary melts, **38,** 2165
effect of composition of TiB_2-C composite cathodes, **38,** 663
from cryolite baths: effect of added TiO_2 and B_2O_3, **37,** 1787
measurement of conductivities of electrolytes in a pyrolytic boron nitride tube-type cell, **38,** 589
recalculation of current efficiency for metal dissolution, **35,** 109
transference numbers and coefficients of suitable molten salt mixtures, **38,** 415
wetting properties of sintered TiB_2 electrodes in cryolite-alumina melts, **37,** 1395
aluminium hydride
formed during hydrogen evolution at Al cathodes in NaCl aq, **35,** 1747
aluminium magnesium oxide
effect of humidity on conduction mechanism in bulk and thin film $MgAl_2O_4$, **38,** 2617
aluminium nitrate
modification of fluorine-cell carbon anodes by impregnation with 0.5M aqueous solution and baking at 1000°C, **38,** 2413
aluminium oxide see also alumina
effect of water content on impedance of thin films on Al, **38,** 1957
growth kinetics for porous films on Al anodes in H_2SO_4 aq, **38,** 2351
amino acids
photoelectrochemical behaviour of Cu/0.3M K_2SO_4-0.01M $CuSO_4$-0.04M AA (AA = glycine, α-alanine or β-alanine), **38,** 2733
amino compounds, primary
radiotracer studies of adsorption at Pt electrodes [R], **35,** 919
3-amino-5-heptyl-1,2,4-triazole
inhibition of corrosion of Cu in 0.5M H_2SO_4 by formation of surface layers, **37,** 2299
p-aminophenol
reduction of nitrobenzene in a packed-bed reactor, **38,** 1753
N-aminopyrrolidin-2-ones
synthesis at Hg cathodes in aqueous ethanol, **35,** 1907
ammonia, liquid
permeation of electrogenerated hydrogen through Fe in, **36,** 283
solvent for cathodic syntheses of $K_2[M(CO)_5]$ where M = Cr, Mo or W, **35,** 1879
amorphous alloys see glassy metals
aniline
anodic polymerization by potentiostatic pulses in 0.5M H_2SO_4, **36,** 1579
effect of molecular mass of added poly(styrene sulphonate) on electrochemical polymerization, **36,** 357
electrosynthesis from nitrobenzene, azoxybenzene etc at Devarda alloy cathodes, **35,** 147
aniline film-covered Pt anodes
adsorption and oxidation of HCOOH, **35,** 1459
anode effect
influence of gas bubbles during discharge of F^- on carbon, **37,** 711
anodic films
the barrier layer/solution interface during breakdown of bismuth oxide, **38,** 511
mechanism of hydration and pore closure during hydrothermal treatment of porous alumina, **37,** 125
anodic stripping
of organic residues from adsorptions of various alcohols on Pt from 0.5M H_2SO_4, **36,** 2003
anodization
of Al in CrO_3-xH_2SO_4 aq, **35,** 955, 961

anodization continued
of Bi in glycol borate buffer [equimolar $(H_2CO)_4BH$-$(H_2CO)_4BNa$], **37,** 2415
of low-doped p-Si in NH_4F aq: nature of oxide layers, **37,** 865
of Si in aqueous acids, **36,** 1611
of valve metals: minimum time to reach a potentiostatic regime, **36,** 739
anodized aluminium
electroplating of Ag and Cu: effects of anions and alloy composition, **35,** 1019
anomalous-resonance X-ray scattering
study of local structure in $NiBr_2(PEO)_8$, **37,** 1663
anthracene
oxidation at Pt microcylinder anodes in MeCN-$TBAPF_6$, **36,** 1475
a spectroscopic and electrochemical study in 1-ethyl-3-methylimidazolium chloride-$AlCl_3$, **37,** 2615
antimonic acid
impedance of solid electrolyte between Pt or carbon electrodes, **35,** 1031
antimony
anodic behaviour in H_2SO_4 aq, **35,** 229, **36,** 2081, 2087, 2093
effect on the anodic behaviour of Pb in H_2SO_4 aq, **36,** 605
effect on kinetics of reduction of the PbO film on Pb-Sb alloy electrodes in H_2SO_4, **38,** 1131
area, active
correction for changes during potential scans, **35,** 1213
determined by weak electroluminescence during oxygen evolution, **36,** 1591
aryl halides
reduction and electroformylation at Cd-modified Au cathodes in DMF, **38,** 613
N-(arylthio)-2,4,6-triphenylanilino radicals
cyclic voltammetry at Pt in 0.1M TEAP-MeCN, **37,** 2095
ascending water electrode see water electrode
ascorbic acid
free radicals formed at Au anodes in aqueous buffers, **36,** 1649
kinetics of oxidation by electrogenerated $Fe(CN)_6^{3-}$, **36,** 203
oxidation at pyrolytic graphite RDE with linear scan of rotation rate and Pt ring, **35,** 1451
asymmetric induction
by β-cyclodextrin during reductions of acetophenones at Hg cathodes in alkaline media, **35,** 1149
by cyclodextrins in cathodic dimerization of acetophenone in DMF-$TBABF_4$, **36,** 1911
by magnetic fields during reduction of glyoxylic acid, **35,** 683
attenuated total reflection
IR spectroscopy using thin sputtered films of Au or Pt on Ge or GaAs IR-transparent crystals, **37,** 2321
Auger analysis
of surfaces of glassy metal anodes containing Ni, Mo and B, **35,** 1919
Auger spectroscopy
of alkali metals electrodeposited on Ag cathodes in alkaline media, **36,** 1947
angle resolved, of freshly-cut Li surfaces, showing accumulation of Na impurity, **37,** 731
of Au single-crystal faces before and after electrochemistry, **35,** 1383
of Cu-Au and Ag-Pd single phase alloys during anodic dissolution, **36,** 49
of passive films on AISI 304 stainless steel in borate buffers, **36,** 315
study of the Ce-Mo process for producing corrosion-resistant Al alloys, **37,** 2277
study of concentration dependence of UPD of Ag on Pt(111) surfaces, **38,** 235
of Ti surfaces passivated in H_2SO_4 aq containing molybdate ions, **36,** 2069
azides
hydrogenation to amines at Pt and Pd dispersed microparticles in poly(pyrrole-alkylammonium) films on carbon felt electrodes, **37,** 1261
azomethine derivatives
anodically oxidized to N-heterocyclics with cation radical mediators in MeCN-TEAP, **35,** 225
azoxybenzenes
redox behaviour of substituted 2-arylazoanthraquinones at Pt electrodes in benzonitrile, **36,** 927

B

band electrodes
novel fabrication of nanometer scale electrodes, **36,** 763
band gaps
of α-Cu_2Te, **38,** 1699
from photocurrent spectra of sputtered thin film Y-Ba-Cu-O electrodes, **35,** 1977
of thermally produced thin films of CdO, **38,** 2199
barium
incorporation into β"-alumina by ion exchange with molten salts, **36,** 563
barium fluoride
as an internal reflection element in IR-ATR spectroelectrochemistry at Au and Pt electrodes, **38,** 695
barrierless discharge
in the HER on Hg cathodes above 100°C in light and heavy water, **36,** 411
batteries
applications of generators with solid-state electrolytes, **37,** 1627
safety and reliability of Li/MoS_2 systems, **38,** 1193
benzalacetone
electrochemical behaviour and effect on electrodeposition of Zn from acid sulphate, **38,** 1351
benzaldehyde
effect of composite-plated PTFE on overvoltages for reduction at Ni cathodes, **37,** 353
electrocatalytic hydrogenation at cathodes of Pd electrodeposited on carbon felt, **37,** 365
reduction at Pd or Pt supported on carbon felt cathodes in 0.1M KOH or 0.1M H_2SO_4 in EtOH aq, **38,** 199
benzaldehyde dimethylacetals
ring-substituted, oxidation at RDE anodes of Pt, graphite and vitreous carbon in methanol, **37,** 1951
benzene
fluorination at Pt anodes in MeCN-$R_4NF.nHF$ and MeCN-$Et_3N.3HF$, **38,** 619
fluorination in liquid $R_4NF.mHF$ at Pt anodes (Me, Et or Pr, m>3.5), **38,** 1123
polymerization in $PhNO_2$-$LiAsF_6$-$CuCl_2$ to form thick poly(*p*-phenylene) films on Pt, **37,** 1093
benzimidazole
chelated with Cu(II): reductions in aqueous and propene carbonate media, **37,** 33
benzoate ion
effect on anodic dissolution and passivation of Fe in benzoate buffers, **37,** 489
benzo-15-crown-5-substituted N-methylpyrrole
synthesis and polymerization, **36,** 1377, 2197
benzohydroxamic acid derivatives
electrochemistry of Fe(II) and Fe(III) complexes at Pt in acetonitrile, **37,** 205
benzoic acid
hydroxylation by oxygen, catalysed by ions of dissolving metals, **37,** 345
benzonitrile
adsorption at Ag electrodes from 0.1M KCl aq, **36,** 1523
1,4-benzoquinone
electron-transfer mediator in a glucose sensor with a composite polypyrrole-glucose oxidase electrode, **37,** 1987
benzoquinone imines
N-aryl- and N-arylsulphonyl-substituted: reduction in acetonitrile and interaction with Hantzsch ester, **37,** 277
N-aryl- and N-arylsulphonyl-derivatives: $E°_{ox}$, $E°_{rd}$ and electron affinities, **36,** 1219
reductions of 1,4-benzoquinone monoimine derivatives in acetonitrile, **35,** 1933
benzo(*b*)selenophene and dibenzo(*b,d*)selenophene
oxidations at Pt or vitreous carbon anodes in 0.1M $LiClO_4$-MeCN, **37,** 1453
benzothiazole derivative
anodic oxidation and inclusion complexes with cyclodextrins, **37,** 149
benzotriazole
effect on naturally grown oxide layers on Cu in aqueous sodium acetate, **38,** 1471
1H-benzotriazole
effects on hydrogen adsorption and absorption at Pd overlayers on Au(111) and Au(100) single-crystal electrodes, **38,** 2145
benzotriazoles
complexation and adsorption on Cu electrodes in aqueous sulphates, **35,** 1011

benzoyloxiranes
reduction at Hg cathodes in 0.1M $TBABF_4$-MeCN, **37,** 1247
benzyl alcohol
indirect anodic oxidation by a monooxoruthenium(V) complex immobilized in Nafion films, **37,** 2645
benzylmethylethers
ring-substituted, oxidation at RDE anodes of Pt, vitreous carbon and graphite in methanol, **37,** 1951
2-benzylthio-6H-1,3-thiazines
reduction at Hg and carbon cathodes in acetate buffers, **35,** 805
Bicuvox.10
conductivity and thermal analysis of $Bi_4V_2O_{11}$ in which 10% of V ions are substituted by Cu, **38,** 969
bifurcation analysis
of instability during anodic dissolution of Fe in H_2SO_4, **36,** 1301
bifurcation behaviour
in the cyclic voltammetric oxidation of lower alcohols in alkaline solutions at Pt anodes, **38,** 519
bifurcation theory
electrochemical instability arising from negative faradaic impedance, **37,** 1771
bilayer membrane
ITO/Nafion[$Ru(bpy)_3^{2+}$]/Nafion[MV^{2+}]/ITO (MV = methylviologen): reduction of MV ion by photoexcited Ru complex, **38,** 1093
bilayers
Pt/poly(2,2'-bithiophene)/poly(xylylviologen)dibromide: transient spectroelectrochemical studies of charge trapping, **37,** 1887
biliverdin
electrode kinetics of oxidation to purpurin at Pt anodes in DMF-TBAP: thin-layer spectroelectrochemistry, **38,** 257
biological sensors
polypyrrole as a conductive polymer matrix: preparation in presence of biological buffers, **37,** 1015
bipyridyl
chelated with Cu(II): reductions in aqueous and propene carbonate, **37,** 33
2,2'-bipyridine derivatives
reductions of new tetradentate ligands at Hg cathodes in DMF-TEAP, **36,** 1997
tris(2,2'-bipyridine) ruthenium (II) cation
enhancement of electrochemiluminescence in MeCN-$TBABF_4$ and in aqueous oxalate by ultrasound, **38,** 307
tris(2,2'-bipyridyl) osmium(II/III)
incorporation into thin poly(styrene sulphonate) coatings on glassy carbon anodes: mediated oxidations, **38,** 1321
4,4'-bipyridyl
adsorption at Au electrodes in acidic and neutral media, **35,** 591
4,4'-bipyridyl disulphide
as a modifier of Au electrodes: adsorption of cytochrome *c* from phosphate buffer solutions, **37,** 403
bismuth
electrodeposition and UPD at Pt, Au and Pd cathodes: ellipsometric study, **37,** 2245
impedance studies of filmed anodes in glycol borate buffer [equimolar $(H_2CO)_4BH$-$(H_2CO)_4BNa$], **37,** 2415
kinetics of anodic oxidation in glycol-borate electrolyte, **38,** 1061
and Pb-Bi alloy cathodes: hydrogen evolution from H_2SO_4 aq, **37,** 269
bismuth oxide
the barrier layer/solution interface during breakdown of anodic films, **38,** 511
behaviour in a carbon paste electrode in 10M KOH, **36,** 1561
impedance studies of filmed Bi anodes in glycol borate buffer [equimolar $(H_2CO)_4BH$-$(H_2CO)_4BNa$], **37,** 2415
δ-bismuth oxide stabilized by erbia
oxygen transfer studied by impedance spectroscopy, DC polarization and ^{18}O exchange, **38,** 1817
bismuth oxyhalide films
photoelectrochemical properties of BiOX formed on Bi film anodes, **35,** 1941
bistable behaviour see also instability
in cyclic voltammograms for oxidations of HCOOH, $HCOO^-$, ethanol, propanol and butanol at Pt, **37,** 673
bisulphite ions
oxidation at graphite anodes, **36,** 1073
boriding
of Fe cathodes in molten sodium tetraborate, **36,** 41

borohydride
activation of a hydrogen storage alloy: misch metal-$Ni_{3.6}Mn_{0.4}Al_{0.3}Co_{0.7}$ in porous Ni substrate, **38,** 659
boron
electrodeposition from LiF-NaF-KF eutectic at 700°C, **37,** 237
boron-substituted carbon
as a negative electrode in secondary lithium cells, **38,** 1179
breakdown of passivity
on Fe in alkaline media: effects of Cl^-, Na^+ and Ca^{2+}, **35,** 1437
break-point method
for determination of reactive area of coated metals, **38,** 1609
of determining the defect area of coated metals, **38,** 1945
bromate ion
current oscillations during potentiostatic oxidation at Hg anodes, **35,** 1095
bromide ions
adsorption at Hg electrodes from propene carbonate solutions, **36,** 1971
bromine/polybromide electrode
electrode kinetics at Pt, **36,** 1403
2-bromoisobutyramides
kinetics of protonation of electrogenerated carbanions, **35,** 81
bronzes
intercalation of precipitated $Na_{1+x}V_3O_8$, by Li^+, **36,** 1549
cycling performances of $Na_{1+x}V_3O_8$ in secondary lithium cells, **37,** 63
bubble formation
under conditions of lowered gravity during water electrolysis at Au electrodes, **38,** 729
bubble size
of hydrogen and oxygen gases in narrow-gap electrolysis cells, **38,** 1381
butanediols
adsorption and oxidation at Au electrodes in aqueous media, **35,** 1345

C

cadmium
anodic behaviour in dilute aqueous alkali, **37,** 665
corrosion in aerated sulphate solutions at 1<pH<6, **37,** 2611
electrodeposited on Au cathodes: reduction and electroformylation of aryl halides in DMF, **38,** 613
electrodeposition from citrate solutions: role of chelate formation, **37,** 631
electrodeposition on Pb in 5M H_2SO_4 aq, **35,** 577
formation and reduction of anodic films in NaOH aq, **35,** 605
potentiometric stripping analysis and speciation in environmental studies, **38,** 807
recovery by electrodeposition from waste solutions containing Fe(III), **38,** 2181, 2191
solvent effects on kinetics of electrodeposition at Hg cathodes, **38,** 721
UPD on polycrystalline Ag, **36,** 1873
UPD on polycrystalline Pt cathodes: effect on oxygen reduction in acidic and neutral media, **37,** 2559
cadmium chloride
diffusion coefficients in water at various concentrations, **35,** 1433
reduction at W cathodes in LiCl-KCl eutectic, **35,** 1201
cadmium electrode
adsorption of thymine at the (0001) basal face: condensed 2-dimensional film behaviour, **37,** 2369
cadmium-glycine complexes
determination of stability constants at Hg microelectrodes, **37,** 1413
cadmium ions
mechanism of polarographic discharge through surfactant monolayers, **35,** 1805
cadmium mercury telluride
current oscillations at anodes in basic solutions of Cs^+ and S^{2-}, **36,** 869
cadmium oxide
characterization of thermally produced thin films by electrolyte electroreflectance and photoelectrochemical measurements, **38,** 2199
hydration, thickness and formation potential of anodic layers, **35,** 605

cadmium selenide electrode
crystallization of Tl_2O_3 from 0.1M NaOH aq containing Tl(I): grain, crystal face and light effects, **37,** 1429
cadmium selenide-cadmium sulphide solid solutions and mixed crystal semiconductor electrodes
photoelectrochemical etching, **38,** 593
cadmium sulphide
deposition at Pt and ITO cathodes from aqueous solutions of Cd^{2+} and $S_2O_3^{2-}$ at 90°C, **38,** 2395
film with Prussian Blue battery in a photochargeable multilayer device, **35,** 291
films on Cd anodes in alkaline Na_2S aq: photoelectrochemical and semiconductor properties, **37,** 1371
photochemical decomposition of HCOOH aq at platinized sintered pellets, **36,** 153
photoelectrochemical behaviour in electrochromic display devices, **38,** 2759
potential-dependent electrolyte electroreflectance, **37,** 957
calcium β"-alumina
preparation, properties and application as a solid electrolyte, **38,** 365
calcium iodide
ion transport in PVC membranes containing dioctylphenyl phosphonate, **38,** 2373
calcium ion
selective membranes based on the ETH1001 ionophore in poly(vinyl chloride), **37,** 2691
calcium ions
adsorption at Pt electrodes induced by adsorbed anions and molecules, **36,** 1453
sorption into copper(II) hexacyanoferrate films, **35,** 811
calorimetry
of anodic intercalation of MnO_2 by Li^+, **36,** 489
study of first-order phase transitions in Li_xMnO_2, **36,** 1469
camphorquinone
reduction at Hg cathodes in aqueous media: product adsorption, **38,** 2217
reduction at Hg and Pt cathodes in aqueous and MeCN solutions, **38,** 2209
cancer cells
killed by TiO_2 powder excited by UV radiation, **38,** 153
capacitance
classification based on mean-field analysis, **36,** 1685
distinction between double-layer- and adsorption pseudo-capacitances for intermediates in faradaic reactions, **37,** 2145
influence of adsorption parameters on the form of *C vs E* curves, **37,** 1273
capacitance studies
of adsorption of $C_{12}H_{25}(OC_2H_4)_xOH$ (x = 4, 8 or 12) at water/nitrobenzene interface, **36,** 1437
of adsorption of DMSO at the Hg/H_3PO_4 interface, **35,** 1901
of adsorption of Forafac ionic perfluorinated surfactants at Au electrodes, **38,** 2203
of adsorption of imidazole from aqueous solutions at a Au electrode, **38,** 947
of adsorption of methylpyridines at Hg electrodes, **38,** 1585
of adsorption of non-ionic surfactants at Au electrodes in Na_2SO_4 aq, **37,** 2377
of adsorption of *p*-toluene sulphonate anions at the polycrystalline Au/aqueous solution interface, **37,** 75
of adsorption of phosphonium cations at a stationary Hg electrode, **37,** 2447
of adsorption of polyacrylamide at Au and mild steel from aqueous acids, **36,** 1315
of adsorption of terminal and vicinal aliphatic diols at Au electrodes from 0.02M $NaClO_4$ aq, **38,** 717
of adsorption of thiourea and anions at Ag electrodes, **35,** 879
of adsorption of thiourea at polycrystalline Ag in methanolic KOH, **36,** 965
of adsorption of thymine at the (0001) basal face of Cd single-crystal electrodes: condensed 2-dimensional film behaviour, **37,** 2369
of adsorption of thymine at the (111) face of Ag single-crystal electrodes, **37,** 2373
of adsorption of trioctylphosphine oxide at Hg, **35,** 379
of adsorption of uracil at Hg electrodes from aqueous phosphate buffer pH8, **37,** 2663
of adsorptions of quinine and flumazenil at Hg electrodes, **35,** 1311
of Au (100) surfaces reconstructed in dilute aqueous acids, **37,** 615
by current-step method for area corrections in electrode kinetics, **35,** 1213
of cathodic reduction of 4,4'-dinitrodibenzyl in EtOH-H_2O, **37,** 1993, 2001, **38,** 471
of ClO_4^- adsorption at the $Hg/HClO_4$ aq and $Hg/HClO_4$-TEAP aq interfaces, **37,** 1753
of effect of annealing on flat-band potential of p-Si in acetonitrile, **37,** 2791
of effect of Cl^- on Ni electrodes in 0.75M Na_2SO_4 aq, **37,** 2437
of effect of ionic strength on rate of adsorption of albumin on vitreous carbon electrodes, **36,** 1811

capacitance studies continued
of frequency dispersion for passive AISI stainless steel in various aqueous and ethanolic electrolyte solutions, **38,** 1615
of the Hg/KCl aq interface from 25 to 300°C, **38,** 1761
of Ni (111), (100), (110) and (210) crystal faces in 0.1M KOH aq at low hydrogen overvoltages, **38,** 2129
of p-GaAs electrodes with thin electrodeposits of Au, **38,** 301
and piezoelectric PZC measurements of Au in NaF aq, **37,** 139
of polyaniline film electrodes, **38,** 2503
of the redox mechanism of poly(3-methylthiophene), **37,** 1417
of specific adsorption of solvent at solid metal electrodes (Cu, Ag, Cd), **36,** 859
to find PZCs for gold {111}, {311}, {110} and {210} surfaces in 0.01M NaF aq, **35,** 1383
transient, of p-Si following removal of anodic polarization in NH_4F aq, **37,** 865
carbanion
cathodic coupling of glucosyl species with acrylonitrile or resorcinol, **36,** 1095
carbanions, electrogenerated
protonation by their parent secondary 2-bromoisobutyramides, **35,** 81
reactions with methoxy-iminium cations, **36,** 819
carbide electrodes
anodic behaviour of WC containing 10 volume % of a metal (Fe, Co or Ni) in H_2SO_4 aq, **37,** 447
oxidation of H_2 in acidic media on bulk and C-supported W-(Mo)-C, **36,** 1543
carbohydrates
oxidation at Cu anodes in aqueous alkali, **37,** 1187
carbon
in Leclanche cells: variation of ESR signal during discharge, **38,** 2511
a new preparation of highly dispersed Pd catalyst, **38,** 2333
carbon blacks
oxidation in hot H_3PO_4 and physicochemical properties, **36,** 1931
carbon dioxide
cathodic reductions on various metal phthalocyanines, **36,** 1309
cathodic replacement of -S(O)Me in PhCH=C(SMe)S(O)Me in DMF, **36,** 1341
formation of CO during reduction at Ni cathodes, **35,** 1777
reactions with radical anions, generated from phenazine at glassy carbon or edge-plane graphite cathodes in 0.1M TBAP-DMSO, **35,** 1405
reactions with radical anions, generated from quinones at glassy carbon or edge-plane graphite cathodes in 0.1M TEAP-DMSO, **35,** 1399
reduction at Cu cathodes in methanol containing benzalkonium chloride at low temperatures, **38,** 2177
reduction at Ni cathodes from aqueous phosphate buffers, **38,** 1391
reduction to CH_4 and C_2H_4 at Cu cathodes in 0.5M $KHCO_3$: on-line MS study, **35,** 771
carbon dioxide-dimethylamine addition compound: properties of a new electrolyte for organic electrosynthesis, **35,** 769
carbon electrodes
discharge of F^- in molten NaF and in molten cryolite, **37,** 705
effect of CO_2 on stability of gas-diffusion electrodes, **35,** 945
effect of crystal structure on suitability as negative electrodes in secondary lithium cells, **38,** 1179
for fluorine cells: modification by impregnation with 0.5M $Al(NO_3)_3$ aq and baking at 1000°C, **38,** 2413
influence of content of Pt catalyst on corrosion of oxygen cathodes in phosphoric acid cells, **37,** 2725
influence of gas bubbles on anode effect during discharge of F^-, **37,** 711
lowering fluorine overvoltage by adding AlF_3 or LiF to KF.2HF melts, **35,** 153
as negative electrodes in secondary lithium cells [R], **38,** 1221, 1233
as negatives in secondary lithium batteries, **38,** 1169
porous: cathodic passivation during reduction of $SOCl_2$-$LiAlCl_4$, **38,** 827
primary film in $LiAlCl_4$-$SOCl_2$, **37,** 1207
for vanadium redox flow batteries, **36,** 1191
carbon felt electrodes
electrodeposited with Pd: electrocatalytic hydrogenation of benzaldehyde, **37,** 365
with electrodeposited poly(pyrrole-alkylammonium) films containing Pt and Pd microparticles: azide hydrogenation, **37,** 1261
mass transfer coefficients assuming plug-flow conditions, **36,** 339
mass transfer studies using hexacyanoferrate and Hg(0/II) couples, **35,** 1369
as supports for Pd and Pt electrocatalysts: cathodic reductions of acetophenone and benzaldehyde, **38,** 199

carbon fibre electrodes
anodic formation and electrochemical properties of polyaniline films in aqueous methanol, **38,** 1559
behaviour of microelectrodes, dip-coated in isopolymolybdic acid, **37,** 1859
microelectrode with a polyaniline film doped with isopolymolybdate anions, **38,** 1029
pitch-based, reversible intercalation of Li^+ from 1M $LiClO_4$-PC, **38,** 1721
carbon fibres
controlled spatial distribution of noble metal catalysts on activated supports, **38,** 793
carbon monoxide
adsorbed at Ni cathodes during reduction of CO_2 from aqueous phosphate buffers, **38,** 1391
adsorbed at Pt electrodes: three types from methanol, HCOOH and reduced CO_2, **37,** 2361
adsorbed on Pt electrodes: quantum chemistry and *in situ* FTIR spectral studies of potential-dependent properties, **38,** 1107
adsorption at Ni electrodes: inhibition of HER and anodic dissolution of Ni, **35,** 1777
co-adsorption and adsorbate competition involving other organic residues, **36,** 2183
effect on Cu(I/II) redox kinetics at a W electrode in molten 1-methyl-3-ethylimidazolium chloride-$AlCl_3$, **38,** 927
formation at Ni cathodes during reduction of CO_2, **35,** 1777
key role in catalytic anodic oxidation of small organic molecules [R], **35,** 691
oxidation at Pt(111) anode surfaces in 0.05M $HClO_4$ aq, **36,** 555
potential oscillations during simultaneous oxidation with H_2 at Pt anodes, **36,** 639
role in the oxidation of HCOOH at Pt anodes, **37,** 37
thermal desorption spectrometry applied to RuO_2-IrO_2- and RuO_2-TiO_2-coated Ti electrodes, **37,** 1029
carbon paste electrodes
analysis and electrochemical behaviour of Pd compounds related to automotive catalytic converters, **37,** 2491
behaviour of CuO, Cu_2O and $YBa_2Cu_3O_7$ in 10M KOH aq, **36,** 1209
behaviour of lead oxides in 0.1M NaOH aq binder, **36,** 277
behaviour of $NaBiO_3$ and Bi_2O_3 in 10M KOH aq, **36,** 1561
electrochemical behaviour of automotive catalytic converters: analysis of Pt, Pd, Pb and Fe, **37,** 2009
electrochemical behaviour of copper selenides, **37,** 1321
reactions of Rh compounds in various media, **38,** 1331
reduction of Na_2SeO_3 in H_2SO_4 aq, **37,** 1165
reductions of Pt(II) and Pt(IV) and oxidations of Pt(II) and Pt black in aqueous acids, **37,** 507
reduction of silver chromate in HCOOH and MeCOOH, **36,** 1505
use of silicone oil instead of Nujol oil in methanolic media: behaviour of phenothiazine derivatives, **37,** 1355
carbon paste electrode, modified by zeolite incorporating methyl viologen
effects of support electrolyte and immersion time in aqueous media, **38,** 2257
ion exchange between MV^{2+} and Na^+ of the zeolite, **38,** 2267
carbon-polymer composite electrodes
in secondary zinc-iodine cells with cation-exchange membranes, **35,** 255
carbon steel
passivity and breakdown in 0.5M $LiAsF_6$-1,2-dimethoxyethane, **38,** 881
carbonyl compounds
acetoxylation of ketones by electrogenerated $Pb(OAc)_4$, **36,** 1165
asymmetric induction by β-cyclodextrin during reductions of acetophenones at Hg cathodes in alkaline media, **35,** 1149
cathodic reductions of 1,3-cyclobutanediones, **36,** 465
comparative reductions of acetophenone and benzaldehyde at Pt and Pd supported on carbon felt cathodes, **38,** 199
oxidation of cyclic 1,3-diketones at PbO_2, Pt and carbon anodes in acid, **36,** 597
reduction of *o*-substituted aromatic ketones to nitrogen heterocyclics, **36,** 2019
carbonyl compounds, aromatic
effect on surface morphology and crystal orientation of Sn electrodeposits from $SnSO_4$ aq, **37,** 2403
carbonylmetallates
reactions of the type $M(CO)_6 + 2e^- \rightarrow CO + [M(CO)_5]^{2-}$ in liquid ammonia, **35,** 1879
catalysis
by RuO_2 Adams catalyst, of oxidation of water to oxygen by Ce(IV), **37,** 1217
catalytic converters, automotive
analysis and electrochemical behaviour of Pd compounds in carbon paste electrodes, **37,** 2491
electrochemical behaviours in carbon paste electrodes, **37,** 2009

catalytic polarographic prewaves
of Ni(II) in presence of SCN^-, **36,** 2119
of Ni(II) in presence of thiourea, **36,** 297, 2119
catalytic reactions, homogeneous
steady-state measurements of pseudo-first- and second-order processes at ultramicrodisc electrodes, **37,** 2695, 2701
catechol see 1,2-dihydroxybenzene
cathodic isomerization
Z→E conversions of some Z 1,2-diarylsulphonyl phenylethenes, **37,** 2467
cellulose acetate
porous films used to bind algae to vitreous carbon electrodes, **35,** 1377
cementation kinetics
of Ag at fixed and rotating planar Cu electrodes in 4.3M NaCl aq, **37,** 1779
enhancement by superimposed cathodic conditions, **35,** 657
cemented carbides
[(Ta, Nb)C, M] where M = Fe, Ni or Co: anodic behaviour in 0.5M H_2SO_4, **37,** 2523
ceramic oxide electrodes [R], **36,** 225
cerium(III) ions
oxidation affected by the presence of oxide on Pt anodes, **35,** 273
cerium(IV) ion
oxidation of water to oxygen in aqueous acids using a RuO_2 Adams catalyst, **37,** 1217
cerium(IV) oxide
modification of RuO_2-TiO_2 electrodes: preparation, voltammetry and stability, **37,** 2511
cesium
hydration or reaction with water co-adsorbed on Cu(110) from the gas phase, **36,** 1883
cetyl alcohol
inhibition of electron transfer by an adsorbed layer, **36,** 421
chalcopyrite photocathode
non-linear and pulse phenomena in hydrogen peroxide reduction, **38,** 115
charge density
effect on second harmonic generation at the metal/electrolyte interface, **36,** 1835
charge trapping
in the Pt/poly(2,2'-bithiophene)/poly(xylylviologen)dibromide bilayer: transient spectroelectrochemical studies, **37,** 1887
charge-transfer complexes
in chemical oxidations and reductions of organic compounds, **36,** 2171
of bis(ethenedithio)-tetrathiofulvalene with trihalide ions: effects of solvent on electrosynthesis, **38,** 2343
of iodine and dialkyl sulphides, **35,** 355
charge-transfer reactions
chemisorption of intermediates in anodic metal oxidations consisting of two successive steps, **38,** 487
experimental determination of dynamic structural parameters, **36,** 1775
solvent effects on interfacial redox and amalgam-formation reactions, **36,** 1767
charge-transfer resistance
expressed as position-dependent resistivity within a crystal, **38,** 1975
chemical dissolution
of n-ZnO: electrochemical measurement of rate, **37,** 827
chemisorption see also adsorption
of an intermediate in electrocatalytic reactions: relations between reaction orders and Tafel slopes, **37,** 51
of halogen atoms (F, Cl and Br) at Ag(111) and of CO at Cu(100) and Pd(100): cluster models, **36,** 1669
of intermediates in anodic metal oxidations consisting of two successive charge-transfer steps, **38,** 487
of intermediates in faradaic reactions: distinction between double-layer- and adsorption-capacitances, **37,** 2145
of methanol at Pt(110) in 0.1M Na_2CO_3 aq, **37,** 1883
of sulpholane and of DMSO at Pt electrodes in 0.5M H_2SO_4 aq, **38,** 175
of three types of CO on Pt electrodes: from methanol, HCOOH and reduced CO_2, **37,** 2361
of 1,1,1-trichlorethane at Pt electrodes in H_2SO_4 aq: on-line mass spectrometry, **38,** 281
chlor-alkali cells
gas bubble formation in stagnant electrolyte in narrow-gap cells, **38,** 1381

chlorate manufacture
effects of added chromate on hydrogen evolution at Fe cathodes and on Fe oxidation in hydroxide and chlorate solutions, **37,** 1873
identification of the layer of reduced chromate on the cathode, **36,** 1605
reduction of chromate at Pt and Au cathodes in 1M NaOH aq, **36,** 1985
chloride ion oxidation
at Pt anodes in aqueous media: effect of pre-polarization in nitromethane solutions, **38,** 1097
chlorine cell cathodes
reduction of cell voltage by use of a membrane-electrode composite, **38,** 2431
chlorine cells
behaviour of gas bubbles in narrow-gap cells, **38,** 1705
chlorine evolution
at Ru-Ti anodes in acidic media, **36,** 19
impedance studies of $Ru_{0.2}Ti_{0.8-x}Sn_xO_2$ ternary oxide electrodes in 1M NaCl aq, **38,** 2239
on Ir- and Rh-implanted Ti anodes, **38,** 1313
on rotating Pt thin-ring anodes in acidic aqueous chloride solutions, **37,** 2715
chlorine gas sensor
redox mechanisms at Ag/Ag-β"-alumina/$AgCl/Cl_2$ interface, **36,** 1823
chloroaluminate
primary film on vitreous and porous carbon electrodes in $LiAlCl_4$-$SOCl_2$, **37,** 1207
surface film on Li electrodes in $LiAlCl_4$-$SOCl_2$, **37,** 1211
chloroplast
from spinach leaves: photocurrents at potentiostatic Pt electrodes in media containing oxygen and photosystem I submembrane fraction, **37,** 2581
chlorosilane derivatives
polymerization at Pt cathodes to polysilanes, **36,** 621
chlorotrifluoroethene
synthesis at Ni cathodes in MeOH-H_2O-NH_4Cl, **35,** 1727
chromate conversion coatings
replacement for the Ce-Mo process for corrosion resistance in Al alloys, **37,** 2277
chromate ions
effects on hydrogen evolution at Fe cathodes and on Fe oxidation in OH^- and ClO_3^- solutions, **37,** 1873
X-ray diffraction study of di- and tri-chromate species in Cr electrodeposition solutions, **37,** 1239
chromate layer
mechanism of formation at Zn electrodes, **35,** 515
chromate reduction
characterization of $Cr(OH)_3$ films on Au and Pt cathodes in chlorate cell electrolytes, **36,** 1605
inhibiting properties of the cathodic film on Au and Pt in 1M NaOH aq, **36,** 1985
chromate-phosphate conversion coatings
on AlMn05Mg05 alloy, characterization by impedance and optical measurements, **38,** 2577
chromium see chromium electrode
chromium(II) chloride
thermodynamic properties of solutions in LiCl-KCl and LiCl-KCl-$BaCl_2$ eutectics from EMF data, **37,** 1445
chromium(II) complexes
with polyaminocarboxylate ligands: organic reduction mediators and phase transfer, **37,** 575
chromium(III)
oxidation: electrocatalytic activities of anode materials, **38,** 437
re-oxidation to Cr(VI) and recycling using supported liquid membranes, **38,** 847
chromium(III) chloride
thermodynamic properties of solutions in LiCl-KCl and LiCl-KCl-$BaCl_2$ eutectics from EMF data, **37,** 1445
chromium (II/III) couple
cyclic voltammetry in HCl aq at graphite, partly covered with Sn catalyst, **36,** 1129
chromium electrode
effects of solution composition on passivity in H_2SO_4 aq, **38,** 2309
electrodeposition: X-ray diffraction study of di- and tri-chromate ions, **37,** 1239
mechanisms of anodic dissolution, **38,** 643
passivation in concentrated aqueous and non-aqueous solutions of H_2SO_4, **37,** 1069
photoelectrochemical behaviour of the passive film in H_2SO_4 aq, **35,** 445
SERS study of passive films in aerated 0.15M NaCl aq, **37,** 2747

chromium electrode continued
studies of the passive films in 0.5M H_2SO_4 aq by potential-modulated ellipsometry and impedance spectroscopy, **38,** 1969
chromium hydroxide
film formed at Pt and Au cathodes in a chlorate cell electrolyte, **36,** 1605
inhibiting properties of the cathodic film on Pt and Au in 1M NaOH-chromate, **36,** 1985
chromium oxides
comparison of Cr_8O_{21} and $LiCr_3O_8$ behaviours towards the insertion of Li^+, **36,** 127
insertion of Li^+ into $AgCr_3O_8$, **38,** 1211
chronocoulometry, potential-step
measurement of surface excesses of quinine and flumazenil at Hg electrodes, **35,** 1311
study of adsorption, diffusion and CMC of a redox surfactant, **35,** 885
chronopotentiometry
EC mechanisms at the DME studied using an $I = I_0 t^q$ perturbation, **35,** 95
cinchonidine
electrochemical transfer across the aqueous/1,2-dichloroethane interface, **38,** 2707
cinnamaldehyde
electrochemical behaviour and effect on electrodeposition of Zn from acid sulphate, **38,** 1351
circular regression analysis of impedance data at solid polymer electrolytes, **36,** 1033
citric acid
anodic behaviour of Sn in 0.5M aqueous solution, **37,** 143
effect of presence in solution on electrodeposition of Cu, **37,** 2497
clathrates
double-layer properties of acid hydrates studied with the frozen-electrolyte technique, **37,** 565
cluster calculations
of electronic properties of CN^- adsorbed at Ag electrodes, **37,** 211
cluster compound
electrochemistry and spectroelectrochemistry of trinuclear ruthenium acetate with pyridine and DMSO ligands in MeCN, **38,** 975
cluster models
for adsorptions of Br, Cl and F at Ag(111) and of CO at Cu(100) and Pd(100), **36,** 1669
clusters
growth kinetics of Ag and Ag-Hg clusters at Pt cathodes, **38,** 535
reactions of Ag particles formed by reduction of Ag^+ ions in presence of polyanions, **36,** 1743
coated metals see also painted metals and polymer-coated metals
containing distributed holes allowing electrolyte penetration: impedance, **37,** 997
delamination of epoxy-polyamine coatings under cathodic protection conditions, **36,** 1915
determination of reactive area: physical meaning and limits of the break-point method, **38,** 1609
effect of roughness on impedance behaviour, **38,** 1867
equivalent circuits for polymer-coated steel and anodized Al alloys and composites: growth rates of corrosion pits, **38,** 1891
impedance spectroscopy of corrosion-resistant fluoropolymer layers on low-carbon steel, **38,** 1945
impedance studies of cathodic degradation of Al metallizations of Si substrates, **38,** 1877
impedance studies of impact-induced corrosion of car bodies, **38,** 2083
impedance studies of polymer and conversion coatings, **35,** 1533
impedance studies used to distinguish between coating porosity and wetted metal area, **38,** 1799
protection of steel by Zn-rich ethyl silicate paint in artificial seawater, **38,** 2029
relationship between adherence of paint films and protection they offer to carbon steel from corrosion in 10^{-3}M NaCl, **38,** 1999
cobalt
current oscillations induced by I^- during pitting corrosion in H_2SO_4 aq, **38,** 835
electrocrystallization mechanism, **38,** 1783
mechanism of deposition of Fe-Co alloys on vitreous carbon cathodes from sulphate baths pH4, **38,** 671
cobalt(II) bromide
conductivities of complexes in poly(tetramethyleneglycol) and poly(ethane-1,2-diol) oligomers, **37,** 1695
cobalt complex, anionic
incorporated into oxidized polypyrrole film electrodes: oxygen reduction electrocatalyst, **37,** 763
cobalt complexes
binuclear, ethyne-bridged: preparation and electrochemical properties, **38,** 1527

cobalt dibenzotetraazaanulene
oxidation of thin films on Pt anodes in 0.1M $LiClO_4$-MeCN, **38,** 907
cobalt(II) hexacyanoferrate
films on glassy carbon electrodes: impedance studies, **38,** 379
films on Pt or vitreous carbon electrodes: preparation and behaviour, **36,** 147
cobalt-nickel spinels
oxygen evolution on $Ni_xCo_{3-x}O_4$ ($0.6<x<1.3$) in alkaline solutions, **38,** 2247
cobalt oxide
semiconducting and electrocatalytic properties of sputtered films, **35,** 975
cobalt oxide electrode
anodic oxygen evolution from aqueous alkali, **35,** 437
physical electrochemistry of ceramic oxides [R], **36,** 225
cobalt oxides
electroreduction of anodically-formed layers in carbonate buffers, **36,** 2147
cobalt phthalocyanine, tetrasulphonated
adsorbed at Pb or graphite cathodes for oxygen reduction in DMF, **35,** 173
adsorption at vitreous carbon electrodes, **36,** 2165, **37,** 769
cobalt tetrakis(4-trimethylammoniumphenyl)porphyrin
catalysed reduction of dithiodipropionic acid at glassy carbon cathodes, **37,** 2591
cobalt tetraphenylporphyrin
catalysis of reductions of 1,2-dibromoethane and tetrabromoethane at Pt ultramicroelectrodes in 0.1M TEAP-DMF, **38,** 1345
oxidation of thin films on Pt anodes in 0.1M $LiClO_4$-MeCN, **38,** 907
pyrolysed: ESCA and electrochemical studies, **37,** 187
pyrolysis of films sublimed on to carbon black surfaces: oxygen reduction catalyst, **38,** 2493
cobaltocene
effect of solvent on differences between oxidation and reduction potentials, **36,** 435
co-enzymes
polarographic reductions of NAD and NADP in aqueous acid, **35,** 753
Cole-Cole plots
for thin oxide layers on pure Al: effect of their water content, **38,** 1957
colloid stability
Monte Carlo simulations of interactions between charged surfaces in electrolytes, **36,** 1723
colloidal metals
reactions of Ag clusters, **36,** 1743
colloids
calculated interactions between a pair of arbitrarily shaped particles, **36,** 1757
counterion binding in solvation shells of ionic colloids, **36,** 1761
electrical double layer around an isolated spherical macroion, **36,** 1747
complex see also crown ether complexes and cryptates
La(III)-alizarin complexone: effect of F^- on reduction mechanism, **35,** 1861
Ni(II)-2,2'-bipyridine: transfer between nitrobenzene and water, **35,** 1965
of nickel ions with bypyridyl: electrochemistry in acetonitrile, **38,** 2515
nickel(II/III) cyclam grafted to polypyrrole and polythiophene, **36,** 15
$[Os(2,2'\text{-bipy})_2(PVP)_nCl]Cl$ films on vitreous carbon electrodes: charge-transfer dynamics, **37,** 159
of pyridine and DMSO with ruthenium acetate clusters: electrochemistry in MeCN, **38,** 975
reduction of Ni(II) salophen at Hg electrodes in DMF, **37,** 113
cis-$[Ru(L)(Cl)(O)]^{2+}$ [L = N,N'-dimethyl-N,N'-bis(2-pyridylmethyl)-1,2-diaminoethane] catalyst for MeOH oxidation, **38,** 1015
complexes
citrate chelates of Cd: effect on electrodeposition of Cd, **37,** 631
of copper ions with cysteine: reduction at Hg cathodes, **35,** 47
of copper ions with glycine, α-alanine or β-alanine; photoelectrochemical behaviour at the interface between aqueous solutions and Cu, **38,** 2733
copper(II) mixed ligand chelates containing β-keto enols and 1,2-diamines: substituent effects on electrochemical behaviour, **38,** 2623
of Cr(II) with EDTA and other polyaminocarboxylate ligands: mediators in organic cathodic reductions, **37,** 575
of Cu with citric acid, nitrilotriacetic acid and EDTA: electrodeposition of Cu, **37,** 2497
of Cu ions with Cl^- in ethan-1,2-diol-water mixtures, **38,** 2291

complexes continued
of Cu(I) and Cu(II) with histidine in aqueous solutions pH6, **38,** 165
of Cu(II) chelated with benzimidazole, phenanthraline or bipyridyl: reductions in various electrolytes, **37,** 33
of Cu(II) and glycine: cathodic deposition of Cu in aqueous solution, **37,** 745
of Cu(II) with L-hydroxyproline and D-allohydroxyproline: dissociation kinetics, **36,** 109
of Cu(II) with L-isoleucine and L-isoleucinate, **35,** 999
of Cu(II) with tris(hydroxymethyl)aminomethane: voltammetric behaviour, **38,** 957
CV and RDE studies of acetylacetonato lanthanide(III) tetraphenylporphyrinates in 0.1M TEAP-DMSO, **38,** 689
of α-, β- and γ-cyclodextrins with ferrocene and its mono- and di-carboxylic acids, **37,** 1939
of cytochrome *c* with Cu(II), Zn(II) and Pb(II), **35,** 473
determination of stability constants using a Hg microelectrode in the steady state, **37,** 1413
of 2,9-dimethyl-1,10-phenanthrolines with Cu^{2+} adsorbed at graphite: catalysis of reductions of oxygen and H_2O_2, **38,** 2423
of Fe(II) and Fe(III) with N-phenylbenzohydroxamic acid and N-methylbenzohydroxamic acid, **37,** 205
of Fe(II) and Fe(III) with phenanthroline in aqueous sulphate: Pourbaix-type diagrams, **35,** 209
of Fe(III) with dionato ligands: reduction at vitreous carbon cathodes in DMF-TBAP containing Cl^-, **38,** 653
formed by anodically dissolving metals: determination of stability constants by pulse voltammetry at microelectrodes, **38,** 1555
inclusion of 2,2'-diazino bis(3-ethyl 6-sulphonate benzothiazole) in α-, β- and γ-cyclodextrins, **37,** 149
of lanthanides(III) with (acac) and diisobutrylmethanate: polarography, **35,** 1713
N_4 chelates of Cu(II) and Co(II): oxidation of thin films on Pt anodes in 0.1M $LiClO_4$-MeCN, **38,** 907
preparation and electrochemical behaviour of two binuclear ethyne-bridged cobalt species, **38,** 1527
of pyrophosphate with Pb(II), Sn(II), Cu(II) etc: reduction at Hg cathodes, **36,** 427
of UO_2^{2+} with acyl-4-pyrazolone-5: reductions at Hg cathodes in PC, **36,** 325
of Zn(II) and Tris buffer solutions, **35,** 673
Zn(II)-paludrine: variation of Arrhenius factors with potential during reduction at Hg cathodes, **38,** 735
composite electrodes: mixture of solid electrolyte with intercalation host
effects of particle size, intercalation level and electrode thickness, **36,** 1643
concentration profiles see also holographic laser interferometry
of $^{137}Cs^+$ in perfluorosulphonic acid ion-exchange membranes, **37,** 221
calculated for liquid junctions, **35,** 361
during electrodeposition of Cu at Ti cathodes, **37,** 1279
during recharge of lead-acid cells with porous electrodes, **36,** 2153
during square-wave potential perturbation of reversible redox systems, **35,** 215
during square-wave potential perturbation of reversible metal discharge, **35,** 483
in potential-step experiments: deflection of probe laser beams, **37,** 429
in a small Cu-refining cell with vertical electrodes, **36,** 1345, **37,** 373
used to calculate liquid-junction potentials, **35,** 367
concrete, reinforced
use of guard rings to define corrosion current distribution in impedance studies, **38,** 2055
conductances see also conductivity
of dimethylamine-CO_2 addition compound, **35,** 769
of perchlorates of Mn(II), Co(II), Ni(II), Cu(II) and Zn(II) in propanone, **35,** 351
of potassium monoethyl benzeneazophosphonates in acetonitrile containing crown ethers, **35,** 59
of pyridine N-oxide acid perchlorates in acetonitrile, **35,** 665
of silver halides and pseudohalides in pyridine, **35,** 509
of solutions of water in $0.467TlNO_3$-$0.214CsNO_3$-$0.319Cd(NO_3)_2$ at 110°C, **37,** 349
conducting polymers
impedance studies, **35,** 1665
Q vs E data for polypyrrole and polythiophene in acetonitrile, **35,** 1815
treatment of poly(vinylalcohol) to give mixed conduction, **36,** 899
conduction, mixed
of polymer electrolytes containing redox species, **37,** 1521
conductive oxide films on metals
A-site substituted perovskite films formed by cathodization in aq acid-chromate-nitrates of La and Ca or Sr, **37,** 2421
conductivity see also conductances
of AgI-{[-$NMe_2(CH_2)_6NMe_2(CH_2)_4$-].2I}, **35,** 951
of AgI-poly(N-alkylene dimethyl-N,N'-piperazinium diiodide) double salts, **35,** 77

conductivity continued
of amorphous methoxy-linked poly(ethene oxide) $Zn(CF_3SO_3)_2$ complex, **37,** 1707
of amorphous PEO containing $LiClO_4$ or $LiCF_3SO_3$: DC polarization between Li electrodes, **37,** 1517
of aqueous solutions of $PbCl_2$: λ° for Pb^{2+} and $PbCl^+$ and K° for $PbCl^+$ and $PbCl_2$, **37,** 2519
of $Bi_4V_2O_{11}$ in which 10% of V ions are substituted by Cu: temperature dependence, **38,** 969
of blended solid polymer electrolytes: PEO with various acrylic polymers, **37,** 1565
of bulk and thin film $MgAl_2O_4$: effect of humidity, **38,** 2617
in calcium β-alumina, **38,** 365
of complexes of $CoBr_2$ in poly(tetramethyleneglycol) and poly(ethane-1,2-diol) oligomers, **37,** 1695
of complexes of PEO with bis(trifluoromethylsulphonyl)imide salts of Cu(II), Pb(II) and Ni(II), **37,** 1743
controlled photochemically through effect on reversible cross-linking *via* anthryl groups, **37,** 1515
of crosslinked poly(oxyethene) complexes with $LiN(CF_3SO_2)_2$, **37,** 1699
of dialkyl sulphide-iodine mixtures, **35,** 355
electronic: dependence on size of polypyrrole fibres formed by template synthesis, **37,** 1611
formulae for accurate interpolation of data over wide concentration ranges, **38,** 799
of lithium salts in organic solvents: electrolytes for lithium cells, **35,** 1257
of manganese oxide-hydroxide: effect of pretreatment temperature, **38,** 2305
mechanism in ionic melts: study of mixed salts with a common anion, **35,** 1761
modification of layer silicates by insertion of PEO or crown ethers to associate interlayer cations, **37,** 1573
of molten fluoride mixtures measured in a pyrolytic boron nitride tube-type cell, **38,** 589
of molten polyiodides, R_4N^+ and R_3S^+ at room temperature, **37,** 379
of Na_3AlF_6-Al_2O_3-(CaF_2)-(MgF_2) ternary and quaternary melts, **38,** 2165
of onium iodide-AgI solid electrolytes, **35,** 1465, 1473
of $[P(EO)_8.LiClO_4]$: relation to correlation times from ^1H and ^7Li relaxation rates, **37,** 1685
of PEO complexes with 5-mercapto-1-methyltetrazoles of Li^+, Na^+ and K^+, **37,** 1645
of PEO solutions of $LiClO_4$, $LiCF_3SO_3$ and $LiN(CF_3SO_2)_2$, **37,** 1579
of $(PEO)_nKCu_xI_{1+x}$, **37,** 1599
of polyaniline film electrodes, **38,** 2503
of polyepoxides, chain-extended, comb-like, with oligo(ethene oxide) units in side chains, complexed with $LiClO_4$, **37,** 1559
of a polymer electrolyte incorporating $LiClO_4$ and based on the glycidyl ethers of PEG and glycerol, **37,** 1569
of polymers: crown-ether groups attached to polyphosphazene backbones and complexed with alkali-metal salts, **37,** 1545
of polypyrrole films containing inserted anions on Pt electrodes, **35,** 567
of polypyrrole films measured by a new method using reusable carbon disc-carbon fibre array electrodes, **38,** 441
relaxation caused by infrared radiation of aqueous electrolytes, **35,** 861
of sequentially-ordered thermotropic liquid-crystalline polymers, **37,** 1479
of silica sols and gels prepared from tetramethoxysilane at various pH, **38,** 371
of solid electrolyte mixtures of AgI with N,N,N',N'-tetramethylhomopiperazinium diiodide and homopiperazinium diiodide, **38,** 565
through the glass transition of ionene polyelectrolytes, **37,** 1491
of uniform, coherent 1μm SPE films formed by simultaneous vapour-deposition of LiI and plasma polymerization, **37,** 1483
of various novel solid polymer electrolytes, **37,** 1539
conductors, ionic and mixed
impedance studies of liquid, semi-solid and glassy systems, **35,** 1609
conformal mapping
of the geometry of a corrosion pit into a semi-infinite strip, **38,** 1649
constant phase-angle behaviour
of the interface between a solid ionic conductor and a blocking electrode, **38,** 2111
irreversibility in the time domain responses of solid electrodes, **38,** 2051
of ramified Cu electrodeposited from $CuSO_4$ aq at high electric fields, **38,** 1941
of WO_3 thin films evaporated on to SnO_2-glass electrodes in 1M $LiClO_4$, **38,** 1935
contact resistance
between active PbO_2 and the Pb grid in Pb-acid cells: effects of time, discharge level and acid concentration, **37,** 1805
convection, free
at a horizontal cylinder electrode with an opposed thermal buoyancy effect, **38,** 2589

convection, free continued
due to density gradients at gas-evolving electrodes, **38,** 1421, 1427
during recharge of a lead-acid cell with porous electrodes, **36,** 2153
and forced at a segmented vertical plate cathode during deposition of Cu below the diffusion limited current, **38,** 1461
influence on cell characteristics under near limiting-current conditions in weak gravitational fields, **38,** 455
influence of support electrolyte in a Cu-refining cell, **37,** 695
in lead-acid cells during cycling, **37,** 681
with low steady currents and excess supporting electrolyte, **35,** 307
in a small Cu-refining cell with vertical electrodes, **36,** 1345, **37,** 373
unsteady, in a Cu electrolysis cell with excess H_2SO_4, vertical electrodes and uniform c.d., **37,** 333
conversion electron Mossbauer spectroscopy see Mossbauer spectroscopy
copolymers
block, from oligo poly(oxyethene) α,ω-dialcoholates with lateral styrene oxide or allylglycidylether, **37,** 1729
of ethene oxide and epichlorohydrin, mixed with oligo EO: conductivity, transport, and elastomeric properties, **37,** 1721
inorganic-organic as solid electrolytes, **37,** 1593
of styrene-maleic anhydride on vitreous carbon electrodes: effect on $Fe(CN)_6^{3-/4-}$ kinetics, **37,** 2573
of various organically substituted silanes formed by the sol-gel method: membrane for methanol fuel cells, **37,** 1615
copper
anodic behaviour of microelectrodes in ethan-1,2-diol-water mixtures containing Cl^-, **38,** 2291
anodic dissolution in 0.1M Na_2SO_4 at pH1.5, **37,** 2195
anodic dissolution in acidic 1M Na_2SO_4 aq, **38,** 2121
anodic dissolution as Cu(I) in aqueous chlorides, **38,** 2781
anodic dissolution in NaCl aq containing traces of SCN^-: analysis of oscillatory behaviour, **37,** 97
anodic dissolution through a precipitated film of CuCl, **36,** 1183
anodic passivation and pitting corrosion in aqueous carbonates, **35,** 1337
cathodic deposition from Cu(II)-glycine complexes in aqueous media, **37,** 745
corrosion by Fe(III) halides in DMSO and water, **36,** 479
current oscillations during anodic dissolution in KSCN-3M NaCl aq, **37,** 2637
deposition on vitreous carbon cathodes from CuI solid electrolyte, **38,** 577
dissolution of fixed and rotating planar electrodes in 4.3M NaCl aq containing Ag^+, **37,** 1779
distribution of thickness of electrodeposits during pulse plating, **37,** 1927
early stages of electrodeposition from $CuSO_4$-0.5M H_2SO_4 at columnar-structured Pt electrodes, **37,** 2203
effect of Cl^- on deposition at Pt cathodes from Cu(II)-histidine complexes at pH6, **38,** 165
effect of magnetic fields on anodic dissolution in NaCl aq containing traces of KSCN, **38,** 2631
effect of SCN^- on corrosion and passivity in borate buffer, **36,** 505
effect of SO_4^{2-} on anodic behaviour in neutral Na_2SO_4 aq, **37,** 2541
effects of Cu concentration and RDE rotation speed on critical potential for electrodeposition of dendrites, **37,** 23
effects of magnetic fields on electrodeposition and dissolution, **36,** 459
effects of pH and chelating agents citric acid, EDTA and nitrilotriacetic acid on electrodeposition on Pt, **37,** 2497
electrochemical behaviour in 1.37HF.NH_4HF_2, **38,** 1951
electrochemical behaviour in 6M H_2SO_4 aq at 30°C, **38,** 981
electrodeposition at Ti cathodes: concentration profiles monitored by laser interferometry, **37,** 1279
electrodeposition in a solenoid-wound cell with a common electrolysis and magnetizing current, **36,** 1907
electrodeposition and UPD at Pt, Au and Pd cathodes: ellipsometric study, **37,** 2245
formation of anodic layers in aqueous phosphate solutions of various pH, **37,** 655
formation and reduction of anodic layers in aqueous carbonate solutions, **38,** 703
impedance studies of ramified electrodeposits from $CuSO_4$ aq at high electric fields, **38,** 1941
impedance study of electrodeposition on a (111) single crystal from 1.25M $CuSO_4$-0.5M H_2SO_4 aq, **35,** 1587
inhibition of corrosion in 0.5M H_2SO_4 by formation of surface layers of 3-amino-5-heptyl-1,2,4-triazole, **37,** 2299
inhibition of oxygen reduction by UPD on Pt cathodes in acidic media, **36,** 1325
initial stages of electrodeposition on Pd cathodes, **35,** 1189
kinetics of pitting corrosion in 0.1M $NaClO_4$ at 8<pH<11, **37,** 1437
magnetic field effect on anodic dissolution in aqueous NaCl-KSCN, **35,** 933

copper continued
mechanism of anodic dissolution in 1M sulphate solution, **38,** 319
mechanism of anodic dissolution in HCl aq, **37,** 2707
nucleation and growth of electrodeposits on Pt and W cathodes: effect of organic additives, **38,** 2455
potentiometric stripping analysis and speciation in environmental studies, **38,** 807
spectroelectrochemical study in KOH aq, of films electroplated on tin oxide/glass, **37,** 17
underpotential deposition on Pt(111): influences of added hydroquinone, coumarin and crystal violet, **38,** 2467
UPD at Pt(100): *in situ* X-ray absorption spectroscopic study, **37,** 1977
UPD on Au(111) and (100) faces: an *in situ* X-ray absorption study, **36,** 1859
UPD on Pt: X-ray absorption fine structure, **36,** 1869
UPD on Pt single crystal electrodes: effects of thiourea and poly(ethane-1,2-diol), **38,** 647
copper(II)
voltammetric behaviour in aqueous solutions of tris(hydroxymethyl)aminomethane buffer, **38,** 957
copper(III)
discharge during intrinsic reduction of perovskite electrodes, **35,** 759
copper chalcogenides
reduction of H_2O_2 at chalcopyrite photocathodes of $CuFeS_2$ and $CuInSe_2$, **38,** 115
copper(I) chloride
pulse voltammetric determination of stability constant of $CuCl_2^-$ using a Cu microelectrode, **38,** 1555
copper(II) complexes
with benzimidazole, phenanthraline or bipyridyl: reductions in various electrolytes, **37,** 33
with mixed ligand cationic chelates: behaviour at carbon fibre electrodes in 0.1M $NaNO_3$-DMSO, **38,** 2623
copper electrode
adsorption of SO_4^{2+} in acidic and neutral media, **36,** 753
anodic oxidation of carbohydrates in aqueous alkali, **37,** 1187
coated with Nafion cation-exchanger: discharge of Cu^{2+}, **36,** 333
complexation and adsorption of benzotriazoles in aqueous sulphate, **35,** 1011
hydrogen evolution during oxidations of aldehydes, **38,** 1067
oxidations of $HCOO^-$, HCHO, hydrazine and methanol in alkaline aqueous media, **36,** 1937
photoelectrochemical behaviour in 0.3M K_2SO_4-0.01M $CuSO_4$-0.04M AA (AA = glycine, α-alanine or β-alanine), **38,** 2733
reduction of CO_2 in methanol containing benzalkonium chloride at low temperatures, **38,** 2177
copper(II) hexacyanoferrate
sorption of Ca^{2+} in films of, **35,** 811
copper indium sulphides
photocatalysis of hydrogen evolution from SO_3^{2-} aq, **37,** 465
copper(I) iodide
deposition of Cu at vitreous carbon cathodes from the solid electrolyte, **38,** 577
copper(I) iodide complexes
ionic conduction in $(PEO)_nKCu_xI_{1+x}$, **37,** 1599
copper ions
complexes with cysteine: reduction at Hg cathodes, **35,** 47
copper(II) ions
complexes with L-isoleucine and L-isoleucinate in aqueous media, **35,** 999
dissociation of complexes with L-hydroxyproline and D-allohydroxyproline, **36,** 109
effect of Cl^- on discharge of histidine complexes at pH6, **38,** 165
copper-nickel alloy
anodic dissolution of RDE in HCl aq, **36,** 2135
copper(I) oxide
behaviour in a carbon paste electrode in 10M KOH aq, **36,** 1209
formation during anodic oxidation of Cu to CuO or $Cu(OH)_2$ in KOH aq and the corresponding cathodic reduction, **37,** 17
photoelectrochemical behaviour of Cu/0.3M K_2SO_4-0.01M $CuSO_4$-0.04M AA (AA = glycine, α-alanine or β-alanine), **38,** 2733
role in cathodic deposition of Cu from glycine complexes of Cu(II) in aqueous media, **37,** 745
copper(II) oxide
behaviour in a carbon paste electrode in 10M KOH aq, **36,** 1209
cathodic reduction of layers formed on Cu anodes in KOH aq, **37,** 17
effect of heat treatment on cathodic discharge in lithium cells, **35,** 245

copper oxides
behaviour of mixtures with Bi_2O_3 and $NaBiO_3$ in carbon paste electrodes in 10M KOH aq, **36,** 1561
photoelectrochemical characterization of layers grown naturally on Cu in aerated aqueous sodium acetate, **38,** 1471
copper(I/II) redox kinetics
effect of CO at a W electrode in 1-methyl-3-ethylimidazolium chloride-$AlCl_3$, **38,** 927
copper-refining cell
calculated and measured concentration and velocity fields, **36,** 1345, **37,** 373
free convection and stratification of electrolyte: influence of support electrolyte, **37,** 695
copper selenides
electrochemical behaviour in the carbon paste electrode, **37,** 1321
electrodeposition from aqueous citric acid solutions containing Cu(II) and Se(IV), **38,** 2387
α-copper(I) telluride
band-gap determination and thermochemistry of reaction with Cu, **38,** 1699
copper ternary alloys
with Al and Ag: anodic oxidation in 0.5M NaOH aq, **36,** 1409
copper tetraphenylporphyrin
oxidation of thin films on Pt anodes in 0.1M $LiClO_4$-MeCN, **38,** 907
copper(II) trifluoromethanesulphonate
conductivity, cyclic voltammetry and calorimetry of complexes with PEO, **37,** 1711
correlation functions
for di- and tri-chromate ions in Cr electrodeposition solutions, **37,** 1239
corrosion
of Ag, Cu, Pd and Au by Fe(III) and Cu(II) in DMSO and aqueous solutions, **36,** 479
of Al in Li_2CO_3-Na_2CO_3 aq: effects of Li^+, CO_3^{2-} and Cl^-, **37,** 2659
of Cd in aerated sulphate solutions at 1<pH<6, **37,** 2611
in chemical process industries: impedance studies, **38,** 2075
of Cu alloys in natural seawater promoted by microorganisms within biofilms, **37,** 2291
of Cu in aqueous carbonate solutions, **38,** 703
of Fe and steel in aerated neutral solutions: impedance studies, **35,** 1501
impact-induced, of car bodies: determination of impact circumstances from impedance data, **38,** 2083
of inhomogeneous surfaces: impedance studies, **37,** 2309
promoted by microorganisms within biofilms, **37,** 2179
of reinforced concrete: use of guard rings to define current distribution in impedance studies, **38,** 2055
of Sb in H_2SO_4 aq, **36,** 2081
of semiconductor electrodes, **37,** 781
of steel with electroless Ni coatings, **38,** 2093
corrosion inhibition <u>see</u> inhibition of corrosion
corrosion, local
detection at large structures buried in soil, **38,** 1857
impedance studies, **35,** 1619, **37,** 2309
of microareas such as single grains and boundaries enabled by use of photo-resists, **37,** 2263
corrosion monitoring
of coated rough metals, **38,** 1867
of metal structures by impedance spectroscopy, **35,** 1573
corrosion nomenclature, **35,** 295
corrosion pits <u>see also</u> pitting corrosion
concentration and distribution on passive Fe in borate buffers with Cl^-, **35,** 1809
initiation by a focused laser beam during impedance studies, **35,** 1619
corrosion potential
of individual metal grains in relation to their residual tensile stress, **37,** 2263
corrosion protection
delamination of epoxy-polyamine coatings under cathodic protection conditions, **36,** 1915
investigations by impedance spectroscopy, **35,** 1533
corrosion rates
of Mg in aerated 0.5M Na_2SO_4 aq, **35,** 555
corrosion resistance
bestowed on Al 6061-T6 by successively boiling in Ce^{3+} aq and anodizing in 0.1M Na_2MoO_4, **37,** 2277
coumarin
influence on UPD of Cu on Pt(111) faces, **38,** 2467

coupled chemical reactions
application of Matsuda theory of pulse polarography, **37,** 1129
coupling, anodic
of morpholine with a disulphide generated *in situ* in water-chloroform emulsion, **36,** 1171
coupling, cathodic
of glucosyl radicals and carbanions with acrylonitrile or resorcinol, **36,** 1095
cresols
synthesis from toluene at the cathode of an O_2-H_2 fuel cell using 0.5M H_3PO_4: effect of $FeCl_3$ mediator, **37,** 2549
12-crown-4 ether
groups attached to poly[bis(1,1,1-trifluoroethoxy)phosphazene] and complexed with alkali-metal salts: conductivities, **37,** 1545
crown ethers see also benzo-15-crown-5-substituted N-methylpyrrole
effect on transfer of alkali-metal ions at the nitrobenzene/water interface, **35,** 127
insertion into layer silicates to change conductivity by association with interlayer cations, **37,** 1573
Si_3N_4 surfaces with styrene / vinylbenzo-[18]-crown-6 copolymer, **35,** 777
crown-ether complexes see also cryptate 222 complexes
of alkali-metal cations in 1,2-dichloroethane: stability constants, **37,** 231
with potassium monoethyl benzeneazophosphonates in acetonitrile, **35,** 59
cryolite
behaviour of sintered TiB_2 electrodes in melts containing Al_2O_3, **37,** 1395
electrodeposition and chemical dissolution of Al using graphite substrates, **36,** 811
oxidation of soluble Al(0) and Al(I) at W and carbon anodes, **36,** 31
temperature- and concentration-dependences of conductivities of mixtures measured in a pyrolytic BN tube-type cell, **38,** 589
cryptate 222 complexes
with silver(I): stability constants in 18 aprotic binary mixed solvents, **37,** 413
stability constants of Ag(I) complexes in DMSO-MeCN mixtures, **36,** 1427
of Tl^+: $E°$ values for Tl/Tl^+ in DMSO, DMF, DMA, MeCN, Me_2CO, sulpholane and PC, **38,** 1043
crystal violet
effects on hydrogen adsorption and absorption at Pd overlayers on Au(111) and Au(100) single-crystal electrodes, **38,** 2145
influence on UPD of Cu on Pt(111) faces, **38,** 2467
crystallization
at charged interfaces: classical and statistical thermodynamics, **37,** 1919
current distribution
at a corrosion pit, **38,** 1649
in pulse electroplating of Cu at a RDE from acidic $CuSO_4$ aq, **37,** 1927
current distributions
at a large structure buried in soil: impedance study, **38,** 1857
current doubling
at p-GaAs caused by oxidizing agents which also etch GaAs chemically, **37,** 909
curvature energies
of electric double layers near charged membranes, **36,** 1757
cyanide ions
adsorbed at Ag electrodes: cluster calculations of electronic properties, **37,** 211
adsorbed at Au, Pt, Pd and Ag: IR spectra, **36,** 1863
co-adsorption with SCN^- at Pt electrodes from 0.1M $NaClO_4$, **36,** 1849
1,1'-biscyanophenyl-4,4'-bipyridylium radical cations
electrodeposition of salts from aqueous solutions, **35,** 1113
cyclam
linking poly[bis(trifluoroethoxy)phosphazene] networks and containing perchlorates of Na or Ni, **37,** 1539
polymerization of compounds with pyrrole, **36,** 15
nickel(II/III) complex grafted to polypyrrole and polythiophene, **36,** 15
polymerization with compounds of pyrrole, **35,** 1051
cyclic voltammetry
at electrodes of non-uniform activity, **36,** 1129
1,3-cyclobutanediones
cathodic reduction in the presence of acetic anhydride, **36,** 465

cyclodextrins
asymmetric induction in the dimerization of acetophenone in DMF-TBABF$_4$, **36,** 1911
effect on partial oxidation of organics at H_2-O_2 fuel-cell $FeCl_3$-graphite cathodes, **37,** 1135
inclusion of 2,2'-diazino bis(3-ethyl 6-sulphonate benzothiazole): association constants, **37,** 149
α-cyclodextrin polymer film host on vitreous carbon electrode
cation-exchange property of guest 4-nitrophenolate, **37,** 1109
β-cyclodextrin
promotion of asymmetric induction during reduction of acetophenones at Hg cathodes in alkaline media, **35,** 1149
α-, β- and γ-cyclodextrins
cyclic voltammetry of ferrocene and its mono- and di-carboxylic acid complexes, **37,** 1939
1,3-cyclohexadiones
oxidation at PbO_2, Pt and carbon anodes in acidic media, **36,** 597
bis[(η^5-cyclopentadienyl)cobalt(η^4-1,3-cyclopentadien-5-exo-yl)]-ethyne
preparation and electrochemical properties, **38,** 1527
1,3-cyclopentadiones
oxidation at PbO_2, Pt and carbon anodes in acidic media, **36,** 597
cyclopropane derivatives
synthesis from electrogenerated monohalomalonate carbanions, **35,** 563
cylindrical electrode
simultaneous heat and mass transfer at a horizontal electrode, **38,** 2589
cylindrical microelectrodes
of Pt: oxidation of anthracene in MeCN-TBAPF$_6$, **36,** 1475
cysteine
complexes with copper ions: reduction at Hg cathodes, **35,** 47
cytochrome *c*
adsorption at Hg and formation of complexes with Cu(II), Zn(II) and Pb(II), **35,** 473
adsorption at pyrolytic graphite electrodes: effect on redox rates, **35,** 177
adsorption on Au electrodes from phosphate buffer solution: effect of 4,4'-bipyridyl disulphide, **37,** 403
incorporation into polypyrrole films formed at Pt anodes in neutral aqueous solution, **38,** 2581
cytochrome c_3
adsorption and redox behaviour at basal plane pyrolytic graphite electrodes, **36,** 1423

D

data analysis
complex non-linear least-squares curve-fitting of impedance data for binary electrolytes, **37,** 1007
in impedance studies: circular regression *vs* non-linear least squares, **36,** 1033
N,N-bis(decaoxyethene)octadecylamine
electrochemical behaviour and effect on electrodeposition of Zn from acid sulphate, **38,** 1351
defects in protective coatings and anodic films
impedance studies, **35,** 1501
delamination of polymer coating see also coated metals
impedance of an electrode with a fractal surface and circular delamination around a defect site, **38,** 1433
impedance of a metal electrode coated with a film containing holes allowing electrolyte access, **37,** 997
dendrites
effects of concentration and RDE rotation speed on critical potential during cathodic discharge of Cu^{2+}, **37,** 23
inhibition by additives during Pb electrodeposition from acidic $PbSiF_6$ aq: effects of potential and RDE speed, **37,** 2249
dendritic deposits
of Ag grown on Pt cathodes from 0.02M Ag^+ solutions, **38,** 1545
dental amalgam
potentiodynamic behaviour in artificial saliva (AFNOR standard S90-701), **38,** 1769
deoxycholic acid
with included ferrocene in 2:1 ratio as a positive electrode for zinc-iodine secondary cells, **38,** 1373

depolarization
of polarized light by defects in chromate-phosphate conversion coatings on AlMn05Mg05 alloy, **38,** 2577
deuterium
coulometric determination of loading in Pd cathodes, **36,** 1515
Devarda alloy cathodes
reductions of nitrobenzene, azoxybenzene etc to aniline, **35,** 147
1,4-diacetate-2-methylnaphthalene
synthesis and oxidation at Pt anodes in HOAc-LiOAc, **35,** 1739
2,4,6-tris(dialkylamino)-1,3,5-triazines
methoxylation of the dimethylamino derivative in methanol at graphite anodes, **38,** 2481
1,2-diaminoethane
adsorption at platinized Pt electrodes from 1M H_2SO_4 aq and from 0.1M NaOH aq, **35,** 111
1,2-diaminoethane-1,2-dioic acid
complexes with Cr(II): organic reduction mediators and phase transfer, **37,** 575
effect of presence in solution on electrodeposition of Cu, **37,** 2497
mechanism of Fe(II/III) reaction at 3.5<pH<6.5 in the presence of, **35,** 1325
diamond electrodes, doped with boron
impedance study of adsorption and partial charge transfer, **37,** 973
Z 1,2-diarylsulphonyl phenylethenes
cathodic catalysis of Z→E isomerizations, **37,** 2467
dibenzo(*b*,*d*)selenopyrane
oxidations of this and related compounds at Pt and vitreous carbon anodes in acetonitrile, **35,** 1855
dibenzo(*c*,*e*)-1,2-diselenine
oxidation at Pt anodes in 0.1M $NaClO_4$-MeCN, **37,** 2077
dibenzo(*c*,*e*)-1,2-dithiine
oxidation at Pt anodes in 0.1M $NaClO_4$-MeCN, **37,** 2077
oxidation at Pt and vitreous carbon anodes in acetonitrile, **37,** 725
1,2-dibromoethane
reduction at Pt ultramicroelectrodes in 0.1M TEAP-DMF catalysed by cobalt tetraphenylporphyrin, **38,** 1345
2,5-dibutylaniline
oxidation at Pt anodes in NH_4F-2.35HF, **36,** 833
dicarbollyl iron
redox reactions of adsorbed and dissolved material at amalgamated Pt electrodes, **36,** 421
bisdicarbollyl nickel
effect of solvent on differences between oxidation and reduction potentials, **36,** 435
β-dicarbonyl compounds
reduction of Fe(III) complexes at vitreous carbon cathodes in DMF-TBAP containing Cl^-, **38,** 653
dichlorocarbosilanes
cathodic polymerization to polycarbosilanes using AC in an undivided cell with Al electrodes in THF or DME, **38,** 529
1,2-dichloroethane/water interface
absolute Galvani potentials based on single ion transfer Gibbs energies, **35,** 1173
dichlorosilane derivatives
polymerization to polysilane derivatives at Pt cathodes in dimethoxyethane, **35,** 1867
di-cobalticenylium-ethyne-di-hexafluorophosphate
preparation and electrochemical properties, **38,** 1527
dielectric properties of the metal/solvent interface
impedance study of Pt in NaF aq, **35,** 1177
dielectric relaxation
through the glass transition of ionene polyelectrolytes, **37,** 1491
differential pulse polarography
application of Matsuda theory to very fast coupled chemical reactions, **37,** 1129
differential thermal analysis
of $Bi_4V_2O_{11}$ in which 10% of vanadium ions are substituted by copper, **38,** 969
diffusion
hemicylindrical, to nanometer scale band microelectrodes, **36,** 763
of hydrogen in metal membrane electrodes: theory of faradaic admittance, **38,** 2645
of reactants through a precipitated porous salt film: impedance spectra, **36,** 1183
diffusion coefficient determinations
by AC-RDE methods when the concentration is unknown, **38,** 681

diffusion coefficient determinations continued
by laser-probe beam deflection in potential-step experiments, **37,** 429
diffusion coefficient, surface
effect of adsorbed Cl^- or pyridine on diffusion of Au atoms on Au electrodes in 0.5 H_2SO_4 aq, **35,** 1331
diffusion coefficients
of anions in polyethyne, **36,** 2025
of atomic hydrogen in Fe and Pt, **36,** 615
of Br^-, $Mo(CN)_8^{4-}$, hydroquinone etc in composite films of PVA and montmorillonite clay, **37,** 1865
of camphorquinone in aqueous and MeCN solutions, **38,** 2209
of Cd^{2+} in LiCl-KCl eutectic, **35,** 1201
of $CdCl_2$ in water at various concentrations, **35,** 1433
chemical, in composite electrodes of solid-state cells, **36,** 1643
of Cl^- during Zn dissolution in low-temperature molten salts, **35,** 89
of Fe(II) and Fe(III) in DMSO, **36,** 471
of H^+ in $Ca(NO_3)_2.4H_2O$ and of NO_3^- in solid $Ca(OH)_2$ at 80°C, **36,** 1639
of H^+ in Nb_2O_5 layers formed by thermal oxidation of Nb, **35,** 765
of Li^+ in 3R-NiS_2, **36,** 935
of Li^+, Na^+, K^+ and NH_4^+ in indium hexacyanoferrate films, **35,** 1057
of Li^+ in MnO_2, **35,** 1849
of Li^+, Na^+ and K^+ inserted in polyethyne, **37,** 1675
of Li^+ in $Na_{1+x}V_3O_8$ and $Li_{1+x}V_3O_8$, **36,** 1549
of Li^+ in new positive electrode materials $MnO_2.xV_2O_5$, **37,** 1039
of Li^+ in polymorphs of TiS_2, **36,** 569
of Li^+ in ScO, TiO and VO, **35,** 17
of Li^+ in $YBa_2Cu_3O_{7-\delta}$ superconductor, **35,** 995
of Mg(II) in molten $BaCl_2$-$CaCl_2$-NaCl, **36,** 155
of protons through electrochromic WO_3 films containing also an oxide of Co, Cr, Fe, Mo, Ni, Ru or Zn, **38,** 1521
of a redox surfactant and its micelles, **35,** 885
of reduced and oxidized forms of cationic dyes in Nafion films, **36,** 881
of Sn^{2+} in LiCl-KCl eutectic at 723K, **35,** 905
of sodium in γ-MnO_2 electrodes, **37,** 603
of traces of Cd^{2+}, Co^{2+}, Cu^{2+}, Ni^{2+} and Zn^{2+} in 0.1-1.0M Na_2SO_4 aq, **36,** 309
of tungstate ion in LiCl-KCl eutectic at 723K, **35,** 1233
of viologen sites in poly(alkeneviologen) complex thin films, **35,** 63
diffusion model
for selective anodic dissolution of Cu-Au and Ag-Pd alloys, **36,** 49
diffusion to fractal surfaces
quasi-random interfaces, **36,** 163
1,4-difluorobenzene
fluorination in liquid $R_4NF.mHF$ at Pt anodes (Me, Et or Pr, m>3.5), **38,** 1123
digital sampling
a method to discriminate against mains noise, **35,** 1797, **36,** 747
dihydrofuran derivatives
syntheses from electrogenerated monohalomalonate carbanions, **35,** 563
1,4-dihydropyridine
interaction of Hantzsch ester with N-aryl- and N-arylsulphonyl-benzoquinoneimines, **37,** 277
dihydropyridine radicals
reductions of 1-methyl-2,4-dicyanopyridinium cations, **35,** 1185
1,4-dihydropyridines, substituted
reduction of 4-(nitrophenyl) derivatives at Hg and solid cathodes in DMF-$TBAPF_6$, **37,** 2599
1,2-dihydroxybenzene
mediated oxidation at glassy carbon anodes coated with poly(styrene sulphonate) containing $Os(bipy)_3^{2+/3+}$, **38,** 1321
diisobutrylmethanate complexes of the lanthanides(III)
polarography in DMSO, **35,** 1713
α-diketones, aromatic
oxidative cleavage by electrogenerated superoxide, **36,** 783
dimensionally stable anodes
effect of preparation conditions on structure of IrO_2-Ta_2O_5, **36,** 991

dimensionally stable anodes continued
impedance and SEM studies of $Ru_{0.2}Ti_{0.8-x}Sn_xO_2$ in 1M NaCl aq, **38,** 2239
preparation of rhodium oxide catalysts on Ti or quartz supports by thermal decomposition of $RhCl_3$ in HCl aq, **38,** 2435
1,3:2,4-di(*p*-methoxycarbonylbenzidene)sorbitol gel
immobilisation of liquid electrolytes in solid state lithium cells, **38,** 1301
1,2-dimethoxyethane with 0.5M $LiAsF_6$
passivity and breakdown of 1018 carbon steel, **38,** 881
dimethyl phthalate
polarography (Tast and DPP) in aqueous media and Et_2O-MeCOOEt emulsions, **36,** 1573
dimethylamine
adduct with SO_2: reduction at Pt cathodes in MeOH and in MeCN, **38,** 553
dimethylamine-CO_2 addition compound
properties of a new electrolyte for organic syntheses, **35,** 769
dimethylamine-SO_2 addition compound
analysis of volatile electrolysis products by mass spectrometry, **37,** 759
dimethylamine-SO_2-methanol addition compound
analysis of volatile electrolysis products by mass spectrometry, **37,** 759
N,N-dimethylamino-N,N-dimethylcarbamate
properties of a new electrolyte for organic electrosyntheses, **35,** 769
N,N-dimethyl-N'-ethyl-1,2-diaminoethane
mixed ligand complexes with (β-dionato)copper(II): behaviour at carbon fibre electrodes in DMSO, **38,** 2623
N,N-dimethylformamide
oxidation at porous Pt anodes in 0.05M H_2SO_4 aq, **38,** 185
N,N-dimethyl-1-naphthylamine
anodic dimerization in nitrobenzene/water emulsions, **35,** 1081
2,9-dimethyl-1,10-phenanthroline
complexes with Cu^{2+} adsorbed at graphite: catalysis of reductions of oxygen and H_2O_2, **38,** 2423
dimethylsulphoxide
adsorption at the Hg/H_3PO_4 aq interface, **35,** 1901
complex with ruthenium acetate clusters: electrochemistry in MeCN, **38,** 975
corrosion of Ag, Cu, Au and Pd by Fe(III) and Cu(II) in, **36,** 479
reactions at Pt electrodes in 0.5M H_2SO_4 aq, **38,** 175
4,4'-dinitrodibenzyl
reductions at Hg, Pt, Sn, Cu, vitreous carbon, and monel cathodes in DMF and EtOH-H_2O, **37,** 1993, 2001, **38,** 471
dinitrogen pentoxide
stabilities in HNO_3 and in protic solvents, **36,** 889
dinitrogen tetroxide
ionic dissociation and redox properties at Pt electrodes in nitromethane, **35,** 389
dinitrogen trioxide
ionic dissociation and redox properties at Pt electrodes in nitromethane, **35,** 389
dioctylphenyl phosphonate
plasticizer in PVC membranes containing CaI_2, **38,** 2373
dioctylsebacate-PVC membranes
in ion-selective electrodes [R], **35,** 1
(β-dionato)copper(II) complexes
behaviour at carbon fibre electrodes in 0.1M $NaNO_3$-DMSO, **38,** 2623
1,3-dioxolane
behaviour of Li and noble metals electrodes in, **35,** 625, 639
FTIR study of exposed lithium surfaces, **37,** 1897
1,3-dioxolane and 4-methyl-1,3-dioxolane
formation of polymer and copolymer hosts for electrolytes, **37,** 1589
1,1'-diphenylene-bispyridinium dications
reductions at Hg cathodes in $TBAPF_6$ solutions in MeCN, DMF and DMSO, **37,** 2481
dipole orientation at interfaces
role of dielectric constants, **36,** 1719
displacement reactions of metals
enhancement of rates by superimposed cathodic condictions, **35,** 657

disulphide redox positive electrodes
PEO complexes with 5-mercapto-1-methyltetrazoles of Li^+, Na^+ and K^+, **37,** 1645
X-ray absorption studies of S-S formation and scission during charge and discharge, **37,** 1635
dithiodipropionic acid
reduction at glassy carbon cathodes catalysed by cobalt tetrakis(4-trimethylammoniumphenyl)porphyrin, **37,** 2591
dodecylbenzene sulphonate
effect on electrochemical behaviour of polypyrrole films, **37,** 1173
synthesis and electrochromic properties of doped polypyrrole films on ITO electrodes, **38,** 869
dodecylsulphate
incorporation into polypyrrole films on Pt electrodes: effect on kinetics of redox processes, **37,** 419
incorporation into polypyrrole films in sub-equivalent amounts, **35,** 1971
double layer
around an isolated spherical macroion, **36,** 1747
classical and statistical thermodynamics of crystallization at charged interfaces, **37,** 1919
curvature energies near charged membranes, **36,** 1757
formation in alkali metal montmorillonite clays in aqueous electrolytes, **36,** 1751
between Hg and the solid polymer electrolyte: short PEO chains linked by $-OCH_2O-$ and containing $LiClO_4$, **37,** 1525
influence of phase transitions on interfacial capacitances, **37,** 81
properties in liquid and frozen electrolytes studied by the frozen-electrolyte technique, **37,** 565
double-layer effects
in potentiometry of suspensions, **36,** 59
double-layer repulsion between highly flexible membranes
entropy-driven expansion, **36,** 1735
double-layer structure
in a surface-inactive electrolyte solution, **36,** 401
double-layer theory
elastically bonded molecular capacity model of the inner layer, **36,** 1703
ion-dipole hard sphere mixture at hard charged wall model, **36,** 1685, 1715
molecular solvent models of the solution side, **36,** 1677
prediction of anisotropic liquid-crystal structures, **36,** 1695
dropping mercury electrode
rigorous model used for power-of-time chronopotentiometric study of EC mechanisms, **35,** 95
dye photocells
high photovoltages generated by multilayers of organic dyes, **38,** 459

E

Ebelsen derivatives
redox behaviour at Pt electrodes in acetonitrile, **35,** 1133, **36,** 631
EC mechanism
kinetic study at the DME using an $I = I_0 t^q$ perturbation, **35,** 95
ECE mechanism
anthracene oxidation at Pt anodes in MeCN-$TBAPF_6$, **36,** 1475
effluent treatment
cathodic recovery of metals from their mixtures, **38,** 2181, 2191
effect of citrate chelates on electrodeposition of Cd, **37,** 631
mechanism of photo-oxidation of organic pollutants over TiO_2 particles, **38,** 47
normalized space velocity as a figure of merit for stirred-tank reactors under mass-transfer limitations, **38,** 465
elastomeric ionic conductors
co-polymers of EO and epichlorohydrin, mixed with oligo-EO and $LiClO_4$, **37,** 1721
electric vehicle batteries
high temperature secondary lithium-sulphide cells, **38,** 1269
electric work method
analysis of exergy efficiency of solid-oxide fuel cells, **38,** 447
local heat changes in Al electrodeposition cells, **36,** 661

electrical double layer see double layer
electroanalysis
of methanol by its effect on zinc acetate coatings on Pt electrodes, **36,** 2109
electroanalytical sensors
expanding technology for their design and fabrication [R], **36,** 243
electrocapillary data
thermodynamic interpretation of data for adsorption of methylpyridines at Hg electrodes, **38,** 1573
electrocapillary equation
for polarizable and reversible interfaces between immiscible solutions, **35,** 715
electrocapillary studies
adsorption of uracil at Hg electrodes from aqueous phosphate buffer pH8, **37,** 2663
of N,N-bis(decaoxyethene)octadecylamine, cinnamaldehyde, benzalacetone and acetonaphthone at Hg cathodes, **38,** 1351
electrocatalysis see also electrocatalysts
at an ultramicroelectrode with a film containing a redox species, **38,** 581
by incipient hydrous oxides during oxidations at Au anodes in 1M NaOH aq, **37,** 585
effect of a Pt film sputtered on to the front surface of a low-Pt loaded SPE fuel cell cathode, **38,** 1661
graphite fibres treated with Pt^{4+}, Pd^{2+}, Au^{4+}, Mn^{2+}, Te^{4+}, In^{3+} or Ir^{3+}, **36,** 513
hydrogen evolution from 5M KOH aq at composite cathodes of Ni electrodeposited from baths containing powders of Ni, Fe or Co, **38,** 1079
of hydrogen oxidation in acidic media by carbides of W and W-Mo, **36,** 1543
hydrogenation at Pd electrodeposited on Ni, **38,** 2683
hydrogenation of organic compounds at palladium black supported on graphite cathodes, **38,** 425
hydrous oxide mediation in oxidations at noble metal anodes in alkali, **35,** 1821, 1829
involving chemisorption: relations between reaction orders and Tafel slopes, **37,** 51
of oxidation of ethane-1,2-diol by Pd-Pt alloy anodes in 0.1M NaOH, **36,** 353
oxygen evolution on $Ni_xCo_{3-x}O_4$ ($0.6<x<1.3$) in alkaline solutions, **38,** 2247
of oxygen and H_2O_2 reductions at graphite cathodes by adsorbed 2,9-dimethyl-1,10-phenanthroline-Cu^{2+}, **38,** 2423
of oxygen reduction at Pt in aqueous acids: activation energy and the Pt-O vibrational quantum, **37,** 1
of oxygen reduction at pyrolysed films of metalloporphyrins of cobalt and iron on carbon black surfaces, **38,** 2493
of oxygen reduction in weak aqueous acid at a glassy carbon RDE by vitamin B_{12}, **38,** 2297
role of CO in oxidation mechanisms of small organic molecules [R], **35,** 691
of $S_2O_8^{2-}$ reduction and the $Fe(CN)_6^{3-/4-}$ reaction at polyaniline films, **36,** 361
electrocatalysts see also electrocatalysis
for cathodic oxygen reduction: polypyrrole films with electrodeposited Pt particles, **35,** 135
controlled spatial distribution of noble metals on activated carbon fibre supports, **38,** 793
for direct oxidation of methanol: characterization of alloys [R], **36,** 2053
electrodeposited Pd on carbon felt electrodes, **36,** 921
finely dispersed metal deposits on semiconductor electrodes, **37,** 781
for HER in 3M KOH aq: Ni electrode modified by cathodization in 1M KOH-WO_4^{2-}-MoO_4^{2-} aq, **37,** 1457
for the HER and HCOOH oxidation: microquantity and UPD deposits of Rh on graphite electrodes, **38,** 1591
improved dispersion and catalytic activity of Pt from pretreatment of graphite substrates with Sn-$PdCl_2$ solutions, **38,** 1551
new preparation of highly dispersed Pd on carbon substrates, **38,** 2333
oxygen evolution at amorphous and crystalline Ni-Co alloy anodes, **37,** 169, 769
Pd and Pt supported on carbon felt cathodes: reductions of acetophenone and benzaldehyde in aqueous ethanol, **38,** 199
perovskite oxides $LaMnO_3$ etc, **35,** 65
physical electrochemistry of ceramic oxides [R], **36,** 225
Pt-Au sputtered on vitreous carbon: methanol oxidation in H_2SO_4, **36,** 947
Pt and Pd microparticles dispersed in poly(pyrrole-alkylammonium) films on carbon felt electrodes: azide hydrogenation, **37,** 1261
Pt and Pt-Fe both supported on carbon: preparations and characterizations, **38,** 2715
Pt utilization in PTFE-bonded gas-diffusion electrodes, **36,** 1049
Pt or WC-MoC for oxidation of gaseous methanol at PTFE-bonded fuel-cell anodes, **37,** 1351
pyrolysed tetraphenylporphyrins of iron and cobalt, **37,** 187
cis-$[Ru(L)(Cl)(O)]^{2+}$ [L = N,N'-dimethyl-N,N'-bis(2-pyridylmethyl)-1,2-diaminoethane] for methanol oxidation, **38,** 1015

electrocatalysts continued
ultrafine Au particles on vitreous carbon anodes: methanal oxidation in alkaline solutions, **37,** 453
electrochemiluminescence
of tris(2,2-bipyridine) Ru(II) in MeCN-TBABF_4 and in aqueous oxalate: enhancement by ultrasound, **38,** 307
radial intensity variations at an RDE with non-uniform current distribution, **35,** 1983
of tryptophan at Pt or glassy carbon anodes in 0.1M NaOH aq containing 1,3-dibromo-5,5-dimethylhydantoin, **37,** 2731
electrochromic behaviour
of BPEI-xH_3PO_4 between WO_3 and IrO_y electrodes, **37,** 1619
of cobalt hexacyanoferrate films, **36,** 147
of 1,1'-biscyanophenyl-4,4'-bipyridylium radical cation, **35,** 1113
and electrochemistry of WO_3 films containing also an oxide of Co, Cr, Fe, Mo, Ni, Ru or Zn, **38,** 1521
Li^+ injection into the nickel oxide electrode, **37,** 1033
of manganese dioxide films on glass-SnO_2 electrodes in 0.1M $Na_2B_2O_7$ aq, **37,** 2015
in non-aqueous media, of chemically-prepared polyaniline films, **36,** 2143
of poly(3-methylthiophene) in PC-$LiClO_4$ with an ITO counter electrode, **35,** 1757
of poly(3-methylthiophenes) electrosynthesized from dimers and tetramers, **38,** 135
of polyaniline or poly(2-chloroaniline) at ITO anodes in 1,2-dichloroethane-0.1M TBA salts: anion effect, **37,** 2101
of poly(methylthiophene)/1M $LiClO_4$-PC/Li_xNiO_y, **36,** 837
of polynaphthidine films on Pt electrodes, **35,** 731
of poly(*o*-anisidine) and poly(*o*-toluidine) films on ITO electrodes in various electrolytes, **37,** 1653
of polypyrrole doped with dodecylbenzene sulphonate, **38,** 869
of single-polymer gel films containing *p*-diacetylbenzene or dialkylterephthalates, **37,** 369
and stress of thin amorphous films of V_2O_5 with the anodic insertion of Li^+ from $LiClO_4$-PC, **38,** 1637
of thin polypyrrole-dodecylsulphate films, **35,** 1145
of WO_3 and polyaniline layers studied by impedance and electro-optical transmittance, **35,** 1553
of WO_3 and Prussian Blue: poly(alkali metal methacrylate) co-oligo(oxyethene) methacrylate solid electrolyte, **37,** 1649
electrochromic devices
viscous liquid polymer electrolytes as separators of self-sealing, laminated, electrochromic glass windows, **37,** 1703
WO_3 containing V_2O_5 or CdS as a light-sensitive layer, **38,** 2759
electrochromic electrode
impedance of WO_3 thin films evaporated on to ITO or fluorine-doped SnO_2 electrodes in 1M $LiClO_4$-PC, **38,** 1935
electrochromic windows
of combined Prussian Blue, WO_3, polyaniline and poly(2-acrylamido-2-methylpropane sulphonic acid) electrolyte, **38,** 1497
glass/ITO/polyaniline film/poly(2-acryamido-2-methylpropane sulphonic acid)/WO_3/ITO/glass: transmission spectra, **37,** 1377
electrochromism
induced by p-doping/undoping of conjugated polymers: basic requirements and effect of conjugation length, **38,** 135
electrocrystallization see also electrodeposition and nucleation and growth
of Fe-group metals, **38,** 1783
electrode potential scales
differences in redox potentials of two oxidation steps of cobaltocene etc, **36,** 435
electrode potentials
open-circuit, for polypyrrole film electrodes: effects of temperature and solution composition, **37,** 1075
electrode potentials, absolute, **36,** 1659
a unifying approach, **35,** 269
electrodeposition
and behaviour of electrochromic WO_3 films containing also an oxide of Co, Cr, Fe, Mo, Ni, Ru or Zn, **38,** 1521
of Cd from citrate solutions: role of chelate formation, **37,** 631
of Cd from waste solutions containing Fe(III), **38,** 2181, 2191
of clusters of Ag and Ag-Hg at Pt cathodes, **38,** 535
of Cu on Pt: effects of pH and chelating agents citric acid, EDTA and nitrilotriacetic acid, **37,** 2497
effect of Ag^+ on deposits of W and WC from chloride melts, **35,** 187

electrodeposition continued
estimation of amounts of deposit using theory of Markov chains, **38,** 1147
general model for nucleation and growth of hemispheroidal centres, **36,** 727
impedance studies of mechanisms, **35,** 1587
of metals with excess inert electrolyte: calculated impedance behaviour, **38,** 1671
of Pb: inhibition of dendrites by additives: effects of potential and RDE speed, **37,** 2249
of Pd on Ni: electrocatalytic hydrogenation of nitrobenzenes to anilines in methanol, **38,** 2683
potentiostatic: morphological stability of a planar metal electrode, **37,** 103
sequential, of Ag and either Pb or Tl on Au single-crystal cathodes, **37,** 2237
of Sn from acidic $SnSO_4$: effect of a surfactant, **36,** 985
of Sn from $SnSO_4$ aq: effect of aromatic carbonyl compounds on surface morphology and crystal orientation, **37,** 2403
of spherical clusters under joint ohmic, diffusion and ion-transfer limitations, **37,** 2229, 2233
of Te from 10^{-3}M Te(IV) in 0.1M K_2SO_4 at pH2.2 through adsorbed intermediates, **38,** 2043
of Ti, Zr, B, TiB_2 and ZrB_2 from LiF-NaF-KF eutectic at 700°C, **37,** 237
of TiB_2 on W or vitreous carbon from NaCl-KCl melts containing $TiCl_3$ and $NaBF_4$: effect of F^-, **37,** 263
of transition metals, laser-induced on (100) p-Si, **36,** 1803
and UPD of Bi, Cu and Ge on Au, Pd and Pt cathodes: ellipsometric study, **37,** 2245
of Zn, Cd and Mn at Hg cathodes: solvent effects, **38,** 721
of Zn at a RDE from $ZnSO_4$-Na_2SO_4-aq, **37,** 439
of Zn on vitreous carbon from zincate solutions, **37,** 1199
of Zn-Ni alloys from aqueous chlorides, **37,** 545
electrodeposition mechanism see nucleation and growth
electrodeposits
modified Michelson interferometer for measuring strain in, **35,** 1989
electrodissolution
potentiostatic: morphological stability of a planar metal electrode, **37,** 103
electrogenerated bases
2-alkoxyquinolines and 3,1,4-benzoxazines from aromatic ketones, **36,** 2019
protonation of carbanions by their parent secondary 2-bromoisobutyramides, **35,** 81
electrogenerated carbanions
monohalomalonate: condensations with Michael acceptors, **35,** 563
electrogenerative oxidation
of ethanol and 2-propanol at Pt supported on a packed graphite bed electrode, **38,** 221
electrogravimetry see quartz crystal microbalance
electrokinetic processes
thermodynamic formulations, **35,** 705, 711
electroless plating
of magnetic materials for the electronics industry [R], **37,** 989
electroluminescence
application of 3-aminophthalhydrazide to study the porosity of chromate-phosphate conversion coatings on AlMn05Mg05 alloy, **38,** 2577
weak, during oxygen evolution at various metal anodes, **36,** 1591
electrolyte electroreflectance
thermodynamic characterization of the semiconductor/electrolyte junction, **37,** 957
electrolyzers see also packed-bed reactors
for effluent treatment: normalized space velocity as a figure of merit under mass-transfer limitations, **38,** 465
with multiple electrodes: uniform potential using external resistors, **36,** 841
plug-flow and batch: modelling of surface electrochemical reactions, **38,** 2155
selective reductions of nitro groups in 4-nitrophenylporphyrins by flow-through cathode and anode in series, **38,** 325
electron microscopy see also scanning electron microscopy
study of Al anodized in CrO_3-xH_2SO_4 aq, **35,** 961
study of grain structure of photoetched CdSe-CdS mixed crystal semiconductor electrodes, **38,** 593
study of grain structure of photoetched $CdSe_xS_{1-x}$ solid solution, **38,** 593
electron paramagnetic resonance see ESR
electron spectroscopy study
of activated graphite felt electrodes intended for use in vanadium redox cells, **37,** 2459
of adsorption of poly(styrene sulphonate) at polyaniline film electrodes, **36,** 799
of Al anodized in CrO_3-xH_2SO_4 aq, **35,** 955

electron spectroscopy study continued
of Al-Zr alloys and their anodic films, **36,** 1227
of alkali metals deposited on Ag cathodes in alkaline media, **36,** 1947
of amorphous Ni-Co-Si-B electrocatalysts and Ni_2Co and Co_2Ni electrodes, **37,** 2029
of anodic layers grown on Ir- and Rh-implanted Ti, **38,** 1313
of anodic oxides formed on n- and p-Si, **37,** 847
of anodic passivation of $Fe_{70}Cr_{10}X_{13}C_7$ where X = P or B in 0.5M H_2SO_4, **37,** 2269
of anodic passivity of Fe in H_2SO_4 aq, **38,** 495
of $Cr(OH)_3$ films on Au and Pt cathodes in chlorate cell electrolytes, **36,** 1605
of effect of Cl^- on adsorption of 1-octyne-3-ol on Fe electrodes in HCl aq, **36,** 1333
of Fe, Ni and Cr polarized anodically in concentrated H_2SO_4, **37,** 1069
of fluorine cell carbon anodes, some modified by impregnation with 0.5M $Al(NO_3)_3$ aq, **38,** 2413
of freshly cut Li surfaces, showing accumulation of Na impurity, **37,** 731
of irreversible doping of polyaniline by a polymer electrolyte, **35,** 827, **36,** 87, 357
of a $Mn(OH)_2$ electrode at different potentials, **36,** 1013
of n-Si after chemical and photoelectrochemical etching, **37,** 877
of passive films on Cr in H_2SO_4 aq: effects of solution composition, **38,** 2309
of passive films on Zn anodes in borate and arsenate solutions pH8.9, **36,** 1491
of porous films formed on Si anodes in 0.5M H_2SO_4, **36,** 1611
of Pt species in porous carbon anodes for methanol fuel cells, **35,** 199
of Pt-Fe alloy oxygen-reduction catalysts supported on carbon, **38,** 2715
of pyrolysed films of metalloporphyrins of cobalt and iron on carbon black surfaces: oxygen-reduction catalysts, **38,** 2493
of pyrolysed tetraphenylporphyrins of iron and cobalt, **37,** 187
of reduction of MnO_2 in aqueous borate, **38,** 341
of sputtered cobalt oxide films, **35,** 975
of surface concentrations on $Cd_xHg_{1-x}Te$ crystal anodes, **36,** 869
of thin hydrous MnO_2 deposits on Au during their discharge in borate pH9.2, **36,** 1485
electron spin resonance see ESR
electron tunnelling
through an adsorbed layer of organic substance on an electrode, **36,** 421
through thin oxide films on a Pt electrode: oxygen evolution in alkaline solutions, **37,** 2533
electron-transfer catalysis
of Z→E isomerizations of some Z 1,2-diarylsulphonyl phenylethenes, **37,** 2467
electron-transfer rates
solvent polarization diffusion, **36,** 395
electron-transfer reactions
at superconducting electrodes: theory, **37,** 2123, 2129
a comparison of electrochemical and chemical conversions of organic species, **36,** 2171
experimental determination of dynamic structural parameters, **36,** 1775
mechanism of oxidation of N-phenyl-*p*-phenylenediamine at electronically-conducting polymer film anodes, **38,** 271
quantum mechanical interpretations of kinetics of transition-metal reactions [A], **36,** 1892
electronic absorption spectra
of $Li[(Pc)Ln(acac)_2]$ and (Pc)Ln(acac) where Ln = Eu, Gd, Dy, Tb, Ho, Er, Tm and Lu, **35,** 1707
electronic materials, advanced
electrochemical aspects [R], **37,** 989
electronic properties
of $Li_xTi_{1+y}S_2$: relation to electrode potential, **36,** 1555
electronic work functions
and zero-charge potentials of gold {111}, {311}, {110} and {210} faces, **35,** 1383
electro-optical impedance methods
absorption and luminescence responses to potential modulation, **35,** 1545
electro-optical transmittance
investigations of electrochromic layers, **35,** 1553
electro-osmotic coefficient
across Nafion 120 membranes separating equimolar 1:1-electrolyte solutions, **36,** 139
electroplating see also pulse plating
of Ag and Cu on anodized Al: effects of anions and alloy composition, **35,** 1019
in a Hull-type cell with a rotating cylinder electrode, **37,** 69

electroplating continued
of magnetic materials for the electronics industry [R], **37,** 989
use of additives to control properties of the deposit, **37,** 2115
electropolishing
of Fe in H_3PO_4-H_2SO_4: rate-limiting mass transfer of Fe(III), **37,** 2469
of mild steel and Al using AC, **36,** 93
electroreflectance
recent theoretical models, **37,** 949
of thermally produced thin films of CdO, **38,** 2199
electrosorption
on fractal surfaces: irreversibility in time domain responses corresponding to constant phase angles, **38,** 2051
electrosynthesis see also organic compounds and heterocyclic compounds etc
of glyoxylic acid at both graphite electrodes, **36,** 1447
ellipsometric study
of Ag(hkl) and Au(hkl) in 0.01M KF and 0.01M KPF_6 aq, **36,** 1839
of anodic dissolution of Si in NH_4F aq, **37,** 889
of anodic films on Cd in NaOH aq, **35,** 605
of effect of 4,4'-bipyridyl disulphide on adsorption of cytochrome *c* on Au electrodes from phosphate buffer solution, **37,** 403
of effects of various cations on anodic behaviour of Fe in alkali, **36,** 1143
of electrodeposition and UPD of Bi, Cu and Ge on Au, Pd and Pt cathodes, **37,** 2245
of growth, cycling and over-oxidation of polypyrrole in 1M $NaClO_4$ aq, **36,** 1263
of growth and cycling of polypyrrole films on Pt, **36,** 2123
of passivation of Fe-Ni alloys in H_2SO_4 aq, **35,** 69
of the passive films on Cr and Fe-Cr alloys in 0.5M H_2SO_4 aq, **38,** 1969
of passivity and breakdown of passivity of Fe in alkaline media, **35,** 1437
of polypyrrole films containing inserted anions on Pt electrodes, **35,** 567
in the range $300<\lambda/nm<850$, of thickness, growth rate and interface properties of barrier and porous anodic oxide films on Al, **38,** 2103
in situ, time-resolved: of 1-octyn-3-ol adsorption on Fe electrodes in HCl aq, **36,** 1333
in situ, of anodic films on Ti in 0.5M H_2SO_4 at high voltage: thickness and optical constants, **37,** 2099
in situ, of anodic oxide formation on n- and p-Si, **37,** 847
in situ, of kinetics of adsorption of acetylenic alcohols on Fe in H_2SO_4 aq, **37,** 317
EMF measurements
calculations of liquid-junction potentials between aqueous bromide solutions, **35,** 371
determination of transport numbers in molten salts suitable for electrodeposition of Al, **38,** 415
of cells including a junction between different solid electrolytes, **35,** 785, 1477
emulsion
anodic dimerization of an aromatic amine in nitrobenzene/water, **35,** 1081
coupling of morpholine with electrogenerated disulphide in $CHCl_3/H_2O$, **36,** 1171
polarography of dimethylphthalate in Et_2O/MeCOOEt (1:9) emulsion, **36,** 1573
enamines
synthesis from methoxy-iminium cations and electrogenerated carbanions, **36,** 819
energy conversion see also solar energy conversion
from an unbiased Fe_2O_3/0.5M Na_2SO_4/Pt cell using intermittent light, **37,** 1101
entropies of activation
for single electrode processes from non-isothermal cell potentials in non-aqueous media, **38,** 997
entropy-driven expansion of electric double-layer repulsion between highly flexible membranes, **36,** 1735
epoxy network
a solid electrolyte incorporating $LiClO_4$ and based on the glycidyl ethers of PEG and glycerol, **37,** 1569
epoxy-polyamine protective coatings
delamination under conditions of cathodic protection, **36,** 1915
equivalent circuit parameters
of montmorillonite clay film-coated quartz crystal oscillators contacting air, moisture and Na_2SO_4 aq, **38,** 747
equivalent circuits
complex non-linear least squares fitting of impedance data, **35,** 1483
of doped diamond-film electrodes, **37,** 973
for electrodeposition processes with adsorption, **38,** 2043
fitting impedance data for illuminated n-GaAs in acetonitrile, **37,** 309
for fuel-cell electrodes, **38,** 2063

equivalent circuits continued
for gas-diffusion electrodes, **38,** 2115
for hydrogen evolution and absorption reactions at metal membrane electrodes, **38,** 2645
for interpretation of impedance studies of corrosion in complex environments, **38,** 2075
for $La_{0.85}Sr_{0.15}MnO_3$ cathodes in Y_2O_3-stabilized ZrO_2 at 1000°C, **38,** 2015
for local corrosion in large metal structures, **35,** 1573
of multilayer oxides: interpretation of Bode diagrams, **38,** 633
for a partially submerged smooth electrode passing a non-zero DC, **38,** 2281
for the poly(3-octylthiophene) film on a Pt electrode in PC-$LiBF_4$, **37,** 1759
for pores in coatings on painted metals, **38,** 2029
for the Pt/NaF aq interface, **35,** 1177
for a redox reaction at the interface between immiscible electrolyte solutions, **36,** 291
representing p-GaAs electrodes with thin electrodeposits of Au, **38,** 301
representing a solid ionic conductor sandwiched between two blocking electrodes, **38,** 2111
of Sb anodes in 0.5M H_2SO_4 aq, **36,** 2087
for the semiconductor/electrolyte interface, **35,** 1631
for super-Nicad cells as functions of voltage and number of cycles, **38,** 2037
for the system Ta/Ta_2O_5/electrolyte, **38,** 285
transmission line representations for macrohomogeneous porous electrodes, **38,** 2653
to explain high-frequency artefacts in impedance studies, **35,** 1125
to fit admittance data for the amorphous WO_3/aqueous electrolyte junction, **36,** 1817
erbia-stabilized δ-bismuth oxide
oxygen transfer studied by impedance spectroscopy, DC polarization and ^{18}O exchange, **38,** 1817
DL-erythritol
oxidation at Ni anodes in 1M KOH, **35,** 375
ESR spectroscopy
of free radicals formed in cathodic reductions of 4-(nitrophenyl) substituted 1,4-dihydropyridines in DMF-$TBAPF_6$, **37,** 2599
of V_2O_5 cathodes intercalated by Li^+ from 1M $LiAsF_6$-PC-EC-DME, **37,** 2755
ESR spectroscopy, *in situ*
of carbon within Leclanche cells: variation during discharge, **38,** 2511
of electrogenerated pyrylium radicals, spin-trapped by nitroso aromatics, **36,** 73
of formyl radicals during oxidations of HCHO or methanol at Pt, **35,** 681
study of cathodic reduction of 4,4'-dinitrodibenzyl in DMF and EtOH-H_2O, **37,** 1993, 2001, **38,** 471
etching
of GaP single crystals: dependence of kinetics and morphology on crystallographic orientation, **37,** 811
of p-GaAs by oxidizing agents e.g. iodate causing photocurrent multiplication, **37,** 909
photoelectrochemical, of n-Si in aqueous fluoride, **37,** 877
photoelectrochemical, of Si in NH_4F aq, **37,** 889
of semiconductors: effect of dopant concentrations, **38,** 889
of Si in aqueous and methanolic HF: pore development followed by gravimetry, **38,** 191
of Si to produce atomically-flat hydrogen-terminated (100) surfaces, **38,** 1367
of Si by H_2O_2 in weak aqueous alkali at 70°C, **35,** 1267
etching, electroless
effect of conditions on morphology of n- and p-GaP electrodes, **35,** 1351
ethanal
adsorption and oxidation on Pt in 0.1M $HClO_4$, **35,** 989
ethane-1,2-diol
anodic behaviour of Cu microelectrodes in mixtures with water containing Cl^-, **38,** 2291
effect of UPD Pb on oxidation at Pt and Au anodes, **36,** 1157
oxidation at Pt-Pd alloy anodes in 0.1M NaOH aq, **36,** 353
ethanol
partial oxidation at Pt supported on graphite particles in a packed-bed anode, **38,** 221
ethene carbonate
mixed solvent electrolytes for secondary lithium cells, **35,** 383
oxidation and reduction at Pt electrodes in aqueous acids, **38,** 541
bis(ethenedithio)-tetrathiofulvalene
solvent effects on electrosynthesis of charge-transfer complexes with trihalide ions, **38,** 2343
ethyl picolinate
reduction at Pb cathodes in H_2SO_4 aq, **37,** 625

ethylene see ethene
ethylene carbonate see ethene carbonate
ethylene diamine see 1,2-diaminoethane
ethylene diamine tetraacetic acid see 1,2-diaminoethane-1,2-dioic acid
ethylene glycol see ethane-1,2-diol
ethyne-bridged binuclear cobalt complexes
  preparation and electrochemical properties, **38,** 1527
europium(II/III)
  solvent effects on kinetics at Hg electrodes, **38,** 721
excess microwave reflectivity
  in situ measurements of anodic oxides on n- and p-Si, **37,** 847
excess thermodynamic functions
  of $AgNO_3$-KNO_3 melts in the range 513-583K, **37, 91,** 1155
extended X-ray absorption fine structure
  study of local structure in $NiBr_2(PEO)_8$, **37,** 1663
  study of mixed-ion polymer electrolytes, **37,** 1529

F

faceting
  of Al during cycling in 0.1M $NaClO_4$ aq containing BPh_4^-, **38,** 1073
faradaic admittance see also impedance
  equations for irreversible reactions under potentiostatic control, **35,** 831, 837
faradaic impedance see impedance
ferrate(VI) ion
  dependence of current yields at an iron anode in 14M NaOH aq upon frequency of superimposed AC, **38,** 1717
ferrocene
  included in deoxycholic acid in 1:2 ratio as a positive electrode for zinc-iodine secondary cells, **38,** 1373
ferrocene carboxylic acid
  cyclic voltammetry of inclusion complexes with α-, β- and γ-cyclodextrins, **37,** 1939
ferrocene derivatives
  redox kinetics at epitaxial $YBa_2Cu_3O_{7-\delta}$ thin films in 0.1M TBAP-MeCN, **35,** 1219
ferrocene derivatives as electron donors
  photo-induced transfer to a sensitizer in an adjacent Langmuir-Blodgett layer, **36,** 1793
ferrocenephanes
  cyclic voltammetry in aqueous methanol, **35,** 93
  substituent effects and electrode kinetics at Au electrodes in MeCN-TEAP, **36,** 689
ferrocenyl undecyltrimethylammonium ion
  adsorption, diffusion coefficient and critical micelle concentration, **35,** 885
ferrocenylalkane thiols
  self-assembled monolayer on Au cathodes: mediator in reduction of Fe(III)-EDTA, **36,** 1799
film potentiometric stripping analysis
  of Pb^{2+} at a vitreous carbon RDE with Fe(III) oxidant, **36,** 2103
flat-band potentials
  of Fe and Fe-Cr alloys covered with passive layers in neutral aqueous media, **38,** 1567
  of GaP electrodes, **35,** 1351
  of illuminated n-WSe_2/1M H_2SO_4, **35,** 1195, **36,** 747, 2037, 2039
  of In_2S_3 thin film electrodes on Ti substrates: effects of pH, solution composition and redox couple, **35,** 345
  measured by electrolyte electroreflectance, **37,** 957
  of n-InP as a pH probe in non-aqueous and mixed solvents, **38,** 781
  of passive films on AISI 304 stainless steel in borate buffers, **36,** 315
  of sputtered thin film Y-Ba-Cu-O electrodes in MeCN-$LiClO_4$, **35,** 1977
  of thermally produced thin films of CdO, **38,** 2199
  of thin anodic oxide films on Ti in H_2SO_4 aq, **35,** 1073
  transient, of p-Si following removal of anodic polarization in NH_4F aq, **37,** 865
flow-modulation technique
  relation of electrohydrodynamic to electrical impedance, **35,** 1637

flow-through electrodes
electrodeposition and dissolution of Zn, **38,** 311
hydrogen evolution on metallized-plastic packed-bed electrodes, **36,** 1899
mass transfer at carbon and graphite felt electrodes, **35,** 1369, **36,** 339
flumazenil
adsorption and reduction at Hg electrodes, **35,** 1311
fluoride ion
discharge at carbon anodes: influence of gas bubbles in the anode effect, **37,** 711
discharge at various carbon and graphite anodes in molten NaF and in molten cryolite, **37,** 705
effect on reduction mechanism of La(III)-alizarin complexone complex, **35,** 1861
in MeCN-10%(mol) H_2O: pF scale and *E vs* pF^- diagrams for Ag, Cu and hydrogen, **35,** 1885
fluorination
of benzene, fluorobenzene and 1,4-difluorobenzene in liquid $R_4NF.mHF$ at Pt anodes (Me, Et or Pr, m>3.5), **38,** 1123
of benzene at Pt anodes in MeCN-$R_4NF.nHF$ and MeCN-$Et_3N.3HF$, **38,** 619
fluorine electrosynthesis
lowering anode polarization by adding AlF_3 or LiF to the KF.2HF melt, **35,** 153
fluorine evolution
from KF.2HF melts: modification of carbon anodes by impregnation with 0.5M $Al(NO_3)_3$ aq and baking at 1000°C, **38,** 2413
fluorobenzene
fluorination in liquid $R_4NF.mHF$ at Pt anodes (Me, Et or Pr, m>3.5), **38,** 1123
fluoropolymer coatings
on low-carbon steel: impedance studies, **38,** 1945
formaldehyde see methanal
formamide
oxidation at porous Pt anodes in 0.05M H_2SO_4 aq, **38,** 185
formic acid see methanoic acid
formylation, electrochemical
of aryl halides at Cd-modified Au cathodes in DMF, **38,** 613
four-dimensional estimation of instantaneous impedance, **37,** 2353
Fourier transform
limitations under non-stationary conditions, **38,** 1919
Fourier transform, rotating
in impedance analysis of non-stationary systems, **37,** 2357
four-probe polarization by sequential, bipolar, rectangular current pulses
application to solid state power sources, **38,** 1289
fractal electrodes
an impedance study of three-dimensional dendritic electrodeposits of Ag on Pt cathodes, **38,** 1545
diffusion to an electrode with quasi-random boundaries, **36,** 163
dispersive behaviour described by a constant phase element, **35,** 1045
impedance of coated metals, **38,** 1867
impedance of a polymer coated electrode with circular delamination around a defect site, **38,** 1433
impedance studies of ramified Cu electrodeposits from $CuSO_4$ aq at high electric fields, **38,** 1941
irreversibility in time-domain responses corresponding to constant phase angles, **38,** 2051
mass transfer to an active fractal region set in an inactive RDE, **35,** 1423
relations between frequency component and Tafel slopes, **35,** 1567
relationship of impedance to statistics of random walks that are reflected from the surface, **38,** 1985
role of surface diffusion during metal deposition studied by Monte Carlo simulations, **37,** 2155
skewed arc impedance plots for irreversible redox reactions, **35,** 141
STM measurements of perimeter and area of intergranular voids in Au films formed by reduction of gold oxide, **37,** 2209
free energies of transfer
of Tl^+ between organic solvents, **38,** 1043
free radicals
of ascorbic acid formed at Au anodes in aqueous buffers, **36,** 1649
cyclic voltammetry of N-(arylthio)-2,4,6-triphenylanilino radicals at Pt in 0.1M TEAP-MeCN, **37,** 2095
frequency exponent
of a blocking fractal electrode and the Tafel slope, **35,** 1567

frozen-electrolyte technique
the study of double-layer properties in liquid and frozen electrolytes, **37,** 565
fuel cells
application of impedance studies to research and development, **38,** 2063
H_2O_2 synthesis in acid cells with Nafion dividers, **35,** 319
impedance studies of changes in electrode morphology in alkaline and molten carbonate cells, **38,** 2115
improved dispersion and catalytic activity of Pt from pretreatment of graphite substrates with Sn-$PdCl_2$ solutions, **38,** 1551
kinetics of oxygen reduction at Au cathodes in Li_2CO_3-K_2CO_3 at 923K, **38,** 2405
modelling of an alkaline cell using the flooded agglomerate electrode model and concentrated electrolyte solution transport equations, **38,** 2599
oxygen reduction at Au cathodes in Li_2CO_3-K_2CO_3 eutectic: effect of CO_2-O_2-He atmosphere, **37,** 1935
oxygen reduction at the $La_{0.85}Sr_{0.15}MnO_3$ cathode in Y_2O_3-stabilized ZrO_2 at 1000°C, **38,** 2015
partial oxidation of hexane and aromatics at cathodes of $FeCl_3$-graphite: effect of cyclodextrins, **37,** 1135
with solid oxide electrolytes: use of local heat produced in the H_2/O_2 cell, **38,** 447
fuel cells, alkaline
modelling and simulation of operation using transport theory for concentrated electrolyte solutions, **37,** 1831
fuel-cell anodes
effect of size and nature of Pt particles on methanol oxidation in H_2SO_4 aq, **35,** 199
oxidation of gaseous methanol at PTFE-bonded anodes with Pt or WC-MoC dispersed on carbon, **37,** 1351
simulation studies for a H_2-O_2 cell with the catalyst bonded to the solid polymer electrolyte, **37,** 2737
fuel-cell cathodes see also phosphoric acid fuel-cell cathodes
of Co tetramethoxyphenylporphyrin: interaction with oxygen, **36,** 999
effect of Pt particle size on oxygen reduction in H_3PO_4, **36,** 1979
effects of PTFE content and sintering temperature on performance, **35,** 1411
influence of amount of Pt catalyst on corrosion of carbon in phosphoric acid cells, **37,** 2725
with low Pt loading: effect of a Pt film sputtered on to the front surface in an SPE cell, **38,** 1661
for methanol fuel cells: thermal preparation of an air electrode based on carbon paper treated with H_2PtCl_6 aq, **37,** 1327
models of NiO cathodes for molten carbonate cells, **38,** 2669
oxidation of carbon blacks in hot H_3PO_4 and their physicochemical properties, **36,** 1931
oxygen reduction in 0.5M H_2SO_4 aq, **37,** 523
fuel-cell electrodes
impedance studies of a partially submerged smooth electrode with non-zero DC, **38,** 2281
fuel-cell gas-diffusion electrodes
anode model for the phosphoric acid H_2-O_2 cell, **36,** 547
effect of CO_2 on stability of cathodes in alkali, **35,** 945
impedance studies, **35,** 1579
simulation and optimization of porous cathodes, **35,** 869
fuel cells, molten carbonate
impedance studies of changes in electrolyte wetting and porosity of Ni sponge anodes and NiO cathodes, **38,** 2115
models of fuel cell NiO cathodes, **38,** 2669
furan-2,5-dicarboxylic acid
synthesis from 5-hydroxymethylfurfural at NiOOH anodes, **36,** 1995
furazano[3,4-b]-quinoxaline 1-oxides
reductions at cathodes of Hg, Pt and Pt(UPD Tl) in $HClO_4$ aq, **38,** 989

G

gallium aluminium arsenide
Mott-Schottky plots, band gaps, band edges and carrier concentrations, **38,** 1993
gallium arsenide
photoelectrochemical processing, **38,** 101
gallium arsenide electrode
chemical and electrochemical reactions of BrO^- in alkali, **36,** 695
photoelectrochemical imaging of sub-monolayer Pb deposits on n-GaAs, **37,** 933
super-high quantum efficiencies for iodate reduction in aqueous alkali at p-GaAs photocathodes, **37,** 909

gallium arsenide electrode continued
theory of electroreflectance and photoreflectance, **37**, 949
n-gallium arsenide electrode
anodic oxidation in acetonitrile solutions, **37**, 309
influence of thin Au electrodeposits on the impedance spectra and current *vs* potential curves, **38**, 1115
physicochemical models for impedance spectroscopy, **38**, 1903
p-gallium arsenide electrode
influence of thin Au electrodeposits on the current *vs* potential curves, **38**, 291
influence of thin Au electrodeposits on impedance, **38**, 301
reduction of oxygen, **35**, 1657
gallium indium phosphide
Mott-Schottky plots, band gaps, band edges and carrier concentrations, **38**, 1993
gallium phosphide
wet etching processes investigated by photoelectrochemistry, **37**, 811
gallium phosphide electrodes
effect of LiCl(4M) on competition between anodic decomposition and stabilization by Fe(II), **37**, 1343
effects of pH, potential and crystal face on etching and redox rates, **35**, 1351
galvanoluminescence
during pore-filling of alumina anodic films, **35**, 825
galvanostatic pulse electrolysis
hydrogenation of phenanthrene at Raney Ni electrodes, **38**, 1377
galvanostatic-step method
correction of electrode kinetic data for electrode area changes, **35**, 1213
gas bubbles
behaviour of oxygen and hydrogen in a narrow-gap cell: application in chlorine production, **38**, 1705
gas evolution
effects on overvoltage of a PTFE array on platinized Pt, **35**, 1089
mass transfer resulting from free convection due to density gradients in the liquid phase, **38**, 1421, 1427
in thin vertical channels of narrow-gap water-electrolysis cells, **38**, 1381
gas sensor
microelectrode coated with poly(ethene oxide)-$LiCF_3SO_3$, **38**, 2315
gas-diffusion electrodes
application of impedance studies to fuel-cell research and development, **38**, 2063
effect of CO_2 on electrochemical stability in alkaline media, **35**, 945
effect of fabrication parameters on oxygen-reduction performance, **35**, 1411
effect of sulphur on reduction of NO (3% in N_2) at Pt black cathodes in H_2SO_4 aq, **36**, 299
effects of phosphoric acid concentration on oxygen reduction and hydrogen oxidation, **37**, 1855
effects of PTFE content and sintering temperature on porosity and acid uptake, **36**, 1049
electrocatalytic activity of, and oxygen adsorption by, $LnMnO_3$ etc, **35**, 65
for hydrogen-oxygen phosphoric acid fuel cells, **35**, 869
model for porous anodes in phosphoric acid H_2-O_2 fuel cell, **36**, 547
modelling of NiO cathodes for molten carbonate fuel cells, **38**, 266
oxygen reduction in 0.5M H_2SO_4 aq, **37**, 523
simulation studies of the anode of a H_2-O_2 fuel cell with a solid polymer electrolyte, **37**, 2737
gelling agent
immobilization of liquid electrolytes for lithium cells in 1,3:2,4-di(*p*-methoxycarbonylbenzidene)sorbitol, **38**, 1301
geraniol
oxidation to citral at MnO_2-modified, Pt-Nafion electrodes, **37**, 1295
germanium
electrodeposition and UPD at Pt, Au and Pd cathodes: ellipsometric study, **37**, 2245
germanium eutectic alloys Ge-Me (Me = Cu, Co, Ni or Fe)
electrochemical behaviour in 0.5M H_2SO_4, **36**, 1247
Gibbs energies of activation
oxygen reduction at Pt electrodes, **35**, 1157
Gibbs energies of formation
of TiB_2 and ZrB_2 at 700°C, **37**, 237
glass transition
in ionene polyelectrolytes as a breakdown of the quasi lattice of bound cationic nitrogen, **37**, 1491
glassy carbon see vitreous carbon

glassy metals
electrocatalysis of the HER in 1M KOH aq, **36,** 537
electrocatalytic activities of some Fe-based alloys in 1M KOH aq, **38,** 821
electrodeposition of Ni-P alloys on glassy carbon cathodes and their anodic dissolution, **38,** 261
$Fe_{70}Cr_{10}X_{13}C_7$ where X = P or B: XPS study of anodic passivation in 0.5M H_2SO_4, **37,** 2269
films on $Fe_{80}B_{20}$ anodes in borate buffer and acidic sulphate solutions, **38,** 205
oxygen evolution at alloy anodes containing mainly Ni, Mo and B, **35,** 1919
voltammetric and XPS studies of Ni-Co-Si-B electrocatalysts in 1M KOH aq, **37,** 2029
glow discharge optical emission spectroscopy
of $Cr(OH)_3$ films on Au and Pt cathodes in chlorate cell electrolyte, **36,** 1605
glucose
effect of UPD Pb on oxidation at Pt or Au anodes, **36,** 1157
oxidation at Au anodes mediated by incipient hydrous oxide, **37,** 1363
oxidation at Pt anodes: effect of UPD Pb, **38,** 2725
D-glucose
adsorption at platinized Pt in 1M H_2SO_4 aq, **37,** 2443
effect of anions on oxidation at single-crystal Au anodes in aqueous acids, **37,** 357
electrocatalytic oxidation at smooth Pd anodes in NaOH aq, **37,** 2651
oxidation in acidic and neutral media at Pt and Au anodes and at Pt modified with UPD Pb, Tl and Bi, **37,** 1333
oxidation in aqueous alkali at Pt and Au anodes, unmodified and modified with UPD Pb, Tl and Bi, **37,** 1909
oxidation at Ni anodes in 1M KOH, **35,** 375
glucose sensor
composite polypyrrole-glucose oxidase films at Pt anodes used with 1,4-benzoquinone electron-transfer mediator, **37,** 1987
glutaric acids
synthesis from 1,3-cyclohexanediones at PbO_2, Pt and carbon anodes, **36,** 597
glycidyl ethers
of PEG and glycerol: components of a solid-electrolyte epoxy network incorporating $LiClO_4$, **37,** 1569
glycine
complexes with Cu(II): cathodic deposition of Cu from aqueous solutions, **37,** 745
α-D-glycopyranosyl bromides
reduction at Hg cathodes in the presence of radical acceptors, **36,** 1095
glyoxal
effect of UPD Pb on oxidation at Pt or Au anodes, **36,** 1157
glyoxylic acid
role of temperature in synthesis from oxalic acid at Pb cathodes, **37,** 1381
simultaneous syntheses from glyoxal at a graphite anode and from oxalic acid at a graphite cathode, **36,** 1447
synthesis from oxalic acid in an undivided cell, **35,** 621
gold see also gold electrodes
comparison of electro- and vapour-deposited films: fractal-surface characterization through STM, **37,** 2209
corrosion by Fe(III) and Cu(II) halides in DMSO and water, **36,** 479
dependence of ellipsometric parameter Δ on crystal face in 0.01M KF and KPF_6 aq, **36,** 1839
effect of thin electrodeposits on current *vs* potential curves at p-GaAs electrodes, **38,** 291
effect of thin electrodeposits on impedance of p-GaAs electrodes, **38,** 301
effect of thin electrodeposits on impedance spectra and current *vs* potential curves at n-GaAs electrodes, **38,** 1115
electrogravimetric transfer function study of oxidation in H_2SO_4 aq, **38,** 1827
impedance study of oxidation in H_2SO_4 aq, **38,** 1023
gold dental alloy
potentiodynamic behaviour in artificial saliva (AFNOR standard S90-701), **38,** 1769
gold electrodes see also gold
in 1M NaOH aq: mediation and inhibition by incipient hydrous oxides during anodic oxidations, **37,** 585
AC voltammetry in acidic solutions, **37,** 2087
adsorption of 4,4'-bipyridyl in acidic and neutral media, **35,** 591
adsorption of Forafac ionic perfluorinated surfactants, **38,** 2203
adsorption of imidazole from aqueous media, **38,** 947
adsorption of non-ionic surfactants from Na_2SO_4 aq, **37,** 2377
adsorption and oxidation of butanediols in aqueous media, **35,** 1345
adsorption of *p*-nitroaniline from aqueous perchlorates, **35,** 1037

gold electrodes continued
adsorption of *p*-toluene sulphonate anions from aqueous solution, **37,** 75
adsorption of polyacrylamide from H_2SO_4 aq and HI aq, **36,** 1315
adsorption of terminal and vicinal aliphatic diols from 0.02M $NaClO_4$ aq, **38,** 717
adsorption of urea and thiourea from acidic and neutral media, **35,** 613
anodic oxidation of sucrose in alkaline solution, **38,** 1679
atomic roughness of the (100) surface induced by potential cycling into hydrogen evolution, **37,** 2169
catalysis of cathodic reduction of nitrate ion in aqueous alkali by UPD Pb, **38,** 2773
coated with poly(*o*-phenylenediamine): kinetics of inorganic redox reactions in 0.5M H_2SO_4, **37,** 635
effect of adsorbed Cl^- or pyridine on surface diffusion of Au adatoms in 0.5M H_2SO_4 aq, **35,** 1331
effect of anions on oxidation of D-glucose at single-crystal Au anodes in aqueous acids, **37,** 357
effect of 4,4'-bipyridyl disulphide on adsorption of cytochrome *c* from phosphate buffer solution, **37,** 403
effect of surface reconstruction on capacitance of (100) surfaces, **37,** 615
effect of UPD of alkali metals on HER in aqueous alkalis, **37,** 2021
effects of As(III), nitrate, sulphate and phosphate on electrocrystallization of PbO_2, **37,** 1811
electrodeposition and UPD of Bi, Cu and Ge: ellipsometric study, **37,** 2245
hydrogen evolution during oxidations of aldehydes, **38,** 1067
in situ FTIR study of phenazine and phenothiazine dye films, **38,** 1619
in situ X-ray absorption study of UPD Cu on (110) and (111) faces, **36,** 1859
modified with Cd electrodeposits: reduction and electroformylation of aryl halides in DMF, **38,** 613
on-line MS analyses of products of oxidation of propargyl, allyl and propyl alcohols in 0.5M H_2SO_4, **38,** 1337
oxidation of D-glucose in acidic and neutral media, **37,** 1333
oxidation of glucose mediated by incipient hydrous oxide, **37,** 1363
oxidation of methanal at (332) faces, **35,** 725
oxidations of hydrazine, methanol, HCHO and $HCOO^-$ in aqueous alkali, **35,** 1829
oxygen reduction in Li_2CO_3-K_2CO_3 eutectic: effect of composition of CO_2-O_2-He atmosphere, **37,** 1935
potentials of zero charge and capacitance minima in NaF aq, **37,** 139
reconstruction of (111) surfaces during UPD of Cd, **36,** 1829
self-assembled monolayers of ferrocenyl alkane mediators in the reduction of Fe(III)-EDTA, **36,** 1799
single-crystal (100) and (111) faces with thin overlayers of Pd: adsorption and absorption of hydrogen, **38,** 2145
single crystal: sequential UPD of Ag and either Tl or Pb, **37,** 2237
unmodified and modified with UPD Pb, Bi and Tl: oxidation of D-glucose in aqueous alkali, **37,** 1909
work functions and PZCs of {111}, {311}, {110} and {210} faces, **35,** 1383
gold oxide, thick hydrous layers
reduction kinetics and roughness of Au overlayers, **35,** 117
grafting
and polymerization of acrylonitrile and methacrylonitrile on metal cathode surfaces, **38,** 1501
grain and grain boundary potentials
localized corrosion studies enabled by use of photo-resists, **37,** 2263
gramicidin
influence on water chains in transmembrane ion channels, **36,** 1753
graphite electrodes see also pyrolytic graphite electrodes
anodic methoxylation of 2,4,6-tris(dimethylamino)-1,3,5-triazine in methanol, **38,** 2481
discharge of F^- in molten NaF and in molten cryolite, **37,** 705
effect of modification with zeolite on oxidations of hydrazine, alcohols and hydroquinones, **38,** 919
intercalation of HOPG in H_2SO_4 aq, **38,** 2005
negative with $LiNi_{1-x}Co_xO_2$ positive electrodes in secondary lithium cells, **38,** 1159
oxidations of SO_3^{2-} and HSO_4^-, **36,** 1073
graphite felt electrodes
activation for use in the vanadium redox cell, **37,** 2459
mass transfer studies using hexacyanoferrate and Hg(0/II) couples, **35,** 1369
thermal pretreatment before use in vanadium redox flow batteries, **37,** 1253
graphite fibre electrodes
treated with Pt^{4+}, Pd^{2+}, Au^{4+}, Mn^{2+}, Te^{4+}, In^{3+} or Ir^{3+}, **36,** 513
graphite intercalation compounds see intercalation
graphite substrates
pretreatment with Sn-$PdCl_2$ solutions leading to improved dispersion and catalytic activity of Pt electrodeposits, **38,** 1551

gravitational systems
a non-equilibrium thermodynamic formulation, **38,** 877
gravity
effect of lowering on bubble formation during water electrolysis at Au electrodes, **38,** 729
D-gulonic acid
selective oxidation at smooth and UPD Pb-modified Pt anodes in 0.1M NaOH aq, **38,** 1359

H

hafnium anode
growth of passive films in 0.5M NH_4HSO_4 aq, **35,** 1897
hafnium electrode
photocurrents at thin oxide films: photoemission at the Hf/HfO_2 interface, **38,** 15
halides, organic
condensations of electrogenerated halomalonate carbanions, **35,** 563
eliminations from 1-fluoro-2-arylvinylphenyl sulphones at Pt, Hg, Pb and C cathodes in MeCN containing proton donors, **38,** 1037
reduction of $CClF_2CCl_2F$ in MeOH-H_2O-NH_4Cl, **35,** 1727
reductions at metalloporphyrin-coated electrodes, **36,** 855
reductions at Pt ultramicroelectrodes in 0.1M TEAP-DMF catalysed by cobalt tetraphenylporphyrin, **38,** 1345
Hall effect
attempts to make measurements on electrolyte solutions, **36,** 979
N-halogen cathodes in power cells with Mg anodes and $Mg(ClO_4)_2$ aq electrolyte
N,N'-dichlorodimethylhydantoin etc, **37,** 1971
Hammett's σ_p-parameters
for oxidations of twenty ferrocenes, **36,** 689
Hansen's reference system
applied to interfaces between two immiscible electrolyte solutions, **35,** 715
hard wall
and a nearby hydrogen molecule: solution of the wave equation, **36,** 1711
and a nearby hydrogen-like atom: exact solution of the wave equation and effect of separation on electronic spectrum, dipole moment etc, **36,** 1711
heat pumps, electrochemical
pairs of similar cells with different temperatures and reaction directions, **35,** 1283
heme protein
adsorption and redox behaviour of cytochrome c_3 at pyrolytic graphite electrodes, **36,** 1423
hemoglobin
redox behaviour at Pt electrodes modified with Methylene Green, **35,** 1139
reduction in 0.5M KCl-PEO, **37,** 1649
reduction at vitreous carbon cathodes modified by thionine, **37,** 595
heterocyclic compounds
anodic synthesis from azomethine derivatives in MeCN-TEAP mediated by radical cations, **35,** 225
behaviour of phenothiazine derivatives and their nitration products at carbon paste electrodes in methanol solutions, **37,** 1355
cathodic synthesis from aromatic ketones *o*-substituted by imino-ether groups, **36,** 2019
coupling of morpholine with electrogenerated bis(2-benzothiazolyl) disulphide in $CHCl_3$-H_2O, **36,** 1171
cyclic voltammetry of quinoxalines and their di-N-oxides in 0.1M TEAP-DMF: substituent effects, **37,** 1433
methoxylation of 2,4,6-tris(dimethylamino)-1,3,5-triazine in methanol at graphite anodes, **38,** 2481
oxidation of dibenzo(*c,e*)-1,2-dithiin at Pt and vitreous carbon anodes in acetonitrile, **37,** 725
oxidations of dibenzo(*b,d*)selenophene and benzo(*b*)selenophene at Pt or vitreous carbon anodes in MeCN, **37,** 1453
oxidations of four 3-hydroxy-4-pyridinones at glassy carbon anodes in aqueous buffers, **38,** 2223
oxidations of Nifedipine derivatives and 4-(*o*-nitrophenyl)-1,4-dihydropyridines at graphite felt anodes, **38,** 1775
polarographic reduction of 2-substituted 3-phenyloxaziridines in DMF-TEAP, **36,** 97
reduction of 3-nitro-1H-1,2,4-triazole at Pt cathodes with UPD Bi, Pb or Tl, **35,** 1957
reduction of 2-, and 4-nitroimidazoles at Hg and at Pt cathodes modified by UPD Pb, Tl or Bi, **37,** 1231

heterocyclic compounds continued
reduction of 3,4-diphenyl-1,2,5-thiadiazole-1,1-dioxide at vitreous carbon cathodes in MeCN-$LiClO_4$, **36,** 167
reduction of isoniazid at Hg cathodes in aqueous acid, **37,** 1147
reduction of nifepidine and related compounds in protic media, **36,** 1135
reductions of 2-benzylthio-6H-1,3-thiazines at Hg and carbon cathodes, **35,** 805
reductions of benzoyloxiranes at Hg cathodes in 0.1M $TBABF_4$-MeCN, **37,** 1247
reductions of furazano[3,4-b]-quinoxaline 1-oxides and 2,3[1H,4H]-quinoxalinedione dioximes in $HClO_4$ aq, **38,** 989
reductions of new tetradentate bipyridine-pyridyl triazine ligands at Hg cathodes in DMF-TBAP, **36,** 1997
reductions of nitrophenyl-pyridines and pyridiniums at Hg cathodes, **38,** 1775
reductions of pyridazin-3-ones at Hg in EtOH-H_2O, **35,** 1907
reductions of pyridinium and sulphonium ylides at Hg cathodes in 0.1M $LiClO_4$-MeOH, **36,** 101
syntheses of macrocyclic diesters using electrogenerated superoxide ion, **36,** 783
heterogeneous electrodes
linear sweep cyclic voltammetry of soluble species, **36,** 1129
heteropolyacids
electrocatalysis of HER in 3M KOH aq on Ni cathodes modified by cathodization in 1M KOH-WO_4^{2-}-MoO_4^{2-} aq, **37,** 1457
hexacarbonyls of group VI metals
kinetically irreversible reductions at Pt and carbon cathodes in liquid ammonia, **35,** 1879
hexacyanoferrate
immobilization by Ti(IV) oxide coated on a silica gel surface: preparation and electrochemical behaviour, **37,** 2477
hexacyanoferrate(II/III)
kinetics at Fe and Fe-Cr alloy electrodes passivated in neutral aqueous media, **38,** 1567
hexacyanoferrate(II)
mediated oxidation at glassy carbon anodes coated with poly(styrene sulphonate) containing $Os(bipy)_3^{2+/3+}$, **38,** 1321
hexacyanomanganate(III)
photogalvanic effect at Pt anodes in aqueous cyanide, **35,** 427
hexacyanoruthenate(II)
mediated oxidation at glassy carbon anodes coated with poly(styrene sulphonate) containing $Os(bipy)_3^{2+/3+}$, **38,** 1321
hexane
partial oxidation at H_2-O_2 fuel-cell cathodes of $FeCl_3$-graphite: effect of cyclodextrins, **37,** 1135
Heyrovsky and polarography
tribute on the centenary of his birth, **36,** 221
high-frequency phase shift
impedance artefacts in low-conductivity media, **36,** 1093, 1385
histidine
reduction of complexes with Cu(II) at Pt cathodes at pH6: effect of Cl^-, **38,** 165
holographic laser interferometry see also concentration profiles
measurements of concentration profiles in a Cu-refining cell, **36,** 1345, **37,** 373
study of a Cu-refining cell: influence of support electrolyte, **37,** 695
study of free convection in a discharging lead-acid cell, **36,** 2153
study of lead-acid cells with and without separators, **37,** 681
homopiperazinium diiodide
solid electrolyte mixtures with AgI: preparation, characterization and total conductivity, **38,** 565
Hull cell
with a rotating cylinder electrode, **37,** 69
humidity sensors
effect of humidity on conduction mechanism in bulk and thin film $MgAl_2O_4$, **38,** 2617
hydrazine oxidation
at noble metal anodes in aqueous alkali, **35,** 1821, 1829
at Pt and Cu anodes in alkaline aqueous media, **36,** 1937
in H_2SO_4 aq at vitreous carbon anodes modified with polyaniline films, **35,** 1425
hydride
coulometric determination of amounts in Pd cathodes, **36,** 1515
effect on rates of hydrogen evolution on Ti in 1M HCl, **35,** 1913

hydrodimerization
of nicotinamide at Hg cathodes at 2<pH<7, **35,** 845
hydrodynamic sensors
frequency response to flow variations of small electrodes operating under convection-diffusion control, **38,** 1847
hydrodynamic structures and instability
formation in systems with concentration polarization and negative resistance, **36,** 143, 321
hydrogen
adsorption and absorption by ultrafine Pd particles on glassy carbon electrodes in $HClO_4$ aq, **36,** 1235
hydration or reaction with water co-adsorbed on Cu(110) or Pt(111) from the gas phase, **36,** 1883
hydrogen absorption
in metal membrane electrodes: theory of faradaic admittance, **38,** 2645
hydrogen adsorption
at Ni (111), (100), (110) and (210) crystal faces in 0.1M KOH aq, **38,** 2129
on polycrystalline Pt electrodes from 0.5M H_2SO_4 aq, **37,** 2629
hydrogen adsorption and absorption
anion and additive effects at single-crystal Au electrodes with overlayers of Pd, **38,** 2145
hydrogen evolution
in 1M NaOH aq at vitreous carbon electrodes supporting ultrafine Pd particles, **37,** 2427
at Ag cathodes: effects of adsorbed thiourea, **35,** 879
at Ag from NaOH aq: effect of UPD Na, **35,** 523
at amorphous Ni-Co-based alloys in 1M KOH aq, **36,** 537
from aqueous sulphite: photocatalytic activity of $CuInS_2$ and $CuIn_5S_8$ cathodes, **37,** 465
at Au in aqueous alkalis: effect of UPD of alkali metals, **37,** 2021
at Bi-Pb alloy cathodes in H_2SO_4 aq: effects of grain macrostructure and surface morphology, **37,** 269
at composite Ni-RuO_2 cathodes in hot strong alkali, **37,** 757
during dissolution of Al cathodes in neutral solutions, **35,** 1743
during oxidations of aldehydes at anodes of Cu, Ag or Au, **38,** 1067
at Fe cathodes in hydroxide and chlorate solutions: effect of chromate, **37,** 1873
formation of oxidizable substances at Al cathodes in NaCl aq, **35,** 1747
at Ge, Fe, $FeGe_2$ and eutectic alloys Ge-Me (Me = Cu, Co, Fe and Ni), **36,** 1247
at Hg above 100°C in light and heavy waters, **36,** 411
from 5M KOH aq at composite cathodes of Ni electrodeposited from baths containing powders of Ni, Fe or Co, **38,** 1079
at metallized-plastic packed-bed electrodes, **36,** 1899
at Ni cathodes: suppression by adsorbed CO, **35,** 1777
at Ni and nickel oxide anodic films, **35,** 1099
at Ni-S_x cathodes prepared by electrodeposition from aqueous solutions of $NiSO_4$ containing thiourea, **38,** 2449
at Raney Ni cathodes in concentrated NaOH aq, **35,** 1251
relation between catalytic activity of transition metals and alloys and their electronic structures, **38,** 557
at Rh cathodes in 1M KOH aq, **37,** 1283
at Ru-Ti cathodes in acidic media, **36,** 19
at Si photocathodes modified with ultrafine Pt particles, **37,** 897
at some Fe-based amorphous alloys in 1M KOH aq, **38,** 821
at Tl in 1M HCl: effect of hydride, **35,** 1913
hydrogen fluoride, liquid
oxidation of 2,5-dibutylaniline at Pt anodes in NH_4F-2.35HF, **36,** 833
hydrogen molecule
near a hard wall: solution of the wave equation, **36,** 1711
hydrogen oxidation
in 1M NaOH aq at vitreous carbon electrodes supporting ultrafine Pd particles, **37,** 2427
in acidic media on bulk and on carbon-supported carbides of W and W-Mo, **36,** 1543
at gas-diffusion electrodes: effect of phosphoric acid concentration, **37,** 1855
potential oscillations during simultaneous oxidation with CO at Pt anodes, **36,** 639
hydrogen permeation
in Fe and Pt cathodes, **36,** 615
through Fe in liquid ammonia, **36,** 283
through membranes of Fe, Pd and stainless steel: effects of visible light, **38,** 89
through a passive film on Fe in borate buffer, **36,** 825

hydrogen peroxide
oxidation at passive Fe rotating disc anodes in alkaline solutions, **37,** 1845
reduction at an Fe cathode in alkaline media, **36,** 5
reduction at chalcopyrite photocathodes: non-linear and pulse phenomena, **38,** 115
reduction at graphite cathodes catalysed by adsorbed complexes of Cu^{2+} with 2,9-dimethyl-1,10-phenanthrolines, **38,** 2423
reduction at n-Si and p-Si electrodes in weak aqueous alkali at 70°C, **35,** 1267
reduction at pyrolytic graphite electrodes modified by iron protoporphyrin, **35,** 1227
synthesis at fuel-cell gold-mesh or carbon cathodes in HCl aq, **35,** 319
hydrogen storage alloys
improved catalytic activity from electrodeposited coatings of Pd, Fe, Co and Ni, **38,** 787
modification by treatment with alkaline KBH_4 solution, **38,** 659
hydrogen sulphide
interference in the response of chlorine gas sensors, **36,** 1823
hydrogenolysis
catalytic, of N-O and N-N bonds: reductions of nitrobenzene etc to aniline at Devarda Cu and Raney Ni cathodes, **35,** 147
hydrolysis of surface bonds
rate-limiting step in chemical dissolution of n-ZnO, **37,** 827
hydrophobic electrode
effect of composite-plated PTFE on overvoltages for HER, OER and reductions and oxidations of organics on Ni, **37,** 353
hydroquinone
influence on UPD of Cu on Pt(111) faces, **38,** 2467
hydrous oxides
on Au anodes: role in oxidation of glucose, **37,** 1363
on Au electrodes in acidic solutions, **37,** 2087
growth and reduction on Pt under potential cycling in $HClO_4$ aq and NaOH aq, **37,** 43
role in electrocatalytic processes at Pt electrodes in methanol-air fuel cells, **37,** 1817
some factors affecting formation on Pt, **38,** 897
α-hydroxyaldehydes
selective reductions of -OH groups using tetraalkylammonium salts, **35,** 1167
2-hydroxybiphenyl
anodic oxidation to 2-phenyl-1,4-benzoquinone and scale-up, **38,** 357
hydroxylation
of benzoic acid by oxygen, catalysed by ions of dissolving metals, **37,** 345
tris(hydroxymethyl)aminomethane: voltammetric behaviour of Cu(II) complexes, **38,** 957
L-hydroxyproline
complexes with Cu^{2+}: kinetics of dissociation, **36,** 109
3-hydroxy-4-pyridinones
oxidations at glassy carbon anodes in aqueous buffers, **38,** 2223
hypernetted-chain approximation: hard charged sphere model for ionic colloidal solutions, **36,** 1761

I

imidazole
adsorption at a Au electrode from aqueous media, **38,** 947
immersion method
a new apparatus for determinations of PZCs of solid electrodes, **35,** 1393
immiscible electrolyte solutions
absolute Galvani potentials based on single ion transfer Gibbs energies, **35,** 1173
adsorption of $C_{12}H_{25}(OC_2H_4)_xOH$ (x = 4, 8 or 12) at nitrobenzene/water, **36,** 1437
alkali-metal ion transfer between water and nitrobenzene assisted by poly(oxyethylene)dodecyl ethers, **37,** 643
anodic dimerization of an aromatic amine in nitrobenzene/water, **35,** 1081
effect of crown ethers on transfer of alkali-metal ions at the nitrobenzene/water interface, **35,** 127
generalized electrocapillary equation, **35,** 715
kinetics of oxidation of ferrocene in nitrobenzene by $Fe(CN)_6^{3-}$ in water, **36,** 291

immiscible electrolyte solutions continued
non-linear regression of impedance data for ion transfer, **35,** 1359
review of interfacial electrochemistry [R], **36,** 253
thermodynamics of transfer of univalent ions from water to 1,2-dichloroethane, **37,** 231
transfer of cinchonidine between aqueous and 1,2-dichloroethane solutions, **38,** 2707
transfer of Ni^{2+} between water and nitrobenzene in the presence of 2,2'-bipyridine, **35,** 1965
impedance see also impedance spectroscopy
instantaneous: four-dimensional estimation, **37,** 2353
negative, modelling of wave propagation at electrode/electrolyte interfaces **38,** 1525
theoretical, for absorption of hydrogen in metal membrane electrodes, **38,** 2645
theoretical, of macrohomogeneous porous electrodes, **38,** 2653
theoretical, of point/plane electrode configurations, **38,** 597
impedance analysis instrumentation
a new experimental device to measure thermoelectrochemical transfer functions $\partial V/\partial T$ and $\partial I/\partial T$, **37,** 1945
use of a sub-sampling algorithm to extend the frequency range above the sampling frequency, **38,** 2079
impedance spectroscopy see also impedance and impedance studies
and admittance studies of low-frequency dispersion, **35,** 1595
of cathodic deposition processes with excess inert electrolyte, **38,** 1671
of coated metals: coating defects, porosity and delamination, **38,** 1609
of coated rough metals, **38,** 1867
complex collection efficiency, electro-optical transmittance and QMBE, **35,** 1553
data analysis for structural and parametrical estimation, **35,** 1493
dependence of Kramers-Kronig transformations on linearity, causality and stability, **35,** 1559
development of physicochemical models, **38,** 1903
of the double layer at rough electrodes, **36,** 1699
of electroactive polymer layers, **35,** 1665
of electrodeposition of metals, **35,** 1587
of electrodeposition reactions with adsorbed intermediates, **38,** 2043
of electrodes coated with precipitated porous salt films, **36,** 1183
of electron-hole recombination in semiconductor electrodes, **37,** 837
flow-modulation methods and electrohydrodynamic impedances, **35,** 1637
of fractal electrodes: frequency exponent and the Tafel slope, **35,** 1567
of fuel cells, **38,** 2063
of a fully dissociated binary equi-valent electrolyte: data analysis, **37,** 1007
high-frequency artefacts in low-conductivity media, **36,** 1093, 1385
interpretation of artefacts in low-conductance media, **35,** 1125
of irreversible electrode reactions, **35,** 831, 837
of irreversible redox reactions at fractal electrodes, **35,** 141
of localized corrosion: review and original instrumentation, **35,** 1619
of localized corrosion phenomena, **37,** 2309
of membrane systems with metal and/or ionic contacts, **35,** 1609
of metal electrodes with polymer coats containing holes which allow electrolyte penetration, **37,** 997
monitoring local corrosion of large metal structures, **35,** 1573
new developments in data analysis by CNLS fitting and by Kronig-Kramers transformations, **38,** 1883
of non-stationary systems, **38,** 1919
non-linear regression of data for ion transfer at liquid interfaces, **35,** 1359
with non-zero DC: study of a partially submerged smooth electrode, **38,** 2281
optimizing information transfer from data to mechanistic model, **35,** 1509
of painted and unpainted metals: an interactive computer analysis programme, **37,** 245
of polymer film electrodes: effects of film thickness and its non-uniformity, **36,** 847, 1527
of polymer film electrodes: a new two-capacitance model, **38,** 773
of polymer protective coatings: distinction between coating porosity and wetted metal area, **38,** 1799
of a polymer-coated electrode with a fractal surface and circular delamination around a defect site, **38,** 1433
of porous, rough and smooth solid electrodes, **35,** 1045
of porous electrodes, **35,** 1579
of porous and solid-liquid composite media, **38,** 1923
of processes involving electrosorbed intermediates: inductive behaviour, **38,** 1803
of rectifying semiconductor/electrolyte interfaces, **35,** 1631
review of treatment of complex mechanisms and concentration overpotential for metal electrodes, **35,** 1527

impedance spectroscopy continued
of rough blocking electrodes: relationship to statistics of random walks that are reflected from the electrode surface, **38,** 1985
of rough electrodes represented by a sinusoidal profile, **36,** 1083
of semiconductor electrodes, **35,** 1545
of solid polymer electrolytes: circular regression analysis, **36,** 1033
of super-Nicad cells as functions of voltage and number of cycles, **38,** 2037
of symmetric cells with potential-dependent steady-state currents, **38,** 1837
theory for Volmer-Heyrovsky mechanism: electrochemical resonance, **37,** 177
thicknesses of multilayer oxides from new interpretations of Bode diagrams, **38,** 633
unsupported conditions and CNLS fitting of data to equivalent circuits, **35,** 1483
validation of data for films of electroactive polymers on electrodes using the Kramers-Kronig transformation, **38,** 1047
validation of experimental data by analysis of discrete response spectra, **38,** 861
at various electrode potentials: three-dimensional impedance diagrams for processes involving electrosorbed intermediates, **38,** 1803
impedance studies see also impedance spectroscopy
in 0.5M K_2SO_4 aq at 20-200°C of the oxide layer formed on Zircaloy in water vapour at 400°C, **38,** 1961
in 1M $LiClO_4$-PC, of polyacrylonitrile electrodes formed by compression of thermally structurized powder, **37,** 2453
of adsorption of $C_{12}H_{25}(OC_2H_4)_xOH$ (x = 4, 8 or 12) at the nitrobenzene/water interface, **36,** 1437
of adsorption and partial charge transfer at boron-doped diamond electrodes, **37,** 973
of amorphous Nb_2O_5 anodic films in aqueous sulphate, **35,** 99
of anodes of cemented carbides [(Ta, Nb)C, M] where M = Fe, Ni or Co in 0.5M H_2SO_4, **37,** 2523
of anodic behaviour of electrodeposited Ni-P alloys (6%<P<28%) in 0.1M NaCl aq and in 0.05M Na_2SO_4 aq, **38,** 1979
of anodic behaviour of Fe-Cr alloys in 0.5M H_2SO_4, **38,** 763
of anodic behaviour of Sb in H_2SO_4 aq, **36,** 2081, 2087
of anodic behaviour of Sb and Pb-Sb eutectic in H_2SO_4 aq, **35,** 229
of anodic dissolution of Cu in 0.1M Na_2SO_4 at pH1.5, **37,** 2195
of anodic dissolution of Cu in acidic 1M Na_2SO_4 aq, **38,** 2121
of anodic films on Bi during breakdown, **38,** 511
of anodic films on $Fe_{80}B_{20}$ in borate buffer and acidic sulphate solutions, **38,** 205
of anodic films on Zr in neutral solutions, **36,** 647
of anodic formation and electrochemical properties of polyaniline films on carbon fibre electrodes in aqueous methanol, **38,** 1559
of anodic oxidation of n-GaAs in acetonitrile, **37,** 309
of Au oxidation in H_2SO_4 aq: application of a quartz crystal microbalance in an AC regime, **38,** 1827
of barrier and porous anodic oxide films on Al, **38,** 2103
of barrier-type films formed on Al in various media, **37,** 2283
of Bi anodes in glycol borate buffer [equimolar $(H_2CO)_4BH$-$(H_2CO)_4BNa$], **37,** 2415
of Ca^{2+} ion selective membranes based on the ETH1001 ionophore in poly(vinyl chloride), **37,** 2691
of cathodic degradation of polyimide-coated Al metallizations of Si substrates, **38,** 1877
of the Ce-Mo process for producing corrosion-resistant Al alloys, **37,** 2277
of a cell consisting of a small non-polarisable disc electrode and a large structure buried in soil, **38,** 1857
of cells with antimonic acid solid electrolyte, **35,** 1031
of chlorine evolution on rotating Pt thin-ring anodes in acidic aqueous chloride solutions, **37,** 2715
and optical measurements of chromate-phosphate conversion coatings on AlMn05Mg05 alloy, **38,** 2577
of conductivities of Li^+ salts in polyacrylonitrile, **37,** 1671
of corrosion of Al in neutral and acidic media, **38,** 1989
of corrosion in chemical process industries, **38,** 2075
of corrosion of Cu alloys in natural seawater promoted by microorganisms within biofilms, **37,** 2291
of corrosion of Mg in aerated 0.5M Na_2SO_4 aq, **35,** 555
of corrosion processes on inhomogeneous surfaces, **35,** 1501
of corrosion protection by coating, inhibition, anodization etc, **35,** 1533
of Cu^{2+} discharge at Cu electrodes coated with Nafion cation exchanger, **36,** 333
of Cu electrodes in 1.37HF.NH_4HF_2, **38,** 1951
of the degradation electroless Ni coatings on steel in acidic NaCl aq, **38,** 2093
of deposition and dissolution of Zn in a flow-through porous electrode, **38,** 311
determination of flat-band potential and concentration of acceptor states in $YBa_2Cu_3O_{7-\delta}$ thin films, **35,** 1219

impedance studies continued
of effect of 1.82% phosphorus content on anodic behaviour of Fe in carbonate buffer solution at 75°C, **38,** 2443
of the effect of dodecylbenzene sulphonate on the behaviour of the polypyrrole film electrode, **37,** 1173
of effect of dodecylsulphate incorporation on polypyrrole film electrodes in 1M $LiClO_4$-PC and 1M $LiAsF_6$-PC, **37,** 419
of effect of humidity on conduction mechanism in bulk and thin film $MgAl_2O_4$, **38,** 2617
of effect of molybdate ion on passivation of Ti in H_2SO_4 aq, **36,** 2069
of effects of electrochemical preteatment and of polymer coatings on redox activity of glassy carbon electrodes, **37,** 2573
of electrochromic WO_3 thin films evaporated on to ITO or fluorine-doped SnO_2 electrodes in 1M $LiClO_4$-PC, **38,** 1935
of electro-codeposition of Zn-Ni alloys from aqueous chlorides, **37,** 545
of electrodeposition of Ni on vitreous carbon cathodes, **38,** 405
of electrosynthesised conducting polymers for use a positive electrodes in secondary Li cells, **38,** 2011
of experimental alkaline and molten carbonate fuel cells, **38,** 2115
of Fe dissolution and passivation in carbonate-bicarbonate buffers, **36,** 117
of fluorine cell carbon anodes, some modified by impregnation with 0.5M $Al(NO_3)_3$ aq, **38,** 2413
of fluoropolymer coatings on low-carbon steel, **38,** 1945
of glassy carbon electrodes modified by films of cobalt(II) hexacyanoferrate, **38,** 379
of grafting and cathodic polymerization of acrylic monomers on metals, **38,** 1501
of the HER on Ni and nickel oxide anodic films, **35,** 1099
of the HER on Raney nickel cathodes in NaOH aq, **35,** 1251
of hydrogen evolution at Rh cathodes in 1M KOH aq, **37,** 1283
of impact-induced corrosion of car bodies, **38,** 2083
of inhibition of corrosion of rusted steel: effect of treatments by tannic, gallic and phosphoric acids, **37,** 1983
of inhibition of corrosion of Zn in NH_4Cl aq by addition of organic surfactants, **38,** 1453
of insertion of Li^+ into various conjugated polymers in 1M $LiClO_4$-PC, **35,** 403
of intercalation of 3R-NbS_2 by Li^+, **36,** 935
of intercalation of highly oriented pyrolytic graphite in H_2SO_4 aq, **38,** 2005
of the interface: Hg/polymer electrolyte (short PEO chains linked by -OCH_2O- and containing $LiClO_4$), **37,** 1525
of kinetics of oxidation of ferrocene in nitrobenzene by $Fe(CN)_6^{3-}$ in water, **36,** 291
of kinetics of oxygen reduction at Au cathodes in Li_2CO_3-K_2CO_3 at 923K, **38,** 2405
of $La_{0.85}Sr_{0.15}MnO_3$ cathodes in Y_2O_3-stabilized ZrO_2 at 1000°C, **38,** 2015
of layer silicates intercalated by PEO or crown ethers, **37,** 1573
of Li^+ insertion into the nickel oxide electrode from 1M $LiClO_4$-PC, **37,** 1033
of Li electrodes in propene carbonate containing organic additives, **37,** 119
of the mechanism of anodic dissolution of Cu in 1M sulphate solution, **38,** 319
of mechanism of formation of the chromate layer on Zn, **35,** 515
of network polymers [poly(propene oxide) polymerized with phenyl isocyanate] complexed with $LiClO_4$, **37,** 1511
of oxidation of Au in H_2SO_4 aq, **38,** 1023
of oxidation of HCOOH at Pt anodes in 0.5M H_2SO_4 aq, **38,** 1899
of oxygen reduction in 0.5M H_2SO_4 aq at a porous fuel-cell cathode, **37,** 523
of oxygen-transfer reactions at solid oxide/noble metal electrodes, **38,** 1817
of p-GaAs electrodes with thin electrodeposits of Au, **38,** 301
of passivation of porous carbon cathodes during reduction of $SOCl_2$-$LiAlCl_4$, **38,** 827
of the passive films on Cr and Fe-Cr alloys in 0.5M H_2SO_4 aq, **38,** 1969
of passive films on Ni(111) in phosphate buffers 9<pH<11, **35,** 1949
of passive films on Ta in acidic and neutral solutions, **38,** 2231
of passive films on Zn anodes in borate and arsenate solutions pH8.9, **36,** 1491
of passive layers formed on Fe and Fe-Cr alloys in neutral aqueous media, **38,** 1567
of passive layers on Li in $SOCl_2$, **35,** 423
of Pd and Pd-plated AISI 304 stainless steel in 1M H_2SO_4 aq, **38,** 2021
of photoelectrochemical evolution of oxygen at n-RuS_2 electrodes in $HClO_4$, 5.5M H_2O, **38,** 1929
of poly(tetracyanoquinodimethane) electrodes in LiCl aq, **36,** 1355
of the primary film on carbon electrodes in $LiAlCl_4$-$SOCl_2$, **37,** 1207
of the protection of steel by Zn-rich ethyl silicate paint in artificial seawater, **38,** 2029
of the Pt/NaF aq interface, **35,** 1177

impedance studies continued
of ramified Cu electrodeposited from $CuSO_4$ aq at high electric fields, **38,** 1941
of $RbAg_4I_5$ between graphite electrodes, **35,** 1649
of the redox mechanism of poly(3-methylthiophene), **37,** 1417
of reinforced concrete: use of guard rings to define current distribution, **38,** 2055
of relationships between adherence of paint films and protection they offer to carbon steel from corrosion in 10^{-3}M NaCl, **38,** 1999
of the reversibility of the Li electrode in polymer electrolytes, **38,** 1199
of reversible Li intercalation into pitch-based carbon fibre electrodes, **38,** 1721
of the roles of Cl^- and SO_4^{2-} in the anodic dissolution of Fe, **35,** 1601
of the roles of Cl^- and SO_4^{2-} in the anodic dissolution of Fe at 0<pH<4, **35,** 1003
of $Ru_{0.2}Ti_{0.8-x}Sn_xO_2$ ternary oxide electrodes in 1M NaCl aq, **38,** 2239
of Si electrodes in HF aq, **36,** 499
of single crystal $GaInP_2$ and $Ga_{1-x}Al_xAs$ interfaces with various aqueous solutions, **38,** 1993
of a solid ionic conductor sandwiched between two blocking electrodes, **38,** 2111
of the surface film on Li electrodes in $LiAlCl_4$-$SOCl_2$, **37,** 1211
of temperature dependence of conductivity and capacitance of polyaniline film electrodes, **38,** 2503
of thin anodic films on Al and Al-0.4%Mn alloy in borate buffer pH7.4, **37,** 1389
of thin oxide layers on pure Al and of their water content, **38,** 1957
of three-dimensional dendritic electrodeposits of Ag on Pt cathodes, **38,** 1545
of transfer of alkali-metal ions across the nitrobenzene/water interface, **35,** 127
under constant current conditions, of plasticised PVC containing neutral carriers of ionic species, **38,** 2691
of yttria-stabilized (3 mol%) zirconia modified with 0.3 mol% CuO: investigation of super-plastic deformation, **38,** 2099
inclusion complexes
of 2,2'-diazino bis(3-ethyl 6-sulphonate benzothiazole) with α-, β- and γ-cyclodextrins, **37,** 149
inclusion compound
of ferrocene in deoxycholic acid (1:2) as a positive electrode for zinc-iodine secondary cells, **38,** 1373
indifferent electrolyte see supporting electrolyte
indirect reduction/oxidation see mediators
indium
anodic behaviour in NaCl aq at 2<pH<12.6, **36,** 2063
anodic behaviour in NaOH aq, **35,** 329
indium arsenide
photoelectrochemical processing, **38,** 101
indium hexacyanoferrate
spectroelectrochemical studies of SnO_2 electrodes modified with, **35,** 1057
indium phosphide
photoelectrochemical etching, **38,** 95
photoelectrochemical processing, **38,** 101
n-indium phosphide
flat-band potential as a pH probe in non-aqueous and mixed solvents, **38,** 781
optoelectrical impedance study of anodic dissolution in HCl aq: competition between electron injection and hole capture, **38,** 2559
optoelectrical impedance study of anodic dissolution in HCl aq: photocurrent enhancement by HIO_3, **38,** 2569
photoanodic behaviour in aqueous electrolytes, **37,** 289
indium selenide electrodes
effects of modification in copper-polyiodide solutions, **35,** 1631
indium sulphide
flat-band potentials of thin film electrodes on Ti substrates, **35,** 345
indium tin oxide electrodes
adsorption of ferrocenyl undecyltrimethylammonium ion, **35,** 885
coated with Nafion film containing tris(2,2'-bipyridine)Ru(II): photoelectrochemical reduction of oxygen with viologen mediator, **38,** 129
dependence of reversibility of Fe(II/III) and $Fe(CN)_6^{3-/4-}$ redox couples on preparation of the thin films, **37,** 2565
deposition of CdS from aqueous solutions of Cd^{2+} and $S_2O_3^{2-}$, **38,** 2395
electrochromic behaviour of poly(*o*-anisidine) and poly(*o*-toluidine) films, **37,** 1653

indium tin oxide electrodes continued
electrochromic behaviour of films of polyanilines formed at ITO anodes in 1,2-dichloroethane-0.1M TBA^+ salt, **37,** 2101
electrochromic behaviour of films of polypyrrole doped with dodecylbenzene sulphonate, **37,** 2101
electrochromic behaviour of WO_3 evaporated thin films in 1M $LiClO_4$ -PC, **38,** 1935
filmed with poly(methylthiophene), **36,** 837
filmed with polypyrrole-dodecylsulphate, **35,** 1145
as terminal layers of a photochemical diode containing a Nafion bilayer including $Ru(bpy)_3^{2+}$ and viologen, **38,** 1093
optically passive counter electrodes in electrochromic devices, **35,** 1757
reduction factor of polyaniline films, **38,** 1643
with sputtered cobalt oxide films: Raman spectroscopy, **35,** 975
visible absorption spectra of poly(pyrrole-alkylammonium) films containing porphyrins of Fe(III), **38,** 2485
inert electrolyte see supporting electrolyte
infrared irradiation
relaxation of conductivity of aqueous electrolyte solutions, **35,** 861
infrared reflectance spectroscopy
electrochemically modulated, study of chemisorption of small organic molecules, **35,** 679
study of effect of cathode material on $SOCl_2$ reduction in $AlCl_3$, **35,** 1787
infrared spectroscopy
attenuated total reflection using BaF_2 with Au and Pt electrodes, **38,** 695
attenuated total reflection using thin sputtered films of Au or Pt on Ge or GaAs IR-transparent crystals, **37,** 2321
of cobalt oxide films sputtered on to Si substrates, **35,** 975
of complexes of branched poly(ethene imine) with CF_3SO_3Li, **37,** 1623
FT studies of $LiNi_{1-x}Co_xO_2$ positive electrodes for secondary lithium cells, **38,** 1159
FT study of Li surfaces in 1,3-dioxolane, **37,** 1897
FT study of $M(CF_3SO_3)_2PEO_n$ with M = Zn or Pb and n = 9, 16 and 24, **37,** 1689
ion association in complexes of PPO with LiSCN, NaSCN, KSCN, $LiClO_4$, $NaClO_4$ and $LiBF_4$, **37,** 1499
of metal phthalocyanines and carbon cathodes doped with them before sintering, **37,** 531
of polypyrroles formed by anodic and chemical oxidations, **36,** 733, **37,** 1227
surface-sensitive FTIR study of electrodes in 1,3-dioxolane-$LiClO_4$, **35,** 625, 639
infrared spectroscopy, electrochemically modulated
of manganese oxide during reduction in aqueous borate, **38,** 341
infrared spectroscopy, *in situ* FTIR study
of adsorbed species at Pt from methanol, HCOOH and reduced CO_2, **37,** 2361
of adsorption of $H_2PO_4^-$ and H_3PO_4 on Pt, **37,** 385
of adsorption and oxidation of ethanal on Pt electrodes in 0.1M $HClO_4$, **35,** 989
cylindrical internal reflection applied to hydrous oxide/aq solution interfaces [A], **36,** 1891
growth, cycling and over-oxidation of polypyrrole in 1M $NaClO_4$ aq, **36,** 1263
of influence of water on oxidation of 0.5M $LiClO_4$-PC at Pt anodes, **36,** 1397
of phenazine and phenothiazine dye films at polycrystalline Au electrodes, **38,** 1619
of potential-dependent properties of CO adsorbed on Pt electrodes, **38,** 1107
second-order Stark effect in SO_4^{2-} adsorbed at Pt electrodes, **37,** 2179
of the Si/electrolyte interface, **37,** 889
theoretical and actual spectra of adsorbed CN^- and SCN^- on solid electrodes, **36,** 1863
infrared thermography
temperature profile in a Nafion membrane during water electrolysis, **36,** 263
inhibition
by adsorbed anions, of the oxidation of D-glucose at single-crystal Au anodes in aqueous acids, **37,** 357
of the $Cd(Hg)/Cd^{2+}$ reaction: a measure of θ for adsorption of surfactants at Hg electrodes, **37,** 2395
of electron transfer by an adsorbed monolayer of cetyl alcohol, **36,** 421
inhibition of corrosion
adsorption of 1-hydroxyethane-1,1-diphosphonic acid at steel, **36,** 981
by adsorption of 1-octyn-3-ol on Fe in HCl aq, **36,** 1333
of Cu in 0.5M H_2SO_4 by formation of surface layers of 3-amino-5-heptyl-1,2,4-triazole, **37,** 2299
of Cu by benzotriazoles, **35,** 1011
of Fe in benzoate buffers, **37,** 489
of Fe and mild steel by adsorption of polyacrylamide, **36,** 1315
investigations using impedance spectroscopy, **35,** 1533

inhibition of corrosion continued
kinetics of adsorption of acetylenic alcohols on Fe from H_2SO_4 aq, **37,** 317
of rusted steel: effect of treatments by tannic, gallic and phosphoric acids, **37,** 1983
of Zn by "Forafac" surfactant in aqueous NH_4Cl and alkali electrolytes, **35,** 479
of Zn in NH_4Cl aq by addition of organic surfactants, **38,** 1453
inhibition of electrodeposition
of Pb dendrites by lignin sulphonate and extract of horse chestnut: effects of potential and RDE speed, **37,** 2249
of Sn from $SnSO_4$ aq by aromatic carbonyl compounds, **37,** 2403
instability see also oscillations
of systems with concentration polarization and negative resistance, **36,** 143, 321
integral transforms
improvements over K-K and Fourier transforms with regard to treatment of noise, **38,** 1883
intercalation see also lithium cells
by Li^+, of $Na_{1+x}V_3O_8$ formed by precipitation, **36,** 1549
by Li^+ of transition-metal oxides and sulphides: analogies with UPD and adsorption processes, **38,** 1249
by Li of pitch-based carbon fibre negative electrodes with radially-oriented graphite structures, **38,** 1721
of carbons by Li: suitable negative electrodes for secondary lithium cells, **38,** 1179
of graphite by metal hydroxides: positive electrodes of alkaline secondary batteries, **36,** 591
of highly oriented pyrolytic graphite in H_2SO_4 aq, **38,** 2005
of layer silicates by PEO or crown ethers to change conductivity by associating interlayer cations, **37,** 1573
of $Li_xV_6O_{13}$ by Li^+: *in situ* X-ray diffaction study, **37,** 1639
of γ-MnO_2 electrodes by Na^+ from 1M $NaClO_4$-PC, **37,** 603
of polyethyne by Li^+, Na^+ and K^+ from PEO-based solid electrolytes, **37,** 1675
of SnS_2 single crystal electrodes by K^+ aq: photoassistance, **36,** 1197
of sol-gel lamellar birnessite $MnO_{1.84}$, $0.64H_2O$ by Na^+, **38,** 1695
of sol-gel laminar birnessite $MnO_{1.84}$,$0.6H_2O$ by Li^+, **36,** 1595
of sputtered thin amorphous V_2O_5 films by Li^+ from $LiClO_4$-PC: electrochromism and stress, **38,** 1637
of thin sputtered nickel oxide films by alkali metal cations, **38,** 2765
of $Ti_{1+y}S_2$ by Li^+: dependence of potential on Fermi levels, **36,** 1555
of various hosts by lithium, particularly carbons and $Li_{1+x}Mn_2O_4$ [R], **38,** 1221
interface between two immiscible electrolyte solutions see immiscible electrolyte solutions
interfacial capacitance
in surface-inactive electrolyte solutions, **36,** 401
interferometer
modified Michelson instrument to measure strain in electrodeposits, **35,** 1989
internal reflection
in thin semiconductor metal oxide films: effect on photocurrents at TiO_2, **38,** 15
International Society for Electrochemistry
its foundation, **36,** 1
iodide ions
induction of current oscillations during pitting corrosion of Co in H_2SO_4 aq, **38,** 835
oxidation at Pt RDE in aqueous and organic $HClO_4$, **36,** 1057
iodine(III or V) organic compounds
reductions at Hg and Pt cathodes in acidic and neutral media, **36,** 1391
iodine-dialkylsulphide mixtures
conductimetric and spectroscopic studies of complexes, **35,** 355
ion association
in complexes of poly(propene oxide) with LiSCN, NaSCN, KSCN, $LiClO_4$, $NaClO_4$ and $LiBF_4$, **37,** 1499
conductances of silver halides and pseudohalides in pyridine solutions, **35,** 509
during chemical oxidations and reductions of organic compounds, **36,** 2171
importance during electrodeposition of Zn from $ZnSO_4$-Na_2SO_4-aq, **37,** 439
of Li^+ and BF_4^- in poly(ethane-1,2-diol), **37,** 1533
in $M(CF_3SO_3)_2PEO_n$ with M = Zn or Pb and n = 9, 16 and 24: FTIR absorption spectra, **37,** 1689
in $NiBr_2(PEO)_8$, **37,** 1663
perchlorates of Mn(II), Co(II), Ni(II), Cu(II) and Zn(II) in propanone solutions, **35,** 351
of potassium monoethylbenzeneazophosphonates with crown ethers in acetonitrile, **35,** 59
of protonated pyridine N-oxides with perchlorate in acetonitrile, **35,** 665
and solvation in polymer hosts: effects of temperature and pressure, **37,** 1505

ion exchange
with acetonitrile solutions: incorporation of Fe(III) ions into Y zeolites, **37,** 2411
between Na^+ and MV^{2+} in zeolite in carbon paste electrodes, **38,** 2257, 2267
mechanisms in films of polypyrrole and poly(N-methylpyrrole) doped with tosylate, **38,** 349
ion exchange, syntheses of new polymer reagents
I^- replacement by anodic oxidation of polymer solutions containing the entering anion, **37,** 751
ion-exchange membranes
calculation of permselectivity at various molarities, temperatures and current densities, **38,** 815
composite with the cathode of a chlorine cell, **38,** 2431
computation of diffusion across a weak acid membrane, **38,** 329
concentration profiles of $^{137}Cs^+$ in perfluorosulphonic acid membranes, **37,** 221
with deposited metal electrode layers: proton transport in Nafion 117 between aqueous and organic solutions, **38,** 2171
impregnated with a layer of conducting polymer: EMF across the bilayer, **37,** 555
oxidation of gaseous methanol in 0.5M H_2SO_4 at Pt-SPE electrodes modified with molybdenum, **35,** 323
property shown by guest 4-nitrophenolate in α-cyclodextrin host films on vitreous carbon electrodes, **37,** 1109
solubility and diffusion coefficient of oxygen in Flemion, **38,** 1727
ion implantation
of Li^+ and K^+ into vitreous carbon with 150keV, **35,** 1279
ion-pair clusters
in concentrated aqueous solutions of monovalent electrolytes, **35,** 861
ion pairing see ion association
ion permeability
in transmembrane channels: influence of peptide charge distribution, **36,** 1753
ion-selective electrodes
electron transfer and adsorption at interfaces between immiscible electrolyte solutions [R], **36,** 253
properties of PVC-based membranes [R], **35,** 1
ion-selective membranes
for Ca^{2+} based on the ETH1001 ionophore in poly(vinyl chloride), **37,** 2691
of plasticised PVC: impedance at constant current, **38,** 2691
ion-sensitive field-effect transistors
photopolymerization of ion-selective membranes on to silicon nitride, **35,** 777
ion solvation
Li^+ by bis[2-(2-methoxyethoxy)ethyl] ether: effect of propene carbonate, **37,** 2043
and pairing in polymer hosts: effects of temperature and pressure, **37,** 1505
ion transfer
across the interface between two immiscible electrolyte solutions [R], **36,** 253
of Ag(I) 222 cryptate between binary aprotic solvent mixtures, **37,** 413
between immiscible electrolyte solutions: absolute Galvani potentials, **35,** 1173
determination of electrostatic component of free energy, **36,** 435
free energy for Ag(I) between acetonitrile and polar solvents, **36,** 1427
from water to 1,2-dichloroethane: standard Gibbs energies for univalent ions, **37,** 231
of NEt_4^+ from water to plasticized PVC membranes, **37,** 1021
conductivity of AgI-poly(N-alkylene dimethyl-N,N'-piperazinium diiodide) double salts, **35,** 77
ion-transfer kinetics
of alkali-metal cations at the water/nitrobenzene interface: role of crown ethers, **35,** 127
of Ni^{2+} between water and nitrobenzene in presence of 2,2'-bipyridine, **35,** 1965
ionene glasses
polyelectrolytes with bound cationic nitrogen and mobile anions: dielectric relaxation, **37,** 1491
ionene polyelectrolyte
NMR study of molecular dynamics of $[-(CH_2)_{10}N^+(CH_3)_2-]_n.nBF_4$, **37,** 1657
ionenes
ionic entropies
from non-isothermal cell potentials in non-aqueous media, **38,** 997
ionic mobilities
of monovalent cations in molten salt mixtures, **35,** 1761
iridium electrode
oxidations of hydrazine, methanol, HCHO and $HCOO^-$ in aqueous alkali, **35,** 1829
oxidation of methanoic acid as a function of pH, **38,** 1631

iridium electrode continued
surface skeleton: behaviour in oxidations of simple organics and various adsorptions, **35,** 191
iridium oxide electrode
electrochromic charge-storage reaction, **37,** 429
physical electrochemistry of ceramic oxides [R], **36,** 225
iridium oxide-tantalum oxide electrode
effect of preparation conditions on structure, **36,** 991
iridium-tin oxide electrode
compared with Ir anodes for the oxidation of methanol, **37,** 1317
iridium-implanted Ti anodes
catalysis of chlorine evolution and XPS characterization of anodic layers, **38,** 1313
iron see also iron electrode
anodic dissolution in aqueous acidic media: roles of Cl^- and SO_4^{2-}, **35,** 1601
anodic dissolution in H_2SO_4 aq: effect of forcing conditions on current or potential oscillations, **37,** 1047
anodic dissolution in LiF-NaF-KF eutectic at 600°C, **37,** 2433
anodic dissolution and passivation: reaction orders with respect to acetate and hydrogen ions, **37,** 477
anodic dissolution and passivation: reaction orders with respect to benzoate and hydrogen ions, **37,** 489
anodic oxidation to ferrate(VI) in 14M NaOH aq: dependence of current yields on frequency of superimposed AC, **38,** 1717
anodic passivation in H_2SO_4 aq, **38,** 495
cathodic boriding in molten sodium tetraborate, **36,** 41
comparison of electrochemical behaviour in 0.5M H_2SO_4 with $FeGe_2$, $FeGe_2$-Ge eutectic and Ge, **36,** 1247
current oscillations induced by Cl^- at anodes in H_2SO_4 aq, **38,** 2321
dissolution and passivation in carbonate-bicarbonate buffers, **36,** 117
effect of 1.82% phosphorus content on anodic behaviour in carbonate buffer solution at 75°C, **38,** 2443
effect of acetonitrile on anodic behaviour of microelectrodes in acidic aqueous perchlorate, **35,** 501
effect of Cl^- on current oscillations at the active-passive transition in 2M H_2SO_4, **37,** 2067
effect of Cl^- on passivity and passivity breakdown in alkaline media, **35,** 1437
effect of SCN^- on corrosion and passivity in borate buffers, **36,** 505
effect of SO_3^{2-} on anodic passivation, **36,** 911
effect of various cations on anodic behaviour in alkali, **36,** 1143
electrocrystallization mechanism, **38,** 1783
electropolishing in H_3PO_4-H_2SO_4: rate-limiting mass transfer of Fe(III), **37,** 2469
hydrogen permeation through passive films in borate buffers, **36,** 825
impedance studies in 1M H_2SO_4 aq, **35,** 1559
impedance studies of passive layers formed on Fe and Fe-Cr alloys in neutral aqueous media, **38,** 1567
influence of surface structure on anodic dissolution mechanism in acidic aqueous sulphates, **35,** 163
mechanism of deposition of Fe-Co alloys on vitreous carbon cathodes from sulphate baths pH4, **38,** 671
mechanism of formation of a passive film in neutral aqueous phosphate, **38,** 2547
Mossbauer spectroscopy of the passive anodic film formed in 0.5M Na_2SO_4-0.001M $NaHSO_3$ aq, **38,** 2253
open-circuit discharge of negative electrodes in Ni-Fe cells, **36,** 369
oscillations during anodic dissolution in H_2SO_4, **36,** 1301
passivation in concentrated aqueous and non-aqueous solutions of H_2SO_4, **37,** 1069
a photoelectrochemical imaging study of passive films in Na_2SO_4 aq and in NaOH aq, **38,** 71
Pourbaix-type diagrams for complexes with phenanthroline in aqueous sulphate, **35,** 209
roles of Cl^- and SO_4^{2-} on anodic dissolution in $0<pH<4$, **35,** 1003
SERS study of passive films in aerated 5M KOH and 0.15M NaCl aq, **37,** 2747
variation of field strength, oxide thickness and anodic current with time in aqueous boric acid, **37,** 327
iron(II) tris(2,2'-bipyridyl) complex
SERS study of adsorption at Ag electrodes, **37,** 2347
iron boride
formation on Fe cathodes in molten sodium tetraborate, **36,** 41
iron chelators
oxidations of four 3-hydroxy-4-pyridinones at glassy carbon anodes in aqueous buffers, **38,** 2223
iron-chromium alloys
anodic behaviour in 0.5M H_2SO_4, **38,** 763
studies of the passive films in 0.5M H_2SO_4 aq by potential-modulated ellipsometry and impedance spectroscopy, **38,** 1969
iron-chromium(-Mo) alloys
role of Mo in passivation in 0.5M H_2SO_4 aq, **36,** 1465

iron(III) complexes
with N-phenylbenzohydroxamic acid and N-methylbenzohydroxamic acid, **37**, 205
iron(II/III) couple
at 3.5<pH<6.5 in the presence of EDTA: mechanism at Pt electrodes, **35**, 1325
electrode kinetics at Pt in DMSO, **36**, 471
iron(III) dionato complexes
reduction at vitreous carbon cathodes in DMF-TBAP containing Cl^-, **38**, 653
iron electrode see also iron
diffusion of cathodically-generated atomic hydrogen, **36**, 615
effect of chromate on oxidation in hydroxide and chlorate solutions, **37**, 1873
kinetics of adsorption of 1-octyn-3-ol in HCl aq, **36**, 1333
kinetics of adsorption of acetylenic alcohols from H_2SO_4 aq, **37**, 317
oxidation of H_2O_2 in alkaline solutions, **37**, 1845
permeation of hydrogen electrogenerated in liquid ammonia, **36**, 283
reduction of hydrogen peroxide in alkaline media, **36**, 5
iron electrode (liquid)
$p(O_2)$ in Fe(l) and in the CaO-Al_2O_3-Fe_2O_3-FeO-CaS melt at 1600°C, **36**, 1027
iron(III) hydroxides
anodic oxidation in alkalis, **36**, 1253
iron(III) hydroxo complexes
adsorption on $Ni(OH)_2$ and NiOOH powders from aqueous alkali, **37**, 469
catalysis of oxygen evolution at nickel hydroxide anodes in aqueous alkali, **37**, 607
iron(III) ions
incorporation into Y zeolites by ion exchange with acetonitrile solutions, **37**, 2411
iron-nickel alloys
effects of Cl^- and alloy composition on passivation in H_2SO_4 aq, **35**, 69
iron oxide
doped with Zn: photoelectrochemical and semiconductor properties, **36**, 1585, **37**, 425
iron(III) oxide electrode
generation of AC and DC electric power from intermittent illumination in aqueous buffer, **37**, 1101
iron, passive
concentration and distribution of pits in borate buffer with Cl^-, **35**, 1809
iron phthalocyanine, tetrasulphonated
adsorption at pyrolytic graphite electrodes, **36**, 2165, **37**, 769
iron(III) porphyrin
incorporated into poly(pyrrole-alkylammonium) films: reactivity towards NO in acidic aqueous media, **38**, 2485
iron porphyrin
oxygen reduction catalysed by a cationic-anionic porphyrin ion complex, **36**, 703
iron protoporphyrin modified electrode
effect of pH on stability of electrocatalytic activity for reduction of H_2O_2, **35**, 1227
iron pyrites
photoanodic oxidation of polyiodides after thermal activation in air, **38**, 123
iron sulphide
electrodeposition on Pt from 1,2-dihydroxyethane containing $FeCl_2$ and S_8, **36**, 581
iron(IV) sulphide
photocurrents and potential-dependent electrolyte electroreflectance of n-FeS_2, **37**, 957
iron sulphide electrodes
as positives in high temperature secondary lithium cells with LiCl-LiBr-KBr eutectic electrolytes, **38**, 1269
iron tetraphenylporphyrin
pyrolysed: ESCA and electrochemical studies, **37**, 187
pyrolysis of films sublimed on to carbon black surfaces: oxygen reduction catalyst, **38**, 2493
irreversible electrode reactions
equations for faradaic admittance under potentiostatic control, **35**, 831, 837
L-isoleucine
complexes with Cu(II) in aqueous media, **35**, 999
Isoniazid
reduction at Hg cathodes in DMF, **36**, 1019
isonicotinic acid hydrazide
reduction at Hg cathodes in aqueous acid, **37**, 1147

isopolymolybdate anions
electrochemical reactions within a polyaniline film on a carbon fibre microelectrode, **38,** 1029
isopolymolybdic acid
modification of carbon fibre microelectrodes by dip-coating, **37,** 1859
preparation of thin films on carbon fibre electrodes, **37,** 11
isotachophoresis
in a capillary: study of electrochemical parameters of micelles derived from ionic surfactants, **37,** 2769
isotope kinetic effect
in HER on Hg above 100°C in light and heavy water, **36,** 411

K

Karl Fischer reagent
oxidations of I^- and SO_2 at Pt RDE in aqueous and organic $HClO_4$, **36,** 1057
Kelvin dynamic-capacitor method
Volta PD of α-cyclodextrin polymer film electrode in 4-nitrophenol aq, **37,** 1109
kinetic effective water content
effect on passivation of Ni in H_2SO_4-H_2O-MeOH, **35,** 9
kink-site density
dependence on current density during anodic oxidations of Nb and Ta, **36,** 1443
Kolbe reaction
at Pt examined by non-steady state potential methods, **35,** 1237
Kramers-Kronig transformations
of impedance spectra for mechanistic models, **35,** 1509
new forms of the relationships and transformation of random errors: alternative new integral transforms, **38,** 1883
sensitivities to linearity, causality and stability, **35,** 1559
validation of impedance data for electrodes with films of electroactive polymers, **38,** 1047

L

Langmuir-Blodgett films
of dimethyldioctadecylammonium salts on vitreous carbon cathodes, **35,** 1167
photo-induced electron transfer from donor to sensitizer in neighbouring layers, **36,** 1793
lanthanide(III) complexes
CV and RDE studies of (acac)Ln tetraphenyl porphyrinates in 0.1M TEAP-DMSO, **38,** 689
lanthanide(III) perchlorates
polarography in DMSO containing TBA(acac) or TBA(dibm), **35,** 1713
lanthanide(III) phthalocyanines
syntheses of $Li[(Pc)Ln(acac)_2]$ and (Pc)Ln(acac) and electrochemistry at Pt electrodes in DMSO-TEAP, **35,** 1707
lanthanum chromium oxides
$La_{1-x}M_xCrO_3$ where M = Sr or Ca: film formation on metals by cathodization and pyrolysis, **37,** 2421
lanthanum(III) ions
incorporation into deposits of NiOOH on Pt anodes from solutions containing Ni^{2+} and La^{3+}, **38,** 1145
lanthanum strontium manganite cathode
oxygen reduction in yttria-stabilized zirconia at 1000°C, **38,** 2015
lanthanum(III) alizarin complexone complex
effect of F^- on reduction mechanism at Hg in $(CH_2)_6N_4$-HNO_3, **35,** 1861
Laplace equation
new solutions for various cell geometries based on Taylor series expansions, **38,** 2525
Laplace transformation
of photocurrent transients to obtain frequency-dependence of the response, **38,** 1913
laser Doppler velocimetry see also velocity profiles
measurements of velocity fields in a Cu-refining cell, **36,** 1345, **37,** 373

laser Doppler velocimetry continued
study of a Cu-refining cell: influence of support electrolyte, **37,** 695
study of free convection in a discharging lead-acid cell, **36,** 2153
study of lead-acid cells with and without separators, **37,** 681
laser light scattering
monitoring of electrodeposits, **37,** 2115
laser-probe beam deflection
by concentration gradients at electrodes: determination of diffusion coefficients in potential-step experiments, **37,** 429
lattice gas, non-interacting
model for ion association and solvation in polymer electrolytes, **37,** 1505
lead see also lead electrode
anodic behaviour in H_2SO_4 aq, **37,** 199
anodic dissolution in 0.5M $HClO_4$ aq, **35,** 1213
anodic formation of a PbO film in H_2SO_4 aq and its reduction under a $PbSO_4$ layer, **37,** 495
anodic formation of $PbSO_4$ in 5M H_2SO_4, **38,** 1513
anodic underpotential monolayer formation of $PbBr_2$ from aqueous media, **37,** 739
effect of H_2SO_4 on anodic dissolution in $HClO_4$, **36,** 197
effect of Sb on anodic behaviour in H_2SO_4 aq, **36,** 605
effect of underpotential deposits at Pt electrodes upon glucose oxidation, **38,** 2725
effect of underpotential deposits on products of oxidation of D-gulonic acid at smooth Pt anodes in 0.1M NaOH aq, **38,** 1359
inhibition of electrodeposition of dendrites by lignin sulphonate and extract of horse chestnut, **37,** 2249
kinetics of passivation in phosphate solutions, **35,** 799
potentiometric stripping analysis and speciation in environmental studies, **38,** 807
potentiostatic reduction of anodic, Pb^{2+}-containing layers in 5M H_2SO_4, **37,** 1119
simultaneous UPD with Tl at Ag electrodes, **36,** 1291
slow structural transformations of UPD Pb on Ag(111) at low coverages, **36,** 1259
underpotential-deposited: catalysis of reduction of nitrate in aqueous alkali at Au cathodes, **38,** 2773
UPD on Ag(111): model for transformations at high coverages, **38,** 387
UPD on Ag from acidic aqueous perchlorate, **36,** 1959
UPD on Ag single crystals, **37,** 2173
UPD at Ag(111): slow structural changes at high coverages, **36,** 2077
UPD on polycrystalline Ag, **36,** 1873
lead-acid cell
contact resistance between active PbO_2 and the Pb grid: effects of time, discharge level and acid concentration, **37,** 1805
free convection during discharge, **36,** 2153
free convection and stratification of electrolyte during cycling, **37,** 681
mathematical model of oxygen transport in a hermetically sealed cell, **38,** 935
lead-bismuth alloys
effects of grain macrostructure and surface morphology on hydrogen evolution in H_2SO_4 aq, **37,** 269
lead bromide
underpotential monolayer formation on Pb anodes in aqueous media, **37,** 739
lead(II) chloride
conductivity of aqueous solutions: $\lambda°$ for Pb^{2+} and $PbCl^+$ and $K°$ for $PbCl^+$ and $PbCl_2$, **37,** 2519
lead dioxide
deposition on vitreous carbon anodes from various aqueous Pb^{2+} solutions, **36,** 2031
effects of As(III), nitrate, sulphate and phosphate on electrocrystallization on Au anodes, **37,** 1811
formation from Pb(II) on a SnO_2/Ti anode: effects of Cu(II) and acetate ions, **38,** 2749
lead dioxide anodes
electrocatalytic activity in oxidation of Cr(III), **38,** 437
lead electrode see also lead
electrodeposition of Cd in 0.5M H_2SO_4 aq, **35,** 577
cathodic reduction of ethyl picolinate in H_2SO_4 aq, **37,** 625
ring-disc studies of soluble intermediates formed in H_2SO_4 aq, **36,** 953
lead ions
adsorption at Hg electrodes induced by Br^-, **35,** 1701
lead oxide see also lead dioxide
kinetics of reduction of the film on Pb-Sb alloy electrodes in H_2SO_4 aq, **38,** 1131

lead(II) oxide
cathodic reduction of a film on Pb under a $PbSO_4$ layer, **37,** 495
potentiostatic reduction of layers formed on Pb anodes in 5M H_2SO_4, **37,** 1119
lead oxides
electrochemical behaviour in a carbon paste electrode in 0.1M NaOH binder, **36,** 277
electrochemical behaviour in H_2SO_4 aq, **37,** 199
lead phosphate
kinetics of formation at Pb anodes, **35,** 799
lead sulphate
electrochemical behaviour in H_2SO_4 aq, **37,** 199
formation on Pb anodes in 5M H_2SO_4, **38,** 1513
potentiostatic reduction of layers formed on Pb anodes in 5M H_2SO_4, **37,** 1119
lead tetraacetate
electrogenerated from $Pb(OAc)_2$: acetoxylation of ketones, **36,** 1165
lead(IV)-thallium(III) mixed oxide
deposition at stainless steel anodes from 0.005M $TlNO_3$-0.1M $Pb(NO_3)_2$-5M NaOH aq, **38,** 2551
ligands, tetradentate
reductions at Hg cathodes in 0.1M TBAP-DMF, **36,** 1997
limonene
oxidation at Pt anodes in MeCN-$LiClO_4$ containing Br^-, **35,** 497
oxidation at Pt anodes in MeOH-TEABr, **35,** 1163
liquid chromatography
peak broadening data to obtain diffusion coefficients of trace ions, **36,** 309
liquid crystalline polymers
containing triad aromatic mesogenic blocks and flexible ion-complexing oligo-oxyethene blocks, **37,** 1479
liquid-junction potentials
between aqueous bromide solutions, from EMF data, **35,** 371
calculated from concentration profiles, **35,** 367
calculation of concentration profiles from simulated diffusion, **35,** 361
calculated for KCl(4M)//X(0.001-4M) where X = NaCl, LiCl, HCl, NaOH, $LaCl_3$, Li_2SO_4 etc, **37,** 719
calculated temperature-dependence, **37,** 719
liquid/liquid interface <u>see</u> immiscible electrolyte solutions
lithium <u>see also</u> lithium electrode
accumulation of Na impurity at freshly cut surfaces: effect on passive layer formation in $LiAlCl_4.3SO_2$, **37,** 731
FTIR study of surfaces exposed to 1,3-dioxolane, **37,** 1897
reaction with THF modelled by THF reaction with Na-Cs alloy, **35,** 1061
lithium-aluminium alloys
effect of Li^+ and CO_3^{2-} on corrosion of pure Al, **37,** 2659
lithium cells
ESR spectroscopy of V_2O_5 cathodes intercalated by Li^+ from 1M $LiAsF_6$-PC-EC-DME, **37,** 2755
immobilization of liquid electrolytes in 1,3:2,4-di(*p*-methoxycarbonylbenzidene)sorbitol gel, **38,** 1301
influence of CuO microstructure on cathodic discharge, **35,** 245
intercalation of $Ti_{1+y}S_2$ by Li^+: dependence of potential on Fermi level, **36,** 1555
organic solvents for lithium salt electrolytes, **35,** 1257
with superconductor $YBa_2Cu_3O_7$ cathodes, **36,** 381
lithium cells, secondary
$AgCr_3O_8$ positive electrodes, **38,** 1211
analogies between intercalated positive electrode behaviour and adsorption and UPD processes, **38,** 1249
capacity loss due to crystalline-to-amorphous transition with cycling of V_6O_{13} positive electrode, **37,** 1715
cathode materials, anode materials and electrolytes [R], **38,** 1169
composite polyaniline-2,5-mercapto-1,3,4-thiadiazole positive electrode, **37,** 1851
direct comparisons of positive electrodes in cycling tests, **37,** 63
effect of crystal stucture on suitability of carbons as intercalated negative electrodes, **38,** 1179
effect of incorporation of dodecylsulphate on performance of polypyrrole-film positive electrodes, **37,** 419
heat generation due to irreversible transitions in Li_xMnO_2, **36,** 489
high temperature Li(Al)/FeS and Li(Al)/FeS_2 cells with LiCl-LiBr-KBr eutectic electrolytes, **38,** 1269
history of development in Japan [R], **38,** 1169
impedance study of electrosynthesised conducting polymers used as positive electrodes, **38,** 2011
improvements in the behaviour of WO_3 positive electrodes, **38,** 431

lithium cells, secondary continued
intercalation of cubic and layered polymorphs of TiS_2 by Li^+, **36,** 569
intercalation of precipitated $Na_{1+x}V_3O_8$ by Li^+, **36,** 1549
intercalation of sol-gel laminar birnessite $MnO_{1.84}$,$0.6H_2O$ by Li^+, **36,** 1595
the $Li_{1+x}Mn_2O_4$ rocking chair system [R], **38,** 1221
with $LiAsF_6$ electrolyte in EC-HCOOMe, EC-MeCN and EC-MeCOOMe solvents, **35,** 383
$LiNi_{1-x}Co_xO_2$ positive electrodes in 1M $LiClO_4$-PC, **38,** 1159
memory effect due to first-order phase transition in Li_xMnO_2, **36,** 1469
negative electrodes of pitch-based carbon fibres with radially-oriented graphite structures, **38,** 1721
new PEO-based electrolyte for lithium-polybithiophene cells, **35,** 1781
3R-NiS_2 as a positive electrode material, **36,** 935
passivation of porous carbon cathodes during reduction of $SOCl_2$-$LiAlCl_4$, **38,** 827
polybithiophene positive electrode with PEO-$LiClO_4$ electrolyte, **35,** 251
poly(N-oxyalkylpyrrole) positive electrodes in $(PEO\text{-}SEO)_{20}LiClO_4$ and liquid electrolytes, **37,** 1631
preparation and electrochemical behaviour of new positive-electrode materials MnO_2.xV_2O_5, **37,** 1039
reversible insertions of Li^+ into Cr_8O_{21} and $LiCr_3O_8$, **36,** 127
synthesis and structural stability of ramsdellite MnO_2, a positive electrode material, **38,** 1259
thick film poly(*p*-phenylene) positive electrodes: preparation and performance, **37,** 1093
vanadium oxide xerogels as positive electrodes, **38,** 1215
various aspects of current research and development [R], **38,** 1233
X-ray absorption study of organo-disulphide positive electrode based on poly(trithiocyanuric acid), **37,** 1635
lithium electrode
cycling in solutions of $LiClO_4$ in 1,3-dioxolane, **35,** 625, 639
effect of organic additive on impedance behaviour and cycling efficiency in propene carbonate, **37,** 119
reversibility in polymer electrolytes, **38,** 1199
surface film in $LiAlCl_4$-$SOCl_2$, **37,** 1211
lithium-ion conductors
polyethers from acrylate esters of polyols, plasticized with PC or EC, **37,** 1681
lithium ions
anodic insertion into ScO, TiO and VO, **35,** 17
conduction in complexes of branched poly(ethene imine) with CF_3SO_3Li, **37,** 1623
conduction in solid electrolytes based on poly(dimethylsiloxane), **37,** 1183
conduction in solid polymers of 1,3-dioxolane and of tetrahydrofuran, **36,** 773
insertion into $AgCr_3O_8$, **38,** 1211
insertion into the nickel oxide electrode: electrochromic behaviour, **37,** 1033
insertion into sputtered thin amorphous V_2O_5 films from $LiClO_4$-PC: electrochromism and stress, **38,** 1637
insertion into various conjugated polymers from 1M $LiClO_4$-PC, **35,** 403
insertion into $YBa_2Cu_3O_{7-\delta}$ superconductor from 1M $LiClO_4$-PC, **35,** 995
specific inhibition of dissolution of synthetic goethite in alkalis, **36,** 1253
structural modifications in V_2O_5 caused by intercalation of, **35,** 889
lithium-MnO_2 cells
a study of relaxation processes, **35,** 1849
lithium polysulphide
phase diagram for Li_2S-Na_2S-S at 400°C, **36,** 673
preparation, density and electrical conductivity of molten $Li_2S_{3.9}$, **36,** 667
sulphur activity and chain length distribution at 400°C, **36,** 679
lithium salts
host copolymers of inorganic oxide backbones bound by organosilanes to organic polymers eg PEO, **37,** 1593
for polymer electrolytes: $N(SO_2CF_3)_2^-$ Li^+ and $C(SO_2CF_3)_3^-$ Li^+, **37,** 1551
lithium secondary batteries
safety and reliability of Li/MoS_2 systems, **38,** 1193
lithium-sulphur battery
phase diagram for Li_2S-Na_2S-S at 400°C, **36,** 673
sulphur activity and chain length distributions at 400°C in molten polysulphides, **36,** 679
lithium-thionyl chloride cells
interpretation of impedance of passive layer, **35,** 423
metal phthalocyanine dopants for carbon cathodes, **37,** 531

lithium bis(trifluoromethylsulphonyl)imide
compared with $LiClO_4$ and $LiCF_3SO_2$ electrolytes in PEO: conductivity etc, **37,** 1579
complex with condensation products of polyacid chlorides and diamine poly(oxyethene-co-oxypropene), **37,** 1737
complexes with cross-linked block copolymers with combined mechanical properties and conductivity, **37,** 1729
solutions in a new PEO network polymer: conductivity, glass transition and mechanical properties, **37,** 1585
solutions in polymers and copolymers of 1,3-dioxolane and 4-methyl-1,3-dioxolane, **37,** 1589
solvation by bis[2-(2-methoxyethoxy)ethyl] ether: effect of propene carbonate, **37,** 2043
stability and conductivity in THF: suitability as a polymer electrolyte, **37,** 1551
stability ranges and conductivities of complexes based on pristine POE and modified POE, **37,** 1699
thermodynamics of insertion into the gel-like spinel $Li_xMn_2O_4$, **37,** 1301
lithium tris(trifluoromethylsulphonyl)methide
stability and conductivity in THF: suitability as a polymer electrolyte, **37,** 1551
Loprazolam
reduction at Hg cathodes in DMF, **36,** 1019
low-conductivity electrolytes
high-frequency phase shifts in impedance measurements, **36,** 1093, 1385
low-energy electron diffraction
of Au single-crystal faces before and after electrochemistry, **35,** 1383
study of concentration dependence of UPD of Ag on Pt(111), **38,** 235
low-frequency dispersion
interpretations of a common phenomenon in admittance studies, **35,** 1595
luminescence see photoemission
luminol
application of 3-aminophthalhydrazide to study the porosity of chromate-phosphate conversion coatings on AlMn05Mg05 alloy, **38,** 2577

M

magnesium
anodic behaviour in carbonate buffers at 9<pH<11, **37,** 1403
corrosion in aerated 0.5M Na_2SO_4 aq, **35,** 555
magnesium(II)
properties in molten $BaCl_2$-$CaCl_2$-NaCl, **36,** 155
magnesium aluminium oxide
effect of humidity on conduction mechanism in bulk and thin film $MgAl_2O_4$, **38,** 2617
magnesium power cells with $Mg(ClO_4)_2$ aq electrolyte
N-halogen organic cathodes e.g. N,N'-dichlorodimethylhydantoin, **37,** 1971
magnetic field effect
on anodic dissolution of Cu in NaCl-KSCN aq, **35,** 933
claimed asymmetric induction during reduction of phenylglyoxylic acid, **35,** 683
on current oscillations during anodic dissolution of Cu in NaCl aq containing traces of SCN^-, **37,** 97
on electrodeposition and dissolution of Cu, **36,** 459
on mass transport: statistical analysis of existing data, **35,** 929
optimization of reactors with a common electrolysis and magnetizing current, **36,** 1907
on pre-oscillatory formation kinetics of anodic oxide layers, **38,** 2631
mains interference
elimination by a digital sampling method, **35,** 1797, **36,** 747
manganate(VI) ion
oxidation to Mn(VII) at vitreous carbon and NiOOH RDE anodes in 2.5M KOH aq, **36,** 173
manganese(II)
anodic oxidation to MnO_4^- in 30% H_2SO_4 aq catalysed by Ag(I), **36,** 1363
oxidation to MnO_2 at Pt anodes in 30% H_2SO_4 aq, **35,** 281
manganese dioxide see also manganese dioxide electrodes
cathodic insertion of Na^+ into sol-gel lamellar birnessite $MnO_{1.84}$,$0.64H_2O$, **38,** 1695
cycling performances of Li_xMnO_2 and other positive electrodes in secondary lithium cells, **37,** 63
deposits on tantalum: reanodization at constant current, **35,** 855

manganese dioxide continued
electrodeposited on Au: reduction in aqueous borate, **38,** 341
formation from Mn(II) at Pt anodes in 30% H_2SO_4 aq, **35,** 281
heat arising from irreversibility of Li^+ insertion, **36,** 489
Li^+ insertion into sol-gel lamellar birnessite $MnO_{1.84}.0.6H_2O$, **36,** 1595
memory effect due to first-order phase transition in Li_xMnO_2, **36,** 1469
oxidation of geraniol to citral at MnO_2-modified, Pt-Nafion electrodes, **37,** 1295
synthesis of the ramsdellite form and its structural stability especially as a positive electrode in secondary lithium cells, **38,** 1259
thermodynamics of insertion of Li^+ into the gel-like spinel $Li_xMn_2O_4$, **37,** 1301
manganese dioxide electrodes
in 1M Na_2SO_4 aq containing Mn(II) at 4<pH<6: exchange currents of individual ions, **35,** 539
discharge in borate buffer pH9.2, **36,** 1485
electrocatalytic activity in anodic oxidation of Cr(III), **38,** 437
kinetic studies in non-aqueous and alkaline media, **35,** 1889
as positive electrodes in secondary lithium cells [R], **38,** 1221
preparation of, and Li^+ insertion into, positive-electrode materials $MnO_2.xV_2O_5$, **37,** 1039
γ-manganese dioxide electrode
intercalation of Na^+ from 1M $NaClO_4$-PC, **37,** 603
manganese dioxide films
on glass-SnO_2 electrodes: electrochromic behaviour in 0.1M $Na_2B_2O_7$ aq, **37,** 2015
manganese dioxide-lithium cells
a study of relaxation processes, **35,** 1849
manganese hydroxide
oxidation of a layer on Pt in alkaline media, **36,** 1013
manganese oxide-hydroxide
ionic conductivity and reduction rates of non-stoichiometric material compared with those of γ-MnO_2, **38,** 2305
manganese porphyrin films
oxygen reduction in acetonitrile, **38,** 1747
manganese-nickel spinels, $Cu_xNi_{0.6-0.2x}Mn_{2.4-0.8x}O_4$: extents of reduction in H_2SO_4 aq, **35,** 1303
Markov chains
application of theory to estimations of amounts of electrodeposits, **38,** 1147
mass spectrometry, on-line, study
of analyses of products of oxidation of propyl, allyl and propargyl alcohols at Au anodes in 0.5M H_2SO_4, **38,** 1337
of chemisorption of 1,1,1-trichlorethane at Pt electrodes in H_2SO_4 aq, **38,** 281
of effect of water on oxidation of 0.5M $LiClO_4$-PC at Pt anodes, **36,** 1397
of electrolyses of electrolytes containing dimethylamine, **37,** 759
of hydrogen evolution during oxidations of aldehydes at anodes of Cu, Ag or Au, **38,** 1067
of oxidation and reduction of propene carbonate, ethene carbonate and 1,2-propanediol at Pt electrodes, **38,** 541
of oxidations of HCOOH, $HCONH_2$ and DMF at porous Pt anodes in 0.05M H_2SO_4 aq, **38,** 185
of reduction of CO_2 to CH_4 and C_2H_4 at Cu cathodes in 0.5M $KHCO_3$ aq, **35,** 771
of reductions of NO_2^- and NO_3^- at porous Pt cathodes in H_2SO_4 aq, **36,** 877
of role of adsorption in reactions of sulpholane and DMSO at Pt electrodes in 0.5M H_2SO_4 aq, **38,** 175
mass transfer
across a weak acid ion-exchange membrane, **38,** 329
at carbon and graphite felt electrodes, **35,** 1369
at gas-evolving electrodes as a result of free convection due to density gradients within the liquid phase, **38,** 1421, 1427
at a horizontal cylinder electrode with an opposed thermal buoyancy effect, **38,** 2589
at a segmented vertical plate cathode with mixed convection during Cu deposition below the diffusion limited current, **38,** 1461
controlled in a Hull-type cell with a rotating cylinder electrode, **37,** 69
in Cu-electrolysis cells with excess H_2SO_4, vertical electrodes and uniform c.d., **37,** 333
during Cu plating at a RDE with square cathodic current pulses, **36,** 625
statistical indeterminacy of effect of magnetic fields on, **35,** 929
mediators
acetoxylation of ketones by electrogenerated $Pb(OAc)_4$, **36,** 1165

mediators continued
Ag(I) catalysis of anodic oxidation of Mn(II) to MnO_4^- in 30% H_2SO_4 aq, **36,** 1363
1,4-benzoquinone in polypyrrole-glucose oxidase composite films, **37,** 1987
cation radicals in the anodic syntheses of N-heterocycles from azomethine derivatives in MeCN-TEAP, **35,** 225
Ce(IV) in the oxidation of water to oxygen catalysed by Adams RuO_2, **37,** 1217
Cr(II) complexes with polyaminocarboxylate ligands: organic reductions and phase transfers, **37,** 575
ferrocenylalkane thiol layer on Au cathodes in the reduction of Fe(III)-EDTA, **36,** 1799
$FeCl_3$ in the oxidation of toluenes to cresols at a fuel-cell oxygen cathode in H_3PO_4, **37,** 2549
located in a film on an ultramicroelectrode, **38,** 581
MnO_2 in the oxidation of geraniol to citral at Pt-Nafion electrodes, **37,** 1295
$Os(bpy)_3^{2+}$ in oxidation of 1,2-dihydroxybenzene at glassy carbon anodes coated with poly(styrene sulphonate), **38,** 1321
oxidation of xylenes by Ce(IV): effect of oxide at Pt and Au anodes, **35,** 273
Ru(V) mono-oxo complex within Nafion films for benzyl alcohol oxidation **37,** 2645
viologen species in the reaction of oxygen with photoexcited $Ru(bpy)_3^{2+}$ in a Nafion film, **38,** 129
Meldola Blue
diffusion coefficients in Nafion films, **36,** 881
membrane cells
impedance studies of symmetric cells with potential-dependent steady-state currents, **38,** 1837
membranes
charged: curvature of nearby double layers, **36,** 1757
highly flexible: entropy-driven expansion of electric double-layer repulsion, **36,** 1735
impedance studies of ion exchangers and mixed conductors, **35,** 1609
influence of peptide charge distribution on water chains in ion channels, **36,** 1753
ion transport in PVC containing dioctylphenyl phosphonate and CaI_2, **38,** 2373
of plasticised PVC containing neutral carriers of ionic species: impedance at constant current, **38,** 2691
properties of plasticized PVC used in ion-selective electrodes [R], **35,** 1
membranes, supported liquid
use of Aliquot 336 in the recycling of Cr(VI) re-oxidized from Cr(III), **38,** 847
2,5-mercapto-1,3,4-thiadiazole
composite with polyaniline: positive-electrode material for lithium cells, **37,** 1851
mercury
electrodeposition on Pt single crystal cathodes from $Hg_2(ClO_4)_2$ aq, **35,** 339
mercury channel electrode
photoelectrochemical reduction of pyrene in acetonitrile, **35,** 1837
mercury electrode see also organic compounds, reductions
adsorption of adenosine from neutral aqueous sulphates, **35,** 1291
adsorption of Br^- from propene carbonate solutions, **36,** 1971
adsorption of ClO_4^- from $HClO_4$ aq and $HClO_4$-TEAP aq, **37,** 1753
adsorption of Pb^{2+} induced by Br^-, **35,** 1701
adsorption of phosphonium cations from Ph_4PCl and cetylBu_3PBr in 0.1M NaF, **37,** 2447
adsorption of surfactants: θ inferred from *cv* ΔE for Cd^{2+}/Cd(Hg), **37,** 2395
adsorption of uracil from aqueous phosphate buffer pH8, **37,** 2663
adsorptions and reductions of quinine and flumazenil, **35,** 1311
capacitance *vs* potential curves in KCl aq from 25 to 300°C, **38,** 1761
current oscillations during potentiostatic oxidation of BrO_3^-, **35,** 1095
solvent effects on kinetics of discharge of metal ions in mixed solvents, **38,** 721
transitions in thymine adsorbate films in NaCl aq, **36,** 1855
mercury microelectrode
preparation and steady-state application to determine Cd-glycine complexation constants, **37,** 1413
mesogenic blocks in co-polymers with poly(ethene oxide)
terephthaloyl bis(1,4-oxybenzoyl-) and terephthaloyl bis(2,6-oxynaphthoyl-), **37,** 1479
metal/electrolyte solution interface structure, **36,** 1659
metallic state cluster
variation of Fermi level to model electrode potential changes of Pt with adsorbed CO, **38,** 1107
metalloporphyrin electrocatalysts
coatings in reductions of organic halides, **36,** 855
interaction of O_2 with Co tetramethoxyphenylporphyrin, **36,** 999

metalloporphyrins see also porphyrin
cobalt tetrakis(4-trimethylammoniumphenyl)porphyrin: catalysed reduction of dithiodipropionic acid at glassy carbon cathodes, **37,** 2591
of cobalt and iron: pyrolysis of films sublimed on to carbon black surfaces, **38,** 2493
of manganese, zinc and iron: incorporation into poly(pyrrole-alkylammonium) films, **38,** 2485
oxygen reduction at manganese porphyrin films on carbon electrodes in acetonitrile, **38,** 1747
methanal
adsorption and oxidation at surface skeleton Ir electrodes, **35,** 191
oxidation at Au(332) electrodes, **35,** 725
oxidation at electrodes of Cu, Ag and Au: concomitant hydrogen evolution, **38,** 1067
oxidation at noble metal anodes in aqueous alkali, **35,** 1821
oxidation at Pt and Cu anodes in alkaline aqueous media, **36,** 1937
oxidation: study of radical intermediates by modulated infrared reflectance spectroscopy, **35,** 679
oxidation at vitreous carbon anodes supporting ultrafine Au particles in alkaline solutions, **37,** 453
potential oscillations during oxidation at Pt anodes in acidic media, **38,** 503
methanoate oxidation
at noble metal anodes in aqueous alkali, **35,** 1821, 1829
at Pt and Cu anodes in alkaline aqueous media, **36,** 1937
methanoic acid
adsorption and oxidation at Pt anodes modified with polyaniline or aniline, **35,** 1459
adsorption and oxidation at surface skeleton Ir electrodes, **35,** 191
effect of size of Pt particles on anodic oxidation, **36,** 973
oxidation at Ir anodes at various pH, **38,** 1631
oxidation at porous Pt anodes in 0.05M H_2SO_4 aq, **38,** 185
oxidation at Pt anodes in 0.5M H_2SO_4 aq, **38,** 1899
photochemical decomposition at Pt-coated sintered CdS pellets, **36,** 153
potential oscillations during oxidation at Pt anodes, **37,** 37
potential oscillations and periodic variations in amount of chemisorbed species during oxidation at Pt anodes, **38,** 2385
methanol
adsorption and oxidation at surface skeleton Ir electrodes, **35,** 191
anodic stripping of adsorbed residues from Pt electrodes in 0.5M H_2SO_4, **36,** 2003
chemisorption at Pt(110) in 0.1M Na_2CO_3 aq, **37,** 1883
methanol fuel cell
thermal preparation of an air electrode based on carbon paper treated with H_2PtCl_6 aq, **37,** 1327
methanol oxidation see also methanol
at anodes of Rh-Sn oxide, Pt-Sn oxide, Ir-Sn oxide compared with those at Rh, Pt and Ir respectively, **37,** 1317
characterization of alloy electrocatalysts [R], **36,** 2053
direct, at Pt-Ru electrocatalysts and source of CO species adsorbed at Pt, **37,** 2361
effect of size of Pt particles evaporated on vitreous carbon anodes, **36,** 973
effect of UPD Pb on Pt and Au anodes, **36,** 1157
electrocatalytic, by *cis*-$[Ru(L)(Cl)(O)]^{2+}$, [L = N,N'-dimethyl-N,N'-bis(2-pyridylmethyl)-1,2-diaminoethane], **38,** 1015
in H_2SO_4 aq at vitreous carbon anodes sputtered with Pt and Au, **36,** 947
influence of size and nature of Pt particles in porous carbon anodes in H_2SO_4 aq, **35,** 199
at noble metal anodes in aqueous alkali, **35,** 1821, 1829
at Pt anodes activated by adsorbed molybdenum ions, **35,** 849
at Pt and Cu anodes in alkaline aqueous media, **36,** 1937
at Pt-SPE electrodes modified by molybdenum in 0.5M H_2SO_4 aq, **35,** 323
at PTFE-bonded fuel-cell anodes fed with gaseous methanol, **37,** 1351
on platinized Pt anodes in alkaline media, **36,** 519
rapid transient measurements at Pt and Pt-SPE electrodes in acidic media, **36,** 1043
study of radical intermediates by modulated infrared reflectance spectroscopy, **35,** 679
DL-methionine S-methylsulphonium chloride
reduction at Hg cathodes in mildly alkaline buffers, **36,** 1925
bis[2-(2-methoxyethoxy)ethyl] ether
solvation of Li^+: effect of propene carbonate, **37,** 2043

methyl viologen
incorporated in a zeolite-modified carbon paste electrode: dependence of reduction on support electrolyte and immersion time, **38,** 2257
incorporated in a zeolite-modified carbon paste electrode: ion exchange between MV^{2+} and Na^+ of the zeolite, **38,** 2267
reduction of MV^{2+} by photoexcited $Ru(bpy)_3^{2+}$ in adjacent Nafion layers sandwiched between ITO electrodes, **38,** 1093
1-methyl-2,4-dicyanopyridinium ion
reductions at Hg and carbon cathodes in acetonitrile and DMF, **35,** 1185
Methylene Blue
diffusion coefficients in Nafion films, **36,** 881
Methylene Green
adsorption at Pt electrodes: redox behaviour of hemoglobin, **35,** 1139
2-methylnaphthalene
acetoxylation at Pt anodes in glacial acetic acid-lithium acetate, **35,** 1739
N-methylphenothiazine: influence on polymerization of pyrrole at Pt anodes in acetonitrile, **37,** 513
methylpyridines
capacitance studies of adsorption at Hg electrodes, **38,** 1585
thermodynamic interpretation of electrocapillary data for adsorption at Hg electrodes, **38,** 1573
methylpyridinium salts
photogalvanic effect in aqueous and MeOH-H_2O media, **36,** 1287
micelle catalysis
of anodic dimerization of aromatic amines in nitrobenzene/water, **35,** 1081
micelles
from ionic surfactants: study of electrochemical properties by isotachophoresis, **37,** 2769
molecular dynamics simulation of sodium octanoate in water, **36,** 1729
Michelson interferometer
modified to measure strain in electrodeposits, **35,** 1989
microelectrodes
carbon fibre array used for transmission spectroelectrochemistry, **36,** 203
carbon fibres modified with isopoly- and heteropoly-oxometallate thin films, **37,** 11
of Cu in ethan-1,2-diol-water mixtures containing Cl^-, **38,** 2291
effect of acetonitrile on anodic behaviour of Fe in aqueous perchlorates, **35,** 501
mercury: preparation and steady-state application to determine Cd-glycine complexation constants, **37,** 1413
novel fabrication of submicrometre band electrodes, **36,** 763
oxygen reduction at Pt cathodes in concentrated phosphotungstic acid at 25 and 60°C, **38,** 1733
pulse voltammetric determination of stability constants of complexes formed by anodically dissolving metals, **38,** 1555
microorganisms
role in the corrosion of Cu alloys in natural seawater, **37,** 2291
uptake of redox couples by algae bound to vitreous carbon electrodes, **35,** 1377
within biofilms: influence on corrosion processes, **37,** 2179
microwave conductivity
photo-induced at n-Si, p-Si and n-WSe_2: dependences on potential and time, **38,** 141
microwave photoconductivity scanning microscopy
of semiconductor surfaces using laser scanning, **37,** 919
microwave photoelectrochemistry
a theoretical basis, **37,** 919
mild steel
electropolishing using alternating current, **36,** 93
Misch metal alloys
hydrogen storage electrodes in the Ni-H battery, **38,** 787, 1087
Mitoxantrone
adsorption and redox behaviour at Hg electrodes in 0.5M Na_2SO_4-McIlvaine buffers, **37,** 2059
mixed (ionic-electronic) conductors
from oxidation and hydrolysis of poly(vinylalcohol), **36,** 899
modified electrodes
adsorptions and oxidations at surface skeleton Ir, **35,** 191
an ultramicroelectrode with a film containing a redox species, **38,** 581

modified electrodes continued
Au treated with 4,4'-bipyridyl disulphide: adsorption of cytochrome *c* from phosphate buffer solution, **37,** 403
carbon fibres, dip-coated in isopolymolybdic acid, **37,** 1859
effect on gas evolution overvoltage of a PTFE array on platinized Pt, **35,** 1089
effects of implantations of Li^+ and K^+ into vitreous carbon, **35,** 1279
film of $[Os(2,2'\text{-bipy})_2(PVP)_nCl]Cl$ on vitreous carbon : charge-transfer dynamics, **37,** 159
glassy carbon coated with benzylated poly(ethene imine) and treated with anthraquinone-2,6-disulphonate, **37,** 2765
hemoglobin reduction at vitreous carbon supporting thionine, **37,** 595
Hg^{2+} with layers of zeolite A coated on vitreous carbon substrates, **36,** 383
iron protoporphyrin on pyrolytic graphite: effect of pH on stability of catalytic activity for H_2O_2 reduction, **35,** 1227
isopoly- and heteropoly-oxymetallate thin films on carbon fibres, **37,** 11
Methylene Green adsorbed at Pt, **35,** 1139
oxidized graphite fibres treated with Pt^{4+}, Pd^{2+}, Au^{4+}, Mn^{2+}, Te^{4+}, Ir^{3+} and In^{3+}, **36,** 513
polypyrrole and polythiophene grafted with nickel cyclam, **36,** 15
Pt or vitreous carbon with films of cobalt hexacyanoferrate, **36,** 147
redox rates affected by proteins adsorbed at pyrolytic graphite, **35,** 177
uptake of redox couples by algae bound to vitreous carbon, **35,** 1377
modulation method
to study hydrogen permeation through a passive film on Fe, **36,** 825
molecular dynamics
segmental, of ionene polyelectrolyte $[-(CH_2)_{10}N^+(CH_3)_2-]_n.nBF_4$, **37,** 1657
simulation of the metal/aqueous solution interface: anisotropic liquid-crystal structures, **36,** 1695
simulation of sodium octanoate micelles in water, **36,** 1729
molecular orbital calculations
CNDO/2 method applied to some 3-phenyloxaziridines, **36,** 97
molecular orbital interpretations
of products from CO_2 reduction at metal phthalocyanine cathodes, **36,** 1309
molten borate
boriding of Fe cathodes in sodium tetraborate, **36,** 41
molten calcium aluminates (slags)
measurement of oxygen in $CaO\text{-}Al_2O_3\text{-}Fe_2O_3\text{-}FeO\text{-}CaS$ at 1600°C, **36,** 1027
molten carbonates see also fuel cells, molten carbonate
electrochemistry of oxygen and superoxide, oxide and peroxide ions in $Na_2CO_3\text{-}K_2CO_3$ eutectic, **36,** 1063
kinetics of oxygen reduction at Au cathodes in $Li_2CO_3\text{-}K_2CO_3$ at 923K, **38,** 2405
oxygen reduction at Au cathodes in $Li_2CO_3\text{-}K_2CO_3$ eutectic: effect of $CO_2\text{-}O_2\text{-}He$ atmosphere, **37,** 1935
molten chlorides
effect of Ag^+ on electrodeposits of W and WC from, **35,** 187
effect of CO on the Cu(I/II) redox kinetics at a W electrode in 1-methyl-3-ethylimidazolium chloride-$AlCl_3$, **38,** 927
effect of NaF on electrodeposition of TiB_2 on W or vitreous C from NaCl-KCl melts containing $TiCl_3$ and $NaBF_4$, **37,** 263
effect of organic co-solvents on electrodeposition of Al from $[Me_3PhN][Al_2Cl_7]$ melts, **38,** 245
electrochemical and spectroscopic study of anthracene in 1-ethyl-3-methylimidazolium chloride-$AlCl_3$, **37,** 2615
kinetics of the Sn(0/II) reaction at W and liquid Sn electrodes in LiCl-KCl eutectic at 723K, **35,** 905
the O_2(Pt) electrode in molten NaCl, KCl and CsCl: exchange with O^{2-}, O_2^- and O_2^{2-}, **37,** 2681
oxide ion exchange between Mg(II) and PbO in $PbCl_2$-KCl at 475°C, **38,** 1743
reduction of $CdCl_2$ at W cathodes in LiCl-KCl eutectic, **35,** 1201
reduction of Sn at W and liquid Sn cathodes in LiCl-KCl eutectic: novel electrode-kinetic analysis, **37,** 1149
reduction of tungstate to W at Ni cathodes in LiCl-KCl eutectic at 723K, **35,** 1233
solubilities and dissociation constants of metal oxides in CsCl-KCl-NaCl eutectic at 600°C, **38,** 1481
solubilities of MgO and CaO and the *E vs* pO^{2-} diagram in $BaCl_2\text{-}CaCl_2\text{-}NaCl$, **36,** 155
thermodynamics of $CrCl_2$ and $CrCl_3$ solutions in LiCl-KCl and LiCl-KCl-$BaCl_2$ eutectics from EMF data, **37,** 1445
molten chloroaluminates
increased conductivity and decreased viscosity by use of aryl chloride and aryl fluoride co-solvents, **37,** 1061

molten fluorides
anodic dissolution of Fe and Ni in LiF-NaF-KF eutectic at 600°C, **37,** 2433
apparent E° for Ti/Ti(III) electrode in LiF-NaF-KF eutectic at 700°C, **36,** 1009
cathodic deposition of Ti, Zr, B, TiB_2 and ZrB_2 from LiF-NaF-KF eutectic at 700°C, **37,** 237
conductivities of Na_3AlF_6-Al_2O_3-(CaF_2)-(MgF_2) ternary and quaternary mixtures, **38,** 2165
discharge of F^- in NaF and in cryolite on various graphite and carbon anodes, **37,** 705
effect of added TiO_2 and B_2O_3 on Al deposition from cryolite, **37,** 1787
electrochemical behaviour of Cu in 1.37HF.NH_4HF_2, **38,** 1951
oxidation of soluble Al(0) and Al(I) at W and carbon anodes in NaF-AlF_3-Al_2O_3, **36,** 31
temperature- and concentration-dependences of conductivities measured in a pyrolytic boron nitride tube-type cell, **38,** 589
transference numbers and coefficients in salt mixtures suitable for electrodeposition of Al, **38,** 415
molten halides
LiCl-LiBr-KBr eutectic as electrolyte in high temperature secondary lithium cells with FeS or FeS_2 positive electrodes, **38,** 1269
thermodynamics of solutions of K in melts of its mixed halides, **35,** 529
molten nitrates
anodic behaviour of Ni in KNO_3 at 350-400°C, **36,** 655
electrical conductance and viscosity of solutions of water in 0.467$TlNO_3$-0.214$CsNO_3$-0.319$Cd(NO_3)_2$, **37,** 349
EMF studies of $AgNO_3$-KNO_3 in the range 513-583K, **37,** 91, 1155
EMF studies in $AgNO_3$-KNO_3-$NaNO_3$, **38,** 1139
reactions at Pt electrodes in wet and dry KNO_3, $NaNO_3$ and their equimolar mixture at 300 and 340°C, **38,** 2611
molten polyiodides
of R_4N^+ and R_3S^+: electrical conductivities at room temperature, **37,** 379
molten polysulphides
the phase diagram for Li_2S-Na_2S-S at 400°C, **36,** 673
preparation, density and electrical conductivity of $Li_2S_{3.9}$, **36,** 667
sulphur activity and chain length distributions at 400°C, **36,** 679
molten salts
ionic mobilities of monovalent cations in mixtures, **35,** 1761
low-temperature, diffusion and stoichiometry in the dissolution of Zn, **35,** 89
used to incorporate Ba^{2+} into β"-alumina, **36,** 563
molten silicates
electrochemical studies of multivalent elements in molten oxide glasses, **38,** 479
molten sodium sulphate
stabilities of reference electrodes at 1200K, **35,** 1065
molybdate ions
effect on passivation of Ti in H_2SO_4 aq, **36,** 2069
modification of Pt-SPE electrodes for oxidation of gaseous methanol in 0.5M H_2SO_4, **35,** 323
molybdenum
role in passivation of Fe-Cr(-Mo)alloys in 0.5M H_2SO_4, **36,** 1465
molybdenum ions
activation of Pt anodes in the oxidation of methanol, **35,** 849
molybdenum trioxide
$Mo_8O_{26}^{4-}.4H^+$ thin films on carbon fibre electrodes, **37,** 11
voltammetry of the solid between two vitreous carbon electrodes, **37,** 5
monolayers, self-assembled
of ferrocenylalkane thiol mediators on Au cathodes, **36,** 1799
Monte Carlo calculations
adsorption isotherms of S and H at Pt(111), of naphthalene at Cu and of decylamine at Ni, **36,** 1689
estimates of colloid stabilities, **36,** 1723
Monte Carlo simulations
of bias and statistical uncertainty in CNLS fitting of impedance data to equivalent circuit models, **35,** 1483
of solvation of Na^+ in TIP4P water, **38,** 1405
Monte Carlo study
of complex non-linear least squares fitting of impedance data, **38,** 1883

montmorillonite clay
composite films with poly(vinyl alcohol) on graphite: kinetics of confined $Ru(NH_3)_6^{3+/2+}$, **37,** 1865
composite films with poly(vinyl alcohol) on graphite: permeation by neutral and anionic species from solution, **37,** 1865
film coatings on quartz crystal oscillators in air, moisture and Na_2SO_4 aq, **38,** 747
insertion of PEO or crown ethers to form intercrystalline polymer-salt complexes, **37,** 1573
swelling pressure in alkali-metal ion electrolytes, **36,** 1751
morphological stability
of a planar metal electrode during potentiostatic electrodeposition and dissolution, **37,** 103
Mossbauer spectroscopy
conversion electron emission study of passive films on low-carbon steel in 0.5M Na_2SO_4 aq: effect of sulphite, **38,** 253
study of ferric hydroxo complexes adsorbed on Ni hydroxide and oxyhydroxide powders from aqueous alkali, **37,** 469
study of nickel hydroxide electrodes containing Fe(III) hydroxo complexes, **37,** 607
study of the passive anodic film formed on Fe in 0.5M Na_2SO_4-0.001M $NaHSO_3$ aq, **38,** 2253
study of polypyrroles formed by anodic and chemical oxidations, **36,** 733
study of effect of SO_3^{2-} on passivation of Fe and steels, **36,** 911
study of Ni-Sn alloy electrodeposits on Cu, **35,** 55
study of various hydroxides of Fe(III) and Ni-Fe and their anodic products in alkali, **36,** 1253
Mott-Schottky plots
effect of annealing on flat-band potential of p-silicon in acetonitrile, **37,** 2791
for MoS_2 with and without illumination, **36,** 2037, 2039
for n-GaAs in acetonitrile, **37,** 309
for passive films on AISI 304 stainless steel in 1M $NaClO_4$ aq, **36,** 345
for passive films on AISI 304 stainless steel in borate buffers, **36,** 315
of passive layers formed on Fe and Fe-Cr alloys in neutral aqueous media, **38,** 1567
positive shifts for n-WSe_2/1M H_2SO_4 caused by white light, **35,** 1195, **36,** 747
for Si electrodes in HF aq, **36,** 499
of single-crystal $GaInP_2$ and $Ga_{1-x}Al_xAs$ in various aqueous solutions, **38,** 1993
for thin anodic films on Al and Al-0.4%Mn alloy in borate buffer pH7.4, **37,** 1389
for thin film In_2S_3 electrodes, **35,** 345
transient, of p-Si, following removal of anodic polarization in NH_4F aq, **37,** 865

N

Nafion 117
with deposited metal electrode layers: proton transport between aqueous and organic solutions, **38,** 2171
Nafion 120
calculation of permselectivity at various molarities, temperatures and current densities, **38,** 815
SPE with Pt anodes modified by molybdate: oxidation of gaseous methanol, **35,** 323
Nafion films
containing ruthenium(II) tris(2,2'-bipyridine) complex: photocurrents, **38,** 129
incorporation of *cis*-$[Ru(L)(Cl)(O)]^{2+}$ [L = N,N'-dimethyl-N,N'-bis(2-pyridylmethyl)-1,2-diaminoethane] catalyst, **38,** 1015
Nafion membranes
concentration profiles of $^{137}Cs^+$, **37,** 221
internal temperature profile during water electrolysis, **36,** 263
ITO/Nafion[$Ru(bpy)_3^{2+}$]/Nafion[MV^{2+}]/ITO (MV = methylviologen): reduction of MV ion by photoexcited Ru complex, **38,** 1093
potentials in non-isothermal systems with alkali-metal chloride solutions, **36,** 135
separating equimolar 1:1 electrolytes, electrokinetic effects, **36,** 139
Nafion-coated electrodes
containing a monooxoruthenium(V) complex: indirect anodic oxidation of benzyl alcohol, **37,** 2645
Cu^{2+} discharge at a Cu cathode, **36,** 333
diffusion coefficients for reduced and oxidized forms of cationic dyes, **36,** 881
ruthenium bimolecular substitution reactions within the film, **35,** 419

naphthidine
polymerization to conducting films at Pt anodes in acetonitrile, **35,** 731
1-naphthylamine
mechanism of polymerization at Pt anodes in aqueous acid, **35,** 741
negative faradaic impedance
modeling of wave propagation at electrode/electrolyte interfaces, **38,** 1535
network polymers
from poly(glycidylethers) and triols: high conductivity with low temperature-dependence, **37,** 1725
neural network analysis
of impedance data for painted metal subjected to impact-induced corrosion, **38,** 2083
neutron diffraction studies
of transformations between ramsdellite and spinel forms of lithiated MnO_2, **38,** 1259
nickel
anodic behaviour in molten KNO_3, **36,** 655
anodic dissolution in LiF-NaF-KF eutectic at 600°C, **37,** 2433
anodic oxidation in 0.1M H_2SO_4 with and without Cl^-: stresses induced by the active-passive transition, **37,** 2051
effect of pH on electrodeposition from acidic 1.22M $NiCl_2$ aq: impedance study, **35,** 1587
effect of water content on passivation in H_2SO_4-H_2O-MeOH, **35,** 9
electrocrystallization mechanism, **38,** 1783
electrodeposition at vitreous carbon cathodes from low concentration baths: influence of pH and anion type, **38,** 405
electroless coating on steel: impedance studies of degradation in NaCl aq, **38,** 2093
impedance study of passive anodic films in phosphate buffer 9<pH<11, **35,** 1949
passivation in concentrated aqueous and non-aqueous solutions of H_2SO_4, **37,** 1069
repassivation kinetics in 0.75M Na_2SO_4 aq using electrode abrasion: effect of Cl^-, **37,** 2437
study of passive films by potential step chronoamperometry, **35,** 1719
suppression of anodic dissolution by adsorbed CO, **35,** 1777
variation of field strength, oxide thickness and anodic current with time in Na_2SO_4 aq, **37,** 327
nickel(II) 2,2'-bipyridine complex
chemical step coupled to ion transfer between water and nitrobenzene, **35,** 1965
nickel bipyridyl complexes
electrochemistry in acetonitrile, **38,** 2515
nickel-cadmium cells
cycling performance of pressed cells with a polyethene binder, **36,** 1433
impedance studies as functions of voltage and number of cycles, **38,** 2037
nickel-cobalt alloys
amorphous Ni-Co-Si-B and crystalline Ni-Co: voltammetric and XPS studies in 1M KOH aq, **37,** 2029
electrocatalysts for anodic oxygen evolution, **37,** 169, 769
nickel-cobalt hydrous oxides
from fast square potential waves on alloy anodes, **36,** 1963
nickel(II) complex
with salophen: reduction at Hg cathodes in DMF, **37,** 113
nickel composite cathodes
electrodeposits from baths containing powders of Ni, Fe or Co: hydrogen evolution from 5M KOH aq, **38,** 1079
nickel(II/III) cyclam
grafted to polypyrrole and polythiophene, **36,** 15
nickel electrodes see also nickel
adsorption of CO during reductions of CO and CO_2, **35,** 1777
capacitance of single crystals in 0.1M KOH aq at low hydrogen overvoltages, **38,** 2129
containing RuO_2 particles: preparation and hydrogen evolution from hot alkali, **37,** 757
effect of anodic oxide films on the HER, **35,** 1099
effect of composite-plated PTFE on overvoltages for HER, OER and reductions and oxidations of organics, **37,** 353
with electrodeposited Pd: catalytic hydrogenation of nitrobenzenes to anilines, **38,** 2683
modified by cathodization in 1M KOH-WO_4^{2-}-MoO_4^{2-} aq: electrocatalysts for HER in 3M KOH aq, **37,** 1457
oxidation of D-glucose and polyalcohols in 1M KOH aq, **35,** 375
porous, electrodeposited as an anode for water electrolysis in KOH aq, **37,** 29
reduction of CO_2 in aqueous phosphate buffers, **38,** 1391

nickel hexacyanoferrate
formation and redox behaviour of films on carbon electrodes, **36**, 1537
nickel-hydrogen battery
effect of alloy composition on discharge behaviour of the hydrogen storage electrode, **38**, 1087
improved hydrogen storage by electrodepositing coatings of Pd, Fe, Co and Ni, **38**, 787
modification of a hydrogen storage alloy by treatment with alkaline KBH_4 solution, **38**, 659
nickel hydroxide
AC electrogravimetric study of cation exchange, **36**, 743
adsorption of ferric hydroxo complexes from aqueous alkali on $Ni(OH)_2$ and NiOOH powders, **37**, 469
nickel hydroxide electrode
activation by insertion of $Ni(OH)_2$ in graphite, **36**, 591
catalysis of oxygen evolution in aqueous alkali by Fe(III) hydroxo species, **37**, 607
potential decay of charged electrodes on open circuit, **36**, 759
nickel(II) ions
catalytic polarographic prewaves in the presence of SCN^-, **36**, 2119
surface catalytic prewaves at the DME in the presence of thiourea, **36**, 297
nickel-iron (4:1) binary hydroxides
anodic oxidation in alkalis, **36**, 1253
nickel-manganese spinels, $Cu_xNi_{0.6-0.2x}Mn_{2.4-0.8x}O_4$: extents of reduction in H_2SO_4 aq, **35**, 1303
nickel oxide
anodes for the oxidation of manganate (VI) to (VII) in 2.5M KOH aq, **36**, 173
effect of anodic films on the HER on Ni, **35**, 1099
effect of La^{3+} on deposition of NiOOH on Pt anodes from solutions containing Ni^{2+} and La^{3+}, **38**, 1145
electrochemical intercalation of thin sputtered films by alkali metal ions, **38**, 2765
nickel oxide electrodes
coupled with a poly(methylthiophene) electrochromic window, **36**, 837
electrocatalytic activity in anodic oxidation of Cr(III), **38**, 437
Li^+ injection and electrochromic behaviour, **37**, 1033
modelling of cathodes for molten carbonate fuel cells, **38**, 2669
oxidation of 5-hydroxymethylfurfural to 2,5-furandicarboxylic acid, **36**, 1995
nickel phosphide
electrodeposition of Ni-P alloys on glassy carbon cathodes and their anodic dissolution, **38**, 261
electroless Ni coatings on steel: impedance studies of degradation in NaCl aq, **38**, 2093
nickel-phosphorus alloys
anodic behaviour in 0.1M NaCl and in 0.05M Na_2SO_4 aq, **38**, 1979
nickel sulphide electrodes
amorphous: electrocatalysis of hydrogen evolution, **38**, 2449
nicotinamide
reduction to dimers and dihydropyridines at Hg cathodes at $2<pH<7$, **35**, 845
nicotinamide adenine dinucleotide and NADP
polarographic reductions in aqueous acid, **35**, 753
Nifedipine
and N-methyl derivatives: oxidation at graphite felt anodes in aqueous ethanol, **38**, 1775
Nifedipine and related compounds
reduction in protic media, **36**, 1135
niobium
anodic oxidation in acidic sulphate solutions, **36**, 1443
thickness of pentoxide films formed anodically in 1% H_3PO_4 aq, **36**, 1297
niobium carbide
NbC and tantalum carbide TaC, sintered with Fe, Ni or Co: anodic behaviour in 0.5M H_2SO_4, **37**, 2523
niobium disulphide
intercalation host in composite electrodes of solid-state cells, **36**, 1643
kinetics and thermodynamics of material intercalated by Li^+, **36**, 935
niobium oxide
an impedance study of amorphous anodic films in aqueous sulphates, **35**, 99
optical measurements of thickness of anodic films, **37**, 1105, 1107
thickness of anodic films formed in 1% H_3PO_4 aq, **36**, 1297
transport of H^+ through films formed by thermal oxidation, **35**, 765
niobium triselenide
cycling performance in secondary lithium cells, **37**, 63

nitrate ions
catalysis of reduction at Au cathodes in aqueous alkali by UPD Pb, **38,** 2773
oxidation at Pt anodes in HNO_3, sulpholane and propene carbonate, **36,** 889
reduction at porous Pt cathodes in H_2SO_4 aq, **36,** 877
reduction of molten $Ca(NO_3)_2.4H_2O$ at Pt cathodes at 80°C, **36,** 1639
nitration
of aromatic hydrocarbons at Pt electrodes in nitromethane, **35,** 389
nitric oxide
interaction with poly(pyrrole-alkylammonium) films containing iron(III) porphyrin, **38,** 2485
reduction at Pt black gas-diffusion electrodes in H_2SO_4 aq: effect of sulphur, **36,** 299
nitrilotriacetic acid
effect of presence in solution on electrodeposition of Cu, **37,** 2497
nitrite ions
reduction at porous Pt cathodes in H_2SO_4 aq, **36,** 877
nitro groups
selective reductions in 4-nitrophenylporphyrins by flow-through cathode and anode in series, **38,** 325
p-nitroaniline
adsorption at Ag and Au electrodes from aqueous perchlorates, **35,** 1037
nitroaromatic compounds
effect of benzoic acid on polarographic waves in DMF, **35,** 399
reduction of Nifepidine and related compounds in protic media, **36,** 1135
nitrobenzene
adsorption at Ag electrodes from 0.1M KCl aq, **36,** 1523
reduction to *p*-aminophenol in a packed-bed reactor, **38,** 1753
nitrobenzenes
electrocatalytic hydrogenation to anilines in MeOH at Ni cathodes with electrodeposited Pd, **38,** 2683
nitrobenzene/water emulsions
anodic dimerizations of N,N-dimethyl-1-naphthylamine, **35,** 1081
nitrobenzene/water interface
absolute Galvani potentials based on single ion transfer Gibbs energies, **35,** 1173
adsorption of $C_{12}H_{25}(OC_2H_4)_xOH$ (x = 4, 8 or 12), **36,** 1437
effect of crown ethers on transfer of alkali-metal ions, **35,** 127
kinetics of transfer of Ni^{2+} in presence of 2,2'-bipyridine, **35,** 1965
kinetics of oxidation of ferrocene in nitrobenzene by $Fe(CN)_6^{3-}$ in water, **36,** 291
transfer of alkali-metal cations aided by poly(oxyethene)dodecyl ethers, **37,** 643
nitrobenzodiazapines
reduction of Loprazolam at Hg cathodes in DMF, **36,** 1019
α-nitrobenzylic compounds: reduction to oximes
at Hg cathodes in buffered aqueous ethanol, **38,** 963
at Hg and porous graphite cathodes, **38,** 2379
nitrogen
photoreduction on Cr_2O_3-TiO_2 in presence of water vapour, **38,** 11
nitrogen-centred free radicals
cyclic voltammetry of N-(arylthio)-2,4,6-triphenylanilino radicals at Pt in 0.1M TEAP-MeCN, **37,** 2095
nitroimidazoles
reductions at Hg and at Pt cathodes modified by UPD Pb, Tl or Bi, **37,** 1231
nitromethane solution
stability of Pt surfaces and surface effect in anodic oxidation of Cl^-, **38,** 1097
nitronium complexes
dissociation constants in sulpholane, **36,** 889
nitronium ion
reactions at Pt electrodes in nitromethane, **35,** 389
4-(*o*-nitrophenyl)-1,4-dihydropyridines
oxidation at graphite felt anodes in aqueous ethanol, **38,** 1775
nitrophenyl-pyridines and pyridiniums
reductions at Hg cathodes, **38,** 1775
nitroso aromatics
spin traps for cathodically-generated pyrylium radicals, **36,** 73
nitrosobenzene
two-stage electrosynthesis from nitrobenzene in 0.2M TBAP-benzoic acid-THF, **38,** 677

p-nitrosodimethylaniline
adsorption at flat Ag single crystals, **36,** 1879
3-nitro-1H,-1,2,4-triazole
reduction at Pt cathodes with UPD Pb, Tl or Bi, **35,** 1957
NMR spectroscopic study
of anthracene in 1-ethyl-3-methylimidazolium chloride-$AlCl_3$, **37,** 2615
and conductivity of poly(ethane-1,2-diol) complexed with Li^+ salts, **37,** 1533
of complex of H_3PO_4 with blended PEO-poly(methylmethacrylate), **37,** 1733
to determine activation energies for Li^+ mobility in polyacrylonitrile from ^7Li line widths, **37,** 1671
of the effect of organic co-solvents on electrodeposition of Al from $[Me_3PhN][Al_2Cl_7]$ melts, **38,** 245
of molecular dynamics of ionene polyelectrolyte $[-(CH_2)_{10}N^+(CH_3)_2-]_n.nBF_4$, **37,** 1657
of PEO films with and without $M(CF_3SO_3)_2PEO_n$, M = Zn or Pb, $8<n<25$, **37,** 1487
of $[P(EO)_8.LiClO_4]$: relaxation behaviour of ^1H and ^7Li, **37,** 1685
noble metal anodes
oxidations of hydrazine, methanol, HCHO and $HCOO^-$ in aqueous alkali, **35,** 1821, 1829
noise interference
discrimination against mains hum by a digital sampling method, **35,** 1797, **36,** 747
nomenclature
conventions for corrosion, **35,** 295
non-equilibrium thermodynamics
balances of extensive variables in open electrochemical systems, **35,** 749
formulation for gravitational systems, **38,** 877
non-isothermal cell potentials
evaluation of entropies of ions and of activation for single electrode processes in non-aqueous media, **38,** 997
non-isothermal cells
potentials across Nafion membranes in alkali-metal chloride solutions, **36,** 135
non-linear regression
of impedance data for ion transfer across liquid/liquid interfaces, **35,** 1359
non-stationary impedance spectroscopy, **38,** 1919
non-stationary systems and impedance spectroscopy, **37,** 2353, 2357
nuclear magnetic resonance see NMR
nucleation
of Ag on Pt: effect of extent of cathode oxidation, **35,** 1873
exclusion zones arising from interactions with existing nuclei, **37,** 2503
nucleation and growth see also electrocrystallization
of adsorbed layers of adenosine at Hg electrodes, **35,** 1291
of Ag deposits on polyfaceted spherical Pt cathodes from acidic Ag_2SO_4 aq, **37,** 2215
of Ag during electroreduction of Ag(I) oxide, **35,** 595
of Ag on polyaniline film electrodes, **36,** 1151
of Ag(I) oxide on polycrystalline Ag electrodes in 0.1M NaOH aq, **35,** 489
of Au overlayers during reduction of thick layers of hydrous gold oxide, **35,** 117
of Co centres during reduction of anodically-formed oxide in carbonate buffers, **36,** 2147
of corrosion pits in Cu in 0.1M $NaClO_4$ at $8<pH<11$, **37,** 1437
of Cu electrodeposits on Pt and W cathodes: effect of organic additives, **38,** 2455
of Cu from $CuSO_4$-0.5M H_2SO_4 at columnar-structured Pt electrodes, **37,** 2203
of Cu on glassy carbon from solid CuI electrolyte, **38,** 577
during potentiostatic reduction of Pb^{2+}-containing, anodic layers on Pb electrodes in 5M H_2SO_4, **37,** 1119
of etch pits during anodic dissolution of Fe in aqueous acidic sulphate, **35,** 163
of Fe-Co alloys from sulphate baths pH4 at vitreous carbon cathodes, **38,** 671
a general model for hemispheroidal electrodeposits, **36,** 727
of Hg on Pt single-crystal cathodes, **35,** 339
involving anodic layers on Cu in aqueous carbonate solutions, **38,** 703
layer-by-layer, for poly(thiophene-3-acetic acid) on Pt anodes in 0.1M $LiClO_4$-MeCN, **37,** 393
of metals: Monte Carlo simulations used to relate deposit smoothness to surface diffusion, **37,** 2155
of Pb on Ag single crystals: scanning tunnelling microscopy, **37,** 2173
of PbO_2 on Au electrodes: effects of As(III), sulphate, nitrate and phosphate ions, **37,** 1811
of PbO_2 on a SnO_2/Ti anode: effects of Cu(II) and acetate ions, **38,** 2749
of PbO_2 on vitreous carbon anodes in 0.1M Pb^{2+} aq at various pH, **36,** 2031
of $PbSO_4$ on Pb anodes in 5M H_2SO_4, **38,** 1513
of polyaniline at Au and Pt microanodes: initial compact layer and later branching, **37,** 2255

nucleation and growth continued
of pores in anodized Si in aqueous and methanolic HF: gravimetry, **38,** 191
of structured laser-induced photoelectrodeposition of transition metals on p-Si, **36,** 1803
of TiB_2 and ZrB_2 on Cu and graphite cathodes in LiF-NaF-KF eutectic at 700°C, **37,** 237
of two-dimensional layers of mitoxantrone on Hg electrodes from 0.5M Na_2SO_4-McIlvaine buffers, **37,** 2059
of Zn at a vitreous carbon cathode from zincate solution, **37,** 1199

O

1-octyn-3-ol
kinetics of adsorption at Fe electrodes in HCl aq, **36,** 1333
ohmic overvoltage compensation
in cyclic voltammetry of oxygen reduction at glassy carbon electrodes in DMF-TEAP, **36,** 2113
ohmic potential drop
calculated for various cell geometries, **38,** 2525
in passivation processes in potentiodynamic experiments, **38,** 2699
optical transmittance
of nickel oxide electrodes: effect of Li^+ insertion from 1M $LiClO_4$-PC, **37,** 1033
opto-electrical impedance
photocurrent response to supra-bandgap illumination of semiconductors, **35,** 1657
studies of passive films of WO_3 and ZrO_2 on W and Zr respectively, **38,** 1965
study of anodic dissolution of n-InP in HCl aq, **38,** 2559, 2569
opto-electrical impedance methods
photocurrent and photopotential responses to modulated illumination, **35,** 1545
optoelectrochemical measurements, *in situ*
of Nb_2O_5 anodic films, **37,** 1105, 1107
organic cathodes for power cells
N,N'-dichlorodimethylhydantoin, triisocyanuric acid, diisocyanuric acid and trichloromelamine, **37,** 1971
organic compounds see also heterocyclic compounds, carbonyl compounds or halides, organic
a comparison of chemical and electrochemical conversions, **36,** 2171
organic compounds, adsorption at electrodes
effects of nature and crystal face of the metal and of substituents in aromatics, **37,** 2137
organic compounds, fluorination see fluorinations
organic compounds, hydrogenation
mechanisms at palladium black deposits on graphite, **38,** 425
of phenanthrene at Raney Ni electrodes using pulsed-current electrolysis, **38,** 1377
organic compounds, isomerizations
Z→E conversions of some Z 1,2-diarylsulphonyl phenylethenes, **37,** 2467
organic compounds, oxidation
of 5-hydroxymethylfurfural at NiOOH anodes, **36,** 1995
at TiO_2 photocatalysts, **38,** 47
at TiO_2 photocatalysts: comparison of anatase and rutile, **38,** 43
of benzothiazole derivatives and inclusion compounds with cyclodextrins, **37,** 149
of carbohydrates at Cu anodes in aqueous alkali, **37,** 1187
conversion of 2-hydroxybiphenyl to 2-phenyl-1,4-benzoquinone and scale-up, **38,** 357
of dibenzo(*c,e*)-1,2-dithiine at Pt and vitreous carbon anodes in acetonitrile, **37,** 725
of 2,5-dibutylaniline at Pt anodes in NH_4F-2.35HF, **36,** 833
effect of UPD Pb on glucose oxidation at Pt anodes, **38,** 2725
effect of UPD Pb on products of oxidation of D-gulonic acid at Pt anodes in 0.1M NaOH aq, **38,** 1359
of geraniol to citral at MnO_2-modified, Pt-Nafion electrodes, **37,** 1295
of D-glucose in acidic and neutral media at Pt and Au anodes and at Pt modified with UPD Pb, Tl or Bi, **37,** 1333
of D-glucose in aqueous alkali at Pt and Au anodes, unmodified and modified with UPD Pb, Tl and Bi , **37,** 1909
of D-glucose at smooth Pd anodes in NaOH aq, **37,** 2651
hydroxylation of benzoic acid by oxygen, **37,** 345
of limonene at Pt anodes in MeCN-TEABr, **35,** 497
partial, of hexane and aromatics at fuel-cell $FeCl_3$-graphite cathodes: role of cyclodextrins, **37,** 1135

organic compounds, oxidation continued
photocatalytic reactions with oxygen at small semiconducting particles, **38,** 3
of ring-substituted toluenes, benzylethers and benzaldehydes, **37,** 1951, 1959
synthesis of cresols from toluene at the cathodes of O_2-H_2 fuel cells: effect of $FeCl_3$ mediator, **37,** 2549
of xylenes by anodically-generated Ce(IV): effect of oxide on Pt and Au anodes, **35,** 273
organic compounds, reduction
of N-aryl- and N-arylsulphonyl- substituted benzoquinoneimines, **37,** 277
of azides to amines at Pt or Pd microparticles in poly(pyrrole-alkylammonium) films on carbon felt electrodes, **37,** 1261
of benzaldehyde at cathodes of Pd supported on carbon felt, **37,** 365
of benzaldehyde at Ni cathodes containing PTFE, **37,** 353
of 1,4-benzoquinonemonoimine derivatives in acetonitrile, **35,** 1933
of benzoyloxiranes at Hg cathodes in 0.1M $TBABF_4$-MeCN, **37,** 1247
competitive eliminations from 1-fluoro-2-arylvinylphenyl sulphones at Pt, Hg, Pb and C in MeCN containing proton donors, **38,** 1037
correlation of reduction potentials of N-substituted benzoquinoneimines with spectroscopic electron affinities, **36,** 1219
of 4,4'-dinitrodibenzyl at Hg, and solid cathodes in DMF and EtOH-H_2O, **37,** 1993, 2001, **38,** 471
of ethyl picolinate in H_2SO_4 aq, **37,** 625
and formylations of aryl halides in DMF at Au cathodes modified with Cd, **38,** 613
of α-D-glycopyranosyl bromides at Hg cathodes in the presence of radical acceptors, **36,** 1095
of hemoglobin at vitreous carbon cathodes modified by thionine, **37,** 595
of Isoniazid at Hg cathodes in aqueous acid, **37,** 1147
of Loprazolam at Hg cathodes in DMF, **36,** 1019
of Mitoxantrone at Hg electrodes in 0.5M Na_2SO_4-McIlvaine buffers, **37,** 2059
of nicotinamide to dimers and dihyropyridines at Hg cathodes at 2<pH<7, **35,** 845
of α-nitrobenzylic compounds to oximes at Hg and porous graphite cathodes, **38,** 2379
of 2- and 4-nitroimidazoles at Hg and at Pt cathodes modified by UPD Pb, Tl or Bi, **37,** 1231
of 4-(nitrophenyl) substituted 1,4-dihydropyridines at Hg and solid cathodes in DMF-$TBAPF_6$, **37,** 2599
of -OH groups in α-hydroxyaldehydes selectively using tetraalkylammonium salts, **35,** 1167
of phenyliodonio-bis(acyloxy)methanides at Hg and Au cathodes in methanolic media, **35,** 455
of bispyridinium dications at Hg cathodes in $TBAPF_6$ solutions in acetonitrile, **37,** 2481
rates of protonation of electrogenerated carbanions by parent 2-bromoisobutyramides, **35,** 81
syntheses of cyclopropanes and dihydrofurans using electrogenerated monohalomalonate carbanions, **35,** 563
of triphenylmethane in DMF to Ph_3C^-, **35,** 239
organic metals
effects of solvent on electrosynthesis of charge-transfer complexes of bis(ethenedithio)-tetrathiofulvalene with trihalide ions, **38,** 2343
organic polyhalides, activated
reduction in the presence of methoxy-iminium cations, **36,** 819
organic solvents
for lithium salt electrolytes in lithium cells, **35,** 1257
organoiodine(III or V) compounds
cleavage of O-I bonds at Hg and Pt cathodes in acidic and neutral media, **36,** 1391
organopolysilanes
synthesis from Me_2SiCl_2-Ph_3SiCl mixture at Pt in 0.4M $TBABF_4$-DME, **36,** 621
synthesis from organodichloromonosilanes at Pt cathodes in dimethoxyethane, **35,** 1867
organoselenium compounds
oxidation of dibenzo(*c,e*)-1,2-diselenine at Pt anodes in 0.1M $NaClO_4$-MeCN, **37,** 2077
oxidation of N-aryl-1,2-benzisoselenazol-3(2H)-one at Pt anodes in acetonitrile, **36,** 631
oxidations of dibenzo(*b,d*)selenophene and benzo(*b*)selenophene at Pt or vitreous carbon anodes in MeCN, **37,** 1453
oxidations of selenoxanthenes at Pt and vitreous carbon anodes in acetonitrile, **35,** 1855
redox behaviour at Pt in acetonitrile related to pharmacological activities, **35,** 1133
organosulphur compounds
cathodic carboxylation of PhCH=C(SMe)S(O)Me, **36,** 1341
oxidation of dibenzo(*c,e*)-1,2-dithiine at Pt anodes in 0.1M $NaClO_4$-MeCN, **37,** 2077
reduction of dithiodipropionic acid at glassy carbon catalysed by cobalt tetrakis(4-trimethylammoniumphenyl)porphyrin, **37,** 2591

oscillations see also instability
damped, during anodic dissolution of Si in aqueous fluoride, **38,** 1627
during anodic dissolution of Al-In alloys in 4M KOH aq, **36,** 79
during anodic dissolution of Fe in H_2SO_4, **36,** 1301
during anodic dissolution of Fe in H_2SO_4 aq: effect of forcing conditions, **37,** 1047
resulting from negative faradaic impedance: a simplified approach to modeling wave propagation at electrode/electrolyte interfaces, **38,** 1535
oscillations of current
at the active-passive transition of Fe in 2M H_2SO_4: effect of Cl^-, **37,** 2067
at $Cd_xHg_{1-x}Te$ crystal anodes in basic solutions of Cs^+ and S^{2-}, **36,** 869
at Hg anodes in solutions of BrO_3^- and bromine in aqueous acids, **35,** 1095
at illuminated n-Si(111) in NH_4F aq, **37,** 847
during anodic dissolution of Cu in KSCN-3M NaCl aq, **37,** 2637
during the anodic dissolution of Cu in NaCl aq containing traces of KSCN: effect of magnetic field, **38,** 2631
during anodic dissolution of Cu in NaCl aq containing traces of SCN^-, **37,** 97
during anodic dissolution of p-Si in NH_4F aq, **37,** 889
during pitting corrosion of Co in H_2SO_4 aq induced by I^-, **38,** 835
during reduction of H_2O_2 at chalcopyrite photocathodes, **38,** 115
induced by Cl^- at Fe anodes in H_2SO_4 aq, **38,** 2321
in systems with negative faradaic impedance, **37,** 1771
oscillations of potential
during anodization of Si in H_2SO_4 aq, **36,** 1611
during galvanostatic oxidation of methanal at Pt anodes in acidic media, **38,** 503
during oxidation of H_2 and CO at Pt anodes in 0.5M H_2SO_4 aq, **36,** 639
during oxidation of HCOOH at Pt anodes, **37,** 37
during oxidation of hydrogen at Pt anodes in acid containing traces of Ag^+, **35,** 431
and periodic variations in amount of chemisorbed species during oxidation of methanoic acid at Pt anodes, **38,** 2385
osmium(II/III)
charge-transfer dynamics within $[Os(2,2'\text{-bipy})_2(PVP)_nCl]Cl$ films on vitreous carbon electrodes, **37,** 159
osmotic activity of multilamellar phases, **36,** 1735
oxalic acid
reduction to glyoxylic acid in undivided cells, **35,** 621
role of temperature in reduction to glyoxylic acid at Pb cathodes, **37,** 1381
oxide electrodes
$Ru_{0.3}Ti_{0.7-x}Ce_xO_2$: preparation, voltammetry and stability, **37,** 2511
oxide ion
potentiometric study of exchange between MgO and PbO in $PbCl_2$-KCl at 475°C, **38,** 1743
oximes, synthesis from α-nitrobenzylic compounds
by reduction at Hg and porous graphite cathodes, **38,** 2379
at Hg cathodes in buffered aqueous ethanol, **38,** 963
oxygen
chemisorption at porous Pt catalyst films in yttria-stabilized zirconia at 350 and 650°C, **38,** 2533
permeation through Flemion perfluorinated carboxylate ion-exchange membranes, **38,** 1727
oxygen adsorption and reduction
on $LnMnO_3$ perovskite-type electrocatalysts, **35,** 65
oxygen electrode
at yttria-stabilized zirconia or erbia-stabilized δ-bismuth oxide with noble metal contacts, **38,** 1817
in molten NaCl, KCl and CsCl: exchange with O^{2-}, O_2^- and O_2^{2-}, **37,** 2681
$Pt(O_2)|ZrO_2$ in CsCl-KCl-NaCl eutectic at 600°C, **38,** 1481
at semiconducting, cobalt oxide, film catalysts, **35,** 975
oxygen evolution
at amorphous and crystalline Ni-Co alloy anodes, **37,** 169, 769
at glassy metal anodes containing mainly Ni, Mo and B, **35,** 1919
at the nickel hydroxide anode in aqueous alkali: catalysis by Fe(III) hydroxo species, **37,** 607
at Pt anodes in alkaline solutions: electron transfer through thin oxide films, **37,** 2533
at Ru-Ti alloy anodes in acidic media, **36,** 19
at n-RuS_2 photoanodes in $HClO_4$,5.5H_2O, **38,** 1929
at thick cobalt oxide films in aqueous alkali, **35,** 437
at various metal anodes: weak electrochemiluminescence, **36,** 1591

oxygen evolution continued
effect of preparation conditions on structure of IrO_2-Ta_2O_5 anodes, **36,** 991
on $Ni_xCo_{3-x}O_4$ spinel electrodes ($0.6<x<1.3$) in alkaline solutions, **38,** 2247
ultra-weak photoemission at the Pt anode in aqueous electrolytes, **38,** 267
using a Ce(III/IV) mediator and a RuO_2 Adams catalyst in aqueous acids, **37,** 1217
oxygen isotope study
of Fe25Cr alloy surfaces exposed to air after electrochemical polarization, **36,** 1623
oxygen partial pressure in molten slags, **36,** 1027
oxygen redox species
electrochemistry of oxygen and oxide, superoxide and peroxide ions in Na_2CO_3-K_2CO_3 eutectic, **36,** 1063
oxygen reduction
in 0.5M H_2SO_4 aq at a porous fuel-cell cathode, **37,** 523
in alkaline solution at Ru cathodes: effect of UPD Tl or Pb, **37,** 457
at Au cathodes in Li_2CO_3-K_2CO_3 eutectic: effect of composition of CO_2-O_2-He atmosphere, **37,** 1935
at cathodes of cobalt tetramethoxyphenylporphyrin, **36,** 999
at gas-diffusion cathodes in phosphoric acid fuel cells, **35,** 1411
at gas-diffusion electrodes: effect of phosphoric acid concentration, **37,** 1855
at a glassy carbon RDE catalysed by vitamin B_{12} in weak aqueous acid, **38,** 2297
at graphite cathodes catalysed by adsorbed complex of Cu^{2+} with 2,9-dimethyl-1,10-phenanthrolines, **38,** 2423
at the $La_{0.85}Sr_{0.15}MnO_3$ cathode in Y_2O_3-stabilized ZrO_2 at 1000°C, **38,** 2015
at manganese porphyrin films on carbon electrodes in acetonitrile, **38,** 1747
at oxidized polypyrrole film electrodes containing anionic cobalt complexes, **37,** 763
at polypyrrole-modified electrodes with incorporated Pt particles, **35,** 135
at Pt on carbon black electrodes in H_3PO_4: effect of Pt particle size, **36,** 1979
at Pt cathodes: pH dependence of Gibbs energies of activation, **35,** 1157
at Pt microcathodes in concentrated phosphotungstic acid at 25 and 60°C, **38,** 1733
at Pt and Pt-Fe both supported on carbon: effect of particle size, **38,** 2715
at pyrolysed films of metalloporphyrins of cobalt and iron on carbon black surfaces, **38,** 2493
at UPD Pb on Hg electrodes in 0.1M $NaClO_4$ $4<pH<10$, **36,** 529
at vitreous carbon cathodes modified by iron porphyrin-ion complex, **36,** 703
in DMF at graphite or Pb cathodes with CoTSPc ad-layers, **35,** 173
effect of CO_2 on stability of gas-diffusion cathodes in alkali, **35,** 945
effects of humidity, current density and temperature on operation of an alkaline fuel cell, **37,** 1831
influence of Pt area and H_3PO_4 uptake on performance of PTFE-bonded porous carbon-Pt cathodes, **38,** 913
on Pt cathodes in acidic media: inhibition by UPD Cu, **36,** 1325
kinetics at Au cathodes in Li_2CO_3-K_2CO_3 at 923K, **38,** 2405
in molten carbonate fuel cells, **38,** 2281
in neutral and acidic media on polycrystalline Pt cathodes with UPD Cd, **37,** 2559
new preparation of highly dispersed Pd on carbon substrates, **38,** 2333
photoassisted, at polyaniline film electrodes, **37,** 1003
in proton-exchange membrane fuel cells: effect of a Pt film sputtered on to the front surface of a low-Pt loaded electrode, **38,** 1661
on Pt in aqueous acids: activation energy increments and the Pt-O vibrational quantum, **37,** 1
to superoxide at vitreous carbon cathodes in DMF-TEAP: electrode kinetics, **36,** 2113
oxygen sensors
impedance studies of yttria-stabilized (3 mol%) zirconia modified with 0.3 mol% CuO: investigation of super-plastic deformation, **38,** 2099
oxygen transport
across the separator membrane of a hermetically sealed lead-acid cell, **38,** 935

P

packed-bed electrodes
of metallized plastic: hydrogen evolution, **36,** 1899
partial oxidation of ethanol and 2-propanol at Pt supported on graphite anodes, **38,** 221
packed-bed reactor
reduction of nitrobenzene to *p*-aminophenol, **38,** 1753

paint films see also coated metals
relationship between adherence and protection of carbon steel from corrosion in 10^{-3} NaCl aq, **38,** 1999
painted metals see also coated metals and polymer-coated metals
and unpainted metals: interactive computer analysis of impedance data, **37,** 245
pair correlation functions see correlation functions
palladium
corrosion by Fe(III) and Cu(II) halides in DMSO and water, **36,** 479
electrodeposition on to carbon felt: electrocatalyst for hydrogenations, **36,** 921
electrodeposits on Ni: electrocatalytic hydrogenation of nitrobenzenes to anilines in methanol, **38,** 2683
a new preparation of highly dispersed catalyst on carbon, **38,** 2333
particles (2-10nm) on vitreous carbon electrodes: adsorption and absorption of hydrogen, **36,** 1235
STM study of surface mobility: polycrystalline Pd in atmospheric and aqueous conditions, **37,** 2331
thin films on Au(111) and (100) electrodes: anion and additive effects on hydrogen adsorption and absorption, **38,** 2145
ultrafine particles supported on vitreous carbon: the HER in 1M NaOH aq, **37,** 2427
palladium black
on a graphite substrate: mechanisms of cathodic hydrogenation of organic compounds, **38,** 425
palladium chloride
effect on the AgCl gas-sensitive layer in chlorine gas sensors, **36,** 1823
palladium compounds
analysis and electrochemical behaviour in a carbon paste electrode, **37,** 2491
palladium electrodes see also palladium
attempts to detect neutrons and γ-rays during D_2O reduction, **36,** 1127
cathodic uptake of hydrogen by thin films, **36,** 1203
coulometric determination of loadings with hydrogen and deuterium, **36,** 1515
effect of surface roughness on impedance in 1M H_2SO_4 aq, **38,** 2021
electrocatalytic oxidation of D-glucose in NaOH aq, **37,** 2651
electrodeposition and UPD of Bi, Cu and Ge: ellipsometric study, **37,** 2245
initial stages of Cu electrodeposition, **35,** 1189
oxidations of hydrazine, methanol, HCHO and $HCOO^-$ in aqueous alkali, **35,** 1821
tritium-deuterium separation factor during electrolysis of 0.1M LiOD-D_2O, **37,** 215
particle-size effects
on HER in 1M NaOH aq on vitreous carbon supporting ultrafine Pd particles, **37,** 2427
on hydrogen adsorption and absorption by Pd on glassy carbon electrodes in $HClO_4$ aq, **36,** 1235
on quantum yield in photochemical oxidations of organic molecules by oxygen on semiconductors, **38,** 3
in the oxidation of methanal in alkaline media at Au evaporated on to vitreous carbon anodes, **37,** 453
in the oxidation of methanol at platinized porous carbon anodes in H_2SO_4 aq, **35,** 199
in oxidations of HCOOH and MeOH at Pt evaporated on vitreous carbon anodes, **36,** 973
in oxygen reduction at Pt and Pt-Fe both supported on carbon, **38,** 2715
in oxygen reduction at Pt supported on carbon black cathodes in H_3PO_4, **36,** 1979
in potentiometry of suspensions, **36,** 59
passivation
of Cd in dilute aqueous alkali, **37,** 665
and corrosion of Cu in aqueous carbonate solutions, **38,** 703
of Cu in aqueous carbonates at $8<pH<12$, **35,** 1337
of Cu in aqueous phosphate solutions, **37,** 655
of $Fe_{70}Cr_{10}X_{13}C_7$ where X = P or B: XPS study of anodes in 0.5M H_2SO_4, **37,** 2269
of Fe in acetate buffers, **37,** 477
of Fe anodes in H_2SO_4 aq, **38,** 495
of Fe in benzoate buffers, **37,** 489
of Fe in carbonate-bicarbonate buffers, **36,** 117
of Fe in neutral aqueous phosphate, **38,** 2547
of Fe, Ni and Cr in concentrated aqueous and non-aqueous solutions of H_2SO_4, **37,** 1069
of Fe and steels: effect of SO_3^{2-}, **36,** 911
of Fe-Ni alloys in H_2SO_4 aq: effects of Cl^- and alloy composition, **35,** 69
of Fe-Cr(-Mo) alloys in 0.5M H_2SO_4: role of Mo, **36,** 1465
of low-alloy steels in carbonate buffer solutions, **35,** 35
mechanistic models for analysis of impedance data, **35,** 1509
of Ni in 0.1M H_2SO_4 with and without 500ppm Cl^-: stresses produced, **37,** 2051
of Ni in H_2SO_4-H_2O-MeOH, **35,** 9

passivation continued
of Ni using electrode abrasion: effect of Cl^- on repassivation kinetics in 0.75M Na_2SO_4 aq, **37,** 2437
of Pb in 5M H_2SO_4, **38,** 1513
of Pb in phosphate solutions, **35,** 799
reaction and ohmic overvoltages in potentiodynamic experiments, **38,** 2699
of Sb anodes in H_2SO_4 aq by an amorphous gel-like film, **36,** 2087, 2093
of Sn in H_2SO_4 aq, **37,** 1797
of Ti in H_2SO_4 aq: effect of molybdate ions, **36,** 2069
passive films
on AISI 304 stainless steel in 1M $NaClO_4$ aq, **36,** 345
on AISI 304 stainless steel in borate buffer: temperature effect, **36,** 315
on AISI 304 stainless steel in various electrolyte solutions: frequency dispersion of interfacial capacitance, **38,** 1615
on Al in aggressive (0.5M NaCl) and non-aggressive (0.5M Na_2SO_4-0.1M ammonium tartrate) media, **37,** 2283
on Al-Mn alloys: photoelectrochemical behaviour, **36,** 1179
on Al-Zr alloys: solid solutions $Al^{3+}_xZr^{4+}_{1-x}O^{2-}_yOH^-_{4-2y-x}$, **36,** 1227
on Cr and Fe-Cr alloys in 0.5M H_2SO_4 aq, **38,** 1969
on Cr in H_2SO_4 aq: dependence of composition on solution concentrations, **38,** 2309
on Fe25Cr stainless steel anodes studied by SIMS, **36,** 1623
on $Fe_{80}B_{20}$ anodes in borate buffer and acidic sulphate solutions, **38,** 205
on Fe in aerated 5M KOH aq and on Fe and Cr in aerated 0.15M NaCl aq: a SERS study, **37,** 2747
on Fe anodes in 0.5M Na_2SO_4-0.001M $NaHSO_3$ aq: transformation from amorphous oxide to crystalline γ-FeOOH, **38,** 2253
on Fe in borate buffer: permeation of hydrogen, **36,** 825
on Fe in Na_2SO_4 aq and NaOH aq studied by photoelectrochemical imaging, **38,** 71
formed on Zn anodes in borate and arsenate solutions pH8.9, **36,** 1491
growth on Hf and Zr anodes in 0.5M NH_4HSO_4 aq, **35,** 1897
growth on Ti in neutral and acidic solutions, **36,** 189
on In anodes in NaCl aq at 2<pH<12.6, **36,** 2063
investigation of growth mechanisms by impedance studies, **35,** 1509
on low-carbon steel: effect of SO_3^{2-} on composition and thickness in 0.5M Na_2SO_4 aq, **38,** 253
model for formation on Al and hydrogen evolution, **38,** 2541
model for movement of metal cation vacancies contributing to further growth of oxide on Ni and Fe, **37,** 327
on Ni studied by potential-step amperometry, **35,** 1719
on Nb and Ta in acidic sulphate solutions, **36,** 1443
on Ni(111) anodes in phosphate buffers 9<pH<11, **35,** 1949
on Zircaloy-2 and Zircaloy-4 anodes in aqueous media, **37,** 281
on Zn, Zn-Co and Zn-Ni: influence of donor states on semiconducting properties, **35,** 1501
passivity
of 1018 carbon steel in 0.5M $LiAsF_6$-1,2-dimethoxyethane, **38,** 881
of Cu in neutral Na_2SO_4 aq: effect of SO_4^{2-}, **37,** 2541
of Fe in alkaline media: influence of various cations, **36,** 1143
of Fe in alkaline media : effects of Cl^-, Na^+ and Ca^{2+}, **35,** 1437
Peltier effect
at an electrochemical interface, studied by acoustic calorimetry, **35,** 25
in Al electrodeposition cells, **36,** 661
perchloric acid, anhydrous
effect on reduction of quinones in acetonitrile, **38,** 607
perfluorinated carboxylate ion-exchange membranes
solubility and diffusion coefficient of oxygen in Flemion, **38,** 1727
permselectivity
of ion-exchange membranes calculated for various molarities, temperatures and current densities, **38,** 815
perovskite oxides
cathodic formation of precursors $(LaOH)_{1-x}M_xCrO_4.nH_2O$ for A-site substituted films, **37,** 2421
electrocatalytic activity and oxygen adsorption property of $LnMnO_3$ where Ln = lanthanide, **35,** 65
perovskite superconductor electrodes
insertion of Li^+ into $YBa_2Cu_3O_{7-\delta}$ from 1M $LiClO_4$-PC, **35,** 995
intrinsic redox processes of Y-Ba-Cu mixed oxide in 1M NaOH, **35,** 759
redox activity of excimer laser-deposited $YBa_2Cu_3O_{7-\delta}$ epitaxial films, **35,** 1219

peroxide ion
the O_2(Pt) electrode in molten NaCl, KCl and CsCl: exchange with O^{2-}, O_2^- and O_2^{2-}, **37,** 2681
peroxodisulphate reaction
catalysed at polyaniline film electrodes, **36,** 361
pH measurement
voltammetrically with glassy carbon electrodes coated with benzylated poly(ethene imine) and incorporating certain quinones, **37,** 2765
pH probe
in non-aqueous and mixed solvents: the flat-band potential of n-InP, **38,** 781
phase diagrams
for PEO solutions of $LiClO_4$, $LiCF_3SO_3$ and $LiN(CF_3SO_2)_2$, **37,** 1579
for PEO-sulphamide: basis for proton-vacancy conducting polymers, **37,** 1603
phase-transfer agents see also immiscible electrolyte solutions
Bu_4N^+ ion for chromium complexes with EDTA and other polyaminocarboxylate ligands, **37,** 575
phase transitions
in adsorbed monolayers: a statistical mechanical treatment, **38,** 1441
of adsorbed phosphonium cations from Ph_4PCl and cetylBu_3PBr in 0.1M NaF at a stationary Hg electrode, **37,** 2447
in adsorbed thymine films at Hg electrodes in NaCl aq, **36,** 1855
at charged interfaces: classical and statistical thermodynamics, **37,** 1919
and surface layer reorientation: thermodynamics of adsorption of methylpyridines on Hg electrodes, **38,** 1573, 1585
within adsorbed layers on electrodes, **36,** 447, **37,** 81
phenanthrene
hydrogenation by galvanostatic pulse electrolysis at Raney Ni electrodes, **38,** 1377
phenanthroline
chelated with Cu(II): reductions in aqueous and propene carbonate media, **37,** 33
Pourbaix diagrams for complexes with Fe(II) and Fe(III) in aqueous sulphate, **35,** 209
phenazine
effects of proton donors on reduction at Pt cathodes in THF, **36,** 803
reaction of radical anions generated at glassy carbon or edge-plane graphite cathodes with CO_2 in 0.1M TBAP-DMSO, **35,** 1405
phenazine dye
polarization-modulation FTIR study of Neutral Red polymer films on polycrystalline Au electrodes, **38,** 1619
phenol
in aqueous solutions: photo-oxidation on Cr_2O_3-TiO_2, **38,** 11
phenothiazine derivatives
and their nitration products: behaviour at carbon paste electrodes in methanol solutions, **37,** 1355
phenothiazine dyes
polarization-modulation FTIR study of thionine polymer and leuco Methylene Blue films on polycrystalline Au electrodes, **38,** 1619
2-phenyl-1,4-benzoquinone
anodic synthesis from 2-hydroxybiphenyl and scale-up, **38,** 357
1,1'-phenylene-bispyridinium dications
substituent effects in reductions at Hg cathodes in $TBAPF_6$ solutions in MeCN, DMF and DMSO, **37,** 2481
N,N'-1,2-phenylene-bis(salicylideneiminato)nickel(II)
reduction at Hg cathodes in DMF, **37,** 113
phenylglyoxylic acid
reduction to mandelic acid at Hg cathodes in magnetic fields, **35,** 683
phenyliodonio-bis(acyloxy)methanides
reductions at Hg and Au cathodes in methanolic media, **35,** 455, 1995
3-phenyloxaziridines, 2-substituted
polarography in TEAP-DMF, **36,** 97
N-phenyl-*p*-phenylenediamine oxidation
electron transfer at Pt anodes coated with polythiophene or poly(3-methylthiophene) in MeCN, **38,** 271
phosphate ion
adsorption of $H_2PO_4^-$ and H_3PO_4 at Pt electrodes from acidic aqueous fluorides, **37,** 385
phosphonium cations
from Ph_4PCl and cetylBu_3PBr in 0.1M NaF: adsorption at a stationary Hg electrode, **37,** 2447

phosphoric acid
adsorption of DMSO at the interface with Hg, **35,** 1901
phosphoric acid fuel-cell cathodes
effects of PTFE content and sintering temperature on performance, **35,** 1411
influence of Pt area and H_3PO_4 uptake on oxygen reduction at PTFE-bonded porous carbon-Pt, **38,** 913
phosphorus
effect of 1.82% content on anodic behaviour of Fe in carbonate buffer solution at 75°C, **38,** 2443
phosphotungstic acid
oxygen reduction at Pt microcathodes at 25 and 60°C, **38,** 1733
photoacoustic spectroscopy
of UPD Pb on Ag electrodes using a chopped argon-ion laser beam, **36,** 1959
photocapacitance spectroscopy
derivation of surface electronic features of semiconductor electrodes, **37,** 781
photocatalytic activity
of $CuInS_2$ and $CuIn_5S_8$ cathodes towards hydrogen evolution from aqueous sulphite, **37,** 465
of semiconductors: principles and examples, **38,** 11
of small semiconducting particles in the oxidation of organic molecules by oxygen, **38,** 3
photochargeable device
multilayers of CdS films and Prussian Blue batteries, **35,** 291
photochemical control of ionic conductivity
through effect on reversible cross-linking *via* anthryl groups, **37,** 1515
photochemical decomposition
of HCOOH at Pt-coated sintered CdS pellets, **36,** 153
photochemical diode
ITO/Nafion[$Ru(bpy)_3^{2+}$]/Nafion[MV^{2+}]/ITO (MV = methylviologen): reduction of MV ion by excited Ru complex, **38,** 1093
photocurrent action spectrum
for SnS_2 electrode with adsorbed oxazine sensitizer, **37,** 943
photocurrent onset potentials
of n-WSe_2 in 1M H_2SO_4 aq, **35,** 1195
photocurrent response
of an unbiased Fe_2O_3/0.5M Na_2SO_4/Pt cell using intermittent light, **37,** 1101
to periodic intensity-modulated supra-bandgap illumination of semiconductor electrodes, **35,** 1657
photocurrent spectroscopy, intensity modulated
of dissolution of Si in NH_4F aq, **37,** 889
studies of p-type semiconductors with quantum efficiencies exceeding 100%, **37,** 909
photocurrent transients: transformations to obtain frequency-dependence at n-Si electrodes, **38,** 1913
photocurrents
for anodic dissolution of n-InP in HCl aq, **38,** 2559, 2569
at GaAs electrodes in alkaline solutions of BrO^-, **36,** 695
at GaP electrodes in electrolytes containing Fe(II) ions: effect of LiCl(4M), **37,** 1343
for n-InP anodes in aqueous electrolytes, **37,** 289
at In_2S_3 thin-film electrodes on Ti substrates, **35,** 345
at an ITO electrode coated with a Nafion film containing tris(2,2'-bipyridine) ruthenium(II) complex, **38,** 129
at laser-deposited $YBa_2Cu_3O_{7-\delta}$ epitaxial thin films, **35,** 1219
at layered n-WSe_2 anodes, **36,** 2037, 2039
at oxide-covered Bi anodes in phosphoric acid, **38,** 511
at oxidized Cu electrodes in aerated aqueous sodium acetate with and without benzotriazole, **38,** 1471
potential dependence at n- and p-Si single-crystal electrodes in NH_4F aq, **37,** 919
potential-dependent measurements made simultaneously with photoinduced microwave conductivity, **38,** 141
at potentiostatic Pt electrodes in media containing oxygen and photosystem I submembrane fraction: effect of durohydroquinone, **37,** 2581
of n-Si(111) in NH_4F aq, **37,** 847
spatial variations dependent on composition and microstructure of an electrode scanned by a focussed light beam, **38,** 57
at thermally produced thin films of CdO in 0.2M Na_2SO_4-0.2M Na_2SO_3, **38,** 2199
at thin oxide films on electrodes of Ti, Al and Hf: effect of film thickness and roles of individual interfaces, **38,** 15
at n-TiO_2 anodic films formed in 20M NaOH: dependence on stress, **38,** 37

photodecomposition
of small-bandgap semiconductors, **38,** 101
photoeffects
on the permeation of hydrogen through membranes of Fe, Pd and stainless steel, **38,** 89
photoelectrochemical behaviour
of amorphous thin Si films, **36,** 915
of BiOCl, BiOBr and BiOI formed at Bi film anodes, **35,** 1941
of CdS films formed on Cd anodes in alkaline Na_2S aq: effects of thickness, λ and *E*, **37,** 1371
of Cu in 0.3M K_2SO_4-0.01M $CuSO_4$-0.04M AA (AA = glycine, α-alanine or β-alanine), **38,** 2733
of electrochromic display devices containing V_2O_5 or CdS as well as WO_3, **38,** 2759
of films on Fe and Cu in borate buffers containing SCN^-, **36,** 505
of n-GaAs in acetonitrile, **37,** 309
of GaP: investigations of wet etching processes, **37,** 811
of iron pyrites anodes prepared by screen printing and thermally activated in air, **38,** 123
of oxidized Al-Mn alloys, **36,** 1179
of the passive film on Cr in H_2SO_4 aq, **35,** 445
of passive films formed on AISI 304 stainless steel in 1M $NaClO_4$ aq, **36,** 345
of passive films formed on AISI 304 stainless steel in borate buffer, **36,** 315
of polyaniline film electrodes, **37,** 1003
of polyaniline films on Pt: pH effect in 1M NaCl aq, **36,** 2015
of Si modified with ultrafine Pt islands, **37,** 897
of sintered iron oxide doped with Zn, in borate buffer pH8.4, **36,** 1585
of sintered iron oxide electrodes doped with Zn, **37,** 425
of sputtered thin film Y-Ba-Cu-O electrodes in MeCN-$LiClO_4$, **35,** 1977
of sub-monolayer Pb deposits on n-GaAs, **37,** 933
of thylakoid and sub-thylakoid membrane preparations, **38,** 757
of TiO_2 thin anodic films grown at high rates in 0.5M H_2SO_4 aq, **38,** 29
of two kinds at polyaniline film electrodes, **36,** 361
photoelectrochemical cells
multilayer organic dye photocells generating high photovoltages, **38,** 459
photoelectrochemical effect
on cancer cells in contact with TiO_2 excited by UV light, **38,** 153
photoelectrochemical etching
of $CdSe_xS_{1-x}$ solid solution and CdSe-CdS mixed crystal semiconductor electrodes, **38,** 593
of III-V semiconductors in device processing, **38,** 101
of n-Si in aqueous fluoride, **37,** 877
principles and applications with special reference to III-V semiconductors, particularly InP, **38,** 95
photoelectrochemical evolution of oxygen
at n-RuS_2 electrodes in $HClO_4$,5.5MH_2O, **38,** 1929
photoelectrochemical imaging
of metal membranes through which hydrogen is permeating, **38,** 89
spatial variations in photo-effects at an electrode scanned by a focussed light beam, **38,** 57
a study of passive oxide films on Fe in Na_2SO_4 aq and NaOH aq, **38,** 71
photoelectrochemical laser imaging
of passive films on AISI stainless steel in 1M $NaClO_4$ aq, **36,** 345
photoelectrochemical microscopy
study of thin oxide films on electrodes of Ti, Al and Hf, **38,** 15
photoelectrochemical quantum yield
measurement of frequency-dependence for n-Si in fluoride and KOH solutions using transient excitation, **38,** 1913
spectra for Zr and W electrodes at 10-12V in 1M H_3PO_4, **38,** 1965
photoelectrochemical solar cell
What has prevented commercialization? [R], **36,** 1107
photoelectrodeposition
of Tl_2O_3 on CdSe anodes from 0.1M NaOH containing Tl(I): grain and crystal face effects, **37,** 1429
photoelectrodeposition, laser-induced structured
of transition metals on (100) p-Si in an aqueous Schottky junction configuration, **36,** 1803
photoemission
at the metal/metal oxide interface of thin insulating oxide films on Al and Hf, **38,** 15
ultra-weak: at a Pt anode during oxygen evolution in aqueous electrolytes, **38,** 267

photoexcitation
of pyrene radical anions formed at Hg channel cathodes in acetonitrile, **35,** 1837
photogalvanic behaviour
of alkyl pyridinium salts in aqueous and MeOH-H_2O media, **36,** 1287
of $K_3Mn(CN)_6$ at Pt anodes in aqueous cyanide solutions, **35,** 427
photo-induced deposition of platinum on sprayed SnO_2 films
effect of the film substrate: n-Si(100) wafer or glass sheet, **36,** 1787
photo-induced electron transfer
in Langmuir-Blodgett films with sensitizer and electron donor in adjacent layers, **36,** 1793
photo-induced microwave conductivity
potential dependence at single-crystal n- and p-Si, **37,** 919
photo-initiated deposition of metals
on III-V semiconductors in device processing, **38,** 101
photo-oxidation
of organic compounds at TiO_2: comparison of rutile and anatase, **38,** 43
of organic pollutants at TiO_2 catalysts, **38,** 47
of water at a $SrTiO_3$-TiO_2 anode with a sulphonated PTFE SPE membrane, **38,** 107
photopolymerization, masked
of styrene / vinylbenzo-[18]-crown-6 mixture on Si_3N_4 surfaces, **35,** 777
photoreflectance
recent theoretical models, **37,** 949
photo-resists
application to corrosion studies localized to microareas, **37,** 2263
photosynthesis
photo-induced electron transfers in sub-membrane fractions enriched with PSI and PSII, **38,** 757
photosystem I submembrane fraction
photocurrents at potentiostatic Pt electrodes in oxygenated media: effect of durohydroquinine electron donor, **37,** 2581
photovoltage
spatial variations dependent on composition and microstructure of an electrode scanned by a focussed light beam, **38,** 57
photovoltaic cell
water electrolysis using a triple junction device with thin films of amorphous Si, **38,** 111
phthalocyaninatolanthanide(III) acetylacetonato complexes
synthesis and electrochemistry at Pt electrodes in DMSO-TEAP, **35,** 1707
phthalocyanine
of cobalt, tetrasulphonated, adsorbed at Pb or graphite cathodes: electrocatalyst for oxygen reduction in DMF, **35,** 173
of Fe(II), effect on cathodic passivation of porous carbon cathodes in $SOCl_2$-$LiAlCl_4$, **38,** 827
phthalocyanines
as dopants for carbon cathodes in Li/$SOCl_2$ cells: influence of metal and sintering temperature, **37,** 531
effect of the complexed metal on cathodic reduction products of CO_2, **36,** 1309
tetrasulphonated, of Co and Fe: adsorption at vitreous carbon electrodes, **36,** 2165, **37,** 769
physiological activity
and redox properties of some organoselenium compounds, **35,** 1133, **36,** 631
piezoelectric measurements
of PZC of Au electrodes in NaF aq, **37,** 139
piperazine ethylsulphonate
and other biological buffers: anodic polymerization of pyrrole, **37,** 1015
pitting
in Ni anodes in 0.1M H_2SO_4 with and without Cl^-: relation to passivation-induced stress, **37,** 2051
pitting corrosion
of Al studied by impedance spectroscopy, **37,** 2283
an analysis of reaction distribution over a pit, **38,** 1649
of anodically polarized Fe in 0.5M Na_2SO_4-0.001M $NaHSO_3$ aq, **38,** 2253
of Co in H_2SO_4 aq: current oscillations induced by I^-, **38,** 835
of coated metals: rate data from impedance studies, **38,** 1891
comparison of arc-melted and sputter-deposited Al-Zr alloys, **36,** 1227
of Cu in 0.1M $NaClO_4$ at 8<pH<11, **37,** 1437
of Cu in aqueous carbonates at 8<pH<12, **35,** 1337

pitting corrosion continued
effects of pretreatment of Al-5.03%Zn-1.67%Mg-0.23%Cu alloy on pitting and repassivation in NaCl-Na_2SO_4 aq, **38,** 2741
of low-carbon steels in 0.5M Na_2SO_4 aq caused by SO_3^{2-}, **38,** 253
spatial distribution of pits on stainless steel anodes in buffered aqueous chloride, **35,** 289
pitting potential
of aluminium in aqueous media, **38,** 2541
plasticized polymers
effect of plasticizers PC and EC on polyethers formed from acrylate esters of polyols and Li^+ salts, **37,** 1681
PEO containing $ZnBr_2$ and LiBr with poly(ethane-1,2-diol dimethylether) as plasticizer, **37,** 1667
platinized platinum electrode
adsorption of D-glucose from 1M H_2SO_4 aq, **37,** 2443
anodic oxidation of methanol in alkaline media, **36,** 519
effect on gas evolution overvoltage of a PTFE array on the surface, **35,** 1089
platinized porous carbon electrodes
effects of Pt crystallite size and nature on methanol oxidation in H_2SO_4 aq, **35,** 199
platinized titanium anodes
synthesis of glyoxylic acid in undivided cells, **35,** 621
platinum
anodic dissolution from Pt-C fuel-cell oxygen cathodes in phosphoric acid: effect on corrosion of the carbon, **37,** 2725
effect of a film sputtered on to the front surface of a low Pt loaded fuel cell cathode, **38,** 1661
effect of particle size on oxygen reduction in H_3PO_4 at cathodes supported on carbon black, **36,** 1979
multilayer oxide growth under potential cycling conditions in NaOH aq and $HClO_4$ aq, **37,** 43
particles electrodeposited into polypyrrole films: effect of deposition current on subsequent cathodic oxygen reduction, **35,** 135
platinum alloy
electrocatalysts for direct oxidation of methanol: characterization [R], **36,** 2053
platinum compounds
electrochemical behaviour at a carbon paste electrode in aqueous acids, **37,** 507
platinum electrodes see also platinum
activated by molybdenum ions for methanol oxidation, **35,** 849
adsorption of acetate ion and its effect on zinc acetate coatings, **36,** 2109
adsorption of Ca^{2+} induced by adsorbed anions and molecules, **36,** 1453
adsorption of CN^- and SCN^- from 0.1M $NaClO_4$ aq, **36,** 1849
adsorption of $H_2PO_4^-$ and H_3PO_4 acidic aqueous fluorides, **37,** 385
adsorption and oxidation of ethanal in 0.1M $HClO_4$, **35,** 989
adsorption of propargyl, allyl, methyl and propyl alcohols from 0.5M H_2SO_4 aq, **36,** 2003
anodic fluorination of benzene in MeCN-$R_4NF.nHF$ and MeCN-$Et_3N.3HF$, **38,** 619
bistable cyclic voltammograms for oxidations of HCOOH, $HCOO^-$, ethanol, propanol and butanol, **37,** 673
chemisorption of adsorbed CO species from MeOH, HCOOH and reduced CO_2, **37,** 2361
chemisorption of methanol at the (110) face in 0.1M Na_2CO_3 aq, **37,** 1883
chemisorption of 1,1,1-trichlorethane in H_2SO_4 aq, **38,** 281
columnar structured: early stages of Cu electrodeposition from $CuSO_4$-0.5M H_2SO_4, **37,** 2203
competitive and co-operative adsorptions of organic residues and CO, **36,** 2183
concentration dependence of UPD of Ag at (111) surfaces, **38,** 235
CV of porous catalyst films in 8% yttria-stabilized zirconia at 350 and 650°C with a wide range of oxygen pressures, **38,** 2533
diffusion of cathodically-generated atomic hydrogen, **36,** 615
effect of extent of oxidation on nucleation of Ag electrodeposits, **35,** 1873
effect of polarization in nitromethane on the hydrogen adsorption capacity and on oxidation of Cl^- in aqueous media, **38,** 1097
effect of protons on reduction of nitrate in molten $Ca(NO_3)_2.4H_2O$ at 80°C, **36,** 1639
effect of sputtered Au on methanol oxidation in H_2SO_4 aq, **36,** 947
effect of UPD Pb on oxidation of glucose, **38,** 2725
effect of UPD Pb on products of anodic oxidation of D-gulonic acid in 0.1M NaOH aq, **38,** 1359
effect of UPD of Bi, Pb or Tl on reduction of 3-nitro-1H-1,2,4-triazole, **35,** 1957
effect of UPD Pb, Bi and Tl on oxidation of D-glucose in acidic and neutral media, **37,** 1333
effect of water on oxidation in 0.5M $LiClO_4$-PC, **36,** 1397
effects of thiourea and poly(ethane-1,2-diol) on UPD of Cu on (111) and (110) faces, **38,** 647

platinum electrodes continued
electrocatalytic activity in oxidation of Cr(III), **38,** 437
electrodeposition of Ag single crystals from 0.5M $AgNO_3$-1M HNO_3 aq, **37,** 2233
electrodeposition and UPD of Bi, Cu and Ge: ellipsometric study, **37,** 2245
electrodispersed: effects of roughness and potential scan rate on Ag electrodeposits, **36,** 1617
Gibbs energies of activation for oxygen reduction at, **35,** 1157
impedance studies of chlorine evolution in acidic aqueous chloride solutions: rotating Pt thin-ring electrodes, **37,** 2715
influences of added hydroquinone, coumarin and crystal violet on UPD of Cu on (111) faces, **38,** 2467
inhibition of oxygen evolution by UPD Cu in acidic media, **36,** 1325
kinetics of cathodic deposition of Hg at, **35,** 339
Kolbe reaction examined by non-steady state potential methods, **35,** 1237
modified by reduced CO_2: interaction with propargyl alcohol and allyl alcohol in 0.5M H_2SO_4, **37,** 1083
modified with UPD Cd: oxygen reduction in acidic and neutral media, **37,** 2559
multilayer oxide growth under potential cycling in H_2SO_4 aq, **35,** 967
oxidation of CO at (111) surfaces in 0.05M $HClO_4$, **36,** 555
oxidation of HCOOH at anodes modified with aniline and polyaniline, **35,** 1459
oxidations of $HCOO^-$, HCHO, hydrazine and methanol in alkaline aqueous media, **36,** 1937
oxidations of HCOOH, $HCONH_2$ and DMF in 0.05M H_2SO_4 aq, **38,** 185
oxidation of HCOOH in 0.5M H_2SO_4 aq, **38,** 1899
oxidations of hydrazine, methanol, HCHO and $HCOO^-$ in aqueous alkali, **35,** 1821
oxidations and reductions of sulpholane and DMSO in 0.5M H_2SO_4 aq, **38,** 175
oxygen evolution in alkaline solutions: electron transfer through thin oxide films, **37,** 2533
oxygen reduction in aqueous acids: activation energy increments and the Pt-O vibrational quantum, **37,** 1
oxygen reduction at microcathodes in concentrated phosphotungstic acid at 25 and 60°C, **38,** 1733
polyfaceted and spherical: nucleation and growth of Ag electrodeposits from Ag_2SO_4 aq, **37,** 2215
potential oscillations during anodic oxidation of HCOOH, **37,** 37
potential oscillations during methanal oxidation in acidic media, **38,** 503
potential oscillations during simultaneous oxidation of CO and H_2, **36,** 639
potential oscillations and periodic variations in amount of chemisorbed species during oxidation of methanoic acid, **38,** 2385
quantum chemistry and *in situ* FTIR spectral studies of potential-dependent properties of adsorbed CO, **38,** 1107
radiotracer studies of adsorption of primary amino compounds at [R], **35,** 919
reactions in wet and dry KNO_3, $NaNO_3$ and their equimolar mixture at 300 and 340°C, **38,** 2611
reductions NO_3^- and NO_2^- in H_2SO_4 aq, **36,** 877
role of incipient hydrous oxide species in the methanol-air fuel cell, **37,** 1817
second-order Stark effect: bond restrictions in adsorbed SO_4^{2-} caused by the applied electric field, **37,** 2179
some factors affecting the formation of "unusually reactive" Pt, **38,** 897
specific adsorption of hydrogen from 0.5M H_2SO_4 aq on polycrystalline Pt, **37,** 2629
unmodified and modified with UPD Pb, Bi and Tl: oxidation of D-glucose in aqueous alkali, **37,** 1909
voltammetry of sulphide, thiosulphate, sulphite, dithionite and sulphate in 0.5M NaCl aq, **37,** 2785
with and without SPE: transient measurements of methanol oxidation in acid, **36,** 1043
X-ray adsorption fine structure of UPD Cu, **36,** 1869
X-ray absorption spectroscopic study of UPD of Cu on the (100) face, **37,** 1977
platinum electrodeposits
on graphite: improved dispersion and catalytic activity from pretreatment with Sn-$PdCl_2$ solutions, **38,** 1551
platinum oxides
formed by potential cycling in H_2SO_4 aq, **35,** 967
platinum-tin oxide electrode
compared with Pt anodes for the oxidation of methanol, HCHO and $HCOO^-$, **37,** 1317
point/plane electrode configurations
theoretical impedances, **38,** 597
Poisson distribution
of corrosion pits on passive Fe in borate buffers with Cl^-, **35,** 1809
of etch pits on stainless steel anodes in buffered aqueous chloride, **35,** 289
polarography
a tribute to its inventor on the centenary of his birth, **36,** 221
polarons
and bipolarons: charge carriers in polypyrrole, **36,** 1263

pollution see effluent treatment
polyacetylene see polyethyne
polyacrylamide
adsorption at Au and mild steel from H_2SO_4 aq and HI aq, **36,** 1315
electrogeneration in DMF solutions: effect of pH, **37,** 2083
poly(2-acrylamido-2-methylpropane sulphonic acid)
combined with polyaniline, Prussian Blue and WO_3: electrochromic window electrolyte, **38,** 1497
poly(2-acrylamido-2-methylpropane sulphonic acid)-poly(ethene imine)
solid polymer electrolyte electrochromic window, **37,** 1377
polyacrylonitrile
complexes with Li^+ salts: conductivity and NMR studies, **37,** 1671
grafting and polymerization on metal cathode surfaces, **38,** 1501
polyacrylonitrile electrodes
formed by compression of thermally structurized powder: impedance in 1M $LiClO_4$-PC, **37,** 2453
polyalcohols
oxidation at Ni anodes in 1M KOH aq, **35,** 375
poly(alkeneviologen)-poly(*p*-styrene sulphonic acid) complex films
kinetics of cathodic one-electron reduction of the viologen dication, **35,** 63
poly(N-alkylene dimethyl-N,N'-piperazinium diiodide)-AgI double salts
total electrical conductivities, **35,** 77
polyamide-ether electrolytes
hosts by condensation of polyacid chlorides and α,ω-diamine poly(oxyethene-co-oxypropene), **37,** 1737
polyaniline
combined with Prussian Blue, WO_3 and poly(2-acrylamido-2-methylpropane sulphonic acid) in electrochromic windows, **38,** 1497
composite with the disulphide, 2,5-mercapto-1,3,4-thiadiazole: positive electrode for lithium cells, **37,** 1851
effect of molecular mass on added poly(styrene sulphonate), **36,** 357
incorporation of Cl^- and SO_4^{2-} ions, **35,** 899
incorporation of polymeric sulphonates, **36,** 87
ion-selective irreversible doping by polymer electrolyte, **35,** 827
layer formed at one side of a cation-exchange membrane, **37,** 555
nucleation and growth at Au and Pt microanodes: initial compact layer and subsequent branching, **37,** 2255
polyaniline film electrodes
adsorption and oxidation of HCOOH, **35,** 1459
adsorption of poly(styrene sulphonate) by anion exchange with ClO_4^- dopant, **36,** 799
coulombic irreversibility of the switching charge, **38,** 1711
effect of film thickness on rate of nucleation of Ag, **36,** 1151
electrocatalytic and two types of photochemical behaviour, **36,** 361
impedance studies, **35,** 1665
influence of pH on semiconductor and photoelectrochemical behaviours, **36,** 2015
photoassisted reduction of oxygen, **37,** 1003
on Pt substrates: effects of pH and electrolyte concentration on CV response, **35,** 27
stability of films formed by potentiostatic pulse polymerization in 0.5M H_2SO_4, **36,** 1579
temperature dependence of conductivity and capacitance, **38,** 2503
on vitreous carbon substrates: oxidation of hydrazine in H_2SO_4 aq, **35,** 1425
polyaniline films
on carbon fibre electrodes in aqueous methanol: anodic formation and electrochemical properties, **38,** 1559
on a carbon fibre microelectrode: electrochemistry of the isopolymolybdate dopant, **38,** 1029
effects of pH and solution composition on electrochemical behaviour, **38,** 393, 1051
formed at ITO anodes in 0.1M TBA salt-1,2-dichloroethane: anion effect on electrochromic behaviour, **37,** 2101
incorporation of hydrolysis products during anodic formation by cyclic potential scanning in 0.2M aniline-1M $HClO_4$ aq, **38,** 1395
on ITO electrodes: determination of reduction factors by visible absorption spectra and cyclic voltammetry, **38,** 1643
on ITO glass: anode for a SPE electrochromic window with a WO_3/ITO/glass cathode, **37,** 1377
prepared chemically: electrochromic behaviour, **36,** 2143
polyaniline-polypyrrole electrodes for secondary lithium cells, **38,** 2011
poly(*o*-anisidine)
films on ITO electrodes in various electrolytes: electrochromic behaviour, **37,** 1653

polybithiophene
positive electrode in secondary lithium cells with new polymer electrolyte, **35**, 1781
positive electrode in solid state secondary lithium cells, **35**, 251
poly(2,2'-bithiophene), n-doped
solvent and electrolyte effects on electrochemical behaviour, **35**, 463
poly(2,2'-bithiophene)/poly(xylylviologen)dibromide bilayer on Pt: transient spectroelectrochemical studies of charge trapping, **37**, 1887
polycarbosilanes
cathodic formation from dichlorocarbosilanes using AC in an undivided cell with Al electrodes in THF or DME, **38**, 529
poly(2-chloroaniline) films
formed at ITO anodes in 1,2-dichloroethane-0.1M TBA salts: anion effect on electrochromic behaviour, **37**, 2101
poly(dimethylsiloxane)
a basis for novel single- and double-ion type solid electrolytes, **37**, 1183
poly(1,3-dioxolane)
Li^+ conduction in solid electrolyte complexes, **36**, 773
poly(1,3-dioxolanes)
polymer and copolymer hosts for electrolytes, **37**, 1589
polyepoxides
chain-extended, comb-like, with oligo(ethene oxide) units in side chains: synthesis and complexation with $LiClO_4$, **37**, 1559
poly(ethane-1,2-diol)
complexes with Li^+ salts: conductivity and ^7Li NMR studies, **37**, 1533
effect on UPD Cu on Pt single crystal electrodes, **38**, 647
oligomers containing $CoBr_2$: comparison of conductances with $CoBr_2$ complexes in poly(tetramethyleneglycol), **37**, 1695
poly(ethane-1,2-diol dimethylether)
plasticizer in PEO containing $ZnBr_2$ and LiBr, **37**, 1667
poly(ethene imine), benzylated
coating on a glassy carbon electrode incorporating quinones: voltammetric pH measurement, **37**, 2765
poly(ethene imine), branched
complexes with CF_3SO_3Li: conductivity, calorimetry and IR spectra, **37**, 1623
complexes with H_3PO_4: conductivity, stability and hygroscopicity, **37**, 1619
poly(ethene imine)-poly(2-acryamido-2-methylpropane sulphonic acid)
solid polymer electrolyte electrochromic window, **37**, 1377
poly(ethene oxide)
amorphous, containing $LiClO_4$ or $LiCF_3SO_3$: DC polarization between Li electrodes, **37**, 1517
amorphous methoxy-linked, $Zn(CF_3SO_3)_2$ complex: conductivity, transport and interfacial studies, **37**, 1707
blends with various acrylic polymers: matrices for solid electrolytes, **37**, 1565
complexes with sulphamide and a proton-vacancy dopant (e.g. guanidine): phase diagrams and conductivities, **37**, 1603
conduction by complex Cu(I) iodides in $(PEO)_nKCu_xI_{1+x}$, **37**, 1599
conductivities of complexes with bis(trifluoromethylsulphonyl)imide salts of Cu(II), Pb(II) and Ni(II), **37**, 1743
conductivity of complexes with 5-mercapto-1-methyltetrazoles of Li^+, Na^+ and K^+, **37**, 1645
conductivity, cyclic voltammetry and calorimetry of complexes with $Cu(CF_3SO_3)_2$, **37**, 1711
conductivity and thermal properties compared for $LiClO_4$, $LiCF_3SO_3$ and $LiN(CF_3SO_2)_2$, **37**, 1579
containing alkali metal salts: insertion of Li^+, Na^+ and K^+ into polyethyne, **37**, 1675
containing $LiCF_3SO_3$: diffusion rates of electroactive species, **38**, 2315
containing $LiClO_4$ and lithium tetracyanoquinodimethane: ion-electron mixed conduction, **37**, 1521
containing pairs of inorganic salts: conductivity and local structure, **37**, 1529
containing $ZnBr_2$ and LiBr with poly(ethane-1,2-diol dimethylether) as plasticizer, **37**, 1667
copolymer with styrene macromonomer of PEO: lithium cell electrolyte, **35**, 1781
FTIR spectra of $M(CF_3SO_3)_2PEO_n$ with M = Zn or Pb and n = 9, 16 and 24, **37**, 1689
insertion into layer silicates to change conductivity by association with interlayer cations, **37**, 1573
ion-complexing oligomers copolymerized with triad aromatic ester mesogenic blocks, **37**, 1479
local structure in $NiBr_2(PEO)_8$, **37**, 1663
NMR study of $[P(EO)_8.LiClO_4]$, **37**, 1685

poly(ethene oxide) diisocyanates
condensed with PEO triols: with and without $Li(CF_3SO_2)_2N$ or $LiClO_4$, **37**, 1585
poly(ethene oxide) films
NMR spectroscopy of $M(CF_3SO_3)_2PEO_n$, M = Zn or Pb, $8<n<25$, **37**, 1487
poly(ethene oxide) triols
condensed with PEO diisocyanates: with and without $Li(CF_3SO_2)_2N$ or $LiClO_4$, **37**, 1585
poly(ethene oxide)-lithium salt electrolytes
reversibility of the Li electrode, **38**, 1199
polyether oligomers
conductances of solutions of $CoBr_2$ in poly(tetramethyleneglycol) and poly(ethane-1,2-diol), **37**, 1695
polyethers
e.g. 2-(2-methoxyethoxy)-ethylglycidylether: condensation with triols to form network polymers, **37**, 1725
radiation-induced polymers of acrylate esters of polyols and Li^+ salts with PC and EC plasticizers, **37**, 1681
Raman study of ion-ion and ion-polymer interactions in low molecular-weight complexes with $LiCF_3SO_3$, **37**, 1495
polyethylene see polyethene
polyethyne
p-doped: model for galvanostatic charging tested in 1M $LiClO_4$-PC, **35**, 467
impedance studies, **35**, 1665
intercalation by Li^+, Na^+ and K^+ from PEO-based solid electrolytes, **37**, 1675
voltammetric behaviour of films in 1M $LiClO_4$-PC, **36**, 2025
poly(glycidylethers)
condensation with triols to network polymer hosts for $LiClO_4$: high conductivities and low temperature-dependences, **37**, 1725
polyheterocyclic conducting polymers
solvent and electrolyte effects on behaviour of poly(2,2'-bithiophene), **35**, 463
polyimide
coatings on Al metallizations of Si substrates: impedance studies of cathodic degradation, **38**, 1877
poly(itaconic acid ester)
with oligo(ethene oxide) side chains and $Ca(ClO_4)_2$ or oligo(propene oxide) side chains and $ZnCl_2$, **37**, 1539
polymer blends
polymerization of methylmethacrylate in presence of PEO: protonic conduction of complex with H_3PO_4, **37**, 1733
polymer electrodes
impedance study of Li^+ insertion from 1M $LiClO_4$-PC, **35**, 403
polymer electrolytes see also solid polymer electrolytes
applications in electrochromics, sensors and biology, **37**, 1649
based on copolymers of SO_2 and either ethene oxide or various vinyl monomers, **37**, 1555
copolymers of EO and epichlorohydrin, mixed with oligo EO and $LiClO_4$: Li^+-conducting elastomers, **37**, 1721
containing pairs of inorganic salts: relationships between local structure and conductivity, **37**, 1529
crown-ether groups attached to polyphosphazene backbones and complexed with alkali-metal salts: conductivities, **37**, 1545
highly-conducting Li^+ salts of $N(SO_2CF_3)_2^-$ and $C(SO_2CF_3)_3^-$, **37**, 1551
hosts: condensation of α,ω-diamine poly(oxyethene-co-oxypropene) with polyacid chlorides, **37**, 1737
incorporation of polymeric sulphonates into polyaniline, **36**, 87
incorporation of polymeric sulphonates into polypyrroles, **35**, 1245
ion-selective irreversible doping of polyaniline by, **35**, 827, **36**, 357
ion solvation and association: effects of temperature and pressure, **37**, 1505
ionene glasses with bound cationic nitrogen and mobile anions, **37**, 1491
$LiClO_4$ complexed with poly(propene oxide) polymerized with phenyl isocyanate, **37**, 1511
new PEO-styrene-based polymer for lithium-polybithiophene cells, **35**, 1781
$(PEO\text{-}SEO)_{20}LiClO_4$ with poly(N-oxyalkylpyrrole) positive electrodes in secondary lithium cells, **37**, 1631
poly(1,3-dioxolane) and poly(tetrahydrofuran) solid complexes with $LiClO_4$, **36**, 773
polyepoxides, chain-extended, comb-like, with oligo(ethene oxide) units in side chains, complexed with $LiClO_4$, **37**, 1559
reversibility of the Li electrode, **38**, 1199
in secondary lithium cells [R], **38**, 1233
in solid-state power cells: studied by four-probe polarization with sequential, bipolar, rectangular current pulses, **38**, 1289

polymer electrolytes continued
viscous liquids as separators of self-sealing, laminated, electrochromic glass windows, **37,** 1703
polymer film electrodes
effects of film thickness and its variations on impedance data, **36,** 847, 1527
impedance studies explained by a two-capacitance model, **38,** 773
styrene-maleic anhydride copolymer on vitreous carbon electrodes: effect on $Fe(CN)_6^{3-/4-}$ kinetics, **37,** 2573
validation of impedance data using the Kramers-Kronig transformation, **38,** 1047
polymer films
coating technologies and adhesion in relation to device requirements, **37,** 1471
polymer films, conducting
pyrrole or aniline polymerized into one side of a cation-exchange membrane, **37,** 555
pyrrole groups attached to amines, **35,** 1273
pyrrole groups attached to aza-macrocycles, **35,** 1051
polymer gel films
containing *p*-diacetylbenzene or dialkylterephthalates: electrochromic behaviour, **37,** 369
polymer syntheses
I^- replacement through anodic oxidation of polymer solutions containing the entering anion, **37,** 751
polymer-coated metals see coated metals and painted metals
polymerization
of acetylenic alcohol corrosion-inhibitors adsorbed on an Fe surface from H_2SO_4 aq, **37,** 317
of acrylonitrile and methacrylonitrile on metal cathode surfaces, **38,** 1501
of an adsorbed amphiphilic N-substituted pyrrole at graphite and ITO electrodes, **38,** 2485
of aniline in 1M $HClO_4$: effect of molecular mass of added poly(styrene sulphonate), **36,** 357
of aniline or 2-chloroaniline at ITO anodes in 1,2-dichloroethane-0.1M TBA salts: anion effect, **37,** 2101
of aniline at Au and Pt microanodes: initial compact layer and later branching, **37,** 2255
of aniline at carbon fibre anodes in aqueous methanol, **38,** 1559
of aniline by anodic potentiostatic pulses in 0.5M H_2SO_4, **36,** 1579
of aniline by potential scanning in 0.2M aniline-1M $HClO_4$: incorporation of hydrolysis products into the film, **38,** 1395
of aniline and pyrrole: preparation of positive electrodes for lithium cells, **38,** 2011
of benzene in $PhNO_2$-$LiAsF_6$-$CuCl_2$ to form thick poly(*p*-phenylene) films on Pt, **37,** 1093
of benzo-15-crown-5-substituted N-methylpyrrole, **36,** 1377
of dichlorocarbosilanes using AC in an undivided cell with Al electrodes in THF or DME, **38,** 529
electrochemical of acrylamide in DMF solutions: effect of pH, **37,** 2083
kinetic study of anodic polymerization of pyrrole: effects of concentration, electrolyte and temperature, **37,** 297
of Me_2SiCl_2-Ph_3SiCl mixture to polysilanes at Pt cathodes in 0.4M $TBABF_4$-DME, **36,** 621
of naphthidine to form thin conducting films at Pt anodes in MeCN-$NaClO_4$, **35,** 731
of 1-naphthylamine at Pt anodes in $HClO_4$ aq, **35,** 741
of organodichloromonosilanes to organopolysilanes at Pt cathodes, **35,** 1867
plasma, of dimethyl-2-[(2-ethoxyethoxy-)ethoxy]-vinylsilane: SPE with vapour-deposited LiI, **37,** 1483
of pyrrole, **36,** 2123
of pyrrole: decomposition of propene carbonate by protons liberated in the anodic process, **37,** 2595
of pyrrole in aqueous media: minimization of degradation, **37,** 1227
of pyrrole at Ag electrodes, **35,** 315
of pyrrole at Ag electrodes: a SERS study, **35,** 315
of pyrrole at a graphite particle bed anode periodically fluidized by pulsing, **36,** 1953
of pyrrole at Pt anodes in acetonitrile: influence of N-methylphenothiazine, **37,** 513
of pyrrole at Pt anodes in acetonitrile with water, **35,** 1841
of pyrrole at Pt anodes in presence of glucose oxidase, PIPES buffer, $LiClO_4$ and sodium dodecylsulphate, **37,** 1987
of pyrrole attached to amine groups in 0.1M $TEABF_4$-MeCN, **35,** 1273
of pyrrole attached to aza-macrocycles, **35,** 1051
of pyrrole from a dispersion of 0.4μm anatase particles to form a composite TiO_2-polypyrrole film, **37,** 1265
of pyrrole and N-methylpyrrole in $NaClO_4$ aq: effect of incorporated polymeric sulphonates on surface morphology, **35,** 1245
of pyrrole on particles of a pulsed-bed electrode: mass-transfer study, **38,** 217
of pyrrole in the presence of biological buffers e.g. piperazine ethylsulphonate, **37,** 1015
of pyrrole within the cylindrical pores of a microporous membrane, **37,** 1611
of pyrroles, **36,** 733

polymerization continued
of silica gels formed by hydrolysis of tetramethoxysilane at various pH: time-dependence of conductivity, **38,** 371
of thiophene-3-acetic acid at Pt anodes in 0.1M $LiClO_4$-MeCN, **37,** 393
of *o*-toluidine and *o*-anisidine : electrochromic efficiency of the films on ITO electrodes, **37,** 1653
of vinyl ferrocene and methoxy-nona(ethene oxide)methacrylate containing $LiClO_4$: mixed conducting polymer, **37,** 1521
polymethacrylonitrile
grafting and polymerization on metal cathode surfaces, **38,** 1501
1,1'-polymethylene-bispyridinium dications
reductions at Hg cathodes in $TBAPF_6$ solutions in MeCN, DMF and DMSO, **37,** 2481
poly(N-methylpyrrole)
effect of incorporated polymeric sulphonates on surface morphology, **35,** 1245
ion-exchange mechanisms in tosylate-doped films on Au electrodes, **38,** 349
poly(methylthiophene)
electrochromic window, **36,** 837
poly(3-methylthiophene)
electrochromic electrode in PC-$LiClO_4$ with an ITO counter electrode, **35,** 1757
impedance study of the redox mechanism, **37,** 1417
poly(methylthiophene) film electrode
mechanism of electron transfer from N-phenyl-*p*-phenylenediamine in MeCN, **38,** 271
poly(3-methylthiophenes)
electrosynthesized from dimers and tetramers: electrochromic behaviour, **38,** 135
polynaphthidine
preparation and properties of thin conducting films on Pt, **35,** 731
poly(1-naphthylamine)
mechanism of formation at Pt anodes in aqueous acid, **35,** 741
poly(3-octylthiophene) film electrode
preparation on a Pt substrate and impedance behaviour in PC-$LiBF_4$, **37,** 1759
poly(N-oxyalkylpyrrole)
positive electrodes in lithium cells with $(PEO\text{-}SEO)_{20}LiClO_4$ and liquid electrolytes, **37,** 1631
poly(oxyethene)
complexes with $LiN(CF_3SO_2)_2$: stability ranges and conductivities, **37,** 1699
poly(*p*-phenylene)
thick films on Pt: anodic synthesis from benzene and performance as a positive electrode in secondary cells, **37,** 1093
poly(*o*-phenylenediamine)
films on Au electrodes: kinetics of inorganic redox reactions in H_2SO_4, **37,** 635
poly(propene oxide)
ion association in complexes with LiSCN, NaSCN, KSCN, $LiClO_4$, $NaClO_4$ and $LiBF_4$, **37,** 1499
polymerized with phenyl isocyanate and complexed with $LiClO_4$: conductivity, **37,** 1511
polypyrrole
comparison of specimens formed by anodic and chemical oxidations, **36,** 733
doped with dodecylbenzene sulphonate: synthesis on ITO anodes and electrochromic properties in KCl aq, **38,** 869
effect of incorporated polymeric sulphonates on surface morphology, **35,** 1245
effect of water on mechanism of formation at Pt anodes in acetonitrile, **35,** 1841
enhanced conductivities through template synthesis within pores of a microporous membrane, **37,** 1611
formation at Ag electrodes, **35,** 315
growth, cycling and over-oxidation in 1M $NaClO_4$ aq, **36,** 1263
influence of N-methylphenothiazine on formation at Pt anodes in acetonitrile, **37,** 513
ion-exchange mechanisms in tosylate-doped films on Au electrodes, **38,** 349
layer formed at one side of a cation-exchange membrane, **37,** 555
mimimization of degradation during formation in aqueous media, **37,** 1227
polypyrrole film electrode
containing TiO_2 particles on Pt or stainless steel substrates, **37,** 1265
effect of polymerization in the presence of dodecylbenzene sulphonate, **37,** 1173
effects of temperature and solution composition on open-circuit electrode potentials, **37,** 1075
ellipsometric study of polymerization and subsequent cycling, **36,** 2123
with incorporated anionic cobalt complex: oxygen reduction electrocatalyst, **37,** 763

polypyrrole film electrode continued
incorporating glucose oxidase: glucose sensor when used with 1,4-benzoquinone electron-transfer mediator, **37,** 1987
incorporating sub-equivalent amounts of dodecylsulphate, **35,** 1971
polymerization of pyrrole grafted with nickel cyclam, **36,** 15
Q vs E data for reversible oxidation in acetonitrile, **35,** 1815
polypyrrole films
anodic preparation in the presence of biological buffers, **37,** 1015
containing dodecylsulphate: electrochromic behaviour, **35,** 1145
effect of dodecylsulphate incorporation on kinetics of redox processes, **37,** 419
effects of dopant and solvent on conductivity and electrochemical activity, **38,** 441
formed at Pt anodes in neutral aqueous solution: electrochemical behaviours in various support electrolytes, **38,** 2581
formed at Pt anodes in neutral aqueous solution: incorporation of cytochrome *c*, **38,** 2581
impedance studies, **35,** 1665
on Pt electrodes: influence of inserted anions on electrochemical behaviour, **35,** 567
substituted with benzo-15-crown-5: synthesis and polymerization of the monomer, **36,** 1377, 2197
polypyrrole-modified electrode
with incorporated Pt particles: reduction of oxygen at, **35,** 135
polypyrroles formed by anodic and chemical oxidations
charge capacity, infrared spectroscopy and conductivity under pressure, **37,** 1227
polysiloxane
film base for viologen mediators in reaction of oxygen with photoexcited $Ru(bpy)_3^{2+}$ in a Nafion layer, **38,** 129
poly(styrene sulphonate)
coating containing $Os(bipy)_3^{2+/3+}$ on glassy C anodes: oxidations of hexacyanometallates and catechol, **38,** 1321
ion-selective adsorption at polyaniline film electrodes, **36,** 799
poly[styrene-4-vinyl(N-methylpyridinium iodide)]
anion replacement by anodic oxidation in solutions of the entering anion, **37,** 751
poly[styrene-4-vinyl(pyridinium hydroiodide)]
cross-linked, anion replacement by anodic oxidation in solutions of the entering anion, **37,** 751
polysulphites
copolymers of SO_2 and ethene oxide: matrices for polyelectrolytes, **37,** 1555
polysulphones
copolymers of SO_2 and various vinyl monomers: matrices for polymer electrolytes, **37,** 1555
poly(tetracyanoquinodimethane) film electrodes
effects of film thickness and its variations on impedance data, **36,** 847, 1527
effects of temperature and LiCl electrolyte concentration on impedance, **36,** 1355
poly(tetrafluoroethene)
effect on overvoltages for HER, OER and oxidation and reduction of organics at Ni electrodes, **37,** 353
poly(tetrahydrofuran)
Li^+ conduction in solid-electrolyte complexes, **36,** 773
poly(tetramethyleneglycol)
oligomers containing $CoBr_2$: comparison of conductances with $CoBr_2$ complexes in poly(ethane-1,2-diol), **37,** 1695
polythiophene film electrode
mechanism of electron transfer from N-phenyl-*p*-phenylenediamine in MeCN, **38,** 271
polymerization of thiophene grafted with nickel cyclam, **36,** 15
Q vs E data for reversible oxidation in acetonitrile, **35,** 1815
poly(thiophene-3-acetic acid)
layer-by-layer nucleation and growth at Pt anodes in 0.1M $LiClO_4$-MeCN, **37,** 393
poly(*o*-toluidine)
films on ITO electrodes in various electrolytes: electrochromic behaviour, **37,** 1653
poly[bis(1,1,1-trifluoroethoxy)phosphazene]
networks linked by 1,4,8,11-tetraazacyclotetradecane and containing perchlorates of Na or Ni, **37,** 1539
with pendant 12-crown-4 ethers, complexed with alkali-metal salts: conductivities, **37,** 1545
poly(trithiocyanuric acid)
organo-disulphide redox positive electrodes for lithium cells: X-ray absorption, **37,** 1635

poly(vinyl alcohol)
composite films with montmorillonite clay on graphite: kinetics of confined $Ru(NH_3)_6^{3+/2+}$, **37,** 1865
composite films with montmorillonite clay on graphite: permeation by neutral and anionic species from solution, **37,** 1865
mixed conduction salts from oxidation by bromine then hydrolysis by hydroxide, **36,** 899
poly(vinyl chloride)
ion-selective membranes for Ca^{2+} based on the ETH1001 ionophore, **37,** 2691
plasticised membranes containing neutral carriers of ionic species: impedance at constant current, **38,** 2691
properties of membranes in ion-selective electrodes [R], **35,** 1
poly(vinyl chloride) membranes
containing dioctylphenyl phosphonate and CaI_2: ion transport, **38,** 2373
containing plasticizers and electrolytes: equilibrium potentials at the aqueous interface, **37,** 1021
poly(vinyl ether)
with oligo(ethene oxide) side chains and containing perchlorates of Ca^{2+} or Mg^{2+}: conductivities, **37,** 1539
poly(vinylferrocene)
swelling of films studied by the quartz crystal microbalance, **37,** 647
poly(vinylpyridine)-osmium complex
electrodeposition of Ag on vitreous carbon electrodes coated with, **35,** 985
poly(4-vinylpyridine)-osmium-2,2'-bipyridyl complex
charge-transfer reactions of films on vitreous carbon electrodes in neutral solutions, **37,** 159
poly(xylylviologen dibromide)
outer layer on Pt/poly(2,2'-bithiophene) electrode: transient spectroelectrochemical study of charge trapping, **37, 1887**
porosity
of protective coatings on metals, **38,** 1799
porous electrodes
anodic polymerization of pyrrole on graphite particles, **36,** 1953
deposition and dissolution of Zn at flow-through electrodes, **38,** 311
determination of active surface area from weak electrochemiluminescence, **36,** 1591
electrodeposited Pd on carbon felt: electrocatalytic hydrogenation of benzaldehyde, **37,** 365
impedance studies, **35,** 1579
impedance studies, of polyacrylonitrile electrodes formed by compression of thermally structurized powder, **37,** 2453
influence of Pt area and H_3PO_4 uptake on oxygen reduction at PTFE-bonded carbon-Pt cathodes, **38,** 913
platinum utilization and uptake of phosphoric acid, **36,** 1049
theoretical impedance, **38,** 2653
porous films
in alumina: luminescence during pore filling, **35,** 825
effect on reaction and ohmic overpotentials, **38,** 2699
mechanism of hydration and pore closure during hydrothermal treatment of anodic films on Al, **37,** 125, **38,** 1413
porphyrin ion complex
catalysis of oxygen reduction by an anionic-cationic complex, **36,** 703
porphyrins <u>see</u> <u>also</u> metalloporphyrins
substituted with 4-nitrophenyl groups: selective reductions of the nitrogroups with cathode and anode in succession, **38,** 325
positive shifts of Mott-Schottky intercepts and photocurrent onset potentials for n-WSe_2/1M H_2SO_4 caused by white light, **36,** 2039
potassium
SVP and thermodynamic properties of solutions in melts of its mixed halides, **35,** 529
potassium vanadate
doped with neodymium oxide: creation of a transient power cell by application of a high field, **37,** 1143
potential distribution
in multi-electrode cells: use of external resistors to obtain uniformity, **36,** 841
potentials of zero charge
of Au, Cu, Fe and Ni in aqueous media by the inversion-immersion method, **35,** 1393
and capacitance minima of Au electrodes in NaF aq, **37,** 139
temperature coefficients and relationship to the work function, **36,** 1659
and work functions of gold {111}, {311}, {110} and {210} surfaces, **35,** 1383

potentiometric stripping analysis
and speciation of heavy metals in environmental studies, **38,** 807
potentiometric titration
of Mg(II) by PbO in $PbCl_2$-KCl at 475°C, **38,** 1743
potentiometry
with indicator electrodes contacting two adjoining regions of solution, **36,** 69
solubilities of metal oxides in CsCl-KCl-NaCl eutectic at 600°C determined by titration, **38,** 1481
of suspensions: double layer and particle size effects, **36,** 59
of suspensions: interactions between the sediment and the double layer of the indicator electrode, **36,** 943
Pourbaix diagrams
for complexes of phenanthroline with Fe(II) and Fe(III) in aqueous sulphate, **35,** 209
prccipitated salt films
effect on low-frequency impedance spectra, **36,** 1183
probability density
for solvent molecule orientation in the ion-dipole model of the double layer, **36,** 1715
probability density functions
molecular solvent models of the solution side of the double layer, **36,** 1677
probabilty
the Markov chain approach to electrode processes of undetermined mechanism, **38,** 1147
1,2-propanediol
mixtures with water: medium effect on behaviour of the $Zn(Hg)/Zn^{2+}$ electrode in 0.05M $LiClO_4$, **38,** 2459
oxidation and reduction at Pt electrodes in aqueous acids, **38,** 541
propanediols
effect of UPD Pb on oxidation at Pt and Au anodes, **36,** 1157
propanol
anodic stripping of adsorption residues from Pt in 0.5M H_2SO_4, **36,** 2003
on-line MS analysis of products of oxidation at Au anodes in 0.5M H_2SO_4 aq, **38,** 1337
2-propanol
effect of composite-plated PTFE on overvoltages for oxidation at Ni anodes, **37,** 353
partial oxidation at Pt supported on graphite particles in a packed-bed anode, **38,** 221
propanone
conductances of perchlorates of Mn(II), Co(II), Ni(II), Cu(II) and Zn(II) in solutions of, **35,** 351
propargyl alcohol
anodic stripping of adsorption residues from Pt in 0.5 M H_2SO_4, **36,** 2003
interaction with a Pt electrode, modified by reduced CO_2 in 0.5M H_2SO_4, **37,** 1083
on-line MS analysis of products of oxidation at Au anodes in 0.5M H_2SO_4 aq, **38,** 1337
propen-3-ol see allyl alcohol
propene carbonate
decomposition by protons liberated during anodic polymerization of pyrrole, **37,** 2595
effect on solvation of Li^+ by bis[2-(2-methoxyethoxy)ethyl] ether, **37,** 2043
influence of water on decomposition at Pt anodes, **36,** 1397
oxidation and reduction at Pt electrodes in aqueous acids, **38,** 541
propyn-3-ol see propargyl alcohol
proteins
adsorption on graphite electrodes: effect on redox kinetics, **35,** 177
protonation rates
of electrogenerated carbanions by parent 2-bromoisobutyramides, **35,** 81
protonic conduction
by complex of H_3PO_4 with blended PEO-poly(methylmethacrylate), **37,** 1733
of complexes of poly(ethene imine) with H_3PO_4, **37,** 1619
in copolymers of various organically-substituted silanes: membranes for methanol fuel cells, **37,** 1615
proton-vacancy conducting polymers
PEO-sulphamide-proton vacancy dopant (e.g. guanidine), **37,** 1603
Prussian Blue
combined with polyaniline, WO_3 and poly(2-acrylamido-2-methylpropane sulphonic acid) in electrochromic windows, **38,** 1497
Prussian Blue battery
with CdS film in a photochargeable multilayer membrane device, **35,** 291
Prussian Blue films
influence of cation exchanges of K^+, H^+ and Li^+ on electrochemical behaviour, **37,** 501

pulse plating
of Cu at a RDE from acidic $CuSO_4$ aq: effects of pulse and other parameters on thickness distribution, **37,** 1927
of Cu at the RDE with square cathodic currents: mass transfer, **36,** 625
pulse polarography
application of Matsuda theory to very fast coupled chemical reactions, **37,** 1129
pulse voltammetry
oxidation of anthracene at Pt anodes in MeCN-$TBAPF_6$, **36,** 1475
study of multivalent elements in molten oxide glasses, **38,** 479
pulsed-bed reactor
anodic polymerization of pyrrole on graphite particles, periodically fluidized, **36,** 1953, **38,** 217
pyrazolone
substituted: reduction at Hg cathodes of complexes with UO_2^{2+} in propene carbonate, **36,** 325
pyrene
effect of light on reduction at Hg channel cathodes in acetonitrile, **35,** 1837
pyridazin-3-ones
reductions at Hg cathodes in aqueous ethanol, **35,** 1907
pyridine
complexation of silver salts in, **35,** 509
pyridine N-oxide
conductances and association constants of protonated species in acetonitrile, **35,** 665
bispyridinium dications
substituent effects in reductions at Hg cathodes in $TBAPF_6$ solutions in MeCN, DMF and DMSO, **37,** 2481
pyridinium ylides
reductions at Hg cathodes in 0.1M $LiClO_4$-MeOH, **36,** 101
2-(2-pyridyl)-1,3,4-triazine derivatives
reductions of new tetradentate ligands at Hg cathodes in DMF-TBAP, **36,** 1997
pyrolytic graphite electrode
adsorption and redox behaviour of cytochrome c_3 at the basal plane, **36,** 1423
adsorption of tetrasulphonated phthalocyanines of Co and Fe, **36,** 2165, **37,** 769
effect of adsorbed proteins on rates of redox reactions, **35,** 177
pyrophosphate complexes of Pb(II), Sn(II) and Cu(II) etc
reductions at Hg cathodes in weakly alkaline media, **36,** 427
pyrrole
decomposition of propene carbonate by protons liberated during anodic polymerization, **37,** 2595
kinetic study of anodic polymerization: effects of concentration, electrolyte and temperature, **37,** 297
polymerization at a graphite bed anode, periodically fluidized by pulsing, **36,** 1953
polymerization at Pt anodes in acetonitrile: influence of N-methylphenothiazine, **37,** 513
polymerization on particles of a pulsed-bed electrode: mass-transfer study, **38,** 217
pyrroles
polymerization of compounds with aza-macrocycles, **35,** 1051
substituted with amine groups: anodic polymerization in 0.1M $TEABF_4$-MeCN, **35,** 1273
pyrrolin-2-ones
syntheses at Hg cathodes in aqueous ethanol, **35,** 1907
pyrylium radicals
spin-trapped by nitrosoaromatics: *in situ* ESR study, **36,** 73

Q

quartz crystal microbalance
AC electrogravimetry of the nickel hydroxide electrode in alkaline solution, **36,** 743
AC electrogravimetry of oxidation of Au in H_2SO_4 aq, **38,** 1827
combined with absorption spectroelectrochemistry at grazing incidence, **38,** 2277
periodic variations in amount of chemisorbed species during oxidation of methanoic acid at Pt anodes, **38,** 2385
study of anodic dissolution of Cu in 0.1M Na_2SO_4 at pH1.5, **37,** 2195
study of corrosion of Cd in aerated sulphate solutions at 1<pH<6, **37,** 2611
study of effect of UPD Pb on glucose oxidation at Pt anodes, **38,** 2725

quartz crystal microbalance continued
study of effects of thiourea and poly(ethane-1,2-diol) on UPD of Cu on Pt electrodes, **38,** 647
study of influence of pH and solution composition on electrochemical behaviour of polyaniline films, **38,** 393, 1051
study of intercalation of thin sputtered NiO films by alkali-metal ions, **38,** 2765
study of ion-exchange mechanism of polypyrrole and poly(N-methylpyrrole) doped with tosylate, **38,** 349
study of swelling of poly(vinylferrocene) films, **37,** 647
study of titration of α-cyclodextrin host films in 1mM 4-nitrophenol (guest) solution, **37,** 1109
study of UPD of Pb, Cd and Tl on polycrystalline Ag, **36,** 1873
quartz crystal oscillators
coated with montmorillonite clay: equivalent circuit parameters in air, moisture and Na_2SO_4 aq, **38,** 747
quartz microbalance electrogravimetric transmittance
applied to 2- and 3-dimensional film-forming reactions, **35,** 1553
quinine
adsorption and reduction at Hg electrodes, **35,** 1311
quinone imines see benzoquinone imines
quinones
with aminoethylamino side chains: electrode kinetics of $1e^-$ reduction at Hg cathodes in DMF, **36,** 269
effect of anhydrous perchloric acid on reductions in acetonitrile, **38,** 607
reactions of radical anions generated at glassy carbon or edge-plane graphite cathodes with CO_2 in 0.1M TEAP-DMSO, **35,** 1399
redox behaviour of substituted 2-arylazoanthraquinones at Pt electrodes in benzonitrile, **36,** 927
2,3[1H,4H]-quinoxalinedione dioximes
reductions at cathodes of Hg, Pt and Pt(UPD Tl) in $HClO_4$ aq, **38,** 989
quinoxalines and their di-N-oxides
cyclic voltammetry in 0.1M TEAP-DMF: substituent effects, **37,** 1433

R

radial distribution functions
for the system of an Na^+ ion in TIP4P water, **38,** 1405
radical anions
of 3,4-diphenyl-1,2,5-thiadiazole-1,1-dioxide, **36,** 167
generated from pyridinium and sulphonium ylides at Hg cathodes in 0.1M $LiClO_4$-MeOH, **36,** 101
of Ni(II) salophen complex: formation and dimerization during reduction at Hg in DMF, **37,** 113
of PhCH=C(SMe)S(O)Me: reactions with CO_2 and H^+ in DMF, **36,** 1341
of phenazine: formation at Pt cathodes in THF, **36,** 803
of pyrene: generation and photoexcitation in acetonitrile, **35,** 1837
radical cations
of pyrrole: rate-determining coupling during anodic polymerization, **35,** 1841
radiolytically-grafted iridium deposits
on a sprayed SnO_2 film, **36,** 1787
radiotracer studies
of adsorption of corrosion inhibitors on carbon steels in neutral media, **36,** 981
of adsorption of D-glucose at platinized Pt in 1M H_2SO_4 aq, **37,** 2443
of adsorption of 1,2-diaminoethane at platinized Pt electrodes from 1M H_2SO_4 aq and from 0.1M NaOH aq, **35,** 111
of adsorption of HCOOH at Pt anodes modified with aniline or polyaniline, **35,** 1459
of adsorption of primary amino compounds at Pt electrodes [R], **35,** 919
of adsorption of SO_4^{2-} on smooth Cu in acidic and neutral media, **36,** 753
of concentration profiles of $^{137}Cs^+$ in perfluorosulphonic acid ion-exchange membranes, **37,** 221
of effect of Cl^- on adsorption of 1-octyn-3-ol at Fe electrodes in HCl aq, **36,** 1333
of effect of CO_2 on stability of gas-diffusion cathodes in alkali, **35,** 945
of electrodeposition of Cd on Pb in 5M H_2SO_4 aq, **35,** 577
of induced adsorption of Ca^{2+} at Pt and modified Pt electrodes, **36,** 1453
of sorption of Ca^{2+} into copper(II) hexacyanoferrate films, **35,** 811
of sorption of Cl^- and HSO_4^- by polyaniline, **35,** 899
of sorption on metal layers, metal powders and protective coatings, **35,** 817

radiotracer studies continued
of the water content in the passive layer on Al under cathodic conditions, **38,** 2541
Raman scattering, resonance-enhanced
assessment of structural parameters in charge-transfer reactions, **36,** 1775
Raman scattering, surface plasmon assisted
from electrochemically-controlled adsorbates on flat single-crystal Ag, **36,** 1879
Raman spectroscopic study see also surface-enhanced Raman spectroscopy
of cobalt oxide films sputtered on to ITO surfaces, **35,** 975
of the electrical double layer and adsorbates, **36,** 1829
of iodine-dialkyl sulphide mixtures, **35,** 355
of ion association in complexes of PPO with LiSCN, NaSCN, KSCN, $LiClO_4$, $NaClO_4$ and $LiBF_4$, **37,** 1499
of implantation of K^+ and Li^+ into vitreous carbon with 150keV, **35,** 1279
of manganese dioxide during reduction in aqueous borate, **38,** 341
in situ, of surface films on Cu and Fe in borate buffer containing SCN^-, **36,** 505
of ion-ion and ion-polymer interactions in polyether-$LiCF_3SO_3$ complexes, **37,** 1495
of use of second harmonic generation in studies of surface reconstruction, **36,** 1829
Raman spectra, surface resonance
of oxygen interaction with cathodes of cobalt tetramethoxyphenylporphyrin, **36,** 999
ramsdellite-MnO_2
transformations involving the spinels $LiMn_2O_4$ and $Li_2Mn_4O_9$, **38,** 1259
random walk algorithm
to calculate impedances of a 2-dimensional slot and fractal aggregates, **36,** 1699
Raney nickel cathodes
hydrogen evolution in concentrated NaOH aq, **35,** 1251
hydrogenation of phenanthrene by galvanostatic pulse electrolysis, **38,** 1377
reductions of nitrobenzene, azoxybenzene etc to aniline, **35,** 147
rate constant for charge transfer
and transfer coefficient: novel analysis of steady-state polarization data, **37,** 1149
reaction orders
relation to Tafel slopes in reactions involving a chemisorbed intermediate, **37,** 51
reactions, multiple
modelling of parallel and series processes: current efficiencies and selectivities, **38,** 2155
reactors see electrolyzers
recombination rates
impedance studies of III-V semiconductor electrodes, **37,** 837
reconstruction
of Au(100) surfaces in dilute aqueous acids, **37,** 615
redox polymer
Ag deposition on $[Os(bipy)_2(PVP)_{10}Cl]Cl$ coatings on vitreous carbon cathodes, **35,** 985
impedance studies, **35,** 1665
redox surfactant
potential-step chronocoulometric study, **35,** 885
reduced carbon dioxide
at Pt electrodes: interaction with propargyl alcohol and allyl alcohol in 0.5M H_2SO_4, **37,** 1083
reference electrodes
artefacts in impedance measurements in media of low conductivity, **35,** 1125
stabilities in molten acidic sodium sulphate at 1200K, **35,** 1065
reference hypernetted-chain integral-equation approximation
applied to the solution side of the double layer, **36,** 1677
reflectance spectroscopy, potential-modulated
of thin anodic oxide films on Ti in H_2SO_4 aq, **35,** 1073
reinforced concrete
monitoring local corrosion by impedance spectroscopy, **35,** 1573
rhodium
UPD and microquantities on graphite electrodes: adsorption of H and O and electrocatalysis of HCOOH oxidation and the HER, **38,** 1591
rhodium compounds
reactions at a carbon paste electrode in various media, **38,** 1331
rhodium electrodes
hydrogen evolution from 1M KOH aq, **37,** 1283

rhodium electrodes continued
oxidations of hydrazine, methanol, HCHO and $HCOO^-$ in aqueous alkali, **35,** 1821
rhodium oxide electrodes
on Ti or quartz supports: preparation by thermal decomposition of $RhCl_3$ in HCl aq, **38,** 2435
rhodium-implanted titanium anodes
catalysis of chlorine evolution and XPS characterization of anodic layers, **38,** 1313
rhodium-tin oxide electrode
compared with Rh anodes for the oxidation of methanol, **37,** 1317
ring-disc electrode
complex collection efficiencies, **35,** 1553
linear scanning of rotation rate: theory and application, **35,** 1451
ring-disc electrode studies
of anodic behaviour of Fe-Cr alloys in 0.5M H_2SO_4, **38,** 763
of anodic behaviour of Sb and Pb-Sb eutectic in H_2SO_4 aq, **35,** 229
of anodic behaviour of Sn in H_2SO_4 aq, **37,** 1797
of anodic dissolution of Cu in 0.1M Na_2SO_4 at pH1.5, **37,** 2195
of anodic dissolution of Cu in HCl aq, **37,** 2707
of anodic dissolution of Si in NH_4F aq, **37,** 889
of ascorbic acid free radicals formed at Au anodes in aqueous buffers, **36,** 1649
of dehydration kinetics of an N,N'-dihydroxyamine intermediate, **35,** 1957
of effect of N-methylphenothiazine on anodic polymerization of pyrrole in acetonitrile, **37,** 513
of effect of Sb on anodic behaviour of Pb in H_2SO_4 aq, **36,** 605
of effect of UPD Cu on oxygen reduction at Pt in acidic media, **36,** 1325
of effect of LiCl(4M) on competition between decomposition of a GaP anode and its stabilization by Fe(II), **37,** 1343
of effects of pH, potential and crystal face on etching and redox rates, **35,** 1351
of electrochemical behaviour of $Ni(II)(bpy)_3(ClO_4)_2$ in acetonitrile, **38,** 2515
of formation of Fe^{2+} aq during passivation of low-alloy steels in carbonate buffers, **35,** 35
of formation of $PbSO_4$ on Pb anodes in 5M H_2SO_4, **38,** 1513
of GaAs in alkaline solutions of BrO^-, **36,** 695
of hydrogen insertion into Pd and Pd-Ni thin film electrodes, **36,** 1203
of mechanism of the iron(II/III) couple at 3.5<pH<6.5 in the presence of EDTA, **35,** 1325
of the mechanism of the MnO_2 electrode in 1M Na_2SO_4 aq containing Mn(II) at 4<pH<6, **35,** 539
of oxidation of carbohydrates at Cu anodes in aqueous alkali, **37,** 1187
of oxidation of films of N_4 chelates of Co(II) and of Cu(II) in 0.1M $LiClO_4$-MeCN, **38,** 907
of oxidation of methanal at Au(332) electrodes, **35,** 725
of oxygen reduction in acidic and neutral media on Pt cathodes modified with UPD Cd, **37,** 2559
of oxygen reduction in alkaline solution at Ru supporting UPD Tl or Pb, **37,** 457
of oxygen reduction at an iron porphyrin ion complex film, **36,** 703
of oxygen reduction at cobalt oxide sputtered films, **35,** 975
of oxygen reduction at UPD Pb on Hg in 0.1M $NaClO_4$: pH effect, **36,** 529
of oxygen reduction at polypyrrole-modified electrodes, **35,** 135
of reduction of tungstate to W at Ni cathodes in LiCl-KCl eutectic, **35,** 1233
of reductions of furazano[3,4-b]-quinoxaline 1-oxides and 2,3[1H,4H]-quinoxalinedione dioximes, **38,** 989
of reductions of 2- and 4-nitroimidazoles at Hg and at Pt cathodes modified by UPD Pb, Tl and Bi, **37,** 1231
of soluble intermediates formed at Pb polarized in H_2SO_4, **36,** 953
rocking chair secondary lithium cells
the $Li_{1+x}Mn_2O_4$ system [R], **38,** 1221
with MnO_2 or V_3O_8 positives and pitch-based carbon fibre negatives, **38,** 1721
rotating cylinder electrode
in a Hull cell with the counter electrode near one end, **37,** 69
reduction of CO_2 to CH_4 and C_2H_4 at Cu cathodes in 0.5M $KHCO_3$, **35,** 771
Zn dissolution in low-temperature molten salt, **35,** 89
rotating disc electrode
application with AC signals for simultaneous determinations of diffusivity and concentration, **38,** 681
film potentiometric stripping analysis of Pb^{2+} at vitreous carbon with Fe(III) oxidant, **36,** 2103
mass transfer during Cu plating using square cathodic current pulses, **36,** 625
mass transfer to an active fractal region set in an inactive electrode, **35,** 1423
non-uniform current distribution monitored by electrochemiluminescence intensity variation, **35,** 1983
relation between electrohydrodynamic and electrical impedances, **35,** 1637

rotating quartz frequency balance
study of the mechanism of the MnO_2/Mn(II) electrode, **35,** 539
rotating ring-disc electrode see ring-disc electrode
rotation-rate scanning
linear at RDE and RRDE: theory and in a study of ascorbic acid oxidation, **35,** 1451
oxygen reduction at a glassy carbon RDE catalysed by vitamin B_{12} in weak aqueous acid, **38,** 2297
rapid: H_2O_2 reduction at iron protoporphyrin-modified pyrolytic graphite electrodes, **35,** 1227
rough electrodes
electrodeposition of Ag on electrodispersed Pt, **36,** 1617
impedance of an electrode with a sinusoidal profile, **36,** 1083
impedance of coated metals, **38,** 1867
impedance studies of the double layer, **36,** 1699
role of surface diffusion during metal deposition studied by Monte Carlo simulations, **37,** 2155
rubidium silver iodide
between graphite electrodes: impedance studies, **35,** 1649
rust converters
effect of treatments by tannic, gallic and phosphoric acids on electrochemical behaviour of rusted steel, **37,** 1983
ruthenium acetate clusters
incorporating pyridine and DMSO ligands: electrochemistry in MeCN, **38,** 975
ruthenium bimolecular substitution reactions
within Nafion coatings on pyrolytic graphite electrodes, **35,** 419
ruthenium(II) bipyridyl derivative (RuC19) sensitizer
photo-induced electron transfer from donor in an adjacent Langmuir-Blodgett layer, **36,** 1793
ruthenium(II) tris(2,2'-bipyridine) complex
enhancement of electrochemiluminescence in MeCN-$TBABF_4$ and in aqueous oxalate by ultrasound, **38,** 307
in a Nafion film coating on an ITO electrode: photocurrents in the presence of oxygen, **38,** 129
photo-excited, reduction of MV^{2+} in adjacent Nafion layers sandwiched between ITO electrodes, **38,** 1093
ruthenium(V) complex
catalyst for methanol oxidation, **38,** 1015
ruthenium dioxide
incorporated into Ni cathodes: electrode preparation and hydrogen evolution from hot alkali, **37,** 757
ruthenium dioxide electrode
influence of pH and scan rate on voltammetric surface charge, **35,** 263
physical electrochemistry of ceramic oxides [R], **36,** 225
RuO_2-TiO_2 modified by CeO_2: preparation, voltammetry and stability, **37,** 2511
Ti coated with RuO_2-IrO_2 and RuO_2-TiO_2, **37,** 1029
n-ruthenium disulphide electrode
effects of temperature, illumination and electrode potential on impedance in $HClO_4$,5.5H_2O, **38,** 1929
ruthenium electrodes
oxidations of hydrazine, methanol, HCHO and $HCOO^-$ in aqueous alkali, **35,** 1829
with UPD Tl or Pb: oxygen reduction in alkaline solution, **37,** 457
ruthenium(II/III) hexammine couple
confined in composite films of montmorillonite clay and poly(vinyl alcohol) on graphite electrodes, **37,** 1865
ruthenium(V) mono-oxo complex, immobilized in Nafion films
indirect anodic oxidation of benzyl alcohol, **37,** 2645
ruthenium oxide Adams catalyst
for Ce(IV) oxidation of water to oxygen in aqueous acids, **37,** 1217
ruthenium oxide film electrodes
effects of temperature on anodic charge in acidic and unbuffered media, **36,** 27
ruthenium ternary oxides
impedance studies of $Ru_{0.2}Ti_{0.8-x}Sn_xO_2$ electrodes in 1M NaCl aq, **38,** 2239
ruthenium-titanium alloy electrode
evolutions of H_2, O_2 and Cl_2 and corrosion in acidic media, **36,** 19
Rutherford backscattered electron spectroscopy
study of anodic oxidation of titanium silicide in KNO_3 solutions in ethane-1,2-diol, **38,** 399

S

safranine
diffusion coefficients in Nafion films, **36,** 881
salicylaldazine
enhancement of semiconductivity by chelation with *d*-block ions, **35,** 1987
salophen
reduction of the Ni(II) complex at Hg cathodes in DMF, **37,** 113
scandium oxide
cathodic insertion and diffusion coefficient of Li^+ in ScO, **35,** 17
scanning electron microscopy study
of Ag electrodeposits on polyfaceted spherical Pt cathodes from acidic Ag_2SO_4 aq, **37,** 2215
of Al-5.03%Zn-1.67%Mg-0.23%Cu alloy in NaCl-Na_2SO_4 aq, **38,** 2741
of Au overlayers formed by reduction of hydrous gold oxide, **35,** 117
of anodic behaviour of indium in NaCl aq at 2<pH<12.6, **36,** 2063
of barrier-type films formed on Al in various media, **37,** 2283
of carbon surfaces after immersion in $LiAlCl_4$-$SOCl_2$, **37,** 1207
of Cd electrodeposits on Pb in 5M H_2SO_4 aq, **35,** 577
of corrosion pits in Cu in 0.1M $NaClO_4$ at 8<pH<11, **37,** 1437
of Cu surfaces anodized in aqueous phosphate solutions, **37,** 655
of deposition and dissolution of Zn at flow-through porous electrodes, **38,** 311
of effect of Ag^+ on electrodeposition of W and WC from molten chlorides, **35,** 187
of effect of Sb on kinetics of reduction of the PbO film on Pb-Sb alloy electrodes in H_2SO_4, **38,** 1131
of the effects of additives on Zn electrodeposits, **38,** 1351
of electrochemistry of eutectic Ge-Me alloys (Me = Cu, Co, Ni, Fe) in 0.5M H_2SO_4, **36,** 1247
of electrodeposits of Ag and Cu on anodized aluminium, **35,** 1019
and energy-dispersive X-ray analysis of graphite electrodes in Al-cryolite cells, **37,** 1787
of the formation and reduction of anodic layers on Cu in aqueous carbonate solutions, **38,** 703
of indium phosphide etched photoelectrochemically, **38,** 95
of influence of surface structure on dissolution mechanism of Fe anodes in acidic aqueous sulphates, **35,** 163
of initial stages of Cu electrodeposition on Pd cathodes, **35,** 1189
of IrO_2-Ta_2O_3 anodes on various substrates, **36,** 991
of lead(IV)-thallium(III) mixed oxide anodic deposits from 0.005M $TlNO_3$-0.1M $Pb(NO_{33}$-5M NaOH aq, **38,** 2551
of Li and noble metal electrodes in 1,3-dioxolane-$LiClO_4$, **35,** 625, 639
of Li surfaces after immersion in $LiAlCl_4$-$SOCl_2$, **37,** 1211
of Mg electrodes polarized in carbonate buffers at 9<pH<11, **37,** 1403
of NiO cathodes for molten carbonate fuel cells, **38,** 2669
of NiSn and porous Ni electrodeposited anodes for water electrolysis, **37,** 29
of passivation of porous carbon cathodes during reduction of $SOCl_2$-$LiAlCl_4$, **38,** 827
of Pb electrodeposition inhibited by lignin sulphonate and extract of horse chestnut, **37,** 2249
of PbO_2 deposits on SnO_2/Ti anodes, **38,** 2749
of Pd electrodeposits on Ni, **38,** 2683
of photoelectrodeposition of Tl_2O_3 on CdSe anodes from 0.1M NaOH containing Tl(I), **37,** 1429
of polyaniline containing polymeric sulphonates, **36,** 87
of polycrystalline diamond films on W substrates, **37,** 973
of poly(*p*-phenylene) thick films on Pt, anodically synthesised from benzene, **37,** 1093
of polypyrrole films containing inserted anions, **35,** 567
of polypyrrole formed on anodic graphite particles, **36,** 1953
of polypyrrole and poly(N-methylpyrrole) containing polymeric sulphonates, **35,** 1245
of reduced Ag electrode surfaces, **35,** 595
of $Ru_{0.2}Ti_{0.8-x}Sn_xO_2$ electrodes, **38,** 2239
of Sb anodes in 0.5M H_2SO_4 aq, **36,** 2087, 2093
of Si electrodes partly coated with Pt, **37,** 897
of n- and p-Si etched by H_2O_2 in weak aqueous alkali at 70°C, **35,** 1267
of silver chromate: reduction in a carbon paste electrode in HCOOH and MeCOOH, **36,** 505
of Sn anodes in 0.5M citric acid aq, **37,** 143
of Sn anodes in H_2SO_4 aq, **37,** 1797
of Sn electrodeposits from acidic $SnSO_4$: effects of a surfactant, **36,** 985
of Sn electrodeposits from $SnSO_4$ aq containing aromatic carbonyl compounds, **37,** 2403

scanning electron microscopy study continued
of a solid electrolyte mixture of AgI with N,N,N',N'-tetramethylhomopiperazinium diiodide, **38,** 571
of Zn electrodeposits on vitreous carbon from zincate solutions, **37,** 1199
scanning tunnelling microscopy study
in air, of electrochemically etched Si(100) surfaces, **38,** 1367
of effects of thiourea and poly(ethane-1,2-diol) on UPD of Cu on Pt electrodes, **38,** 647
of fractal surface characterizations of electrodeposited and vapour-deposited Au films, **37,** 2209
in situ, of Pd(111) overlayers on Au(111) surfaces, **38,** 2145
in situ, of UPD and normal deposition of Pb on Ag, **37,** 2173
of mobility of Ag(100) and polycrystalline Pd surfaces in atmospheric and aqueous conditions, **37,** 2331
of sequential UPD of Ag and either Pb or Tl on Au single-crystal cathodes, **37,** 2237
of UPD Cu on Au single crystals [A], **36,** 1893
Schiff base ligands
reduction of Ni(II) salophen at Hg cathodes in DMF, **37,** 113
Schottky barrier
at amorphous Nb_2O_5 anodic films in aqueous sulphates, **35,** 99
Schrodinger equation exact solution for a H-like atom near a hard wall
effects of distance on electronic spectrum, atom dipole moment etc, **36,** 1711
scratched electrodes see scribed electrodes
scribed electrodes
calculations of ohmic drop based on Taylor series expansion solutions of Laplace's equation, **38,** 2525
second harmonic generation
at the metal/electrolyte interface treated by electron-density functional calculation, **36,** 1835
secondary electron imaging
of Cu-Al-Ag alloy surfaces after potential cycling in 0.5M NaOH aq, **36,** 1409
secondary-ion mass spectrometry study
of effect of hydride on rates of HER on Ti in 1M HCl, **35,** 1913
of Fe25Cr alloy surfaces exposed to air after abrasion or electrochemical polarization, **36,** 1623
of implantation of K^+ and Li^+ into vitreous carbon with 150keV, **35,** 1279
of nickel oxide electrodes: effect of Li^+ insertion from 1M $LiClO_4$-PC, **37,** 1033
of Sn anodes in H_2SO_4 aq, **37,** 1797
of Ti and Pd cathodes used in electrolysis of 0.1M LiOD-D_2O, **37,** 215
sedimentation equilibrium
a non-equilibrium thermodynamic formulation, **38,** 877
selective reductions
of -OH groups in α-hydroxyaldehydes using tetraalkylammonium salts, **35,** 1167
selenious acid
simultaneous reduction with Cu(II) from aqueous solutions of citric acid to form copper selenides, Cu, Se and H_2Se, **38,** 2387
selenium
oxidation in a carbon paste electrode, **37,** 1321
selenium(IV)
reduction in a carbon paste electrode in H_2SO_4 aq, **37,** 1165
seleno-organic compounds see organoselenium compounds
self-assembled monolayers see monolayers, self-assembled
semiconducting behaviour
of CdS films formed on Cd anodes in alkaline Na_2S aq: effects of thickness, λ and *E*, **37,** 1371
of the poly(3-octylthiophene) film on a Pt electrode in PC-$LiBF_4$, **37,** 1759
of salicylaldazine, enhanced by chelation with *d*-block ions, **35,** 1987
of sintered iron oxide, doped with Zn, in borate buffer pH8.4, **36,** 1585
of sintered iron oxide electrodes doped with Zn, **37,** 425
semiconductor devices
photoelectrochemical methods used in processing, **38,** 101
semiconductor electrodes
with adsorbed sensitizor dyes giving high quantum efficiency, **37,** 943
classical, opto-electric and electro-optic impedance studies, **35,** 1545
comparisons of charge-transfer kinetics at n- and p-type electrodes, **37,** 799
corrosion inhibition for p-Si in acetonitrile containing cobalticene/cobalticinium by treatment with AlF_3, **35,** 413
with deep-level states: physicochemical models for impedance spectroscopy, **38,** 1903

semiconductor electrodes continued
effect of dopant concentration on rate of electrochemical etching, **38,** 889
effect of LiCl(4M) on competition between decomposition of a GaP anode and its stabilization by Fe(II), **37,** 1343
effect of thickness of amorphous WO_3 films on redox kinetics, **36,** 1817
effects of temperature, illumination and electrode potential on impedance of n-RuS_2 in $HClO_4$,5.5H_2O, **38,** 1929
electrochemical measurement of chemical dissolution rate of n-ZnO, **37,** 827
experimental investigations of charge transfer, **37,** 781
flat-band potentials of In_2S_3 thin-film electrodes, **35,** 345
frequency response of photocurrents to periodic supra-bandgap illumination, **35,** 1657
impact on the concepts of electrochemistry [R], **35,** 1677
impedance studies of electron-hole recombination, **37,** 837
impedance studies of rectifying interfaces, **35,** 1631
influence of thin Au electrodeposits on current *vs* potential curves at p-GaAs, **38,** 291
influence of thin Au electrodeposits on impedance of p-GaAs, **38,** 301
influence of thin Au electrodeposits on impedance spectra and current *vs* potential curves of n-GaAs, **38,** 1115
iron pyrites photoanodes prepared by screen printing and thermally activated in air, **38,** 123
non-stoichiometric, sputtered, cobalt oxide films, **35,** 975
optoelectrical impedance study of anodic dissolution of n-InP in HCl aq, **38,** 2559, 2569
photo-oxidation of water at a $SrTiO_3$-TiO_2 anode with a sulphonated PTFE SPE membrane, **38,** 107
photoassisted intercalation of K^+ aq into n-SnS_2, **36,** 1197
photocurrents at layered n-WSe_2 anodes, **35,** 1195, **36,** 747, 2037, 2039
potential dependence of photocurrents and induced microwave conductivity, **37,** 919
principles and applications of photoelectrochemical etching, **38,** 95
redox activity of excimer laser-deposited $YBa_2Cu_3O_{7-\delta}$ epitaxial thin films, **35,** 1219
reduction of H_2O_2 at Si electrodes in weak aqueous alkali at 70°, **35,** 1267
reduction rate of $Fe(CN)_6^{3-}$ at, and etching of, n- and p-GaP, **35,** 1351
simultaneous potential-dependent measurements of photocurrents and photo-induced microwave conductivity, **38,** 141
theory of electroreflectance and photoreflectance, **37,** 949
with ultrafine islands of deposited metals: Pb on n-GaAs, **37,** 933
with ultrafine islands of deposited metals: Pt on n-GaAs, **37,** 781
with ultrafine islands of deposited metals: Pt on Si, **37,** 897
wet etching of GaP investigated by photoelectrochemistry, **37,** 811
semiconductor films
dependence of photocurrents at n-TiO_2 anodic films formed in 20M NaOH on stress, **38,** 37
impedance of amorphous Nb_2O_5 in aqueous sulphate, **35,** 99
photoelectrochemical behaviour of TiO_2 thin amorphous anodic films grown at high rates in 0.5M H_2SO_4 aq, **38,** 29
of polyaniline: pH dependence of transition potential from n- to p-type, **36,** 2015
semiconductor particles
photocatalysis of oxidation of organic molecules by oxygen, **38,** 3
principles of heterogeneous photocatalysis, **38,** 11
semiconductor/electrolyte solution interface
the flat-band potential of n-InP as a pH probe in non-aqueous and mixed solvents, **38,** 781
sensitization
of bismuth oxyhalide formed on Bi film anodes, **35,** 1941
of two-dimensional chalcogenides with adsorbed dyes, **37,** 943
sensors, electroanalytical
expanding technology for their design and fabrication [R], **36,** 243
glucose amperometry with a polypyrrole film electrode incorporating glucose oxidase, **37,** 1987
silanes
organically-substituted: basis of proton-conducting copolymers for methanol fuel-cell membranes, **37,** 1615
silica
conductivity of sols and gels prepared from tetramethoxysilane at various pH, **38,** 371
gel, coated with titanium(IV) oxide: immobilization of hexacyanoferrate ions, **37,** 2477
silicon see also silicon electrode
anodic dissolution in aqueous fluoride: microscopic self-oscillating domains, **38,** 1627

silicon continued
anodic formation and propagation of pores in aqueous and methanolic HF: gravimetry, **38,** 191
anodic oxide formation on n- and p-type Si, **37,** 847
preparation and photoelectrochemical response of amorphous thin films, **36,** 915
STM study in air of (100) surfaces produced by electrochemical etching, **38,** 1367
p-silicon
effect of annealing on flat-band potential in acetonitrile, **37,** 2791
silicon electrode see also silicon
amorphous thin films in photovoltaic cells for water electrolysis, **38,** 111
modified with ultrafine Pt islands: generation of high photovoltages, **37,** 897
anodic oxide films formed in aqueous sulphuric, phosphoric and oxalic acids, **36,** 1611
photodissolution in NH_4F aq, **37,** 889
porous, impedance study, **38,** 1923
potential distribution at the interface with HF aq, **36,** 499
reduction of H_2O_2 in weak aqueous alkali at 70°C, **35,** 1267
n-silicon electrode
behaviour in MeOH-$LiClO_4$ containing the dimethylferrocene couple, **35,** 1631
in fluoride and KOH solutions: frequency-dependence of quantum efficiency of the photocurrent response, **38,** 1913
intensity-modulated photo-oxidation in NH_4F aq, **35,** 1657
photoelectrochemical etching in aqueous fluoride, **37,** 877
p-silicon electrode
low-doped, anodic oxide formation and dissolution, **37,** 865
effect of pretreatment by an AlF_3 etch on its corrosion in acetonitrile containing cobalticene/cobalticinium, **35,** 413
laser-induced deposition of transition metals on a (100) face, **36,** 1803
silver see also silver electrode
anodic behaviour in 0.1M NaOH aq, **35,** 489
chronoamperometry of anodic oxidation to AgO in KOH aq, **35,** 1445
concentration dependence of UPD on Pt(111), **38,** 235
corrosion by Fe(III) and Cu(II) halides in DMSO and water, **36,** 479
dependence of ellipsometric parameter Δ on crystal face and E or σ in 0.01M KF and KPF_6 aq, **36,** 1839
dependence of nucleation of electrodeposits on extent of oxidation of the Pt cathode, **35,** 1873
effect of 0.01M tartaric acid on electrodeposition from 1M $AgNO_3$-0.5M HNO_3 aq: impedance study, **35,** 1587
effects of potential scan rate and roughness of Pt cathode on electrodeposits, **36,** 1617
electrodeposition on glassy carbon coated with $[Os(bipy)_2(PVP)_{10}Cl]Cl$, **35,** 985
electrodeposition on polyaniline film electrode: film thickness and nucleation rate, **36,** 1151
electrodeposition of single crystals on Pt cathodes from 0.5M $AgNO_3$-1M HNO_3 aq, **37,** 2233
growth kinetics of clusters at Pt cathodes, **38,** 535
kinetics of displacement at fixed and rotating planar Cu electrodes in 4.3M NaCl aq, **37,** 1779
nucleation of clusters formed by reduction of Ag^+ in the presence of polyanions, **36,** 1743
nucleation and growth of deposits on polyfaceted spherical Pt cathodes from acidic Ag_2SO_4 aq, **37,** 2215
STM study of mobility of (100) surfaces in atmospheric and aqueous conditions, **37,** 2331
UPD on Au single-crystal cathodes before or after UPD of either Pb or Tl, **37,** 2237
silver β"-alumina solid electrolyte
in a chlorine gas sensor: redox mechanisms, **36,** 1823
silver chromate
reduction in a carbon paste electrode in HCOOH and MeCOOH, **36,** 1505
silver chromium oxide
insertion of Li^+ into $AgCr_3O_8$, **38,** 1211
silver(I) cryptate with cryptand 222: stability constants
in 18 aprotic binary mixed solvents, **37,** 413
in DMSO-MeCN mixtures, **36,** 1427
silver electrode see also silver
adsorption of nitrobenzene and benzonitrile from 0.1M KCl aq, **36,** 1523
adsorption of *p*-nitroaniline from aqueous perchlorates, **35,** 1037
adsorption of *p*-nitrosodimethylaniline at flat single-crystal Ag, **36,** 1879
adsorption of thiourea in methanolic KF, **36,** 965
adsorption of thymine at the (111) face, **37,** 2373

silver electrode continued
an impedance study of three-dimensional dendritic electrodeposits on Pt substrates, **38,** 1545
characterization of reduced surface by SEM and Tl UPD, **35,** 595
cluster calculations of electronic properties of adsorbed CN^-, **37,** 211
effect of Na UPD on hydrogen evolution in NaOH aq, **35,** 523
effects on the HER of the co-adsorption of anions and thiourea, **35,** 879
electron and Auger spectroscopy of alkali-metal electrodeposits, **36,** 1947
hydrogen evolution during oxidations of aldehydes, **38,** 1067
SERS study of adsorption of $Fe(bpy)_3^{2+}$ complex (bpy is 2,2'-bipyridyl), **37,** 2347
SERS study of polypyrrole formation at, **35,** 315
simultaneous UPD of Pb and Tl, **36,** 1291
slow structural transformations of UPD Pb on (111) faces at low coverages, **36,** 1259
underpotential deposits of Pb on the (111) surface: model for transformations at high coverages, **38,** 387
UPD of Pb, Cd and Tl, **36,** 1873
UPD of Pb on (111) faces: slow structural changes at high coverages, **36,** 2077
UPD of Pb from acidic aqueous perchlorate, **36,** 1959
UPD of Pb on single crystals, **37,** 2173
UPD of Tl from a TlI film, chemically-deposited from a saturated solution of TlI, **37,** 1767
silver halides and pseudohalides
ion association in pyridine solutions, **35,** 509
silver iodide
conductivity of double salts with poly(N-alkylene dimethyl-N,N'-piperazinium diiodide), **35,** 77
effect of onium ion on conductivity of onium iodide-AgI mixtures, **35,** 1465, 1473
solid electrolyte mixture with N,N,N',N'-tetramethylhomopiperazinium diiodide: redox stability range and transport numbers, **38,** 571
solid electrolyte mixtures with N,N,N',N'-tetramethylhomopiperazinium diiodide and homopiperazinium diiodide, **38,** 565
solid electrolyte with poly{[-$NMe_2(CH_2)_6NMe_2(CH_2)_4$-].2I}, **35,** 951
silver(I) ion
mediator in anodic oxidation of Mn(II) to MnO_4^- in 30% H_2SO_4 aq, **36,** 1363
silver ion-conducting glass electrolyte $AgI-Ag_2O-B_2O_3$
in composite electrodes with NbS_2 intercalation host, **36,** 1643
silver nitrate
EMF studies of the cells Ag / $AgNO_3$-KNO_3-$NaNO_3$ / NO_2, O_2, Pt, **38,** 1139
silver(I) oxide
formation on polycrystalline Ag anodes in 0.1M NaOH aq, **35,** 489
kinetics of electroreduction in 0.1M NaOH aq, **35,** 595
silver(II) oxide
formation from Ag by potentiostatic steps in KOH aq, **35,** 1445
the nature of material prepared anodically in alkali, **36,** 1533
silver(III) periodate
reduction at Pt microelectrodes in KOH aq at pH13, **35,** 451
silver rubidium iodide
between graphite electrodes: impedance study, **35,** 1649
silver-zinc cell
open-circuit voltages during charge-discharge cycles, **36,** 1533
simulation
an alkaline fuel cell using the flooded agglomerate electrode model and concentrated electrolyte solution transport equations, **38,** 2599
singlet oxygen
ultra-weak photoemission at the Pt anode during oxygen evolution in aqueous electrolytes, **38,** 267
size ratio parameter in adsorption studies, **38,** 2663
society
founding of the ISE, **36,** 1
sodium
thin electrodeposits at Ag cathodes in 1M NaOH aq, **36,** 1947
sodium ions
cathodic insertion into sol-gel lamellar birnessite $MnO_{1.84}$,$0.64H_2O$, **38,** 1695
insertion into γ-MnO_2 electrodes from 1M $NaClO_4$-PC, **37,** 603
structure of the solvation shell in aqueous solutions, **38,** 1405

sodium monoxide
activities in the two phase fields of the Na_2O-α-Al_2O_3 system, **36,** 791
sodium polysulphide
phase diagram for Li_2S-Na_2S-S at 400°C, **36,** 673
sulphur activity and chain length distribution at 400°C, **36,** 679
sodium-sulphur battery
phase diagram for Li_2S-Na_2S-S at 400°C, **36,** 673
sulphur activity and chain length distribution of molten polysulphides at 400°C, **36,** 679
solar energy conversion see also energy conversion
impedance study of electron-hole recombination in III-V semiconductors, **37,** 837
photo-oxidation of water at a $SrTiO_3$-TiO_2 anode with a sulphonated PTFE SPE membrane, **38,** 107
Si photoelectrodes modified with ultrafine Pt islands, **37,** 897
using iron pyrites photoanodes prepared by screen printing and thermally activated in air, **38,** 123
water electrolysis in a photovoltaic cell using a triple junction device with thin films of amorphous Si, **38,** 111
solar rechargeable battery
principles and materials [R], **36,** 1107
solid electrodes
step elastic stretching (potentiostatic): adsorption of polar solvents, **36,** 859
solid electrolyte interfaces
calculation of EMF when respective mobile ions react, **35,** 785, 1477
solid electrolytes
Ag β"-alumina, Ag^+-conducting glass and $RbAg_4I_5$ used with superconductor electrodes, **37,** 2129
analysis of exergy efficiency in oxide fuel cells, **38,** 447
$CaO.6Al_2O_3$ in galvanic cells, **38,** 365
characterization of AgI-poly{[-$NMe_2(CH_2)_6NMe_2(CH_2)_4$-].2I}, **35,** 951
CV of porous Pt catalyst films in 8% yttria-stabilized zirconia at 350 and 650°C with a wide range of oxygen pressures, **38,** 2533
deposition of Cu at vitreous carbon cathodes from CuI, **38,** 577
effect of cation on total conductivity in onium iodide-AgI mixtures, **35,** 1465, 1473
impedance of antimonic acid between carbon or Pt electrodes, **35,** 1031
impedance of $RbAg_4I_5$ between graphite electrodes, **35,** 1649
for lithium cells by immobilising liquid electrolytes in 1,3:2,4-di(*p*-methoxycarbonylbenzidene)sorbitol gel, **38,** 1301
redox stability range and transport numbers of AgI-N,N,N',N'-tetramethylhomopiperazinium diiodide, **38,** 571
of single-(Li^+) and double-ion types (Li^+ and an anion), based on poly(dimethylsiloxane), **37,** 1183
voltammetry of hydrogen molybdenum bronze between vitreous carbon electrodes, **37,** 5
solid polymer electrolyte electrode
for chlorine cell cathodes by electroless plating of Pt on the membrane, **38,** 2431
proton transport in Nafion 117 between aqueous and organic solutions, **38,** 2171
solid polymer electrolyte fuel cells
effect of a Pt film sputtered on to the front surface of a low-Pt loaded cathode, **38,** 1661
solid polymer electrolytes see also polymer electrolytes
amorphous PEO containing $LiClO_4$ or $LiCF_3SO_3$: DC polarization between Li electrodes, **37,** 1517
based on a new PEO network polymer, **37,** 1585
blends of PEO with various acrylic polymers, **37,** 1565
bonded to Pt for transient measurements of methanol oxidation in acid, **36,** 1043
circular regression analysis of impedance data, **36,** 1033
conductivities of several new systems, **37,** 1539
film coating technologies and adhesion in relation to device requirements, **37,** 1471
incorporating $LiClO_4$ and based on the glycidyl ethers of PEG and glycerol, **37,** 1569
inorganic-organic copolymers, **37,** 1593
NMR spectroscopy of PEO and $M(CF_3SO_3)_2PEO_n$, M = Zn or Pb, $8<n<25$, **37,** 1487
oxidation of geraniol to citral at MnO_2-modified, Pt-Nafion electrodes, **37,** 1295
photochemical control of conductivity by effect on reversible cross-linking *via* anthryl groups, **37,** 1515
photo-oxidation of water at a $SrTiO_3$-TiO_2 anode with a sulphonated PTFE membrane, **38,** 107
poly(2-acryamido-2-methylpropane sulphonic acid)-poly(ethene imine) electrochromic window, **37,** 1377
proton-conducting copolymer of various organically-substituted silanes, **37,** 1615

solid polymer electrolytes continued
reversibility of the Li electrode, **38**, 1199
short PEO chains linked by -OCH_2O- and containing $LiClO_4$: the interface with Hg, **37**, 1525
simulation studies of the anode of a H_2-O_2 fuel cell with catalyst particles bonded to the membrane, **37**, 2737
temperature profile in a Nafion membrane during water electrolysis, **36**, 263
uniform, coherent 1μm films by simultaneous vapour-deposition of LiI and plasma polymerization, **37**, 1483
solid-state, high-temperature power cell
by application of a high field across potassium vanadate doped with Nd_2O_3, **37**, 1143
solvation
structure of Na^+ in TIP4P water, **38**, 1405
solvation energy
of $AsPh_4BPh_4$ in plasticized PVC membranes, **37**, 1021
determination of electrostatic component of free energy of ion transfer between solvents, **36**, 435
solvent effects
on electrode kinetics of electron-transfer and amalgam-formation reactions, **36**, 1767
on the $Zn(Hg)/Zn^{2+}$ couple in 0.05M $LiClO_4$ in propane-1,2-diol-water mixtures, **38**, 2459
solvent polarization
effect on the double layer structure, **36**, 401
solvent polarization diffusion
effect on rates of electron transfer, **36**, 395
D-sorbitol
oxidation at Ni anodes in 1M KOH, **35**, 375
space charge
effect in anodic oxidation of Bi in glycol-borate electrolyte, **38**, 1061
space-charge-containing interfaces
new approach to computation of frequency response, **38**, 1975
spatiotemporal phenomena
in spatially distributed systems: modeling of wave propagation at electrode/electrolyte interfaces, **38**, 1535
spectroelectrochemical studies
of adsorption of CN^- and SCN^- at Pt electrodes from 0.1M $NaClO_4$ aq, **36**, 1849
with an array of carbon fibre microelectrodes, **36**, 203
of ascorbic acid free radicals formed at Au anodes in aqueous buffers, **36**, 1649
determination of reduction factors of polyaniline films on ITO electrodes, **38**, 1643
of electrodeposition of cyanophenylparaquat radical cation salts, **35**, 1113
of indium hexacyanoferrate films on tin oxide electrodes, **35**, 1057
in situ FTIR study of phenazine and phenothiazine dye films at polycrystalline Au electrodes, **38**, 1619
in KOH aq, of Cu films electroplated on tin oxide/glass, **37**, 17
of oxidation of biliverdin to purpurin at Pt anodes in DMF-TBAP, **38**, 257
of redox behaviour of hemoglobin at Pt-Methylene Green electrodes, **35**, 1139
of reduction of dithiodipropionic acid at glassy carbon cathodes catalysed by a metalloporphyrin, **37**, 2591
of transient charge trapping in the Pt/poly(2,2'-bithiophene)/poly(xylylviologen)dibromide bilayer, **37**, 1887
visible absorption spectra of poly(pyrrole-alkylammonium) films containing porphyrins of Fe(III), Mn or Zn, **38**, 2485
spectroelectrochemistry
at grazing incidence: combination with quartz crystal microbalance studies, **38**, 2277
BaF_2 as an internal reflection element in IR-ATR spectroscopy of Au and Pt electrodes, **38**, 695
IR attenuated total reflection using thin sputtered films of Au or Pt on Ge or GaAs IR-transparent crystals, **37**, 2321
spectroscopic ellipsometry
study of barrier and porous anodic oxide films on Al, **38**, 2103
specular reflectance, *in situ*
method to determine thicknesses of Nb_2O_5 anodic films, **36**, 1297
spherical clusters
electrodeposition under joint ohmic, diffusion and ion-transfer limitations, **37**, 2229, 2233
spinel electrodes
oxygen evolution on $Ni_xCo_{3-x}O_4$ ($0.6<x<1.3$) in alkaline solutions, **38**, 2247
spinel $NiCo_2O_4$
formed by heating anodic hydrous oxide on Ni-Co 40:60 alloy, **36**, 1963
spinels
$Cu_xNi_{0.6-0.2x}Mn_{2.4-0.8x}O_4$: effect of x on extent of reduction in H_2SO_4 aq, **35**, 1303

spinels continued
transformations of $LiMn_2O_4$ and $Li_2Mn_4O_9$ to and from ramsdellite, **38,** 1259
square-wave electrolysis
evolution of concentration profiles for reversible metal-ion discharge, **35,** 483
evolution of concentration profiles for a reversible redox case, **35,** 215
square-wave voltammetry
anthracene oxidation at Pt anodes in MeCN-$TBAPF_6$, **36,** 1475
electrode kinetic study of $1e^-$ reductions of some quinones at Hg cathodes in DMF, **36,** 269
stability constants see complex and complexes
stainless steel
atmospheric oxidation of abraded and electrochemically polarized Fe25Cr, **36,** 1623
electrochemical behaviour of SO_3^{2-} in 0.5M NaCl aq, **36,** 1367
frequency dispersion of the interfacial capacitance of passive AISI 304 in various aqueous and ethanolic electrolyte solutions, **38,** 1615
influence of temperature on passive films in borate buffers, **36,** 315
passive films in 1M $NaClO_4$, **36,** 345
photoelectrochemical mapping of an AISI 304 electrode through which hydrogen is diffusing, **38,** 89
spatial distribution of etch pits in neutral chloride solution, **35,** 289
staircase voltammetry
oxidation of anthracene at Pt anodes in MeCN-$TBAPF_6$, **36,** 1475
Stark effect
second-order, for SO_4^{2-} adsorbed at Pt electrodes, **37,** 2179
statistical analysis
of data on magnetic field effects on mass transport, **35,** 929
of pit distribution on passive Fe in borate buffer containing Cl^-, **35,** 1809
statistical mechanics
of phase transitions in adsorbed monolayers, **38,** 1441
steel see also carbon steel
adsorption of polyacrylamide from H_2SO_4 aq and HI aq, **36,** 1315
impedance determinations of rates of pitting corrosion of coated metal, **38,** 1891
steel, low-carbon
effect of SO_3^{2-} on composition and thickness of passive films in 0.5M Na_2SO_4 aq, **38,** 253
steel, low-alloy
active-passive transition in carbonate buffer solutions, **35,** 35
Mossbauer spectroscopy of the passive anodic film formed in 0.5M Na_2SO_4-0.001M $NaHSO_3$ aq, **38,** 2253
steel, rusted
effect of treatments with tannic, gallic and phosphoric acids on electrochemical behaviour, **37,** 1983
steel, X20Cr13
anodic behaviour in concentrated aqueous and non-aqueous solutions of H_2SO_4, **37,** 1069
step elastic stretching under potentiostatic conditions
study of specific adsorption of solvent at solid electrodes (Cu, Cd, Ag), **36,** 859
stereochemical factors
distinguishing chemical and electrochemical reactions of organics, **36,** 2171
strain in electrodeposits
measured by a modified Michelson interferometer, **35,** 1989
streaming potential
across Nafion 120 membranes separating equimolar 1:1-electrolytes, **36,** 139
stress
effect on photocurrents at n-TiO_2 anodic films formed in 20M NaOH aq, **38,** 37
and electrochromic behaviour of thin amorphous films of V_2O_5 with the anodic insertion of Li^+ from $LiClO_4$-PC, **38,** 1637
in passive films, Ni anodes in 0.1M H_2SO_4, with and without 500ppm Cl^-, **37,** 2051
stress change studies
of intercalation of thin sputtered NiO films by alkali metals, **38,** 2765
stress corrosion cracking
transmission-line behaviour in impedance studies, **35,** 1619
stripping analysis
of Fe_2Sn alloy layer on tinplate in 1M HCl, **36,** 1501
of hydrogen and deuterium in Pd electrodes, **36,** 1515
potentiometric: of heavy metals in environmental studies, **38,** 807

stripping analysis continued
potentiometric, of Pb^{2+} at vitreous carbon RDE with Fe(III) oxidant, **36,** 2103
sucrose
oxidations at various metal electrocatalysts in alkaline solutions, **38,** 1679
sulphamide
complexes with PEO: a basis for proton-vacancy conducting polymers, **37,** 1603
sulphate ions
adsorbed at Pt: bond restrictions caused by the applied electric field (second-order Stark effect), **37,** 2179
adsorption at smooth Cu electrodes from acidic and neutral media, **36,** 753
effect on anodic behaviour of Cu in neutral Na_2SO_4 aq, **37,** 2541
sulphenamide synthesis
from secondary amine and electrogenerated disulphide in emulsions, **36,** 1171
sulphite ions
effect on passivation of Fe and steels, **36,** 911
effect on passivation of low-carbon steel in 0.5M Na_2SO_4 aq, **38,** 253
electrochemical behaviour at SMO stainless steel electrodes in 0.5M NaCl aq, **36,** 1367
oxidation at graphite anodes, **36,** 1073
sulpholane
reactions at Pt electrodes in 0.5M H_2SO_4 aq, **38,** 175
sulphones
competitive eliminations from 1-fluoro-2-arylvinylphenyl sulphones at Pt, Hg, Pb and C cathodes in MeCN containing proton donors, **38,** 1037
sulphonium dicyanomethylides
reductions at Hg cathodes in 0.1M $LiClO_4$-MeOH, **36,** 101
sulphur
effect on reduction of NO (3% in N_2) at Pt black electrodes in H_2SO_4 aq, **36,** 299
reduction to iron sulphide films from diethylene glycol containing $FeCl_2$, **36,** 581
sulphur dioxide
adducts with Me_2NH and Me_3N: reductions at Pt cathodes in MeOH and in MeCN, **38,** 553
oxidation at Pt RDE in aqueous and organic $HClO_4$, **36,** 1057
units in copolymer main chains: matrices for polymer electrolytes, **37,** 1555
sulphur distribution between liquid Fe and molten slags, **36,** 1027
sulphuric acid
passivation of Fe, Ni and Cr in concentrated aqueous and non-aqueous solutions, **37,** 1069
sulphur-oxygen compounds
equilibrium electrochemical properties [R], **37,** 2775
voltammetry of sulphide, thiosulphate, sulphite, dithionite and sulphate in 0.5M NaCl at Pt electrodes, **37,** 2785
sum frequency generation
study of CN^- and SCN^- adsorbed at Pt electrodes in 0.1M $NaClO_4$ aq, **36,** 1849
supercapacitors
applications of generators with solid-state electrolytes, **37,** 1627
superconductor electrodes
behaviour of $Bi_2Sr_2CaCu_2O_{8-x}$ in a carbon paste electrode in 10M KOH, **36,** 1561
behaviour of Y-Ba-Cu perovskite electrodes in 1M NaOH aq, **35,** 759
behaviour of $YBa_2Cu_3O_7$ in a carbon paste electrode in 10M KOH, **36,** 1209
insertion of Li^+ into $YBa_2Cu_3O_{7-\delta}$ from 1M $LiClO_4$-PC, **35,** 995
photocurrents at sputtered thin-film Y-Ba-Cu-O electrodes in MeCN-$LiClO_4$, **35,** 1977
redox activity of excimer laser-deposited $YBa_2Cu_3O_{7-\delta}$ epitaxial films, **35,** 1219
theory of electron-transfer reactions: rate peaks at the transition temperature, **37,** 2123, 2129
$YBa_2Cu_3O_7$ cathodes for lithium cells, **36,** 381
superoxide ions
diffusion during oxygen reduction at Au cathodes in Li_2CO_3-K_2CO_3 at 923K, **38,** 2405
electrogenerated: oxidative cleavage of aromatic α-diketones, **36,** 783
kinetics of oxygen reduction at vitreous carbon cathodes in DMF-TEAP, **36,** 2113
the O_2(Pt) electrode in molten NaCl, KCl and CsCl: exchange with O^{2-}, O_2^- and O_2^{2-}, **37,** 2681
super-plastic deformation
of yttria-stabilized (3 mol%) zirconia modified with 0.3 mol% CuO: impedance studies, **38,** 2099
supporting electrolyte
comparisons of impedance data in the presence and absence of, **35,** 1483

supporting electrolyte continued
effect on electrodeposition rate of spherical clusters under joint ohmic, diffusion and ion-transfer control, **37,** 2229, 2233
surface diffusion
during electrodeposition of metals: effect on smoothness of deposit, **37,** 2155
surface dissociation constants
for suspensions of ZrO_2, **36,** 2189
surface mobility
of Ag(100) and polycrystalline Pd surfaces in atmospheric and aqueous conditions, **37,** 2331
surface tension
of metal interfaces with non-symmetrical electrolytes, **35,** 545
orientation of dipoles at the interface, **36,** 1719
surface-enhanced Raman spectroscopic study see also Raman spectra
of adsorption on Ag of $Fe(bpy)_3^{2+}$ complex (bpy is 2,2'-bipyridyl), **37,** 2347
of adsorption of benzotriazoles at Cu electrodes in aqueous sulphates, **35,** 1011
of adsorption of imidazole from aqueous solutions at a Au electrode, **38,** 947
of adsorption of *p*-nitroaniline at Ag and Au electrodes, **35,** 1037
of adsorption of nitrobenzene and benzonitrile on Ag electrodes from 0.1M KCl aq, **36,** 1523
of adsorption of urea and thiourea at Au electrodes, **35,** 613
of amorphous films on Ti anodes in 0.15M NaCl, 1M Na_2SO_4 and 1M H_2SO_4, **38,** 2777
of co-adsorption of thiourea and anions at Ag electrodes, **35,** 879
of Cu during anodic dissolution in KSCN-3M NaCl aq, **37,** 2637
in situ, of electrode surfaces, **36,** 1829
of passive films on Fe in aerated 5M KOH aq and on Fe and Cr in aerated 0.15M NaCl aq, **37,** 2747
of pyrrole polymerization at Ag electrodes, **35,** 315
of species adsorbed on electrodeposited metals, **37,** 2115
surface-plasmon excitation
study of phase transitions in thymine films at Hg in NaCl aq, **36,** 1855
surfactants see also additives
adsorption of $C_{10}H_{21}(OC_2H_4)_{11}OH$ and $C_6F_{13}(C_2H_4O)_nH$ on Au, **37,** 2377
adsorption of $C_{12}H_{25}(OC_2H_4)_xOH$ (x = 4, 8 or 12) at the water/nitrobenzene interface, **36,** 1437
adsorption of ionic perfluorinated Forafac at Au electrodes, **38,** 2203
adsorption of ubiquinone-10 and 1-hexanol at Hg electrodes: θ inferred from *cv* ΔE for Cd^{2+}/Cd(Hg), **37,** 2395
effect on anodic dimerization of an aromatic amine in an emulsion, **35,** 1081
effect of N,N-bis(polyoxyethene)octadecylamines on electrodeposition of Sn, **36,** 985
effect of cetylMe_3NBr, $H(CH_2)_{12}SO_4Na$, Brij-35 and Triton X-100 on 4,4'-dinitrodibenzyl reduction at Hg, **37,** 2001
effect of dodecylbenzene sulphonate on the electrochemical behaviour of polypyrrole films, **37,** 1173
influence of adsorption parameters on the form of capacitance *vs* potential curves, **37,** 1273
inhibition of corrosion of Zn in aqueous NH_4Cl and alkali electrolytes by "Forafac", **35,** 479
inhibition of corrosion of Zn in NH_4Cl aq, **38,** 1453
ionic: study of electrochemical properties of micelles by isotachophoresis, **37,** 2769
kinetics of transfer of Cd^{2+} through adsorbed monolayers, **35,** 1805
non-ionic: transfer of alkali-metal ions between water and nitrobenzene aided by poly(oxyethene)dodecyl ethers, **37,** 643
redox: adsorption, diffusion and critical micelle concentration, **35,** 885
suspension effects
due to interaction of the sediment and indicator electrode double layers, **36,** 59, 69, 943
suspensions
of ZrO_2: ionization constants for surface reactions, **36,** 2189
swelling pressure
of alkali-metal montmorillonite clays in aqueous electrolytes, **36,** 1751

T

Tafel plots of semiconductor electrodes
log(photocurrent) *vs* flat-band potential data at various electrodes, **37,** 781

Tafel slopes
relation to reaction orders in reactions involving a chemisorbed intermediate, **37,** 51
tantalum
anodic oxidation in acidic sulphate solutions, **36,** 1443
impedance studies of passive films in acidic and neutral solutions, **38,** 2231
tantalum capacitors
frequency-dependence of capacitance and series resistance of Ta/Ta_2O_5/electrolyte, **38,** 285
minimum time to reach a potentiostatic regime during anodization, **36,** 739
study of the reformation of the MnO_2-Ta_2O_5-Ta system, **35,** 855
tantalum carbide
TaC and niobium carbide NbC, sintered with Fe, Ni or Co: anodic behaviour in 0.5M H_2SO_4, **37,** 2523
tellurium
electrodeposition from 10^{-3}M Te(IV) in 0.1M K_2SO_4 at pH2.2 through adsorbed intermediates, **38,** 2043
tellurium-copper compounds
coulometric analysis at 350-450°C, **38,** 1699
temperature perturbations
a new experimental device to measure thermoelectrochemical transfer functions $\partial V/\partial T$ and $\partial I/\partial T$, **37,** 1945
template synthesis
polymerization of pyrrole within pores of a microporous membrane, **37,** 1611
terpenes
oxidation of limonene at Pt anodes in MeCN-TEABr, **35,** 497
oxidation of limonene at Pt anodes in methanol solutions, **35,** 1163
1,4,8,11-tetra-azacyclotetradecane see cyclam
tetrabromoethane
reduction at Pt ultramicroelectrodes in 0.1M TEAP-DMF catalysed by cobalt tetraphenylporphyrin, **38,** 1345
7,7,8,8-tetracyanoquinodimethane
Li^+ salt dissolved with $LiClO_4$ in PEO: ion-electron mixed conduction, **37,** 1521
tetraethylene glycol dimethyl ether see bis[2-(2-methoxyethoxy)ethyl] ether
tetraglyme see bis[2-(2-methoxyethoxy)ethyl] ether
tetrahydrofuran
reaction with Li electrode modelled by reaction with Na-Cs alloy, **35,** 1061
N,N,N',N'-tetramethylhomopiperazinium diiodide solid electrolyte mixtures with AgI
redox stability range and transport number of Ag^+, **38,** 571
preparation, characterization and total conductivity, **38,** 565
tetraphenylborate ion
effect on surface modification of Al during cycling in 0.1M $NaClO_4$ aq, **38,** 1073
5,10,15,20-tetraphenylporphyrinato Fe(III) [or Co(II)] chloride
coatings catalyse reductions of organic halides, **36,** 855
tetraphenylporphyrins
of cobalt and copper: oxidation of thin films on Pt anodes in 0.1M $LiClO_4$-MeCN, **38,** 907
of iron and cobalt, pyrolysed: ESCA and electrochemical studies, **37,** 187
thallium
simultaneous UPD with Pb at Ag electrodes, **36,** 1291
UPD on Ag from a TlI film, chemically-deposited from a saturated solution of TlI, **37,** 1767
UPD on polycrystalline Ag, **36,** 1873
thallium(0/I) couple
$E°$ values for Tl^+ and Tl^+222 cryptate in various organic solvents: free energies of transfer, **38,** 1043
thallium iodide
UPD of Tl on Ag from a TlI film, chemically-deposited from a saturated solution of TlI, **37,** 1767
thallium(III)-lead(IV) mixed oxide
deposition at stainless steel anodes from 0.005M $TlNO_3$-0.1M $Pb(NO_3)_2$-5M NaOH aq, **38,** 2551
thallium(III) oxide
deposition and photodeposition on CdSe anodes from 0.1M NaOH containing Tl(I): grain and crystal-face effects, **37,** 1429
thallium UPD voltammetry
characterization of reduced Ag electrodes, **35,** 595
thermal desorption spectrometry
of CO, applied to RuO_2-IrO_2- and RuO_2-TiO_2-coated Ti electrodes, **37,** 1029
thermodynamic analysis
of electrochemical heat pumps, **35,** 1283

thermodynamic extensive variables
balances in open electrochemical systems, **35,** 749
thermodynamic method
for determination of the size ratio parameter in adsorption studies, **38,** 2663
thermodynamic properties
of K in melts of its mixed halides, **35,** 529
thermodynamic study
of phase relations and p_{Na} in Na_2O-α-Al_2O_3 from 825 to 1400K, **36,** 791
thermodynamics
classical and statistical, of crystallization at charged interfaces, **37,** 1919
of insertion of Li^+ into the gel-like spinel $Li_xMn_2O_4$, **37,** 1301
of phase transitions in adsorbed layers on electrodes, **36,** 447, **37,** 81
thermodynamics of electrokinetic processes
formulations, **35,** 705
systems with different kinds of electrodes, **35,** 711
thermoelectrochemical impedances
a new experimental device to measure thermoelectrochemical transfer functions $\partial V/\partial T$ and $\partial I/\partial T$, **37,** 1945
thiadiazole derivative
reduction of 3,4-diphenyl-1,2,5-thiadiazole-1,1-dioxide in MeCN-$LiClO_4$, **36,** 167
thin-layer cells
spectroelectrochemical study of oxidation of biliverdin to purpurin at Pt anodes in DMF-TBAP, **38,** 257
with symmetric electrodes, single charge-carrier and excess supporting electrolyte: impedances, **38,** 1837
thiocyanate ions
adsorbed at Pt, Pd, Au and Ag electrodes: infrared spectra, **36,** 1863
co-adsorption with CN^- at Pt electrodes from 0.1M $NaClO_4$, **36,** 1849
effect on corrosion and passivation of Cu and Fe in borate buffer, **36,** 505
thionine
diffusion coefficients in Nafion films, **36,** 881
modified vitreous carbon cathodes: reduction of hemoglobin, **37,** 595
thionyl chloride
effect of cathode material on reduction in $AlCl_3$, **35,** 1787
primary film on vitreous and porous carbon electrodes in $LiAlCl_4$-$SOCl_2$, **37,** 1207
reduction at porous carbon cathodes from $LiAlCl_4$-$SOCl_2$: cathode passivation, **38,** 827
surface film on Li electrodes in $LiAlCl_4$-$SOCl_2$, **37,** 1211
thiosulphate ion
co-reduction with Cd^{2+} at Pt and ITO cathodes at 90°C to form CdS, **38,** 2395
thiourea
adsorption at Au electrodes from acidic and neutral media, **35,** 613
adsorption at polycrystalline Ag in methanolic KF, **36,** 965
co-adsorption with anions at Ag electrodes, **35,** 879
effect on polarography of Ni(II): surface catalytic prewaves, **36,** 297
effect on UPD of Cu on Pt single-crystal electrodes, **38,** 647
three-dimensional phase-sensitive AC voltammetry
study of adsorption of phosphonium cations at a stationary Hg electrode, **37,** 2447
thylakoids
photoelectrochemical behaviour of sub-membrane fractions enriched with PSI and PSII, **38,** 757
thymine
adsorption at the (0001) basal face of Cd single-crystal electrodes: condensed 2-dimensional film behaviour, **37,** 2369
adsorption at the (111) face of Ag single-crystal electrodes, **37,** 2373
study of phase transitions in films at Hg in NaCl aq, **36,** 1855
tin
anodic behaviour in 0.5M citric acid aq, **37,** 143
anodic behaviour in H_2SO_4 aq, **37,** 1797
corroding in H_2SO_4: catalyst for hydroxylation of benzoic acid, **37,** 345
effect of a surfactant on electrodeposits from acidic $SnSO_4$ aq, **36,** 985
electrodeposition at W and liquid Sn cathodes in LiCl-KCl eutectic: novel electrode-kinetic analysis, **37,** 1149
electrodeposition at W and liquid Sn cathodes in LiCl-KCl eutectic: kinetics at 723K, **35,** 905

tin continued
electrodeposits from $SnSO_4$ aq: effect of aromatic carbonyl compounds on surface morphology and crystal orientation, **37**, 2403
tin disulphide
with adsorbed sensitizor dyes giving high quantum yields, **37**, 943
reductive decomposition and intercalation by K^+ aq: effect of light, **36**, 1197
tin(IV) oxide
effect on Pt, Ir and Rh as methanol-oxidation anodes, **37**, 1317
layer on Ti: anode for electrodeposition of PbO_2, **38**, 2749
tin oxide electrode
effect of substrate for the thin films on the photo-induced deposition of Pt, **36**, 1787
modified with indium hexacyanoferrate films, **35**, 1057
tin(IV) oxide electrode, fluorine-doped
with electrochromic evaporated thin WO_3 films: impedance in 1M $LiClO_4$-PC, **38**, 1935
tinplate
anodic stripping voltammetry in 1M HCl, **36**, 1501
titanium
effect of molybdate ions on passivation in H_2SO_4 aq, **36**, 2069
electrodeposition from LiF-NaF-KF eutectic at 700°C, **37**, 237
growth of anodic passive films in acidic and neutral media, **36**, 189
optical constants and thickness of anodic oxide films formed at high voltage in 0.5M H_2SO_4, **37**, 2099
potentiodynamic behaviour in artificial saliva (AFNOR standard S90-701), **38**, 1769
reflectance spectra of thin anodic films in H_2SO_4 aq, **35**, 1073
surface-enhanced Raman spectroscopy of amorphous anodic films in 0.15M NaCl, 1M Na_2SO_4 and 1M H_2SO_4, **38**, 2777
titanium diboride
effect of NaF on deposition on W or vitreous carbon cathodes from NaCl-KCl melts containing $TiCl_3$ and $NaBF_4$, **37**, 263
electro-codeposition from LiF-NaF-KF eutectic at 700°C, **37**, 237
titanium diboride electrode
wetting properties in Al cells containing cryolite-alumina melts, **37**, 1395
titanium diboride-carbon composite cathodes
effect of composition on Al electrodeposition, **38**, 663
titanium dioxide
catalyst in the photo-oxidation of organic pollutants: mechanism, **38**, 47
coated on a silica gel surface: immobilization of hexacyanoferrate ions, **37**, 2477
comparison of activities of anatase and rutile towards photooxidation of organic compounds, **38**, 43
composite film with polypyrrole on Pt or stainless steel electrodes, **37**, 1265
excited by UV light: killing of cancer cells, **38**, 153
photo-oxidation of water at a $SrTiO_3$-TiO_2 anode with a sulphonated PTFE SPE membrane, **38**, 107
photocatalysis of oxidation of organic molecules by oxygen on small semiconducting particles, **38**, 3
photocurrents at thin anodic films grown at high rates in 0.5M H_2SO_4 aq, **38**, 29
photocurrents and potential-dependent electrolyte electroreflectance of n-TiO_2, **37**, 957
photooxidation of aqueous solutions of phenol on Cr_2O_3-TiO_2, **38**, 11
photoreduction of nitrogen on Cr_2O_3-TiO_2 in presence of water vapour, **38**, 11
n-titanium dioxide
anodic films formed in 20M NaOH: dependence of photocurrents on stress, **38**, 37
titanium disulphide
cathodic intercalation by Li^+: dependence of potential on Fermi level, **36**, 1555
cycling performance in secondary lithium cells, **37**, 63
intercalation by Li^+ into cubic and layered polymorphs, **36**, 569
titanium electrodes
apparent E° for Ti/Ti(III) in the LiF-NaF-KF eutectic at 700°C, **36**, 1009
coated with RuO_2-IrO_2 and RuO_2-TiO_2, **37**, 1029
effect of hydride layers on HER kinetics from 1M HCl aq, **35**, 1913
electrodeposition of Cu: concentration profiles monitored by laser interferometry, **37**, 1279
implanted with Ir or Rh near the surface: catalysis of chlorine evolution and XPS characterization of anodic layers, **38**, 1313
photocurrents at thin oxide films: effect of film thickness, **38**, 15
tritium-deuterium separation factor during electrolysis of 0.1M LiOD-D_2O, **37**, 215

titanium(II) oxide
cathodic insertion and diffusion coefficient of Li^+, **35,** 17
titanium silicide
anodic oxidation in solutions of KNO_3 in ethane-1,2-diol, **38,** 399
toluene
oxidation to cresols at the cathode of an O_2-H_2 fuel cell using 0.5M H_3PO_4: effect of $FeCl_3$ mediator, **37,** 2549
toluenes, ring-substituted
oxidations at RDE anodes of Pt, vitreous carbon and graphite in methanol, ethanol and acetonitrile, **37,** 1951
toluenes, 3,4,5-trimethoxy-, 4-methoxy- and 4-chloro-
oxidations at graphite anode in MeOH/EtOH-$NaClO_4$/$TEABF_4$/$NaBF_4$, **37,** 1959
p-toluene sulphonate anions
adsorption at the polycrystalline Au/aqueous solution interface, **37,** 75
transfer coefficient
and charge-transfer rate constant: novel analysis of steady-state polarization data, **37,** 1149
transfer function
between velocity gradients and mass transfer flux at small electrodes, **38,** 1847
photoelectrochemical: photoeffects stimulated by light of modulated intensity, **38,** 2559
transference numbers
of Ag^+ in a solid electrolyte mixture of AgI with N,N,N',N'-tetramethylhomopiperazinium diiodide, **38,** 571
of Li^+ in the cell Li/amorphous PEO containing $LiClO_4$ or $LiCF_3SO_3$/Li, **37,** 1517
in molten salts suitable for electrodeposition of Al, **38,** 415
transition metals and alloys
relation between hydrogen overpotential and electronic structure, **38,** 557
transition-metal monoxides
cathodic insertion of alkali metal ions into, **35,** 17
transition-metal perchlorates
conductances in propanone solutions, **35,** 351
transport number see transference numbers
triazines
methoxylation of 2,4,6-tris(dimethylamino)-1,3,5-triazine in methanol at graphite anodes, **38,** 2481
1,1,1-trichlorethane
chemisorption at Pt electrodes in H_2SO_4 aq, **38,** 281
trichloro-1,1,2-trifluoroethane
catalytic effect of NH_4^+ on reduction in MeOH-H_2O at RDEs of Zn, Ni, Cu or Cd, **35,** 1727
triflates see trifluorosulphonates
bis(trifluoromethylsulphonyl)imide salts of Cu(II), Pb(II) and Ni(II)
complexes with PEO: conductivities, **37,** 1743
trifluorosulphonates
of Li^+ in polyethers: Raman study of ion-ion and ion-polymer interactions, **37,** 1495
of Pb(II) and Zn(II) incorporated in PEO films: NMR spectroscopy, **37,** 1487
trimethylamine
adduct with SO_2: reduction at Pt cathodes in MeOH and in MeCN, **38,** 553
trioctylphosphine oxide
adsorption at Hg from methanolic electrolytes, **35,** 379
triphenylmethyl anion
electrogenerated base for selective organic synthesis in DMF, **35,** 239
tritium enrichment
in the 0.1M LiOD-D_2O electrolyte during electrolysis at Pd or Ti cathodes, **37,** 215
tryptophan
electrochemiluminescence at Pt or glassy carbon anodes in 0.1M NaOH aq containing 1,3-dibromo-5,5-dimethylhydantoin, **37,** 2731
tungstate ion
reduction to W at Ni cathodes in LiCl-KCl eutectic, **35,** 1233
tungsten
effect of Ag^+ on electrodeposits from molten chlorides, **35,** 187
electrodeposition from tungstate in LiCl-KCl eutectic, **35,** 1233
photoelectrochemical behaviour of anodes in 1M H_3PO_4, **38,** 1965
tungsten carbide
containing 10 volume % of a metal (Fe or Co or Ni): anodic behaviour in H_2SO_4 aq, **37,** 447

tungsten carbide continued
effect of Ag^+ on electrodeposits from molten chlorides, **35,** 187
oxidation of hydrogen in acidic media on bulk and carbon-supported carbides, **36,** 1543
tungsten carbide-molybdenum carbide electrocatalysts
for oxidation of gaseous methanol at PTFE-bonded fuel-cell anodes, **37,** 1351
tungsten diselenide
flat-band and photocurrent-onset potentials of n-type layered anodes, **35,** 1195, **36,** 747, 2037, 2039
potential-dependent electrolyte electroreflectance of single crystals, **37,** 957
tungsten electrode
effect of CO on Cu(I/II) redox kinetics in molten 1-methyl-3-ethylimidazolium chloride-$AlCl_3$, **38,** 927
tungsten oxide
electrodeposition and behaviour of electrochromic films containing also an oxide of Co, Cr, Fe, Mo, Ni, Ru or Zn, **38,** 1521
impedance of electrochromic thin films evaporated on to ITO or fluorine-doped SnO_2 electrodes in 1M $LiClO_4$-PC, **38,** 1935
tungsten oxide amorphous anodic films
effect of film thickness on redox kinetics: densities of localized states, **36,** 1817
tungsten oxide film
on ITO glass: cathode for a SPE electrochromic window with a polyaniline/ITO/glass anode, **37,** 1377
tungsten trioxide
combined with Prussian Blue, polyaniline and poly(2-acrylamido-2-methylpropane sulphonic acid) in electrochromic windows, **38,** 1497
improvement of behaviour as a positive electrode for lithium cells, **38,** 431
photoelectrochemical behaviour of electrochromic display devices containing V_2O_5 or CdS as well as WO_3, **38,** 2759
turbulent flow
in a rectangular duct: power spectrum densities of wall velocity gradient fluctuations parallel and perpendicular to the stream, **38,** 1847

U

ubiquinone-10
adsorption at Hg electrodes from HOAc-NaOAc in MeOH-H_2O: θ inferred from *cv* ΔE for Cd^{2+}/Cd(Hg), **37,** 2395
ultrahigh vacuum studies of electrochemical phenomena
co-adsorptions of water and Cs on Cu(110) and of water and hydrogen on Cu(110) and Pt(111), **36,** 1883
ultramicroelectrodes
with arbitrary geometry: general features of homogeneous catalytic reactions in the steady state, **37,** 2587
homogeneous catalytic reactions of pseudo-first- and second-orders, **37,** 2695, 2701
modified with redox species: electrochemical catalysis, **38,** 581
reduction of Ag(III) periodate in KOH aq at pH13, **35,** 451
reductions of 1,2-dibromoethane and tetrabromoethane catalysed by Co tetraphenylporphyrin at Pt in 0.1M TEAP-DMF, **38,** 1345
study of diffusion rates of electroactive species in poly(ethene oxide)-$LiCF_3SO_3$, **38,** 2315
ultrasound
enhancement of electrochemiluminescence of tris(2,2-bipyridine) Ru(II) in MeCN-$TBABF_4$ and in aqueous oxalate, **38,** 307
underpotential deposition
of Ag and Bi at surface skeleton Ir electrodes, **35,** 191
of Ag on Pt(111): concentration dependence, **38,** 235
of alkali metals on gold from aqueous alkalis: effect on HER, **37,** 2021
of Cd at Au(111), **36,** 1829
of Cd on Pb in 5M H_2SO_4 aq, **35,** 577
of Cu at Pt(100): *in situ* X-ray absorption spectroscopic study, **37,** 1977
of Cu on Au(100) and (111) faces: an *in situ* X-ray absorption study, **36,** 1859
of Cu on Au single crystals: scanning tunnelling microscopy [A], **36,** 1893
of Cu on Pd overlayers on Au(111) and (100) single-crystal faces, **38,** 2145
of Cu on Pt(111): influences of added hydroquinone, coumarin and crystal violet, **38,** 2467

underpotential deposition continued
of Cu on Pt single-crystal electrodes: effects of thiourea and poly(ethane-1,2-diol), **38,** 647
and electrodeposition of Bi, Cu and Ge on Au, Pd and Pt cathodes: ellipsometric study, **37,** 2245
of monolayer $PbBr_2$ at Pb anodes in aqueous media, **37,** 739
of Na on Ag in NaOH aq, **35,** 523
of Pb, Cd and Tl on polycrystalline Ag, **36,** 1873
of Pb, Tl or Bi on Pt: effects on reduction of 3-nitro-1H-1,2,4-triazole, **35,** 1957
of Pb on Ag(111): slow structural changes at high coverages, **36,** 2077
of Pb on Ag(111): slow structural changes at low coverages, **36,** 1259
of Pb on Ag from acidic aqueous perchlorate, **36,** 1959
of Pb on Ag single crystals, **37,** 2173
of Pb or Tl on Ru: effect on cathodic reduction of oxygen in alkaline solution, **37,** 457
relation to work functions of substrate and adsorbate [A], **36,** 1889
sequential, of Ag and either Pb or Tl on Au single-crystal cathodes, **37,** 2237
simultaneous UPD of Pb and Tl on polycrystalline Ag, **36,** 1291
of Tl on Ag from a TlI film, chemically-deposited from a saturated solution of TlI, **37,** 1767
two dimensional analog of a model for intercalation of Li^+ into transition-metal oxides and sulphides, **38,** 1249
underpotential deposits
of Cd on polycrystalline Pt: oxygen reduction in neutral and acidic media, **37,** 2559
of Cu on Pt: inhibition of oxygen reduction, **36,** 1325
of Cu on Pt: *in situ* study of X-ray absorption fine structure, **36,** 1869
and microquantities of Rh on graphite electrodes: adsorption of H and O and electrocatalysis of HER and HCOOH oxidation, **38,** 1591
of Pb: catalysis of reduction of nitrate ion at Au cathodes in aqueous alkali, **38,** 2773
of Pb: effect on glucose oxidation at Pt anodes, **38,** 2725
of Pb: effect on products of oxidation of D-gulonic acid at smooth Pt anodes in 0.1M NaOH aq, **38,** 1359
of Pb, Tl and Bi: effect on oxidation products from D-glucose at Pt and Au anodes in aqueous alkali, **37,** 1909
of Pb, Tl and Bi: effect on oxidations of D-glucose at Pt anodes, **37,** 1333
of Pb on Ag(111): model for transformations at high coverages, **38,** 387
of Pb on Hg: effect of pH on electrocatalysis of oxygen reduction, **36,** 529
of Pb on Pt or Au: effect on anodic oxidation of methanol, glyoxal, glucose and diols, **36,** 1157
of Tl: effect on hydrogen adsorption and absorption at Pd overlayers on Au(111) and (100) single-crystal faces, **38,** 2145
uracil
adsorption at Hg electrodes from aqueous phosphate buffer pH8, **37,** 2663
uranium(VI) complexes
substituent effects on reduction of acyl-4-pyrazolone-5 complexes at Hg cathodes in PC, **36,** 325
urea
adsorption at Au electrodes from acidic and neutral media, **35,** 613

V

valinomycin
in plasticised PVC ion-selective membranes: impedance at constant current, **38,** 2691
in PVC-dioctylsebacate membranes of ion-selective electrodes [R], **35,** 1
vanadium
anodic behaviour in acidic solutions, **36,** 577
vanadium(IV)
behaviour of 2M $VOSO_4$-2M H_2SO_4 aq at graphite fibre electrodes modified by metal ions, **36,** 513
vanadium bronzes
cycling performances of $Na_{1+x}V_3O_8$ and other positive electrodes in secondary lithium cells, **37,** 63
intercalation of precipitated $Na_{1+x}V_3O_8$ by Li^+, **36,** 1549
vanadium oxide electrode see also vanadium pentoxide
capacity loss due to crystalline-to-amorphous transition with cycling, **37,** 1715
cathodic insertion and diffusion coefficient of Li^+ in VO, **35,** 17
cycling performances of V_6O_{13} and other positive electrodes in secondary lithium cells, **37,** 63
in situ X-ray study of intercalation by Li^+, **37,** 1639

vanadium oxide xerogels
as positive electrodes for secondary lithium cells, **38,** 1215
vanadium pentoxide see also vanadium oxide electrode
ESR study of cathodic intercalation by Li^+ from 1M $LiAsF_6$-PC-EC-DME, **37,** 2755
photoelectrochemical behaviour in electrochromic display devices, **38,** 2759
preparation of, and Li^+ insertion into, new positive electrode materials MnO_2-xV_2O_5, **37,** 1039
stress and electrochromism introduced by anodic insertion of Li^+ into thin amorphous films, **38,** 1637
structural modifications caused by intercalation by Li^+, **35,** 889
vanadium redox cell
activation of graphite felt electrodes, **37,** 2459
thermal pretreament of graphite felt electrodes, **37,** 1253
vanadium redox flow battery: suitable carbon electrodes, **36,** 1191
velocity distributions
near a cone rotating with modulated velocity about an axis orthogonal to a fixed plane touched by the apex, **38,** 1847
velocity profiles see also laser Doppler velocimetry
vibrational frequency shifts
induced by electric fields for halogen-Ag(111) and Co-metal bonds, **36,** 1669
vibrational quantum
of the Pt-O bond: relation to activation energy for oxygen reduction at Pt in aqueous acids, **37,** 1
vinyl fluorides
cathodic synthesis from 1-fluoro-2-arylvinylphenyl sulphones at Pt, Hg, Pb and C cathodes in MeCN containing proton donors, **38,** 1037
viologen
reduction of dications in poly(alkeneviologen)-poly(*p*-styrene sulphonic acid) complex thin films, **35,** 63
viologen mediators
reaction of oxygen with photoexcited $Ru(bpy)_3^{2+}$ in a Nafion film, **38,** 129
viscosity
of solutions of water in 0.467$TlNO_3$-0.214$CsNO_3$-0.319$Cd(NO_3)_2$ at 110°C, **37,** 349
vitamin B_{12}
catalysis of oxygen reduction at a glassy carbon cathode in weak aqueous acid, **38,** 2297
vitamin U
reduction at Hg cathodes in mildly alkaline buffers, **36,** 1925
vitreous carbon electrode
deposition of PbO_2 from 0.1M Pb^{2+} solutions of various pH, **36,** 2031
diminished electrochemical activity on implantation with Li^+ and K^+, **35,** 1279
effect of ionic strength on rate of adsorption of bovine serum albumin, **36,** 1811
effects of electrochemical pretreatment and of coating by styrene-maleic anhydride copolymer on redox kinetics, **37,** 2573
electrodeposition of Cu from solid CuI electrolyte, **38,** 577
influence of pH and anion type on electrodeposition of Ni from low concentration baths, **38,** 405
modified with $[Os(bipy)_2(PVP)_{10}Cl]Cl$: Ag deposition, **35,** 985
in the oxidation of manganate(VI) to (VII) in 2.5M KOH aq, **36,** 173
primary film in $LiAlCl_4$-$SOCl_2$, **37,** 1207
solvent effect on effectiveness of electrochemical activation, **37,** 371
supporting ultrafine Pd particles: the HER in 1M NaOH aq, **37,** 2427
with thin coatings of poly(styrene sulphonate) containing $Os(bipy)_3^{3+/2+}$: mediated oxidations, **38,** 1321
Volmer-Heyrovsky mechanism
predicted impedance behaviour, **37,** 177
Volta potential difference
at α-cyclodextrin films potentiostically emersed from 4-nitrophenol aq, **37,** 1109
Volta potential measurements
of polypyrrole films incorporating sub-equivalent amounts of dodecylsulphate, **35,** 1971

W

water
in contact with various model planar surfaces [A], **36,** 1891

water electrode
ascending: transfer of cinchonidine to 1,2-dichloroethane solutions, **38,** 2707
water electrolysis
effect of lowered gravity conditions on bubble formation at Au electrodes, **38,** 729
in KOH aq: steel anodes with electrodeposited coatings of NiSn or porous nickel, **37,** 29
photoelectrochemical device for solar energy conversion, **38,** 107, 111
temperature profile in a Nafion membrane, **36,** 263
water, heavy
attempt to detect neutrons and γ-rays during reduction at Pd cathodes, **36,** 1127
electrolysis at Pd and Ti cathodes: tritium enrichment in the electrolyte, **37,** 215
wave propagation
simplified modeling at electrode/electrolyte interfaces, **38,** 1535
work functions, **36,** 1659
of (5 x 20) and (1 x 1) surfaces of Au(100) electrodes, **37,** 615

X

xerogels
vanadium oxide as positive electrodes in secondary lithium cells, **38,** 1215
X-ray absorption studies
of fine structure of PEO containing pairs of inorganic salts, **37,** 1529
in situ, of fine structure of UPD Cu on a Pt electrode, **36,** 1869
in situ, of UPD of Cu on Pt(100) electrodes, **37,** 1977
in situ, of UPD Cu on Au(100) and (111) faces, **36,** 1859
of local structure in $NiBr_2(PEO)_8$, **37,** 1663
of organo-disulphide redox positive electrodes for lithium cells, **37,** 1635
of V_2O_5 intercalated by Li^+, **35,** 889
X-ray diffraction studies
of Al anodized in CrO_3-xH_2SO_4 aq, **35,** 961
of anodic deposits of Sb in 0.5M H_2SO_4 aq, **36,** 2093
of $Bi_4V_2O_{11}$ in which 10% of vanadium ions are substituted by copper, **38,** 969
of carbons used as negatives in secondary lithium cells, **38,** 1179
of CdSe, CdS and $CdSe_xS_{1-x}$, **38,** 593
of cobalt oxide films sputtered on to glass substrates, **35,** 975
of di- and tri-chromate ions in Cr electrodeposition solutions, **37,** 1239
of effect of Ag^+ on electrodeposition of W and WC from molten chlorides, **35,** 187
of inhibition of electrodeposition of Sn from $SnSO_4$ aq by aromatic carbonyl compounds, **37,** 2403
of insertion of Li^+ into $AgCr_3O_8$, **38,** 1211
in situ, of stepwise intercalation of $Li_xV_6O_{13}$ by Li^+, **37,** 1639
of lead(IV)-thallium(III) mixed oxide anodic deposits from 0.005M $TlNO_3$-0.1M $Pb(NO_{33}$-5M NaOH aq, **38,** 2551
of Li^+ insertion into sol-gel lamellar birnessite $MnO_{1.84}.0.6H_2O$, **36,** 1595
of $LiNi_{1-x}Co_xO_2$ positive electrodes for secondary lithium cells, **38,** 1159
of modification of a hydrogen storage alloy by KBH_4 treatment, **38,** 659
of Nb_2O_5 before and after cathodic polarization, **35,** 765
of new positive-electrode materials $MnO_2.xV_2O_5$, **37,** 1039
of Ni-P electrodeposits before and after differential scanning calorimetry to 500°C, **38,** 261
of Pt-Fe alloy oxygen reduction catalysts supported on carbon, **38,** 2715
of solid electrolyte mixtures of AgI with diiodides of N,N,N',N'-tetramethylhomopiperazinium and homopiperazinium, **38,** 565
of surface atomic roughness at Au(100) electrodes induced by potential cycling into hydrogen evolution, **37,** 2169
of transformations between ramsdellite and spinel forms of lithiated MnO_2, **38,** 1259
of tungsten trioxides for use as positive electrodes in lithium cells, **38,** 431
of V_2O_5 intercalated by Li^+, **35,** 889
of V_6O_{13} positive electrodes: crystalline-to-amorphous transition with cycling, **37,** 1715
X-ray energy dispersion analysis
study of passivation of porous carbon cathodes during reduction of $SOCl_2$-$LiAlCl_4$, **38,** 827

X-ray fluorescence, energy-dispersive
studies of Ni-Sn alloy electrodeposits on Cu, **35,** 55
X-ray scattering
electrochemical cell for *in situ* measurements using transmission geometry, **36,** 209
X-ray spectroscopy
ultrasoft study of Al anodized in CrO_3-xH_2SO_4 aq, **35,** 961
xylenes
adsorption and indirect oxidations at Pt and Au electrodes, **35,** 273

Y

Y zeolites
incorporation of Fe(III) ions by ion exchange with acetonitrile solutions, **37,** 2411
ylides
reductions of phenyliodonium ylides at Hg and Au cathodes in methanolic media, **35,** 455, 1995
reductions of pyridinium and sulphonium dicyanomethylides at Hg cathodes in 0.1M $LiClO_4$-MeOH, **36,** 101
yttria-stabilised zirconia electrode
potentiometric study of oxide ion exchange between MgO and PbO in $PbCl_2$-KCl at 475°C, **38,** 1743
yttria-stabilized zirconia
CV of porous Pt catalyst films at 350 and 650°C with a wide range of oxygen pressures, **38,** 2533
effect of Fe implantation on oxygen transfer: impedance, DC polarization and ^{18}O exchange studies, **38,** 1817
equivalent circuit for a solid ionic conductor sandwiched between two blocking electrodes, **38,** 2111
impedance study of the effect of 0.3 mol% of CuO on super-plastic deformation, **38,** 2099
oxygen reduction at a lanthanum strontium manganite cathode at 1000°C, **38,** 2015

Z

zeolite-modified carbon paste electrode, incorporating methyl viologen
effects of support electrolyte and immersion time in aqueous media, **38,** 2257
ion exchange between MV^{2+} and Na^+ of the zeolite, **38,** 2267
zeolite-modified electrode
comparison of pure graphite with 45% zeolite electrodes in oxidations of hydrazine, alcohols and hydroquinones, **38,** 919
zeolites
voltammetric behaviour of layers containing Hg(II) in coatings on vitreous carbon substrates, **36,** 383
zeta potentials
for spherical macroions in 1:1 and 2:2 electrolytes, **36,** 1747
zinc
deposition and dissolution in a flow-through porous electrode, **38,** 311
dissolution in $AlCl_3$/1-methyl-3-ethylimidazolium chloride mixtures, **35,** 89
electrodeposition: effects of N,N-bis(decaoxyethene)octadecylamine, cinnamaldehyde, benzalacetone and acetonaphthone, **38,** 1351
electrodeposition at a RDE from aqueous sulphate solution, **37,** 439
electrodeposition on vitreous carbon from zincate solutions, **37,** 1199
impedance study of electrodeposition from 0.5M ZnO-5M KOH aq, **35,** 1587
inhibition of corrosion in NH_4Cl aq by addition of organic surfactants, **38,** 1453
solvent effects on kinetics of electrodeposition at Hg, **38,** 721
zinc amalgam electrode
medium effect on the $Zn(Hg)/Zn^{2+}$ couple in 0.05M $LiClO_4$ in propane-1,2-diol-water mixtures, **38,** 2459
zinc electrode
impedance study of the formation of a chromate layer, **35,** 515
inhibition of corrosion in aqueous NH_4Cl and alkali electrolytes by the surfactant "Forafac", **35,** 479
passive anodic films formed in borate and arsenate solutions at pH8.9, **36,** 1491
zinc(II) ion
complexes with Tris buffer solutions, **35,** 673

zinc(II) ion continued
conduction and interfacial studies of amorphous methoxy-linked poly(ethene oxide) $Zn(CF_3SO_3)_2$ complex, **37,** 1707
zinc oxide
effect of electrolyte composition on rate of chemical dissolution of n-type single crystals, **37,** 827
zinc-bromide secondary cell
kinetics of the Br_3^-/Br_2 electrode, **36,** 1403
zinc-iodine secondary cell
with porous Nylon-carbon composite positive electrode, **35,** 255
ferrocene:deoxycholic acid 1:2 inclusion compound as a positive electrode, **38,** 1373
zinc-nickel alloys
electro-codeposition from aqueous chlorides, **37,** 545
zinc(II)-palludrine complexes
variation of Arrhenius factors with potential during reduction at Hg cathodes, **38,** 735
zinc-rich ethyl silicate paint
protection performance for steel in artificial seawater studied by impedance spectroscopy, **38,** 2029
Zircaloy
impedance studies in 0.5M K_2SO_4 aq at 20-200°C of the oxide layer formed in water vapour at 400°C, **38,** 1961
Zircaloy-2 and Zircaloy-4
anodic behaviour in aqueous media, **37,** 281
zirconia stabilized by yttria see yttria-stabilized zirconia
zirconium
electrodeposition from LiF-NaF-KF eutectic at 700°C, **37,** 237
impedance study of anodic films in neutral solutions, **36,** 647
photoelectrochemical behaviour of anodes in 1M H_3PO_4, **38,** 1965
growth of passive anodic films in 0.5M NH_4HSO_4 aq, **35,** 1897
zirconium diboride
electro-codeposition from LiF-NaF-KF eutectic at 700°C, **37,** 237
zirconium dioxide
ionization constants for surface reactions in its suspensions, **36,** 2189
zirconium oxides
determination of layer thicknesses from Bode diagrams, **38,** 633

Receive Regular News of Pergamon's Publications

Pergamon mails information on new and existing publications regularly.
If you would like to be added to the mailing list please send us your name and full mailing address, indicating your fields of interest:

ENGINEERING
Energy Sources & Technology, Civil & Structural Engineering, Mechanical Engineering, Electrical & Electronic Engineering, Systems & Control Engineering, Aeronautical & Aerospace Technology, Materials Technology, Chemical Engineering

LIFE SCIENCES & MEDICINE
Biological Sciences (including biochemistry & molecular biology), Agriculture, Veterinary Medicine, Immunology, Cancer Research, Pharmacology, Neuroscience, Vision Science, Clinical Medicine

PHYSICAL SCIENCES
Computer Science, Physics, Chemistry, Mathematics, Earth Science, Environmental Science, Materials Science, Space & Planetary Sciences

SOCIAL SCIENCE & HUMANITIES
Sociology, Women's Studies, Psychology, Education, Political Science, Geography, Economics, Management & Business, Linguistics, Information Science, Librarianship

PERGAMON

An imprint of Elsevier Science

Elsevier Science Ltd
PO Box 800, Kidlington, Oxford OX5 1DX, UK

Elsevier Science Inc.
660 White Plains Road, Tarrytown, NY 10591-5153, USA

COR017/P4

Announcing New and Newly Acquired Journals

Engineering

Control Engineering Practice
1994: Volume 2 (6 issues)
Publishes papers which illustrate the direct application of control theory and its supporting tools in all possible areas of automation. The journal is centred in engineering - especially mechanical, electrical and electronic, aerospace and chemical engineering, but also includes social effects, cultural aspects, project planning and system design and economic and management decisions.

Engineering Failure Analysis
1994: Volume 1 (4 issues)
Publishes original, high quality research papers, communications, and occasional review articles describing the analysis of engineering failures and related studies.
It provides essential reference material and critical feedback into design process thereby contributing to the prevention of engineering failures in the future.

Chemistry

Bioorganic & Medicinal Chemistry
A Tetrahedron Publication
1994: Volume 2 (12 issues)
Provides an international forum for the publication of full original research papers and critical reviews on molecular interactions in key biological targets such as receptors, channels, enzymes, nucleotides, lipids and saccharides. The aim of the journal is to promote a better understanding at the molecular level of life processes, and living organisms, as well as the interaction of chemical agents with these.

Molecular Biology

Cytokine Reviews and Communications
1994: Volume 1 (4 issues)
This new international journal will publish both authoritative reviews and short preliminary communications in the growing field of cytokine research. Articles will focus on all aspects of cytokine research, including cytokine discovery, functional studies, and genetic and molecular experimentation.

Free sample copies of these journals are/or will be available on publication, from your nearest Elsevier Science office

PERGAMON
An imprint of Elsevier Science

Elsevier Science Ltd, PO Box 800, Kidlington,
Oxford, OX5 1DX, UK
Elsevier Science Inc., 660 White Plains Road,
Tarrytown, NY 10591-5153, USA

Social & Behavioural Sciences

European Management Journal
1994: Volume 12 (4 issues)
Publishes leading-edge research from academics and senior industrialists throughout Europe and the United States enabling practitioners and management trainers to broaden their knowledge of the new operational environment.

International Business Review
1994: Volume 3 (4 issues)
This journal provides a forum for academics and professionals to share the latest developments and advances in knowledge and practice of international business. It aims to foster the exchange of ideas on a range of important international subjects and provide stimulus for research and the further development of international perspectives.

International Transactions in Operational Research
1994: Volume 1 (4 issues)
The primary purpose of this journal is to advance the understanding and practice of operational research on an international basis. The scope of the journal will include problems of an international nature (eg. fisheries management, environmental, global competitiveness).

Location Science
1994: Volume 2 (4 issues)
The primary focus of this journal is on research directed to extending and applying the theory and modeling of location decisions. The journal will also publish papers which address the underlying processes related to locational decisions, the determination of parameters associated with location problems, and issues of implementation.

Transportation Research Part C: Emerging Technologies
1994: Volume 2 (4 issues)
This journal is concerned with the impacts of new technology (including IVHS) on transportation system performance characteristics.

Environmental Science & Technology

Spill Science and Technology Bulletin
Sister Journal of *Marine Pollution Bulletin*
1994: Volume 1 (2 issues)
A new international, peer-reviewed journal on oil and chemical spill science and technology, focussing on the effects and control of discharges of oil, oil products and other hazardous substances. Both land and water spill issues will be addressed, and papers linking science and technology with policy and management matters will also be considered appropriate.

SHORT COMMUNICATIONS

PREPARATION OF CAMERA-READY COPY: GUIDELINES FOR AUTHORS

Manuscripts submitted and accepted (including any revisions made necessary by refereeing or Editorial modification) as camera-ready copy benefit from substantially reduced publication times since the normal procedures of typesetting and proof-checking are by-passed. However, where the submitted copy is not of adequate quality or is not sufficiently close to the journal style, the Editors and the Publisher reserve the right to have the material typset in the normal way. Authors are recommended to consult a copy of the journal for examples of the preferred style. The following guidelines may also be of assistance.

Manuscripts submitted as camera-ready copy should be on good quality A4 (29.7 × 21.0 cm) or U.S. Letter (27.9 × 21.6 cm) size paper. Manuscripts will normally be reproduced after photographic reduction to 90% of the original size.

Ideally manuscripts should be laser printed using 10pt Times Roman font, with a maximum of 66 lines text. The text may be in single or double column. All graphics must be inserted in text (if not printed directly then graphics should be glued in place, not taped). All graphics and text should be within an image area of 26 cm height and 16.5 cm width.

Suggested margin settings (in cm) are:

	LH margin	RH margin	Upper margin	Lower margin
U.S. letter	3.2	1.9	0.8	1.2
A4	2.9	1.6	1.6	2.1

Recommended font settings are:

Title of the paper	12pt Times Roman Bold.
Names of Author(s)	10pt Times Roman Capitals.
Address(es) of Author(s)	8pt Times Roman.
Abstract	8pt Times Roman.
Section headings with subheadings in italics	10pt Times Roman Capitals.
Figure headings	8pt Times Roman.

Lettering on figures should be of appropriate size for reproduction after reduction. **References** should be numbered in the text (in square [] brackets), and should be listed in numerical sequence (in 8pt Times Roman) at the end of the paper.

Where these suggestions for type size cannot be followed in detail, authors should above all ensure that they keep as closely as possible to the measurements given above for the image area of a page.

SAMPLE PAGE OF A SHORT COMMUNICATION AFTER REDUCTION TO 90% OF ORIGINAL SIZE

The lines indicating the image area are for information only and should not be included on submitted typescripts

THE MINIMUM VALUE OF THE DIFFERENTIAL CAPACITY OF GALLIUM AT NEGATIVE CHARGES

L. DOUBOVA, A. DE BATTISTI, S. TRASATTI†

Department of Chemistry, University of Ferrara, Via Borsari 46, 44100 Ferrara, Italy

†Department of Physical Chemistry and Electrochemistry, University of Milan, Via Venezian 21, 20133 Milan, Italy

(Received)

Abstract - The minimum values of the differential capacity of Ga at negative charges has been found to be systematically higher than that of Hg by about 20%. These results, in close agreement with recent chronocoulometric experiments, cause the relation between the structure of the interface at Hg and that at Ga to be looked at in a different light.

INTRODUCTION

The interpretation of the differential capacity-charge curves of the electrode/aqueous solution interface rests on two pictures of the boundary region between the metal and the liquid phase differing by the role assigned to the solid. In one group of models whose prototype is that proposed by Watts-Tobin [1] the metal depicted as an infinitely conducting solid wall so that the interphase is reduced to a water monolayer. In the other group [2-4], the water monolayer is in contact with a solid whose electronic structure is taken quantitatively into account through the "jellium" model of a metal surface.

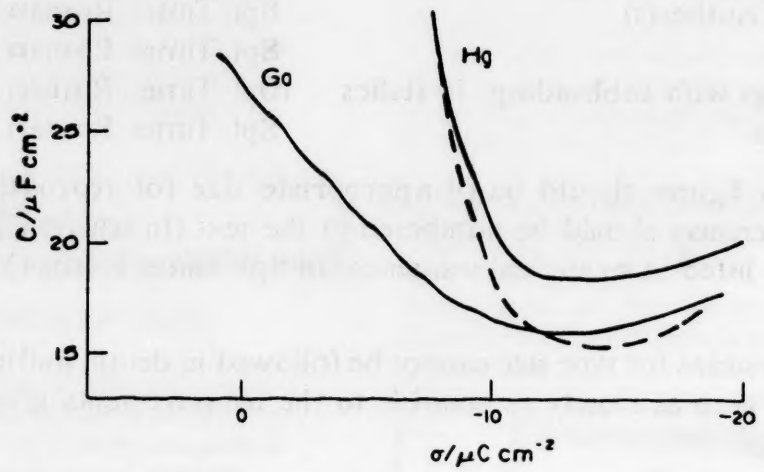

Fig. 1. Differential capacity of dropping Hg and Ga electrodes in 0.5mol dm^{-3} Na_2SO_4 solution. (—) This work; (----) from Ref.[16].

REFERENCES

1. R.J. Watts-Tobin, Phil. Mag. 6, 133 (1961).
2. J.P. Badiali, M.L. Rosinberg and J. Goodisman, J. Electroanal. Chem. 130, 31 (1981).
3. M.A. Vorotyntsev and A.A. Kornyshev, Elektrokhimiya 20, 3 (1984).
4. W. Schmickler and D. Henderson, J. Chem. Phys. 80, 3381 (1984).
5. B.B. Damaskin and A.N. Frumkin, Electrochim. Acta 19, 173 (1974).

GUIDE TO AUTHORS

Papers should be submitted directly to the Editor-in-Chief, except that authors from North America *may* instead send their papers to the North American Regional Editor: E. J. Cairns, Energy & Environment Div. Bldg 90, Lawrence Berkeley Laboratory, University of California, Berkeley, CA 94720, U.S.A.

1. Papers submitted to *Electrochimica Acta* should consist of (i) critical reviews, (ii) full length research papers or (iii) short communications, *not previously published*, in the field of pure and applied electrochemistry. Authors intending to offer critical reviews are advised first to contact the Editor-in-Chief. Short communications should take up no more than *two* printed pages in the journal and will be handled more rapidly if supplied in camera-ready format, in which case papers may be up to *four* pages long. Papers that are accepted may not be published elsewhere in any language without the consent of the Editor-in-Chief. Papers from non-members of Int. Soc. of Electrochemistry are welcome.

2. Papers will only be published if they are likely to be of interest to our subscribers. Thus papers which deal solely with the *dc* polarography of substances will probably not be accepted, whilst papers dealing with conductance or *emf* measurements on ambient temperature electrolytes should generally be submitted in the form of Short Communications. All papers will be refereed.

3. **Only English language papers will be accepted.** An abstract not exceeding 200 words must be provided. For Short Communications an abstract not exceeding 50 words should be provided. Authors must provide **FIVE KEY WORDS** at the end of each abstract.

4. Papers should be submitted **IN TRIPLICATE** to facilitate refereeing. Where there may be postal delays authors are advised to send an additional copy to Newcastle by fax at the same time that they post their three copies. **One top copy** and **two** Xerox copies are acceptable. They should be typed in **double spacing on one side of the paper only.** Detailed descriptions of apparatus etc. should be given only if such apparatus is new.

5. The author responsible for proofs and correspondence must be identified on the manuscript. Failure to do this can be a major cause of delay in publication. **ONCE A MANUSCRIPT HAS BEEN ACCEPTED, QUERIES REGARDING THE PROGRESS OF PUBLICATION SHOULD BE ADDRESSED TO THE PRODUCTION EDITOR** at Elsevier Science Ltd, The Boulevard, Langford Lane, Kidlington, Oxford OX5 1GB, U.K. In the interests of speedy publication galley proofs are not submitted to authors. The difficulty and expense involved in making corrections to page proofs make it essential for authors to prepare their manuscripts carefully so that alteration is not required. The cost of excessive alteration at the proof stage may have to be charged to the author.

6. Illustrations should be on separate sheets the same size as the typescript, in any case no larger than A4 (209 by 296 mm). **Legends for illustrations should also be on a separate sheet;** they should render the illustration intelligible without reference to the text. **ONE SET OF ORIGINAL LINE DRAWINGS** and two sets of photocopies should be furnished, drawn boldly to twice the final size required, with lettering in light pencil. The following standard symbols easily available to the printer for legends should be used:

○ ● + × □ ■ △ ▲ ◇ ◆ ▽ ▼

Photographs and photomicrographs should be included only if absolutely *essential*. If artwork needs to be redrawn this may cause a delay.

7. Tables should be kept to a minimum; no data can be recorded in both graphical and tabular form. Essential tables should be provided with headings, and should be intelligible without reference to the text. In the interest of economy and in order to avoid the introduction of errors, tables will be reproduced by photo-offset means directly from the authors' manuscripts.

8. Authors are requested to provide **FIVE KEY WORDS** for future indexing.

9. References should be indicated in the text in square brackets, and listed at the end of the paper as follows:

1. K. F. Bonhoeffer and H. Gerischer, *Z. Elektrochem.* **52,** 149 (1948).
2. U. R. Evans, *Metallic Corrosion, Passivity and Protection*, 2nd edn, p. 32. Arnold, London (1964).

Abbreviations of journal titles should follow those in *World List of Scientific Periodicals* (Fourth Edition).

10. Each paper should be consistent within itself as to abbreviations, symbols and units. Authors should use wherever possible SI units and when these are not used should provide a conversion factor to SI units. Axes for graphs and headings for tables should be given in quantity calculus form, e.g. times as t/s, potential as E/mV, current density as i/A m^{-2}. Any electrochemical abbreviations should be written without stops, e.g. *emf*, *pd*, *ac*, etc.

11. Reprints can be ordered on the form accompanying proofs.

12. If the above recommendations are followed, it will be possible to publish accepted papers with a minimum of delay. **Papers not conforming to this Guide will, however, inevitably suffer much delay and in extreme cases may have to be rejected entirely.** The Editors will warmly appreciate the co-operation of authors in preparing papers in a manner that will facilitate the complex work of publication.

13. The original manuscript and diagrams will be discarded 1 month after publication unless the Publisher is requested to return original material to the author.

14. Material for the Calendar should be sent to the Editor-in-Chief: Dr R. D. Armstrong, Chemistry Department, The University, Newcastle upon Tyne NE1 7RU, England. **Organizers are asked to submit details at least 6 months before the date of the event.**

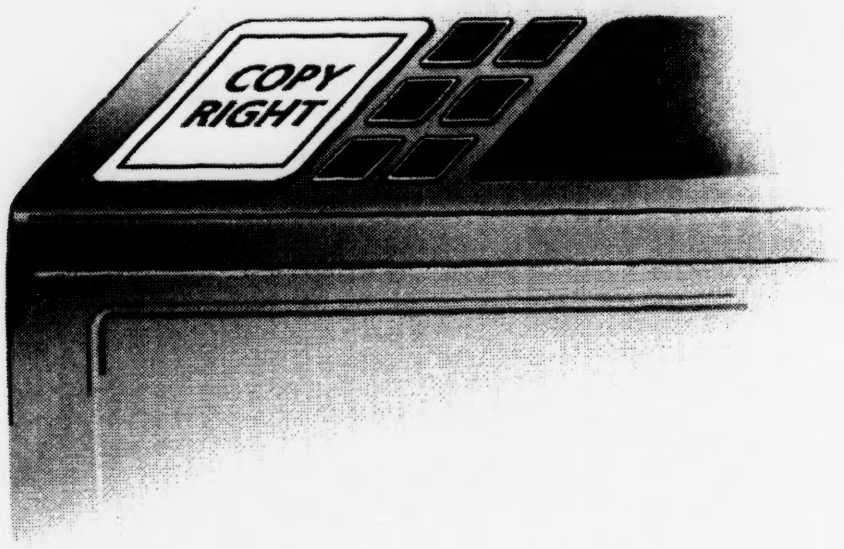

THE Most
~~AN~~ IMPORTANT PART
OF YOUR PHOTOCOPIER
ISN'T PART OF
YOUR PHOTOCOPIER

Having the machine does not permit you to photocopy
books, journals and magazines.
The Copyright Clearance Center DOES.
Contact us to find out
how you too can Copy Right.

COPYRIGHT CLEARANCE CENTER
222 Rosewood Drive, Danvers, MA 01923 ☐ Tel. (508) 750-8400 ☐ Fax (508) 750-4744

© 1991 Copyright Clearance Center

PERGAMON

PRINTED IN GREAT BRITAIN BY BPCC WHEATONS LTD, EXETER